NASA CR-72803

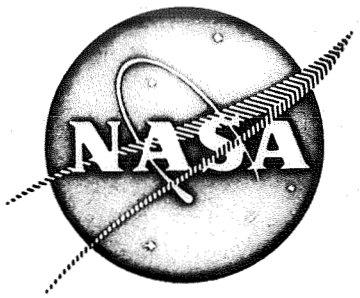

INVESTIGATION OF ELECTROLYTE SYSTEMS FOR LITHIUM BATTERIES

by

R. Keller and J. F. Hon

ROCKETDYNE
A DIVISION OF NORTH AMERICAN ROCKWELL CORPORATION

prepared for

NATIONAL AERONAUTICS AND SPACE ADMINISTRATION

NASA Lewis Research Center
Contract NAS3-12969
Robert B. King, Project Manager

FINAL REPORT

INVESTIGATION OF ELECTROLYTE SYSTEMS FOR LITHIUM BATTERIES

(26 May 1969 to 25 July 1970)

By

Rudolf Keller and John F. Hon

ROCKETDYNE
A Division of North American Rockwell Corporation
6633 Canoga Avenue
Canoga Park, California 91304

Prepared For

National Aeronautics and Space Administration

Contract NAS3-12969

NASA Lewis Research Center
Cleveland, Ohio
Mr. Robert B. King, Project Manager
Space Power Systems Division

NOTICE

This report was prepared as an account of Government sponsored work. Neither the United States, nor the National Aeronautics and Space Administration (NASA) nor any person acting on behalf of NASA:

A.) Makes any warranty or representation, expressed or implied, with respect to the accuracy, completeness, or usefulness of the information contained in this report, or that the use of any information, apparatus, method, or process disclosed in this report may not infringe privately owned rights; or

B.) Assumes any liabilities with respect to the use of, or for damages resulting from the use of any information, apparatus, method or process disclosed in this report.

As used above, "person acting on behalf of NASA" includes any employee or contractor of NASA, or employee of such contractor, to the extent that such employee or contractor of NASA, or employee of such contractor prepares, disseminates, or provides access to, any information pursuant to his employment or contract with NASA, or his employment with such contractor.

Requests for copies of this report should be referred to

National Aeronautics and Space Administration
Office of Scientific and Technical Information
Attention: AFSS-A
Washington, D.C. 20546

FOREWORD

The research described in this Final Report was conducted in Rocketdyne's Research organization, during the period 26 May 1969 through 25 July 1970. The work was done under NASA Contract NAS3-12969, with Mr. Robert B. King, Space Power Systems Division, NASA-Lewis Research Center, as NASA Project Manager.

The authors acknowledge the support of Dr. James N. Foster who performed the major part of the analytical effort on the program, of Mr. Douglas C. Hanson who was responsible for the purification of solvents and for many property measurements, and of Dr. James S. Muirhead who contributed to the NMR effort.

Informal Monthly Progress Reports were submitted to NASA, but no interim reports for wide distribution were prepared.

The Rocketdyne report number for this document is R-8368.

ABSTRACT

Aprotic electrolytes based upon methyl formate, propylene carbonate, and dimethyl formamide as solvents and lithium chloride plus aluminum chloride, lithium hexafluoroarsenate, and lithium perchlorate as solutes were studied. Well characterized components were used to prepare solutions. The affect of additives, other aprotic solvents, other salts and, in some cases, small amounts of water, on species in solution and physical properties was investigated. Physical properties investigated included conductance, solubilities, and stability in the presence of lithium.

CONTENTS

TABLES

ILLUSTRATIONS

SUMMARY

Structural studies and physical property measurements were conducted in aprotic electrolyte systems containing methyl formate (MF), propylene carbonate (PC) or dimethylformamide (DMF) as the primary solvent component, and $LiCl+AlCl_3$, $LiAsF_6$ or $LiClO_4$ as the primary solute. The effect of additives on species and species distribution and physical properties was studied; the additives were solvents such as nitromethane (NM), tetrahydrofuran (THF), acetonitrile (AN), dimethyl sulfoxide (DMSO), as well as the solvents named above (MF, PC, and DMF), or solutes such as $LiClO_4$ and LiBr. In some cases, the effect of the addition of small amounts of water was also investigated.

Well characterized components were used to prepare solutions. Vapor phase chromatography (VPC) was the principal analytical method employed to analyze distilled solvent batches. The water content of the solvents was normally below 50 ppm, and ordinarily a solvent was not utilized if organic impurities were detected at greater levels. Emission spectrography and spark source mass spectrography were the methods used to analyze solutes.

Nuclear magnetic resonance (NMR) techniques were the principal experimental tool used to determine species in the nonaqueous solutions. Often results of these measurements could be compared directly with results obtained from conductance and other physical property measurements. In such instances agreement was found.

In additional studies, solution stabilities were evaluated in simple tests and the solubility of CuF_2 and $CuCl_2$, representing electroactive battery cathode materials, was investigated.

For the complexing of the aluminum ion, the following order of decreasing solvating or complexing strength was found for various solvents and anions:

$$DMSO,\ H_2O,\ DMF,\ Cl^-,\ Br^-,\ PC,\ ClO_4^-,\ AN,\ MF,\ THF,\ NM$$

In some instances the positions in this sequence may be interchanged.

The predominant species found in $LiClO_4$ and $LiAsF_6$ solutions were, as expected, Li^+ ions and ClO_4^- or AsF_6^- ions, respectively. In the case of $LiAsF_6$, the existence of an additional species asymmetric with respect to the As site, was indicated in several electrolytes.

$LiAsF_6$ was found to have a stabilizing effect on methyl formate solutions in contact with metallic lithium, although the mechanism of this stabilizing effect was not determined. It was observed that the hydrolysis reaction involving methyl formate and traces of water was greatly accelerated in the presence of $LiAsF_6$ but not in the presence of $LiClO_4$.

In many cases, the conductance of solutions seem to be affected by solvent additives through a viscosity effect only. In other cases, an interaction with aluminum complexes in solution was indicated, however. For $LiClO_4$/MF solutions, the solution conductance was greatly enhanced in certain cases by addition of solvents such as DMF, presumably because of the break-up of ion pairs.

Solubility values for CuF_2 and $CuCl_2$ often were significantly increased by additives, but it was not always certain to what extent true solubility values were affected and to what extent only dissolution rates, which in some systems appear to be extremely slow, were affected.

The solution stability was frequently affected by additives. A sufficiently pronounced effect was observed for $LiAsF_6$ only, however.

INTRODUCTION

Lithium batteries have the potential to deliver the high energy density beneficial in space and other applications. The NASA-Lewis Research Center therefore supported various efforts in this area, among them work by groups at American University, Globe-Union, Inc., Honeywell's Livingston Electronic Laboratory, P. R. Mallory and Company, Inc., Monsanto Research Corporation, and the Whittaker Corporation.

During the course of such investigations, a lack of knowledge of the properties of nonaqueous electrolytes to be used in lithium batteries became evident. Composition of these electrolytes, relationships of the components of the electrolyte to each other, and interaction of the electrolyte with other battery components should be known to guide the optimization of the battery systems in an efficient manner. A program, NAS3-8521, was therefore performed at Rocketdyne to study aprotic electrolytes with and without dissolved cupric halides; the results were described and discussed in a Final Report, NASA CR-1425 (Ref. 1). Under the investigation described in this report, this effort was extended to electrolytes containing a solvent or solute additive, to study the properties of such mixed electrolytes, and to find electrolytes with improved properties mainly in regard to stability, conductance, and interaction with electroactive materials.

The present investigation, performed with well characterized materials, consisted of nuclear magnetic resonance studies, stability and solubility tests, and physical property determinations. Electrolytes containing $LiClO_4$, $LiAsF_6$, or $LiCl + AlCl_3$ as solutes were studied. Because of the direct practical interest, solutions of $LiAsF_6$ in methyl formate were emphasized during the latter part of the program (after pure $LiAsF_6$ synthesized on another NASA contract had become available).

PREPARATION OF ELECTROLYTES

SELECTION OF ELECTROLYTES AND ADDITIVES

Propylene carbonate (PC), dimethylformamide (DMF), and methyl formate (MF) were selected as the main solvents. Among the main solutes employed were $LiClO_4$, $LiAsF_6$, and $LiCl+AlCl_3$ mixtures. The electrolyte $LiAsF_6$/MF received major attention in the latter part of the program.

The solid and liquid additives were selected for various reasons. The solvents dimethylformamide, dimethyl sulfoxide (DMSO), tetrahydrofuran (THF), nitromethane (NM), acetonitrile (AN), propylene carbonate, methyl formate, and the solids LiBr, $LiClO_4$, and $AlCl_3$ were selected to study the complexing properties of solvents and the possibilities to stabilize aluminum chloride solutions. Phenanthroline and salicylaldoxime were chosen to investigate the effect of these additives on the solubility of copper halides. Some of the additives previously mentioned were also studied to determine their effects on copper halide solubility, and to identify viscosity and other effects on the electrolyte conductance.

PURIFICATION OF SOLVENTS

Starting Materials

The sources of the starting materials are given in Table 1. The coding of solvents is consistent with that in Ref. 1; the first number designates a certain lot of received material, the second number is added for the different purified and analyzed batches.

Distillation Procedures

Solvents were purified by distillation. Methods previously established for the purification of PC and DMF (Ref. 1) consistently furnished solvents with acceptable impurity levels; the procedures are reviewed in Table 2. Procedures developed for the purification of MF, AN, DMSO, NM, and THF are discussed in detail below and are also summarized in Table 2.

TABLE 1

PURCHASED SOLVENTS, GRADES AND SUPPLIERS

Solvent	Source	Quality	Lot No.	Analysis
PC #3	Chemical Procurement Laboratories			
PC #6	Matheson, Coleman and Bell	Chemical		
PC #7	Matheson, Coleman and Bell	Chemical	20	
DMF #7	J. T. Baker Chemical Co.	GC-Spectrophotometric	1-3378	
MF #2	Matheson, Coleman and Bell	Spectro	27	490 ppm methanol
MF #3	Matheson, Coleman and Bell	Spectro	42	
MF #4	Livingston Electronic Laboratory	Special (purified); no detectable H_2O; 40-50 ppm MeOH	43	25 ppm H_2O; 20 ppm MeOH 20 ppm other organic impurity
AN #6	Matheson, Coleman and Bell	Chromato	27	
DMSO #1	Matheson, Coleman and Bell	Reagent	A47	730 ppm H_2O; no organic impurities
NM #1	Eastman Organic Chemicals	Spectro	682A	270 ppm H_2O; $\leq$20 ppm organic impurity
THF #1	J. T. Baker Chemical Co.	Reagent	39215	41 ppm H_2O; 210 ppm BHT; 23 ppm organic impurity
H_2O		Distilled, deionized		

TABLE 2

DISTILLATION PROCEDURES FOR PURIFICATION OF SOLVENTS

Solvent	Quality	Drying Agent	Distillation Column	Condition
PC	Chemical	CaH_2	Vigreux (Packed with Heli-pak)	8 to 15 mm Hg; 100 to 115 C
DMF	Spectro	Molecular Sieves	Vigreux (Packed with Heli-pak)	Atmospheric Pressure; 151 C
MF	Spectro	P_2O_5	Vigreux (Packed with Heli-pak)	Atmospheric Pressure; 31 C
AN	Chromato	P_2O_5	Vigreux (Packed with Heli-pak)	Atmospheric Pressure; 80 C
DMSO	Reagent	CaH_2	Vigreux (Packed with Heli-pak)	~10 mm Hg ~75 C
NM	Spectro	Molecular Sieves (in column)	None	24 hours in molecular sieve column at ambient temperature
THF	Reagent	None	None	None

Methyl Formate. Material of acceptable purity was obtained by treatment with P_2O_5 and distillation with a 1 1/2 ft. Vigreux column (packed with Heli-pak) at atmospheric pressure and 31 C. The MF was stirred with P_2O_5, allowed to settle overnight, and decanted before distillation. To prevent "gelling", the P_2O_5 treatment should not exceed 25 grams per liter of solvent and stirring should be limited to 1/2 hour. Before the above procedure was established, methyl formate had been unsuccessfully treated with molecular sieves, Multrathane M and a lithium dispersion; such batches (MF #2-7, #2-8, #2-9, and #2-10) were discarded.

Acetonitrile. One-liter batches of AN were distilled with a 1 1/2 ft. Vigreux column (packed with Heli-pak) at atmospheric pressure and 80 C. Prior to distillation, the AN was stirred with about 15 grams of P_2O_5 for one hour, allowed to settle overnight, and decanted.

Dimethyl Sulfoxide. Reagent grade DMSO was treated with molecular sieves in a procedure similar to the standard treatment of DMF (Ref. 1). The material was then allowed to stand over CaH_2 for several days, followed by distillation from CaH_2 with a 1 ft. Vigreux column (packed with Heli-pak) at about 10 mm Hg and 75 C. Dry nitrogen was used to bring the system to atmospheric pressure when cutting fractions.

Nitromethane. Due to the potential hazard and low organic impurity content (13 ppm, determined by VPC), spectro grade NM was not distilled. A large molecular sieve column (packed with Linde 4A, 1/16 inch activated pellets) was assembled for water removal. Batches of NM were treated with the column for 24 hours. The column was designed with a nitrogen pressurization system, that enables fractions to be cut without being exposed to the atmosphere.

Tetrahydrofuran. Reagent grade THF, from J. T. Baker Chemical Company, contained 41 ppm H_2O and 23 ppm of an organic impurity (retention time 4.3 minutes) according to a gas chromatographic analysis with a Porapak Q column. An analysis with a SE-30 column indicated 210 ppm of butylated hydroxy-toluene (BHT), which is a stabilizing agent for THF. The material was considered satisfactory for use as received.

Purification Results

Analyses on each batch were performed, as described in the next section; the analysis results are given in Table 3 for each batch.

TABLE 3

CHARACTERIZATION OF SOLVENT BATCHES

Solvent Code	H_2O Content, ppm per weight	Organics, ppm per weight
PC #6-4	<5 (None observed)	None observed*
PC #6-5	<5	<10 (6 min. R.T.**)
PC #6-6	<5	16 (4.5 min. R.T.)
PC #6-7	<5	16 (4.5 min. R.T.)
PC #3-1	<5	None observed
PC #7-1	<5	None observed
PC #7-2	<5	None observed
PC #7-3	<5	10 (6 min. R.T.)
PC #7-4	<5	17 (6 min. R.T.)
PC #7-5	<5	15 (6 min. R.T.)
PC #7-6	<5	≤10 (6 min. R.T.)
PC #7-7	<5	≤10 (6 min. R.T.)
PC #7-8	<5	≤10 (6 min. R.T.)
PC #7-9	<5	None observed
PC #7-10	<5	None observed
DMF #7-3	52	None observed
DMF #7-4	47	None observed
MF #2	106	710 (MeOH)
MF #2-7	74	690 (MeOH)
MF #2-8	86	590 (MeOH)
MF #2-9	94	970 (MeOH)
MF #2-10	65	960 (MeOH)
MF #2-11	30	<20 (MeOH)
MF #2-12	45	<20 (MeOH)
MF #2-13	35	<20 MeOH + 69 (27 min. R.T.)
MF #2-14	32	<20 MeOH + 63 (27 min. R.T.)
MF #3-1	38	<20 MeOH + 28 (27 min. R.T.)
MF #3-2	28	<20 MeOH + 50 (36 min. R.T.)
MF #3-3	34	<20 MeOH + 29 (36 min. R.T.)
MF #3-4	20	<20 MeOH + 35 (36 min. R.T.)
MF #3-5	20	<20 MeOH + 30 (36 min. R.T.)

*The detection limit for most organic species eluted prior to the solvent (but within 20 minutes after sample injection) is about 5 ppm.

**R.T. = Retention Time

TABLE 3 (CONCLUDED)

Solvent Code	H_2O Content, ppm per weight	Organics ppm per weight
MF #3-6	41	<20 MeOH
MF #3-7	38	<20 MeOH + 38 (33 min. R.T.)
MF #3-8	36 (29 after 3 months)	<20 MeOH
MF #4	25	<20 MeOH + 15 (6.5 min. R.T.)
AN #6-1	34	None observed
AN #6-2	30	None observed
DMSO #1	730	None observed
DMSO #1-1	13	None observed
NM #1	270	Not analyzed
NM #1-1	26	5 impurities (see text)
NM #1-2	23	Not analyzed
THF #1	41	23 (4.3 min. R.T.); 210 (BHT)

ANALYSIS OF SOLVENTS

A special effort was made to use only well characterized solvents for experimentation. Each batch of solvent was therefore analyzed for trace impurities, with vapor phase chromatography (VPC) being the main analytical technique employed. Occasionally, other techniques such as Karl Fischer titration and nuclear magnetic resonance (NMR) were also applied.

The general approach to the VPC analysis is described in the Final Report of the previous NASA contract (Ref. 1). The analysis effort was extended for methyl formate, and the experimental conditions for the analysis of new solvents were established; this is described for each solvent in the following.

Propylene Carbonate, Dimethylformamide, Acetonitrile.

A routine analysis employing a Porapak Q column was performed, as described in Ref. 1. The experimental parameters and responses are presented in Table 4.

Methyl Formate.

The operating conditions for the routine analysis for water in MF are listed in Table 4.

To analyze for methanol in methyl formate, a Beckman GC2A gas chromatograph equipped with a thermo-conductivity detector was first used. This detector has only a sufficient sensitivity to determine relatively high methanol contents; hence, a flame ionization detector in conjunction with a Bendix gas chromatograph Series 2100 was employed to enable analysis of samples with low methanol contents. The operating conditions for this analysis are given in Table 5; the conditions were changed for the sampling of MF #2-11 and later batches, because of the much lower methanol content of these batches which were treated with P_2O_5. A chromatogram for MF #2-11 is shown in Figure 1.

Under the conditions given in Table 5, the methanol is eluted as a fairly sharp, symmetrical peak and is eluted prior to methyl formate. A baseline shift appears to occur after the methanol peak which may be due to decomposition of methyl formate on the column. The baseline shift was small compared to the methanol peak height in the case of MF #2-8, MF #2-9, and MF #2-10; therefore, any error due to this shift for samples with a relatively high methanol content would be insignificant. The response of the detector was determined by adding 0.4 percent (by weight) methanol to MF #2-8 and measuring the increase in the area of the methanol peak. The methanol content, on a weight basis, was found to be 0.9 times the ratio of the methanol and methyl formate peak areas.

TABLE 4

EXPERIMENTAL PARAMETERS AND RESPONSE FOR THE ROUTINE DETERMINATION OF WATER IN PROPYLENE CARBONATE, DIMETHYLFORMAMIDE, ACETONITRILE, AND METHYL FORMATE

Conditions[a]	Solvent			
	PC	DMF	AN	MF
Sample Size, microliters	100	100	100	25
Column Dimension	3/16 inch by 6 feet	3/16 inch by 6 feet	3/16 inch by 6 feet	3/16 inch by 6 feet
Column Packing	Porapak Q	Porapak Q	Porapak Q	Porapak Q
Column Temperature, C	165	165	150	150
Injector Temperature, C	175	175	175	175
Carrier Gas	Hydrogen	Hydrogen	Hydrogen	Hydrogen
Flowrate, $cm^3/min.$	25	25	25	25
Detector	Cross section	Cross section	Cross section	Cross section
Detector Temperature, C	165	165	165	165
Response, micrograms H_2O/cm^2	6.0	6.4	7.1[b]	6.2[c]
Response, ppm H_2O/cm^2	50	67	92[b]	64[c]

a. Chromatograph: Aerograph 660, Wilkens Instrument & Research, Inc.
Recorder: Leeds & Northrup Speedomax G; 670 microvolts full scale, 1/2-in./min. chart speed

b. Value used with second Porapak Q column

c. Value based upon average of values for PC and DMF

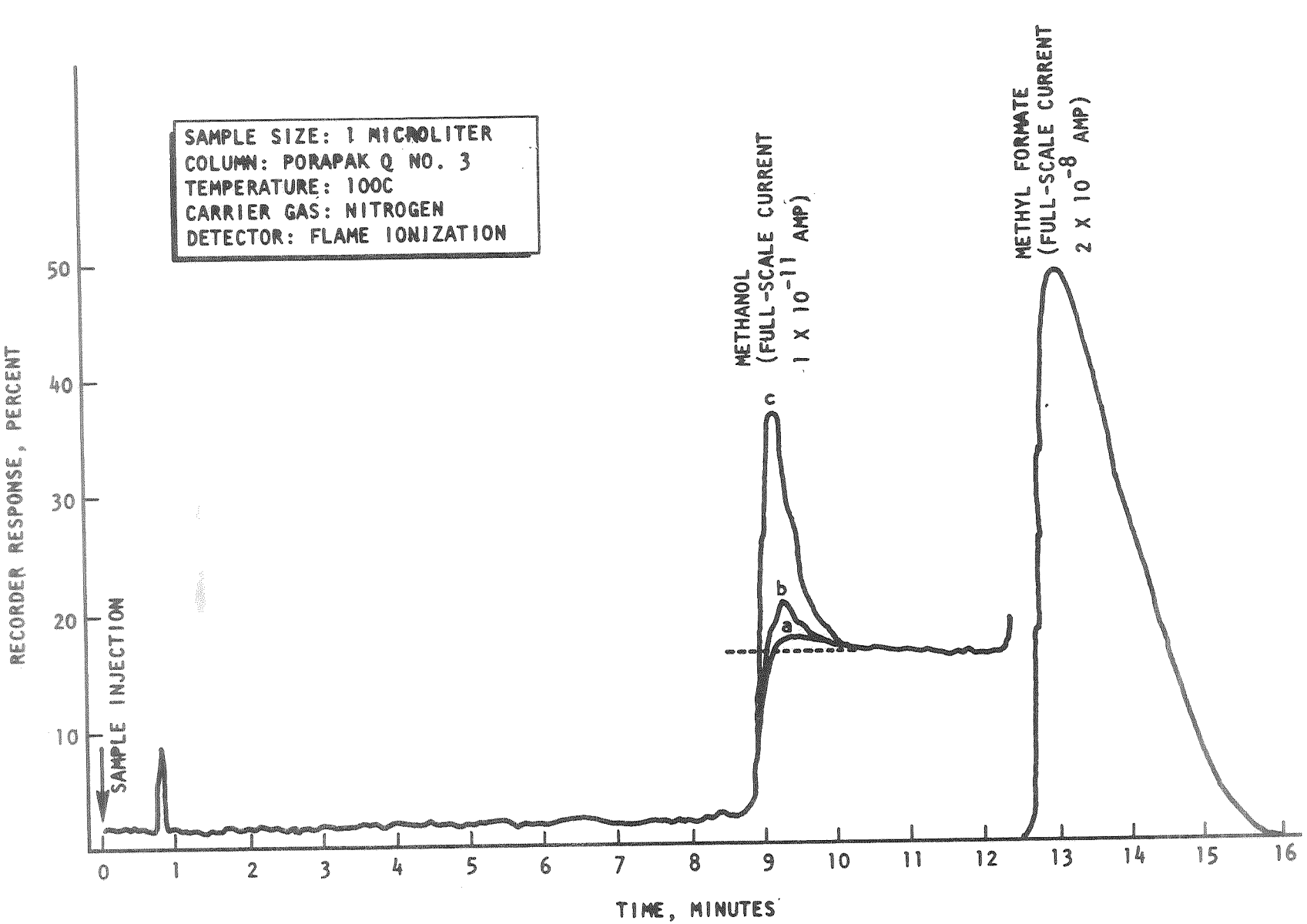

Fig. 1 Initial Portion of Chromatogram of Methyl Formate, MF #2-11, Containing Added Methanol (Curve a: 0 ppm; Curve b: 16 ppm; Curve c: 81 ppm)

TABLE 5

OPERATING CONDITIONS FOR ANALYSIS OF METHYL FORMATE

	MF #2-8, MF #2-9, & MF #2-10	MF #2-11 & MF #2-12
Sample size	0.5 µl	1 µl
Column dimension	3/16 inch x 6 feet	3/16 inch x 6 feet
Packing	Porapak Q	Porapak Q
Column temperature	130 C	100 C
Injector temperature	130 C	100 C
Carrier gas	Nitrogen	Nitrogen
Carrier gas flow rate	30 cc/min	30 cc/min
Flame ionization detector	30 cc/min H_2, 2 CFH air	30 cc/min H_2, 2 CFH air
Detector temperature	215 C	215 C

When the sensitivity of the detector was increased for the analysis of batches with lower methanol content, the baseline shift became significant. Such a baseline shift can be due either to decomposition of methyl formate on the column to produce methanol or to an irreversible methanol adsorption on the column. The latter hypothesis was shown to be invalid: A sample of 10 ppm methanol in isopropanol gave a fairly sharp, symmetrical methanol peak under these conditions. Furthermore, a decrease of the column temperature reduced the amount of baseline shift.

An undisputable interpretation of the type of chromatogram shown in Figure 1 would only be possible if a chromatogram of a solution known to contain no methanol would be available. However, it can be assumed, as a first approximation, that the baseline rises rapidly to its new position and is flat before and after the rise; any methanol originally present in the sample would then appear as the usual peak on a shifted baseline. The area of the peak can easily be measured after extrapolating the baseline under the peak. Figure 1 shows chromatograms of MF #2-11 containing 0, 16, and 81 ppm added methanol. The broken line is an extrapolation of the baseline after the methanol peak, and the ratios of the areas under the methanol peaks and the methyl formate peaks are 8.0×10^{-6}, 14×10^{-6}, and 74×10^{-6}, respectively. Based upon the relative response of methanol and methyl formate found previously, the ratios of the areas would be expected to be 8.0×10^{-6}, 26×10^{-6}, and 98×10^{-6}, respectively. Because the actual area ratios are less than those predicted, the method of measuring the area of the methanol peak is probably not entirely correct. Referring to Figure 1, it can be seen that the baseline shift occurs sooner at greater methanol concentration. This part of the baseline shift is probably due to methanol originally present in the sample which was not accounted for in the simple hypothesis. From the area increase for addition of 16 ppm methanol, the detector response is about 2.5 (weight) ppm per area ppm and the amount of methanol in MF #2-11 would be 20 ppm. The detector response value of 2.5 is an upper bound, the actual value probably being somewhat less, so that the methanol concentration is reported as ≤ 20 ppm.

The gas chromatography of formic acid was studied briefly. The retention time of formic acid under the conditions given in Table 4 for MF #2-11 appeared to vary from 34 to 56 minutes, depending upon the sample size. The peak had a very poor shape with extreme tailing. The use of a thermoconductivity detector for the determination of formic acid was considered but was never put into practice.

In actual analysis, other impurities were often found, with retention times on the order of 50 minutes. These impurity peaks, detected with a flame ionization detector, were symmetrical and did not exhibit tailing. This appears to preclude the impurity peaks being due to formic acid, but they were not identified further, and only the ratio of the responses of the impurity and methyl formate on the flame ionization detector are reported in addition to the retention time. The actual impurity concentration, incidentally, was most likely less than the response ratios might have indicated, because the response of methyl

formate is less than the response of most organic compounds in the flame ionization detector. Batch MF #2-12 and batches of earlier data had not shown any of these impurities, but their presence in these cases cannot be precluded, because replicate injections had been made before the impurity was eluted and the impurity peak may have been obscured by the methyl formate peak.

When a methyl formate sample, MF #2-7, was analyzed by Karl Fischer titration, an apparent end point was reached upon the first addition of titrant, which would correspond to a water content of less than 20 ppm. The same occurred, however, when a sample containing 100 ppm of added water was titrated. Methyl formate, therefore, appears to present similar problems as had been encountered with DMF (Ref. 1), and a direct titration does not seem reliable.

A back titration method was investigated, but neat methyl formate again reacted anomalously. Reproducible values were obtained with $LiAsF_6$/MF solutions, but they were not reliable because they depended on experimental parameters such as amount of titrant matrix, and because inconsistent values were obtained upon addition of known amounts of water.

The use of NMR techniques had been explored on a previous contract (Ref. 1). A hydrolysis of MF had been observed to occur, catalyzed by the presence of $LiAsF_6$. These results were confirmed, as reported in later sections of this report.

Tetrahydrofuran

A chromatogram of reagent grade tetrahydrofuran, THF #1, as supplied, is shown in Figure 2. It was obtained on a Porapak Q column using the same conditions employed for the PC and DMF analysis (Table 1). The detector response for water in THF was determined by adding a measured volume of water to a known volume of the solvent. The addition of 1/2 µl of water to 10 ml of THF increased the water peak area by 1.64 cm^2. This value corresponds to a response of 6.1 µg H_2O/cm^2 or 69 ppm/cm^2.

In addition, THF #1 was also analyzed by VPC under the conditions given in Table 6, and three impurities were found. The largest impurity was identified as 210 ppm of 2,6-di-t-butyl-p-cresol (butylated hydroxytoluene, BHT) by observing the peak enhancement as a known amount of BHT was added to THF. BHT is employed as an anti-oxidant to stabilize the THF and according to the manufacturer the concentration should be 250 ppm. Two other peaks were found on the chromatogram of THF #1; the ratios of their areas to that of the parent peak are 14×10^{-6} and 6×10^{-6}, and the concentrations are certainly less than 50 ppm.

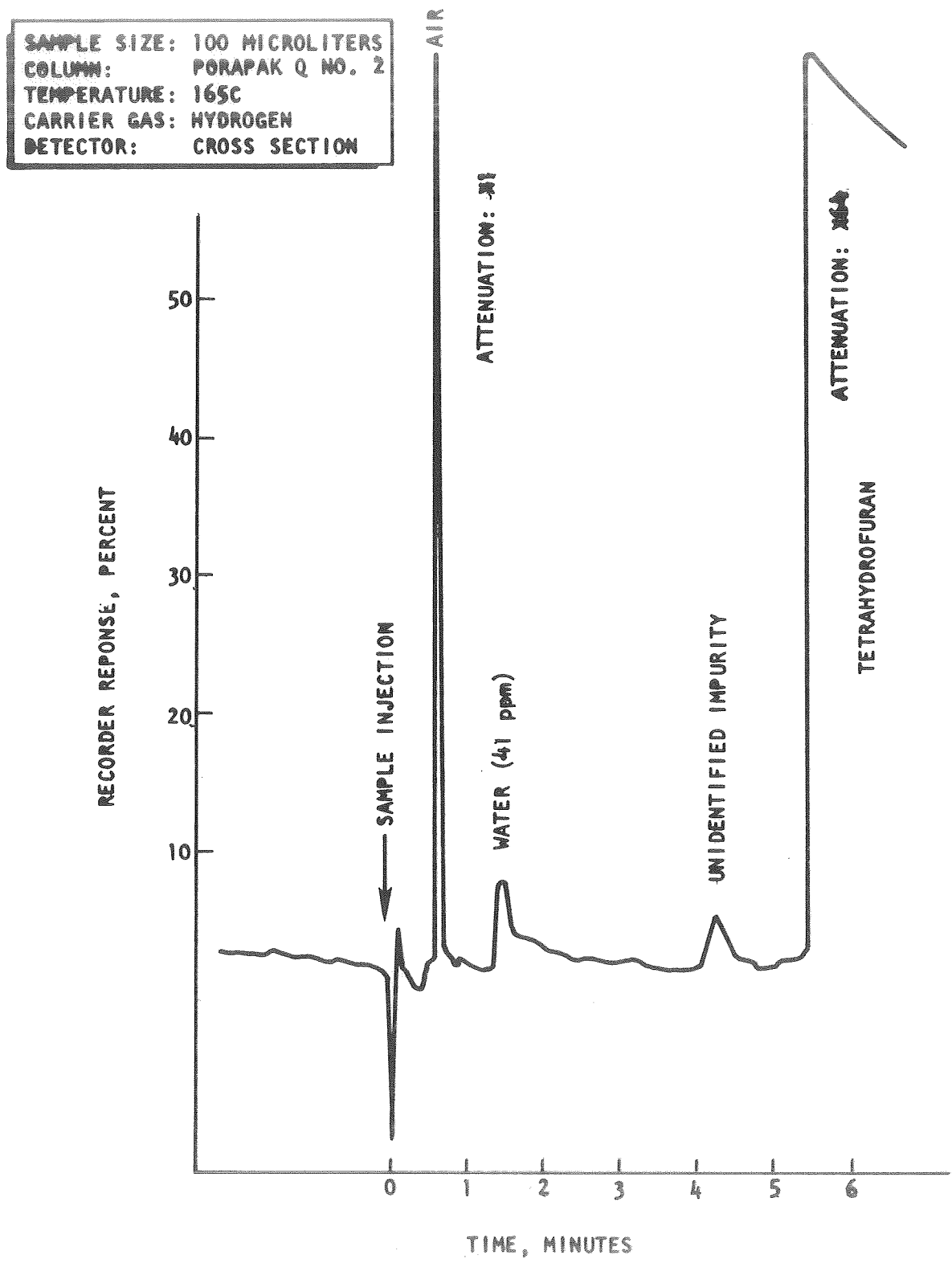

Fig. 2 Initial Portion of Chromatogram of Tetrahydrofuran, THF #1, on Porapak Q Column

TABLE 6

CONDITIONS OF ANALYSIS OF NM #1 AND THF #1 FOR ORGANIC IMPURITIES

Sample size:	1 μl
Column dimension:	5 ft x 1/4 inch
Column packing:	SE-30
Column temperature:	165 C
Injector temperature	165 C
Carrier gas:	N_2
Flowrate:	25 cc/min
Detector:	Flame ionization; 30 cc/min H_2, 2 cfh air
Detector temperature:	165 C

Nitromethane

Spectro grade nitromethane from Eastman Organic Chemicals, NM #1, was analyzed as supplied on the Porapak Q using the standard conditions as employed for the PC and DMF analyses (Table 1), i.e., the column was at 165 C, and the injector at 175 C. The chromatogram was similar to that shown for THF in Figure 2; however, the water peak did not return to the baseline but remained 10 percent above it until the elution of the NM. This behavior would be expected if the hydrogen carrier gas slowly reduced the NM as it was eluted through the column. If the water peak were extrapolated to the baseline in the usual fashion, it would correspond to a water content of 200 to 300 ppm. Because an accurate extrapolation of the water peak was not possible, NM #1 was also analyzed by the Karl Fischer procedure, and the water content was found to be 270 ppm.

Two additional peaks were also found on the Porapak Q column which were eluted after NM. These peaks were about 1 percent the size of the NM peak. However, NM #1 was analyzed on a second solumn (SE-30) using the conditions given in Table 6, and the only impurity peak found corresponded to a concentration of 13 ppm or less. The water content could not be determined in this analysis because a flame ionization detector was employed.

The fact that no large impurity peaks were found on the second column would be consistent with the hypothesis advanced above. According to this hypothesis, NM would be reduced by the hydrogen carrier gas during the analysis on the Porapak Q column to yield water as well as two additional products. Because hydrogen continuously reduced NM, forming water, the water peak would not return to the baseline and water would be continually eluted until NM was eluted from the column.

When NM #1-1 (containing less H_2O than NM #1) was analyzed by gas chromatography employing the conditions given in Table 7, i.e., using nitrogen as the carrier gas, the chromatogram contained six symmetrical well separated peaks. The retention time and area percentage of each peak is given in Table 8. Two main impurities appear to be present at the level of 1 percent or higher (the most probable impurities, higher nitroparaffins, would give a greater response than nitromethane on a weight basis and their concentrations would be less than the area percentage given in Table 8. High resolution NMR spectra taken on NM #1-1 confirmed the presence of two impurities at concentrations consistent with the gas chromatography results. Based on the NMR chemical shifts, the gas chromatographic retention times, and the information supplied by the manufacturer of nitromethane, Commercial Solvents Corporation, it must be assumed that the principal impurities are nitroparaffins such as nitroethane, 1-nitropropane and 2-nitropropane.

Dimethyl Sulfoxide

Two samples of dimethyl sulfoxide were analyzed for water content on a Porapak Q column under the conditions normally used for PC and DMF (Table 2). A water response of 6.2 $\mu g/cm^2$ was used to calculate the water content; this value is an average of the values found previously for PC, DMF, and THF under the same conditions of analysis.

TABLE 7

CONDITIONS USED FOR ANALYSIS OF NITROMETHANE, NM #1-1

Column:	2.5-ft x 3/16-in Porapak Q (120-150 mesh)
Column Temperature:	125 C
Carrier Gas:	100 cc/min N_2
Detector:	Flame ionization; 40 cc/min H_2, 2 cfh air

TABLE 8

PEAKS FOUND ON CHROMATOGRAM OF NM #1-1

Species	Retention time, min.	Area Percentage
Impurity I	3.2	0.01
Nitromethane	4.7	91.7
Impurity II	8.2	0.81
Impurity III	13.6	4.3
Impurity IV	26.4	3.1
Impurity V	40.8	0.1

PURIFICATION AND ANALYSIS OF SOLUTES

Sources and Purification of Solutes

Sources and purities of procured materials to be used as solutes or solid additives are given in Table 9.

Most solutes were used as received, except for $LiClO_4$, LiCl and LiBr which were dried at elevated temperature (about 120 C) under vacuum.

$LiAsF_6$ #1 and $LiAsF_6$ #6 were made by metathesis of $KAsF_6$ and $LiBF_4$ at the Livingston Electronic Laboratory and were supplied in $LiAsF_6$/MF solutions. These solutions were diluted with MF; the solvent code for such $LiAsF_6$/MF solutions designates the MF used for the dilution.

Analysis of Solutes

The analysis of some solutes had been performed and reported on a previous contract (Ref. 1).

Samples of solid (powder) $AlCl_3$ #3 and #4 were run on the broadline NMR spectrometer at both the proton and ^{27}Al frequencies. $AlCl_3$ #3 showed qualitative evidence of protons while $AlCl_3$ #4 did not. The protons in $AlCl_3$ #3 could be due to solvent picked up while the material was stored and used in the dry box. $AlCl_3$ #3 also showed evidence of a paramagnetic impurity by virtue of a shorter relaxation time of the ^{27}Al resonance (evidenced by a lesser tendency to saturate) than for the $AlCl_3$ #4. This is consistent with the analyses of these materials (Ref. 1) which indicated a higher Fe content for $AlCl_3$ #3. $AlCl_3$ #4 was therefore used preferentially.

The results of the analysis of $AlCl_3$ #5 by emission spectrography and spark source mass spectrography are given in Table 10. The emission spectrographic analysis, performed by Pacific Spectrochemical Laboratory, Inc., Los Angeles, showed high contents of heavy metals in a first run, but these impurities were absent according to a second analysis, as well as according to the results of the spark source mass spectrographic analysis, which was done by the Bell & Howell Research Laboratories, Pasadena. For $AlCl_3$ #5, an oxygen content of 410 ppm was found by SSMS, which is lower than the figures obtained for $AlCl_3$ #3 (1300 ppm) and $AlCl_3$ #4 (100-7700 ppm) as reported in Ref. 1. The new product

TABLE 9

SOURCES AND QUALITIES OF PROCURED SOLUTES

Chemical	Source	Lot	Quality	Analysis
$LiClO_4$ #3	Atomergic Chemetals Co.	B7523	99.9%	Ref. 1
LiCl #3	Atomergic Chemetals Co.	B7948	99.9+%(optical)	Ref. 1
$AlCl_3$ #4	Rocky Mountain Research, Inc.	LP03088	99.999%	Ref. 1
$AlCl_3$ #5	Rocky Mountain Research, Inc.	LP08289	99.999%	Table 10
$LiAsF_6$ #1	Livingston Electronic Laboratory		2.2 M $LiAsF_6$/MF	Ref. 1
$LiAsF_6$ #2	Midwest Research Institute	1-45-D	Special	Ref. 2
$LiAsF_6$ #3	Midwest Research Institute		Special	Ref. 2
$LiAsF_6$ #4	Midwest Research Institute	I-66-A	Special	Ref. 2
$LiAsF_6$ #5	Midwest Research Institute	I-96-A	Special	Ref. 2
$LiAsF_6$ #6	Livingston Electronic Laboratory	NASA-16	3 M $LiAsF_6$/MF	
$LiAsF_6$ #7	Midwest Research Institute	I-96-A (second shipment)	Special	Ref. 2
LiBr #2	Gallard-Schlesinger Chemical Mfg. Corp.	B5111	99.99% (optical)	See text
Salicylaldoxime #1	J. T. Baker Chemical Co.	1-4166		Tables 11 & 12
Salicylaldoxime #2	British Drug House Ltd.	0370290	Analytical Reagent	Tables 11 & 12
Phenanthroline #1	J. T. Baker Chemical Co.	1-4032	Analyzed Reagent	Tables 11 & 12
Phenanthroline #2	British Drug House Ltd.		Analytical Reagent	Tables 11 & 12
CuF_2 #4	Battelle-Northwest	5	Special, 99.99%	Ref. 3
$CuCl_2$ #2	Fisher Scientific Co.	752944	Certified Reagent	Ref. 1

TABLE 10

IMPURITY CONCENTRATIONS IN $AlCl_3$ #5,

EMISSION SPECTROGRAPHIC AND SPARK SOURCE MASS SPECTROGRAPHIC ANALYSES

Impurity	Content, ppm per weight		
	Em. Spec. 1st analysis	Em. Spec. 2nd analysis	SSMS
H			13
Li			0.14
C			28
N			1.3
O			410
F			5.1
Na			21
Mg	16	14	51
Si		trace (< 20)	51
P			60
S			35
K			13
Ca	7.7	11	13
V			20
Cr			10
Fe			6.9
Co			11
Cu	1.4	0.51	100
Zn			< 10 (not detected)
Ge			< 10 (not detected)
Br			65
Sn	300		
Pb	2600		
Bi	81		

was not exposed to the laboratory air during sample preparation, a significant improvement over the procedure used previously. The oxygen content of $AlCl_3$ #5 appears to be acceptable. No other impurity at significant levels was found; the relatively high copper content indicated by mass spectrometry was not confirmed by emission spectrography.

The $LiAsF_6$ products supplied by Midwest Research Institute, $LiAsF_6$ #2 through $LiAsF_6$ #5 and $LiAsF_6$ #7, were synthesized and extensively characterized under contract NAS3-12979 (Ref. 2). They were high purity products with no impurities present in significant amounts. $LiAsF_6$ #1 and $LiAsF_6$ #6 were products supplied by Livingston Electronic Laboratory in methyl formate solutions. The 2.2 M $LiAsF_6$ #1/MF stock solution had been analyzed by atomic absorption; a potassium content of 0.035 molar and a boron content of 0.010 molar had been found (Ref. 1).

LiBr #2 was analyzed by emission spectrography. The only impurities indicated were 0.8 ppm Mg, 5.4 ppm Ca and a trace (less than 0.5 ppm) Cu.

The salicylaldoximes and phenanthrolines were analyzed by emission spectrography, and by microanalytical techniques for C, H, and N. The results are given in Table 11 and Table 12, respectively. The phenanthrolines were obviously hydrates; the theoretical values of the elemental C, H, O and N contents for the monohydrate are given in parenthesis. Salicylaldoxime #1 and phenanthroline #2 appeared to be somewhat superior products and were used for studies.

CuF_2 #4 was synthesized under contract NAS3-10942 by Battelle-Northwest. It is a high purity product with a low oxygen content (10 ppm); analysis results obtained with this product are given in Ref. 3.

PREPARATION AND HANDLING OF SOLUTIONS

Solution Code

The solutions generally contained a main electrolyte solute, a main solvent, and an additive component which could be either a solid or a liquid. In the solution code, the components are named in the above order, as illustrated by the following example:

0.5 M LiCl #3 + 1 M $AlCl_3$ #4/PC #3-1 & 0.75 M DMF #7-2

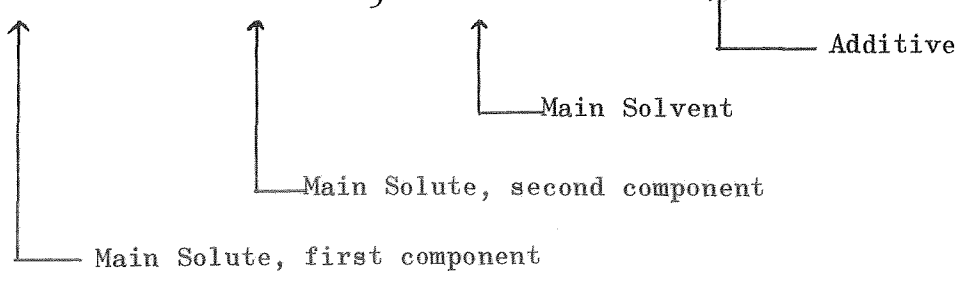

TABLE 11

IMPURITY CONCENTRATIONS IN SALICYLALDOXIMES AND PHENANTHROLINES ACCORDING TO EMISSION SPECTROGRAPHIC ANALYSIS

Impurity	Content, ppm per weight			
	Salicylaldoxime #1	Salicylaldoxime #2	Phenanthroline #1	Phenanthroline #2
B	7.4	4.4		2.0
Na	110	trace (< 200)	650	340
Mg	1.7	7.0	8.5	5.1
Al	7.0	43	76	80
Si	15	270	65	79
Ca	4.0		25	12
Ti		trace (< 1.0)		
Fe	4.1	87	20	15
Ni		trace (< 1.0)		
Cu	0.52	2.9	5.3	2.4
Ag				0.92
Sn		120	14	
Loss on ignition (sulfate ash)	99.9518%	99.3750%	99.72%	99.82%

TABLE 12

ELEMENTAL ANALYSIS RESULTS FOR

SALICYLALDOXIMES AND PHENANTHROLINES

Component	Salicylaldoxime #1	Salicylaldoxime #2	Phenanthroline #1	Phenanthroline #2
C (determined)	61.36%	61.03%	72.08%	72.86%
C (theoretical)	61.308%	61.308%	79.980% (72.712%	79.980% (72.712%)
H (determined)	5.22%	5.33%	5.03%	5.09%
H (theoretical)	5.145%	5.145%	4.475% (5.085%)	4.75% (5.085%)
N (determined)	10.57%	10.23%	14.25%	14.16%
N (theoretical)	10.214%	10.214%	15.545% (14.132%)	15.545% (14.132%)
O (balance)	22.85%	23.41%	8.64%	7.89%
O (theoretical)	23.333%	23.333%	0% (8.071%)	0% (8.071%)

Numbers for Phenanthroline given in parenthesis relate to the monohydrate

All concentrations indicated are given for the final solution, i.e., the additive was not simply added to an original solution of the composition as noted in the code.

Preparation of Solutions

Solutions were prepared in an inert atmosphere chamber (dry box) under a nitrogen atmosphere, as described in Ref. 1.

Dissolution of aluminum chloride in various solvents was performed at low temperatures, employing liquid nitrogen as the coolant, as described in Ref. 1. A similar technique was adopted in other cases of exothermic dissolution, e.g., when $LiClO_4$ or $LiAsF_6$ were dissolved in MF and boiling of the solvent would have presented problems in the absence of precautionary cooling. Boiling off of MF had also to be prevented when adding DMSO to $LiCl+AlCl_3$/MF solutions.

In some cases, a precipitate resulted when the electrolyte-additive system was prepared. The clear supernatant liquid was then normally used for experimentation. This approach was taken, e.g., with the system 1 M $AlCl_3$ #4 + 1 M LiCl #3/MF #2-12 & 1 M DMSO #1-1; the supernatant liquid was found to contain 1.00 M of aluminum, but only 0.43 M of lithium. In an attempt to prepare a 1 M $AlCl_3$ #4 + 1 M LiCl #3/MF #3-3 & 1 M $LiAsF_6$ #3, a supernatant liquid containing 1.873 M of lithium and 0.86 M of aluminum was obtained; additional precipitation appeared to occur later.

A precipitate formed also when water was added by means of a syringe to 1 M $AlCl_3$ + 0.5 M LiCl/PC. The white precipitate with an amorphous appearance formed immediately, and the solution remaining after a day of stirring was used to prepare NMR samples and for other studies. Some of the precipitate subsequently seemed to redissolve very slowly.

When the preparation of a 0.5 M $LiAsF_6$/MF and 0.5 M $AlCl_3$ solution was attempted, a light yellow gel which was stable for several weeks resulted. No measurements were performed in this system.

Handling of Solutions

The solutions were always handled in a manner so that contamination by exposure to the air was eliminated, or at least minimized. Conductivity cells, for instance, were filled in the inert atmosphere chamber and sealed by a stopper. Because these tests were subject to much longer exposure to the laboratory atmosphere, solubility flasks for solubility tests were, in addition to glass stopper seals, capped with polyethylene bags containing inert gas.

A special procedure was developed to prepare sealed NMR tubes. The tubes were filled in the dry box and capped with a long piece of rubber tubing which was closed at the end. The sample content was then frozen

in liquid nitrogen*, the end of the rubber tubing opened to the atmosphere, and the sample quickly sealed. For broad-line NMR samples, screw-cap culture tubes with Teflon liners were often used without torch sealing.

Handling of Glassware

The glassware used for purifying solvents and preparing and storing was treated according to the procedure described in Ref. 1. This procedure involved cleaning in hot nitric acid-water (1:1) and final heating to 250 C.

* Late in the program, some samples were not frozen but merely cooled in granulated dry ice.

SPECIES (NMR) STUDIES

INTRODUCTION

A very large number of electrolytes were investigated using NMR techniques to determine species in solution and the manner in which species and species distributions changed when other solutes and/or solvents were added to the electrolyte.

Most of the NMR techniques employed in this investigation are standard techniques which have been described in numerous text books on the subject (see Ref. 4, 5 and 6). Both high resolution and broadline spectra were recorded. Some techniques were used which have received less attention in text books but have been described in the literature; the latter are referenced as discussed.

Two instruments were employed. High resolution spectra were obtained with a Varian DP-60 which was modified to operate with internal lock. As far as high resolution work is concerned, the instrument, as modified, is the equivalent of the Varian HA-60-IL. High resolution proton (^{1}H), fluorine (^{19}F) and aluminum (^{27}Al) spectra were obtained with this instrument, a different r.f. unit being used for the ^{27}Al spectra. The instrument is equipped with variable temperature apparatus which permits measurements over a range of temperatures. It should be noted that this instrument is not well suited for the ^{19}F resonance in the AsF_6^- ion even when T_1 is long (see later discussion) because of interference caused by internal modulation frequencies. Broadline spectra were obtained from a wide variety of nuclei (^{7}Li, ^{19}F, ^{27}Al, ^{35}Cl and ^{75}As) with an instrument comprised primarily of a Varian variable frequency r.f. unit with matched probes, a Princeton Applied Research coherent amplifier, Model HR-8, a 12-inch Magnion magnet and supplementary electronics.

Almost all of the electrolytes studied can be described as having some simple characteristic accompanied by some or several unexpected complexities. The general subject of species in electrolyte solutions is becoming more and more prevalent in the literature and most of the systems studied here would require a rather major effort (for each) to determine the complete picture of all species in solution, all equilibria which occur and are affected by additions, exchange rate of ions and solvent molecules between the several sites that they can occupy, the distribution of mixed species such as $Al[(S_1)_{6-x}\ (S_2)_x]^{+3}$

where S_1 and S_2 are competing solvent molecules, occupancy of solvent molecules and ions in sites outside the first coordination sphere of Al^{+3}, the still remaining question of the extent of solvation of Li^+, the singular characteristics of $LiAsF_6$ in solution, changes in short term and long term solubilities, catalytic effects of $LiAsF_6$ and many other questions.

The effort described here resulted in a great deal of information regarding species in solution for a large number of electrolytes; but it also uncovered as many, if not more, questions and complexities as it found answers to questions.

In general the organization of this section is determined by primary solvent, PC, MF and DMF, then by electrolyte (e.g., $LiAsF_6$/MF), then by additive. $LiAsF_6$ electrolytes are an exception to the general organization because of the different technique, unique to the AsF_6^- ion, which was used to monitor changes in these electrolytes.

In all spectra, high resolution and broadline, shown in this report the magnetic field increases from left to right.

PROPYLENE CARBONATE ELECTROLYTES

Three electrolytes employing propylene carbonate (PC) as the primary solvent were studied. These were $LiCl+AlCl_3$/PC, $LiClO_4$/PC and $LiAsF_6$/PC. A variety of salts and solvents were added to these electrolytes and the resultant changes in species studied.

$LiCl+AlCl_3$/PC

This system was studied previously (Ref. 1). The results indicate that addition of $AlCl_3$ to PC produced primarily the species $Al[PC]_6^{+3}$ and $AlCl_4^-$. Furthermore, the addition of LiCl results in a decrease in the population of $Al[PC]_6^{+3}$ and an increase in the population of $AlCl_4^-$. This was determined by observing both the high resolution proton spectra of the solvent PC and the broadline aluminum containing species. Examples of these spectra are shown in Figs. 3 through 5 (taken from Ref. 1). The reduction of the concentration of $Al[PC]_6^{+3}$ with the addition of LiCl is displayed both by the decrease in the intensity of the proton peak due to coordinated PC and by the decrease in intensity of the peak ^{27}Al due to $Al[PC]_6^{+3}$. The reduction of $Al[PC]_6^{+3}$ upon the addition of LiCl proceeds almost quantitatively so that in 1 M $AlCl_3$/PC which produces 1/4 M $Al[PC]_6^{+3}$ and 3/4 M $AlCl_4^-$ the addition of approximately 1 M LiCl depletes the system of $Al[PC]_6^{+3}$. This is shown in Fig. 6 (taken from Ref. 1) where the relative intensity of the ^{27}Al line from the coordinated species is plotted as a function of the concentration of LiCl in 1 M $AlCl_3$/PC.

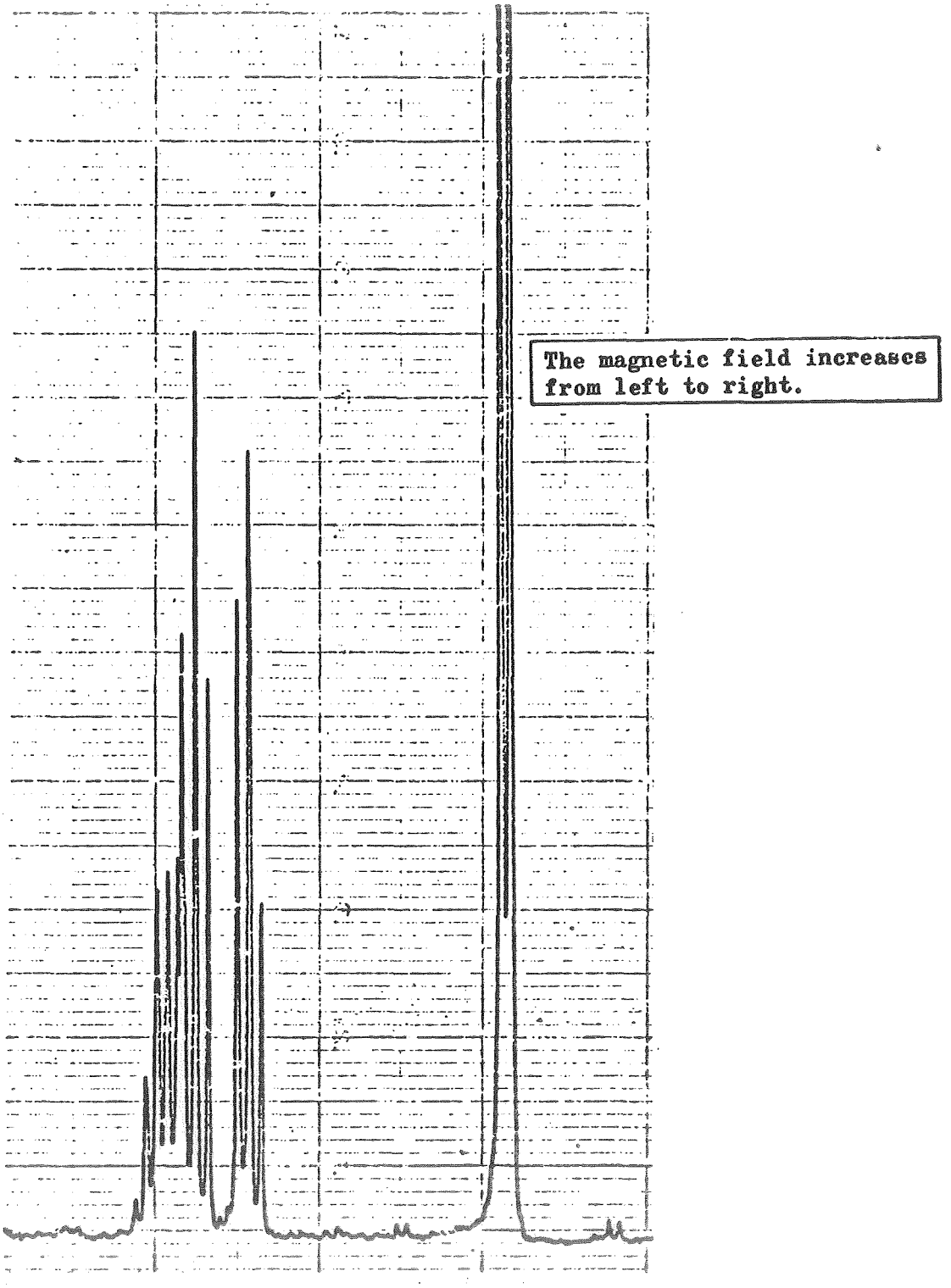

Figure 3 . High-Resolution ^{1}H Spectrum in Pure PC

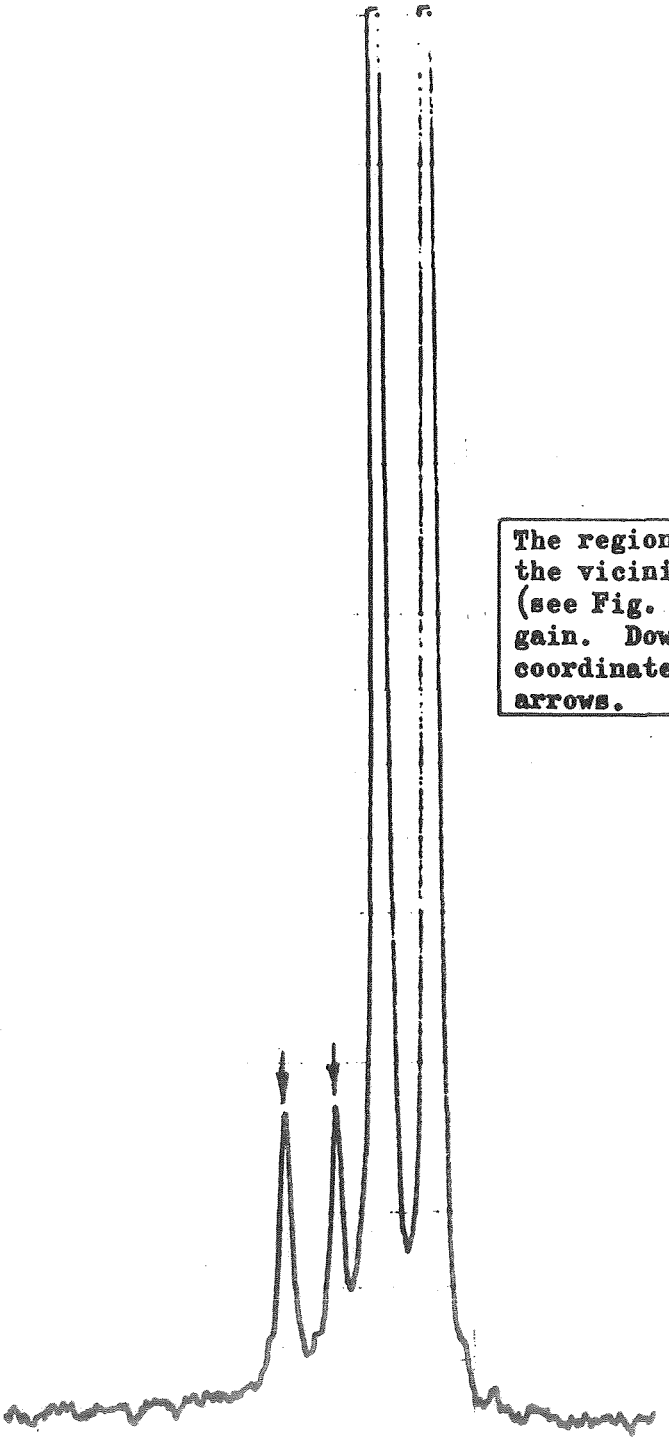

The region scanned is restricted to the vicinity of the high field doublet (see Fig. 3) and recorded at higher gain. Down field shifted peaks due to coordinated PC are denoted by vertical arrows.

Figure 4. High-Resolution ^{1}H Spectrum in 1.00 M $AlCl_3$/PC

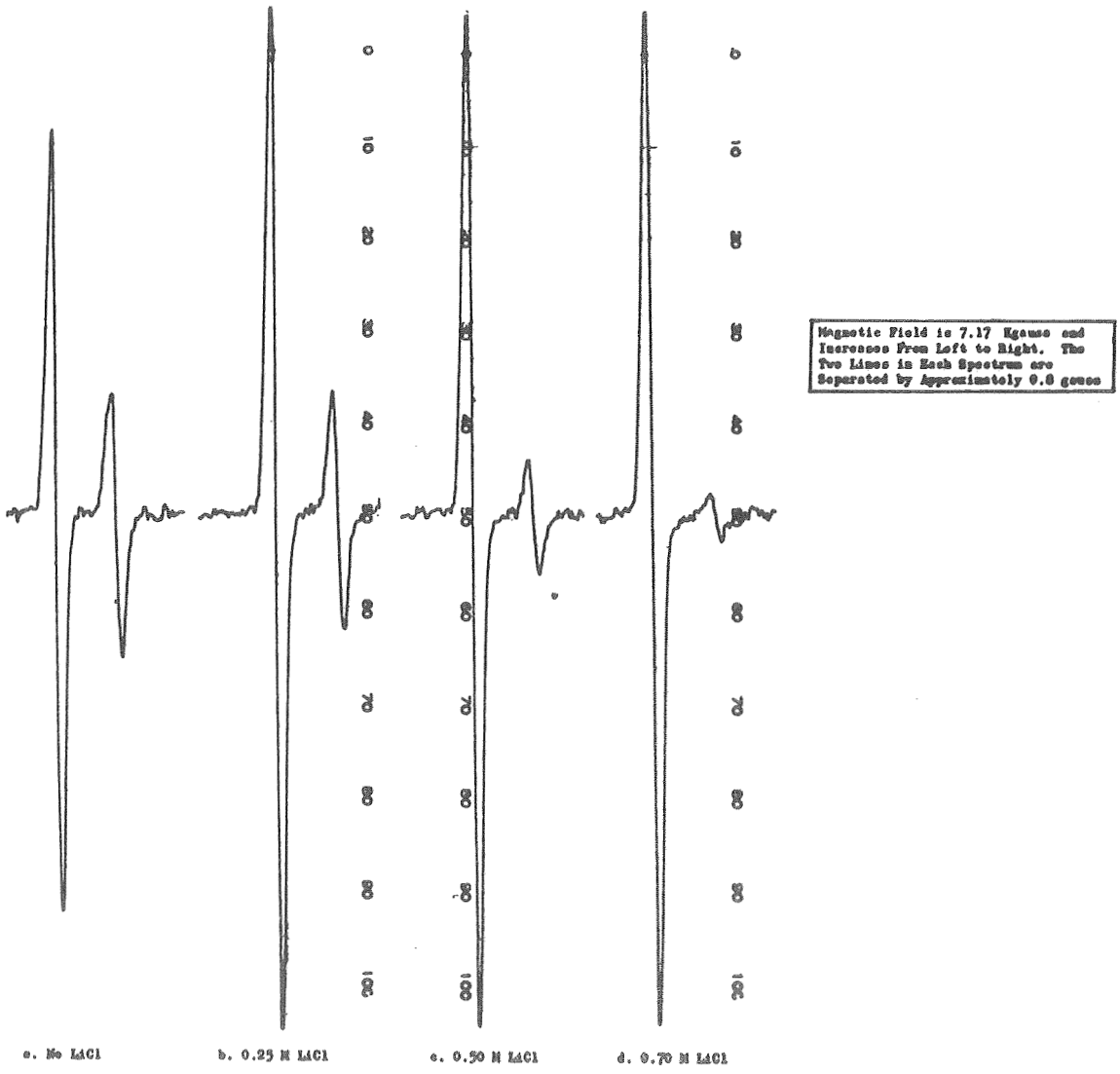

Figure 5. ^{27}Al Nuclear Magnetic Resonance in 1 M $AlCl_3$/PC Containing Various Concentrations of LiCl

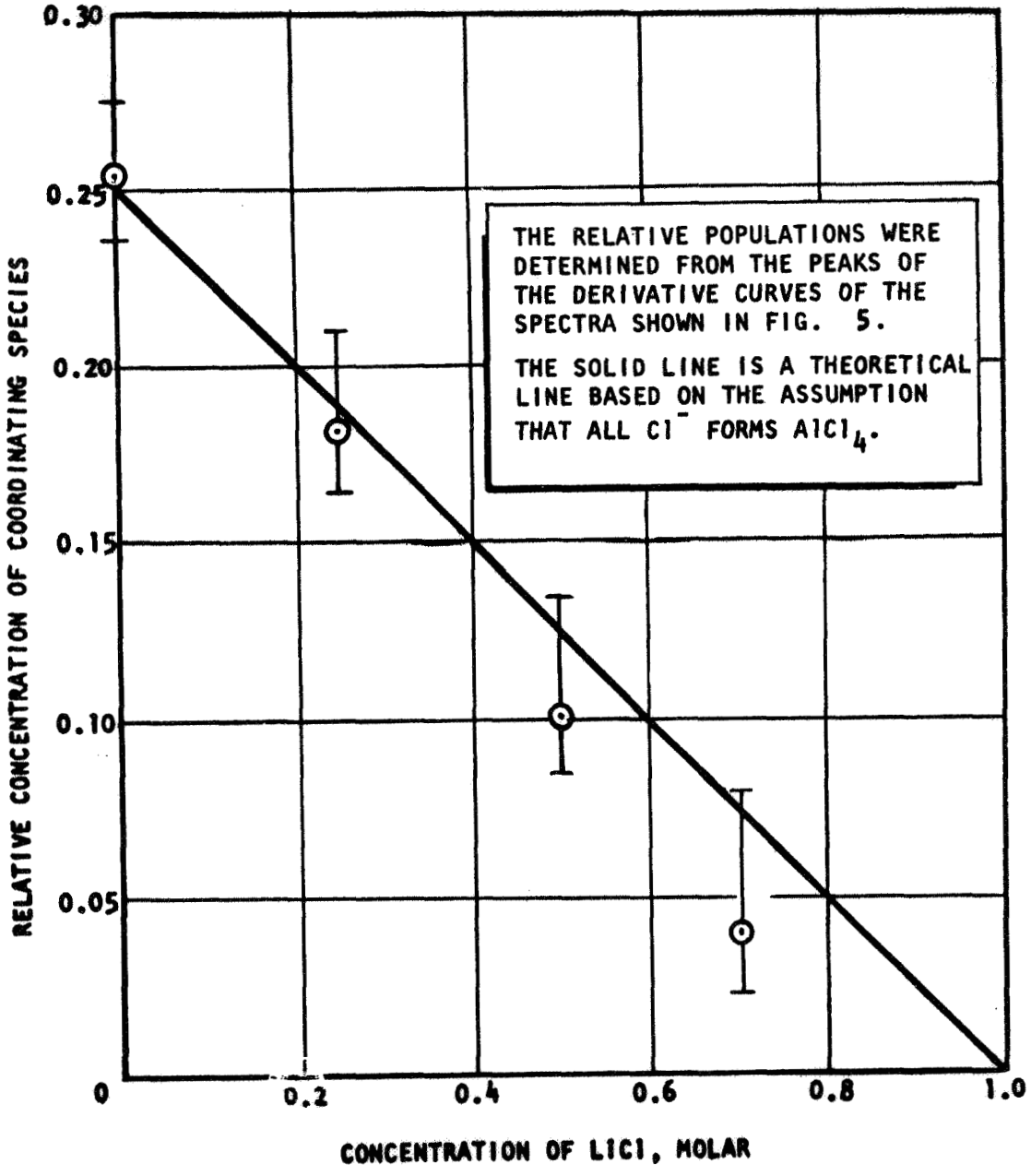

Figure 6 . Approximate Relative Populations of Coordinating Al Species in 1 M $AlCl_3$/PC as a Function of Added LiCl

DMSO As Additive. The species formed and the redistribution of the species caused by addition of DMSO to LiCl+$AlCl_3$/PC electrolytes were studied, utilizing both high resolution proton and broadline ^{27}Al NMR spectra. The information obtained on species using these two resonating nuclei complement one another in a fruitful manner. The results from the ^{27}Al NMR will be discussed first, then the high resolution proton results.

Broadline ^{27}Al NMR spectra for a series of 1 M $AlCl_3$/PC electrolytes containing various concentrations of LiCl and DMSO are shown in Figure 7. Figure 7a, which is for no LiCl and a low concentration of DMSO, shows the usual ^{27}Al spectrum. The narrow line on the left is ascribed to $AlCl_4^-$ and the broader, less intense line on the right is due to the complex $Al[PC]_6^{+3}$. As the concentration of DMSO is increased, the relative intensity of the $Al[PC]_6^{+3}$ line decreases as can be seen from Figures 7b, 7c, and 7d and from the plot in Figure 8. The line due to $Al[PC]_6^{+3}$ is not observable at DMSO concentrations above 0.5 M. At high DMSO concentration (>1 M) in electrolytes containing no LiCl another broadline having a smaller chemical shift relative to the ^{27}Al line in $AlCl_4^-$ appears. This line is more intense in the 1 M DMSO specimen containing 0.4 M LiCl than in the 1 M DMSO specimen containing no LiCl. Also, this line is observed in the 0.5 M DMSO specimen containing 0.8 M LiCl, whereas in the 0.5 M DMSO specimen containing no LiCl, the line due to the complex $Al[PC]_6^{+3}$ is observed. The line appearing at high concentrations of DMSO is attributed to the new complex $Al[DMSO]_6^{+3}$, and the results are interpreted as follows. The DMSO preferentially displaces PC molecules from the Al^{+3} coordination sphere. It is assumed that mixed species of the type $Al[PC]_{6-m}[DMSO]_m^{+3}$ have suffiently enhanced quadrupolar relaxation to broaden the ^{27}Al resonance beyond detection under the operating conditions used to record the $AlCl_4^-$ line. Thus, only $AlCl_4^-$ and the symmetrically solvated $Al[PC]_6^{+3}$ or $Al[DMSO]_6^{+3}$ species are observed. Addition of DMSO converts the PC complex through the series of mixed complexes to the pure DMSO complex. As DMSO is added, a decrease in the intensity of the $Al[PC]_6^{+3}$ line is observed at low concentrations, while at high DMSO concentrations an increase in the intensity of the $Al[DMSO]_6^{+3}$ line is observed. The addition of LiCl converts some of the PC complex to $AlCl_4^-$. The amount of $Al[PC]_6^{+3}$ in the system is thereby reduced, and a smaller amount of DMSO is required to produce the same fraction of $Al[DMSO]_6^{+3}$. Figure 7 shows the data obtained in the screening runs for this system. It is interesting to note that at 1.5 M DMSO the concentration of the DMSO complex is only about 80% of that predicted by the above arguments since 1.5 M DMSO could quantitatively transform all of the PC complex to the DMSO complex. This indicates that there is DMSO that is not tied up in the $Al[DMSO]_6^{+3}$ species.

High resolution proton NMR spectra of 1 M $AlCl_3$/PC solutions containing various concentrations of LiCl and DMSO are shown in Figures 9 through 44. These figures have been organized in the order of increasing DMSO concentration and increasing LiCl concentration to facilitate inter-

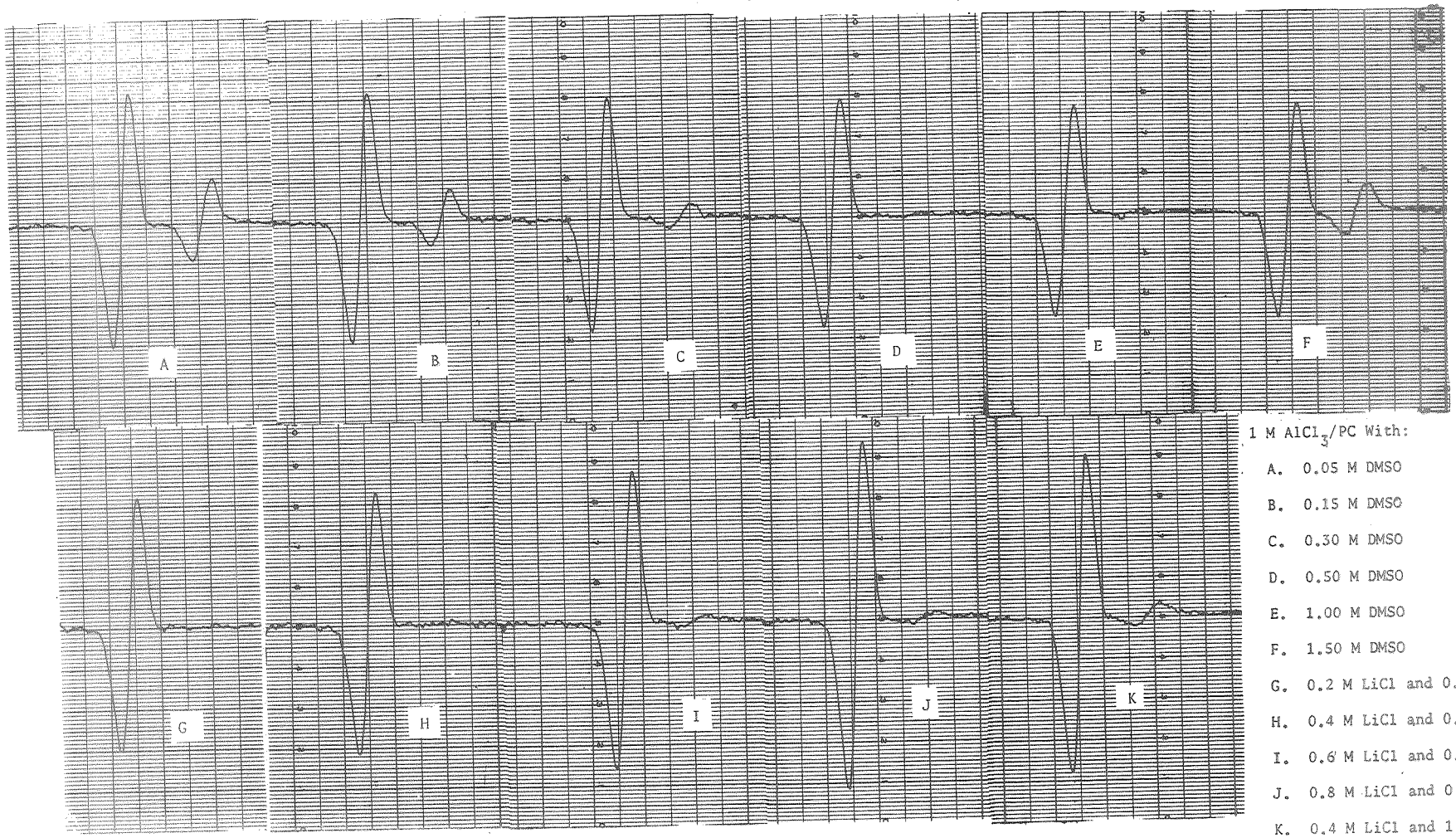

Fig. 7. Broadline ^{27}Al NMR in 1 M $AlCl_3$/PC Containing Various Concentrations of DMSO and LiCl as Noted.

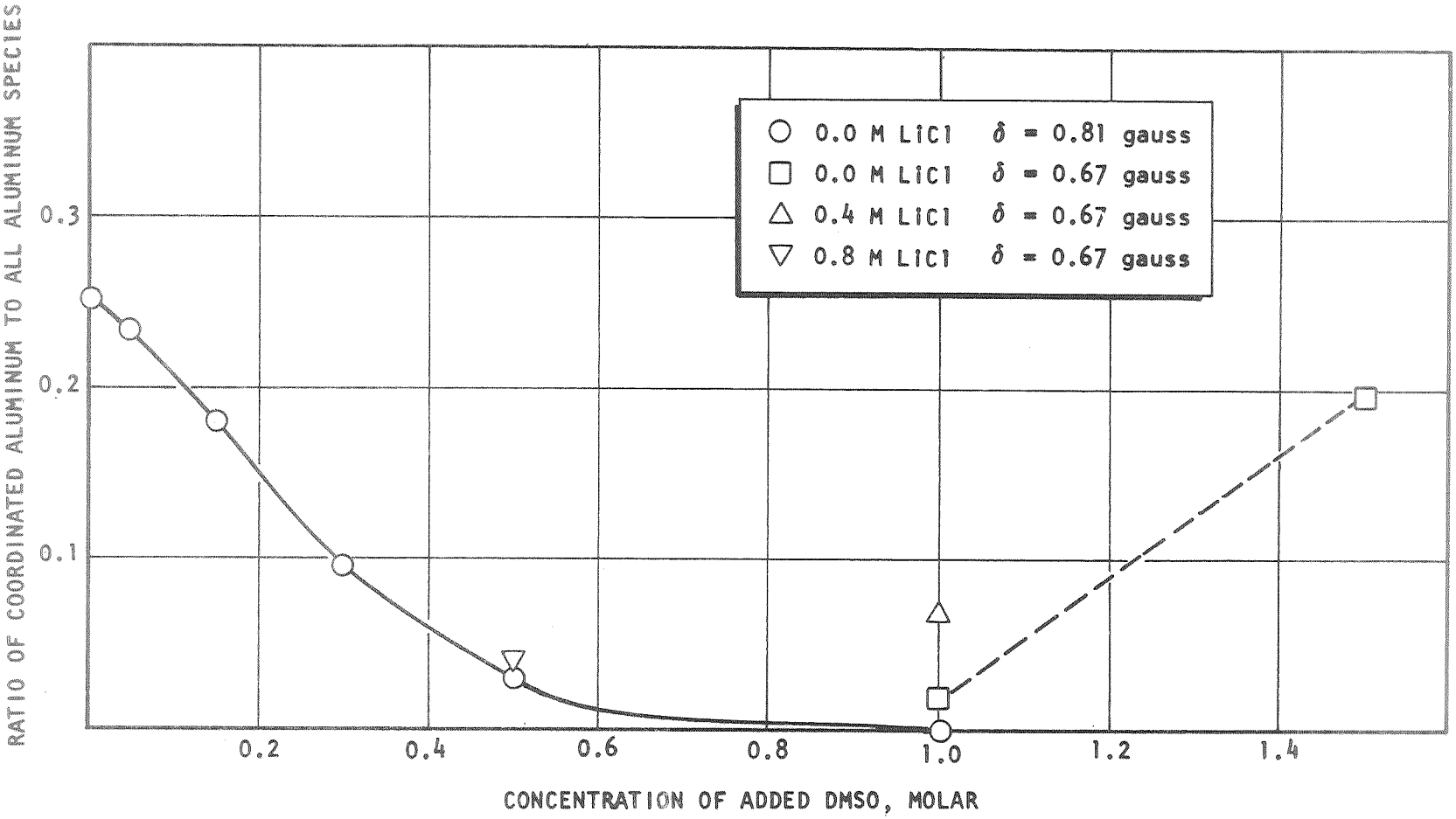

Fig. 8. Ratio, R, of Coordinated Al^{+3} to Coordinated Al^{+3} Plus $AlCl_4^-$ in 1 M $AlCl_3$/PC With Added DMSO and LiCl.

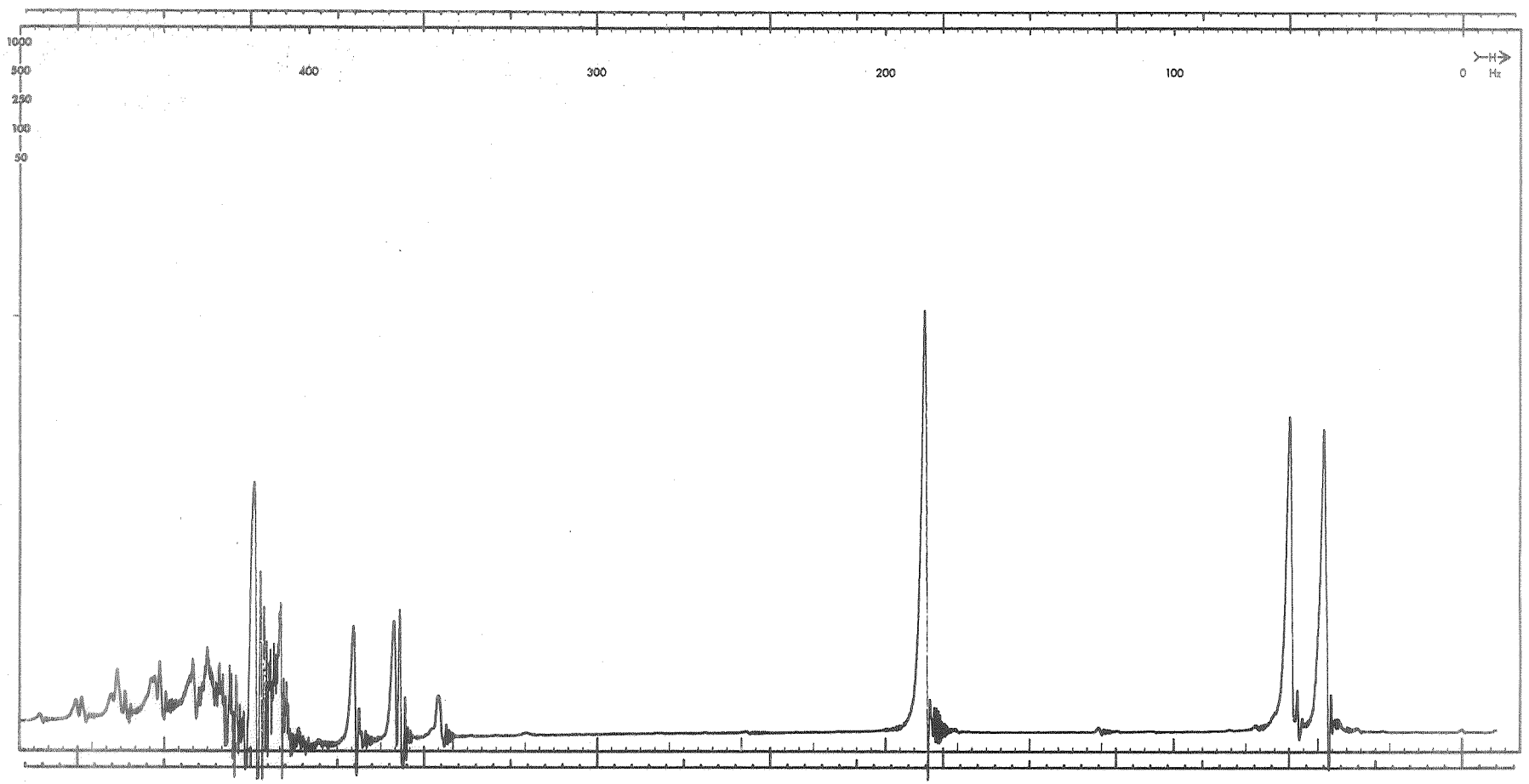

Fig. 9. ^{1}H NMR Spectra In 20 V/o DMSO #1-1 Added To PC #6-6

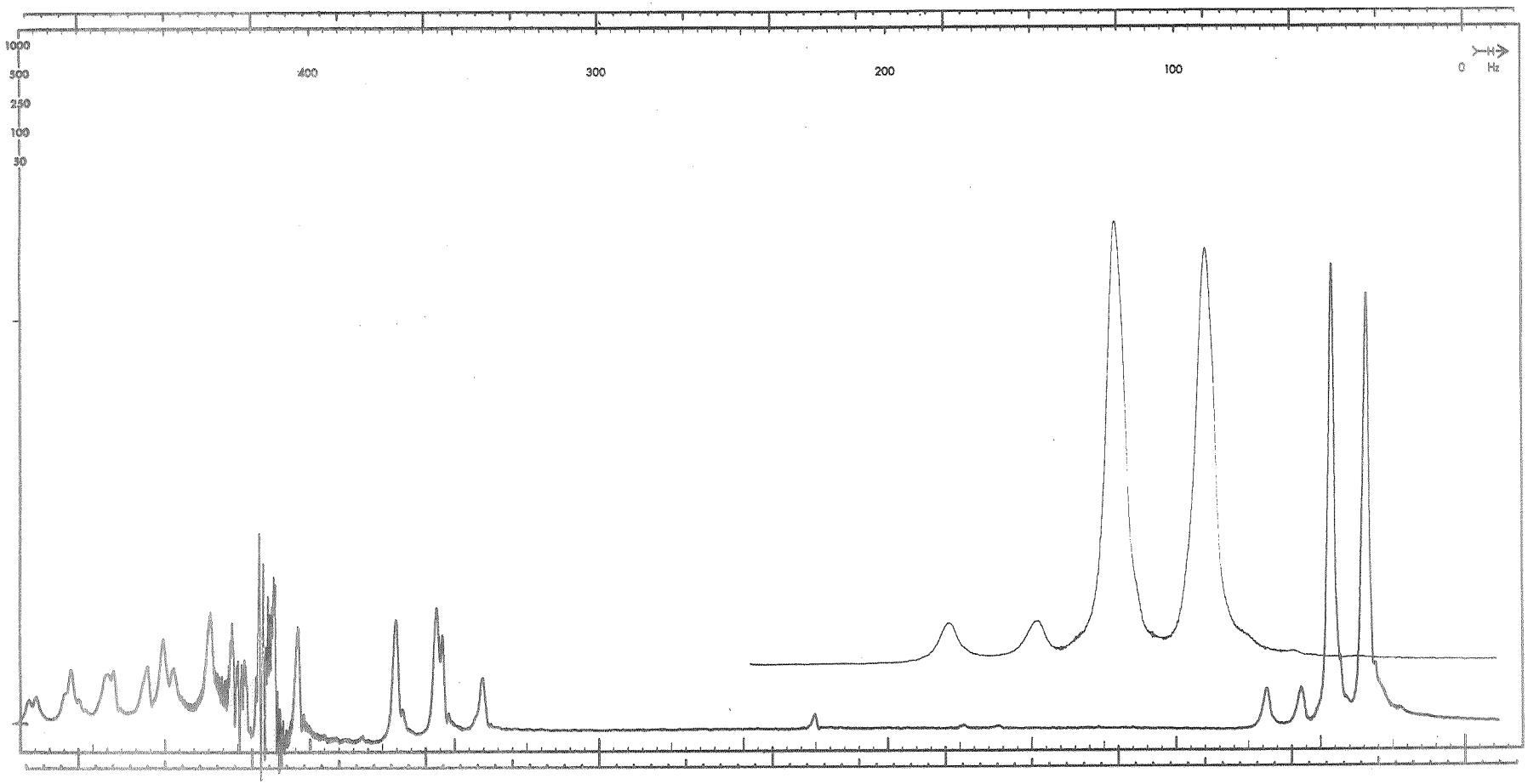

Fig. 10. ^{1}H NMR Spectra In 1M $AlCl_3$ #4/PC #6-6 & 0.05 M DMSO #1-1

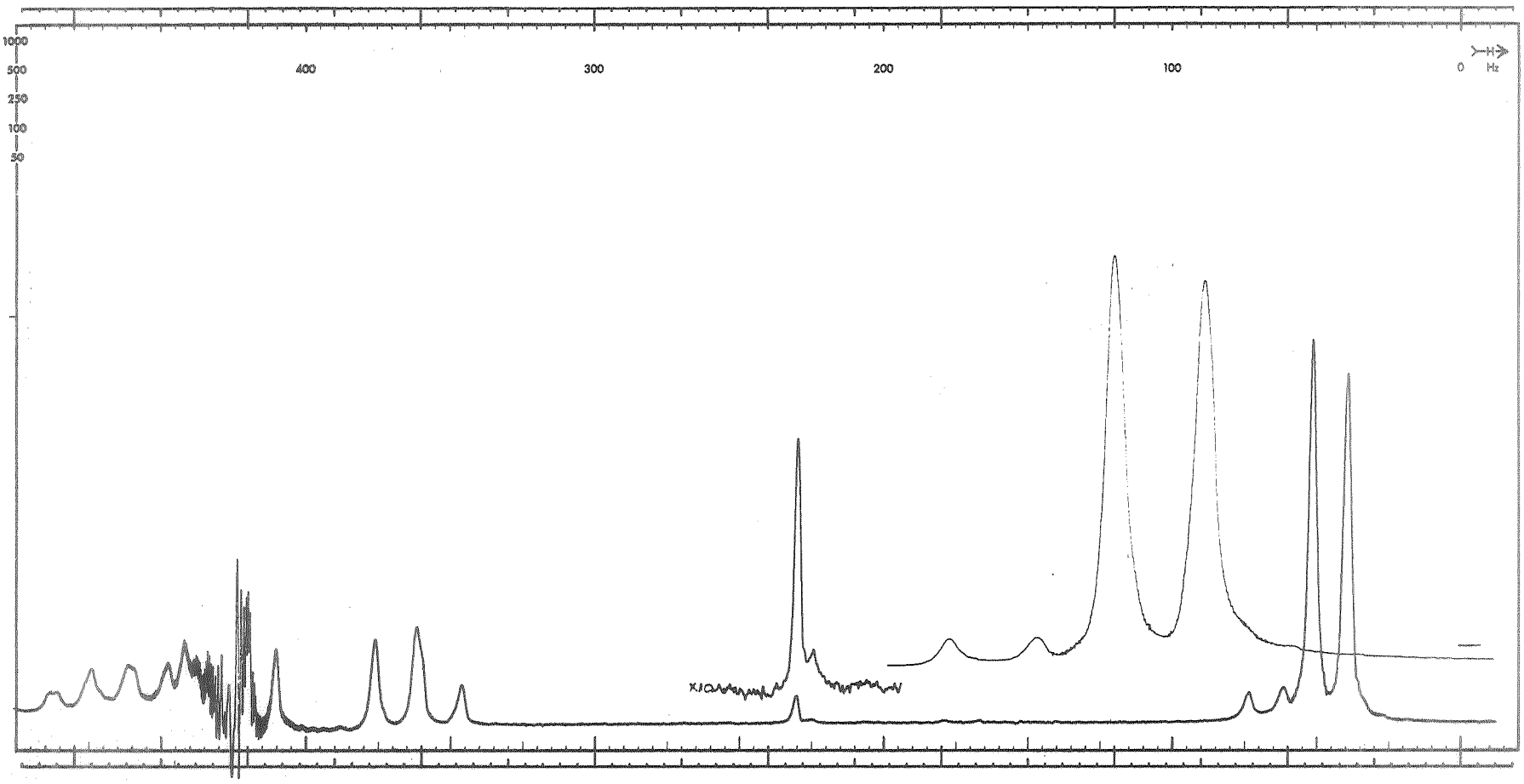

Fig. 11. ^{1}H NMR Spectra In 1M $AlCl_3$ #4/PC #6-6 & 0.15 M DMSO #1-1

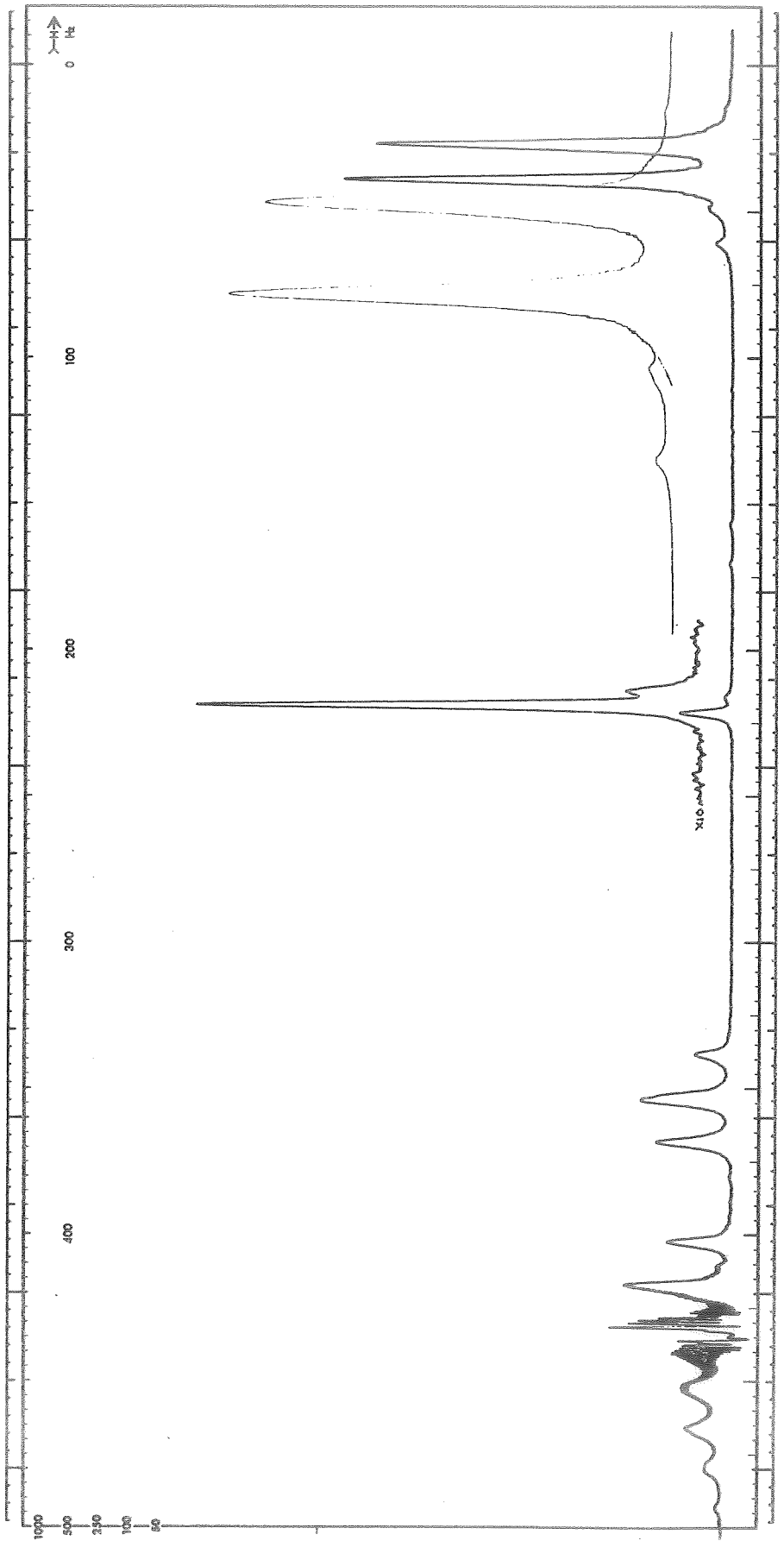

Fig. 12. ^{1}H NMR Spectra In 1M $AlCl_3$ #4/PC #6-6 & 0.30 M DMSO #1-1

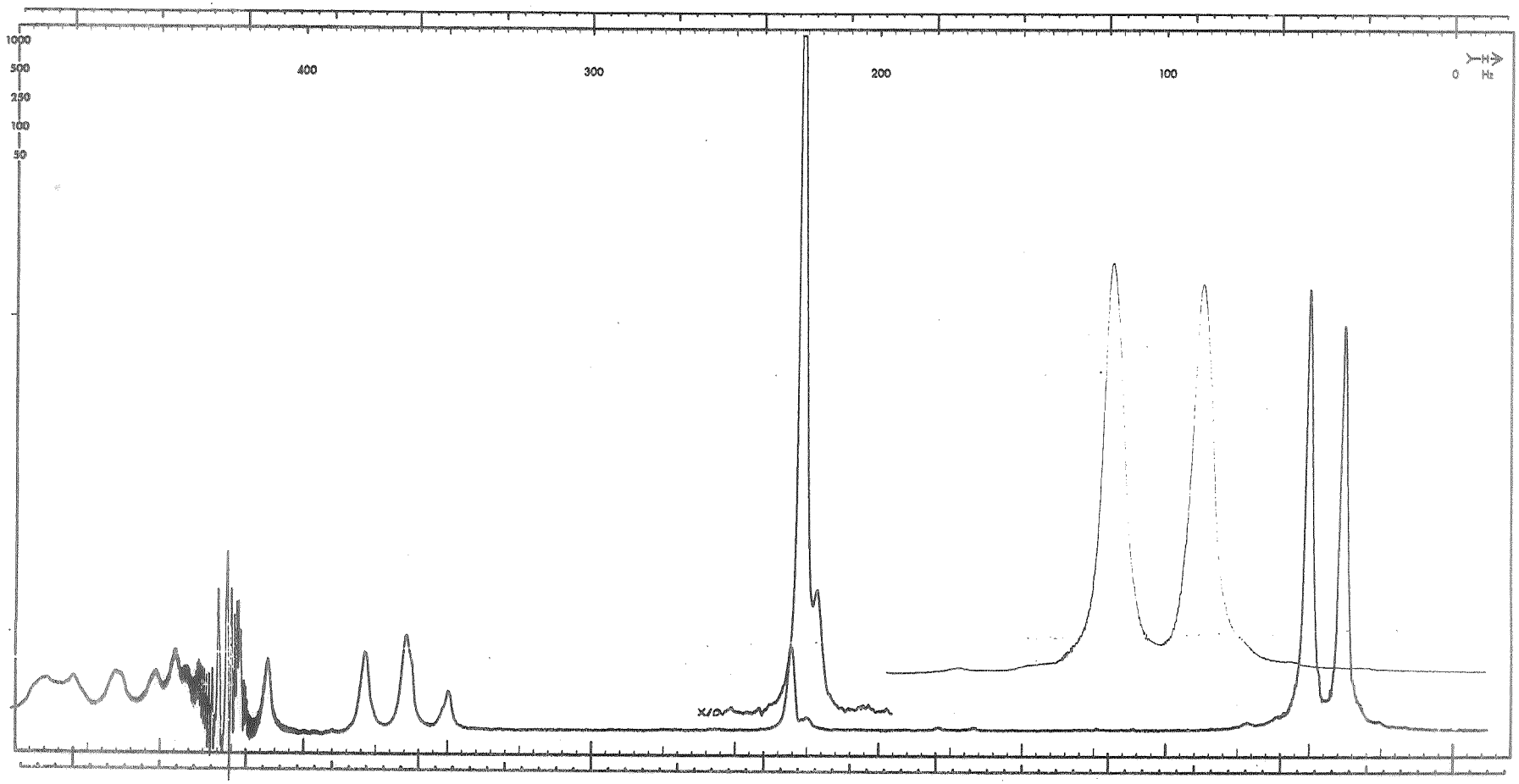

Fig. 13. ^{1}H NMR Spectra In 1M $AlCl_3$ #4/PC #6-6 & 0.50 M DMSO #1-1

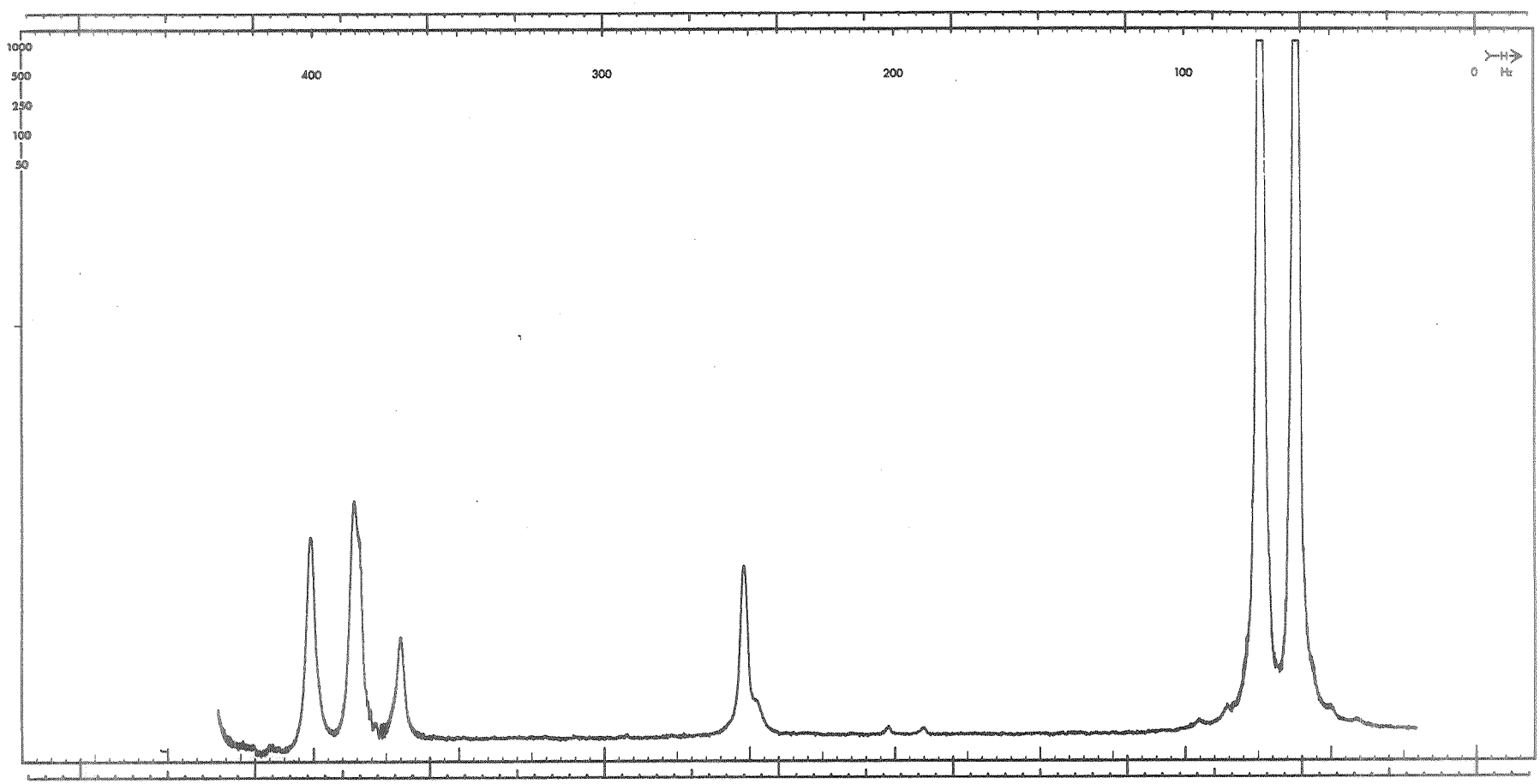

Fig. 14. ^{1}H NMR Spectra In 1M $AlCl_3$ #4/PC #6-6 & 0.5 M DMSO #1-1 Taken Three Months After The Spectra Shown In Fig. 13

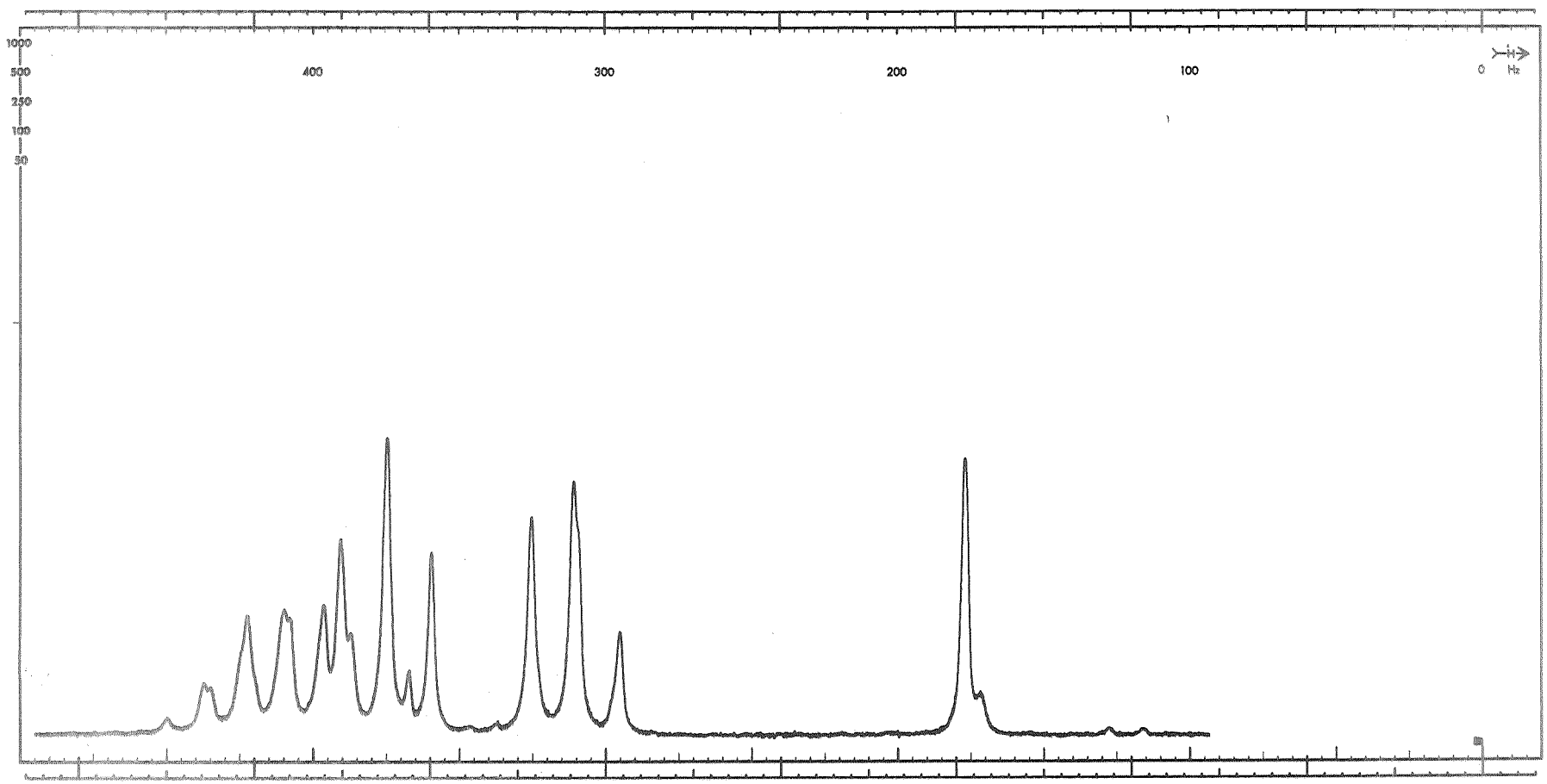

Fig. 15. ^{1}H NMR Spectra In 1M $AlCl_3$ #4/PC #7-4 & 0.7 M DMSO #1-1

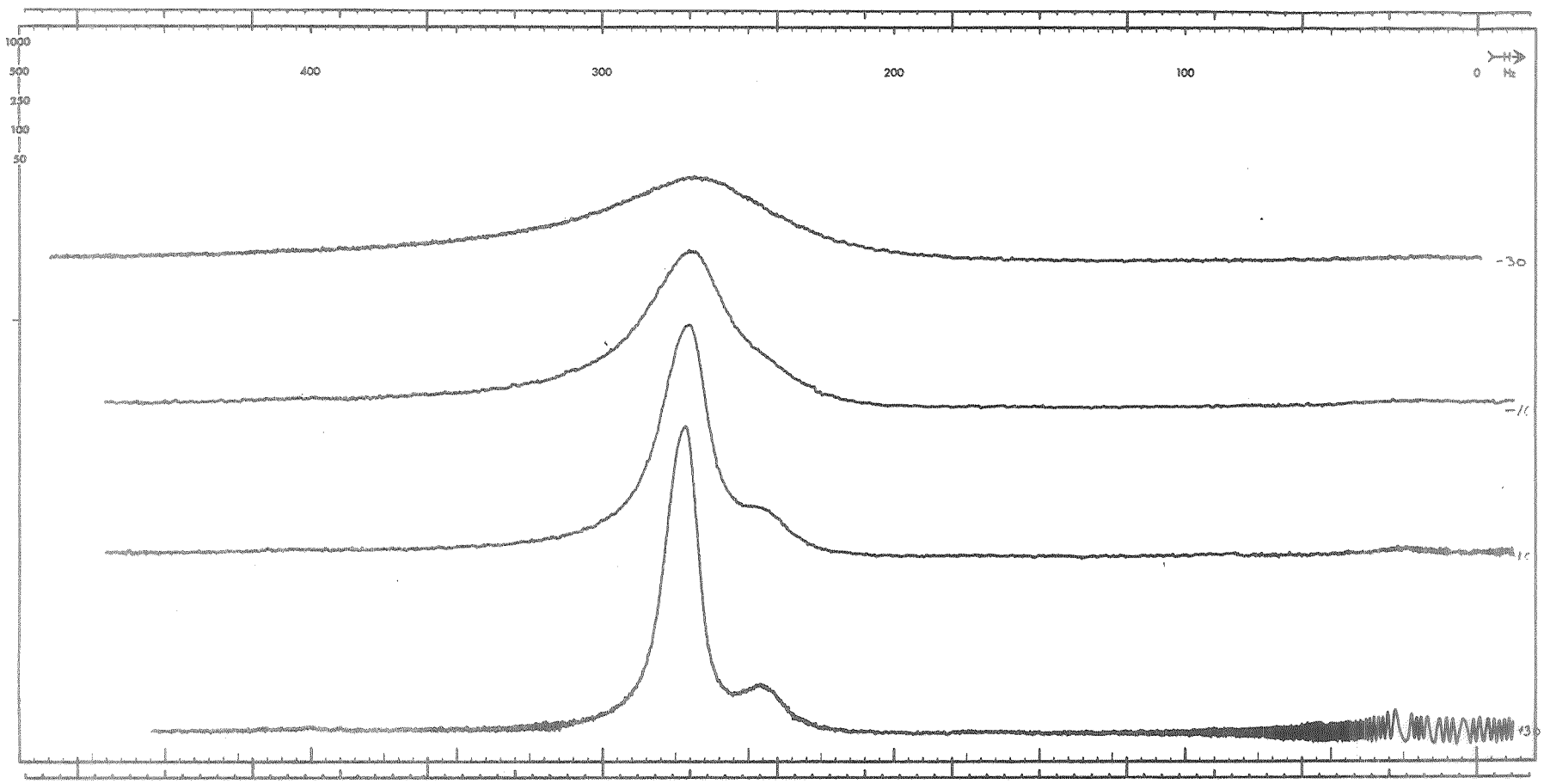

Fig. 16. ^{1}H NMR Spectra In 1M $AlCl_3$ #4/PC #7-4 & 0.7 M DMSO #1-1, Expanded Scale Covering The DMSO Spectra Taken At +30, +10, -10 and -30 C

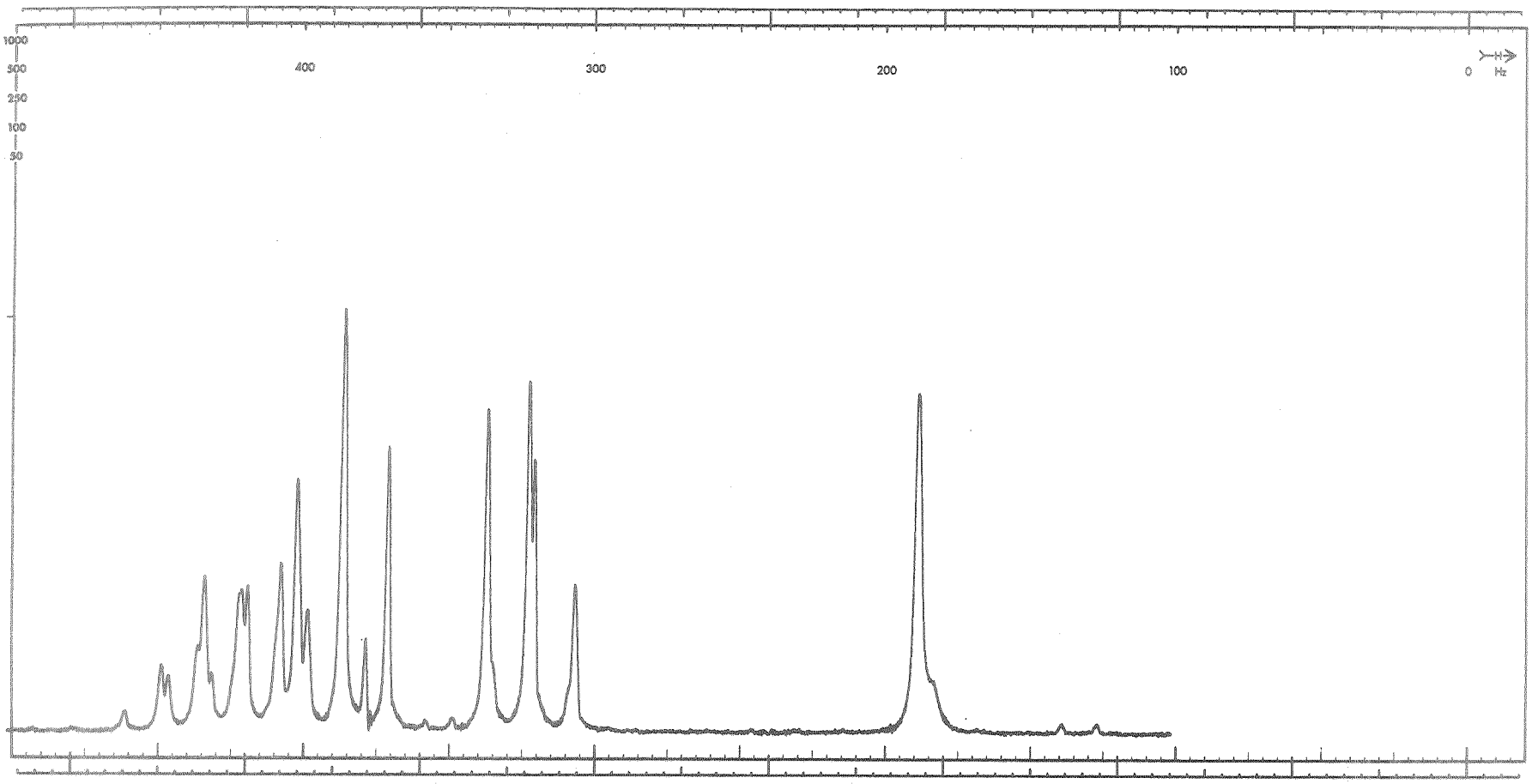

Fig. 17. ^{1}H NMR Spectra In 1M $AlCl_3$ #4/PC #7-4 & 0.9 M DMSO #1-1

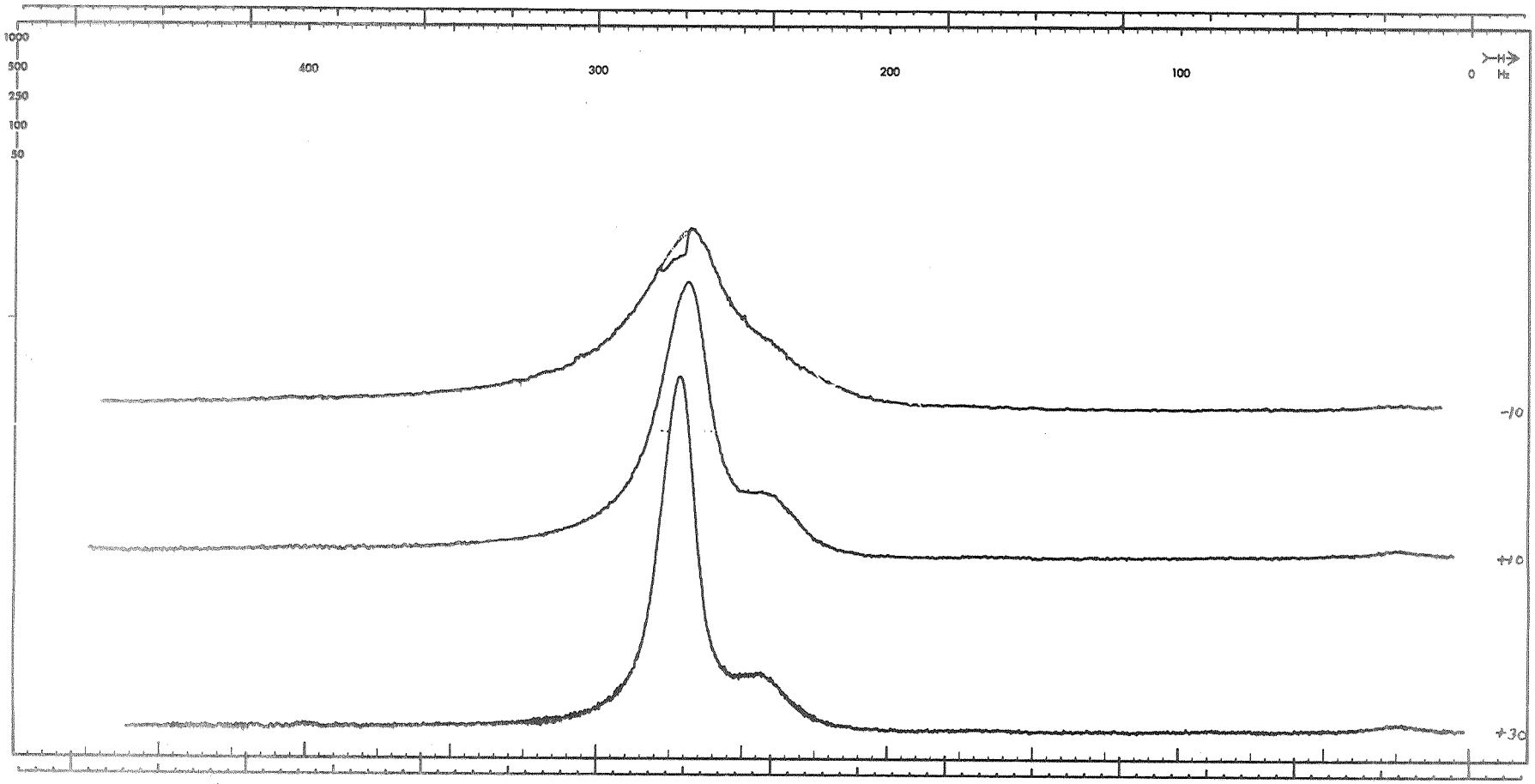

Fig. 18. ^{1}H NMR Spectra In 1M $AlCl_3$ #4/PC #7-4 & 0.9 M DMSO #1-1, Expanded Scale Covering The DMSO Spectra Taken at +30, +10 and -10 C

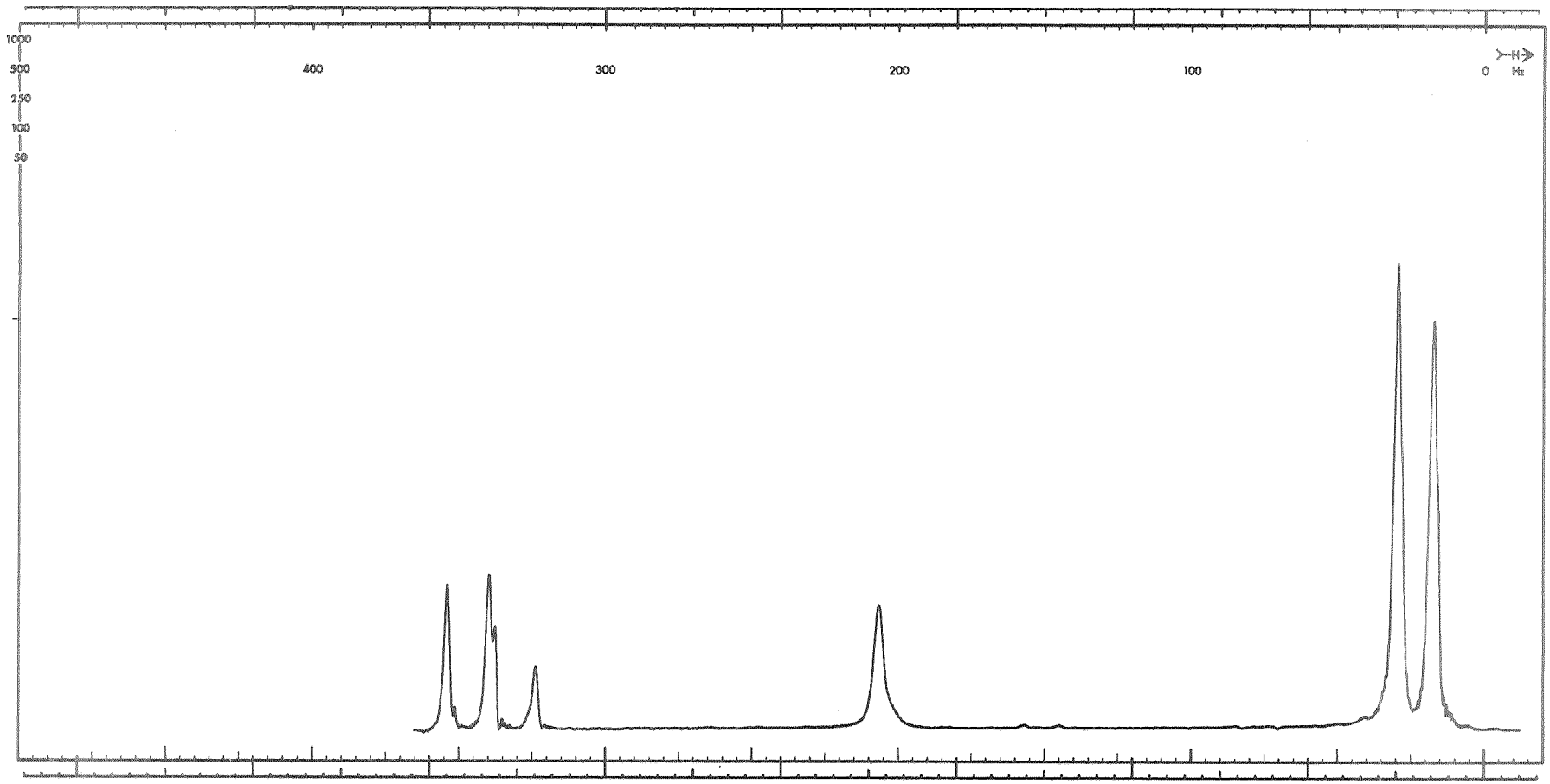

Fig. 19. ^{1}H NMR Spectra In 1M $AlCl_3$ #4/PC #6-6 & 1 M DMSO #1-1

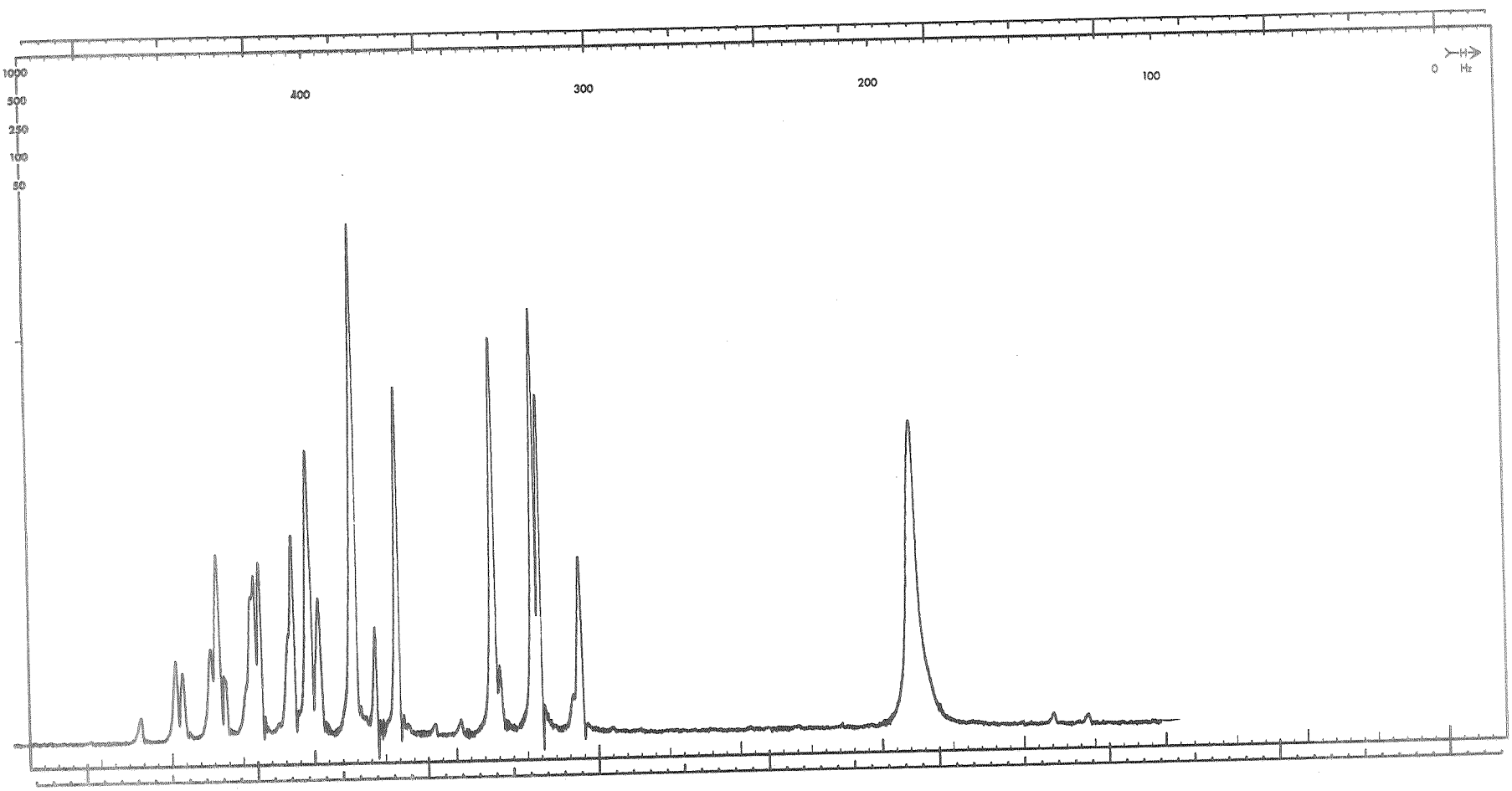

Fig. 20. ^{1}H NMR Spectra In 1M $AlCl_3$ #4/PC #7-4 & 1.1 M DMSO #1-1

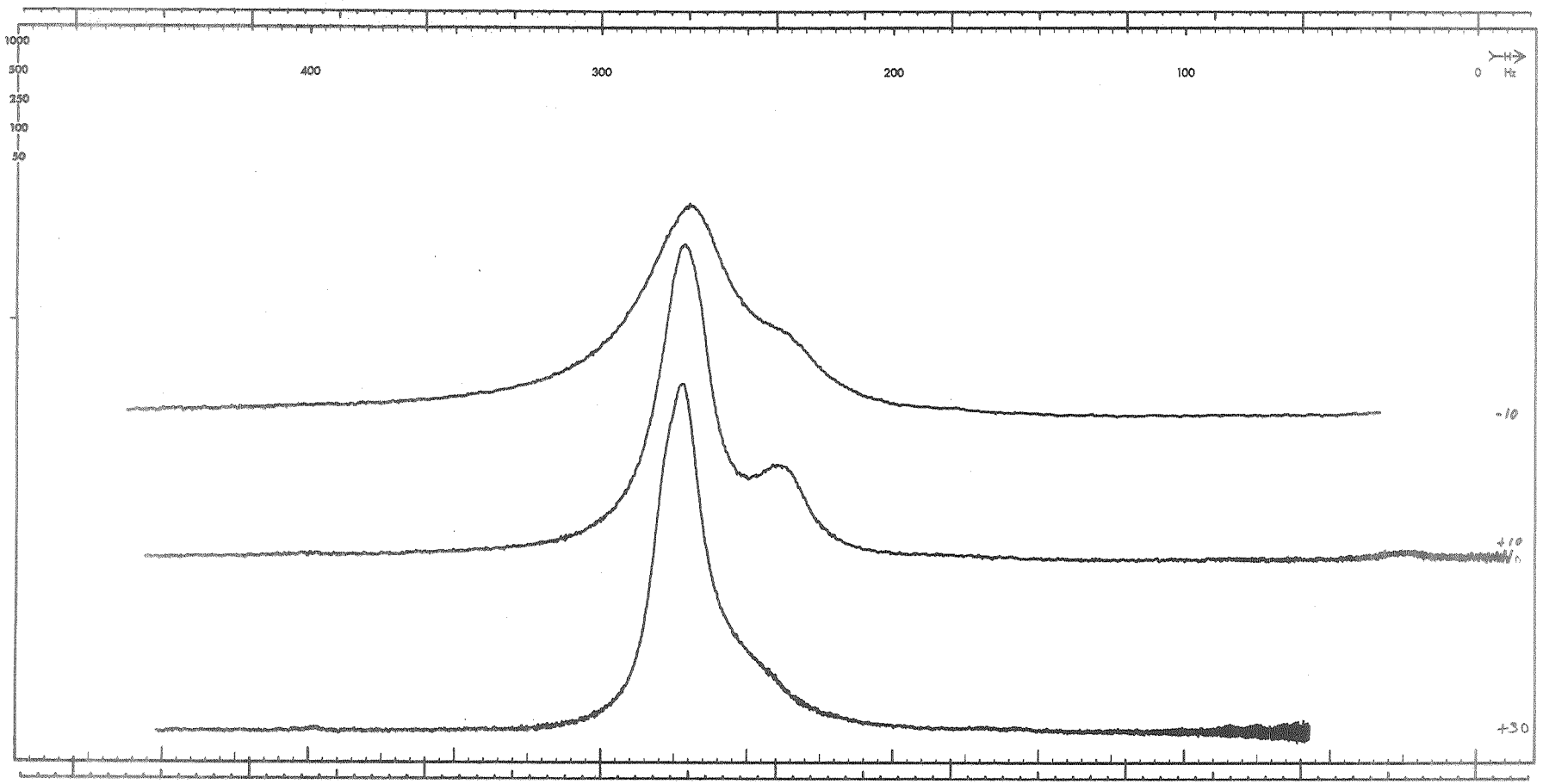

Fig. 21. ^{1}H NMR Spectra In 1M $AlCl_3$ #4/PC #7-4 & 1.1 M DMSO #1-1. Expanded Scale Covering The DMSO Spectra Taken At +30, +10 and -10 C

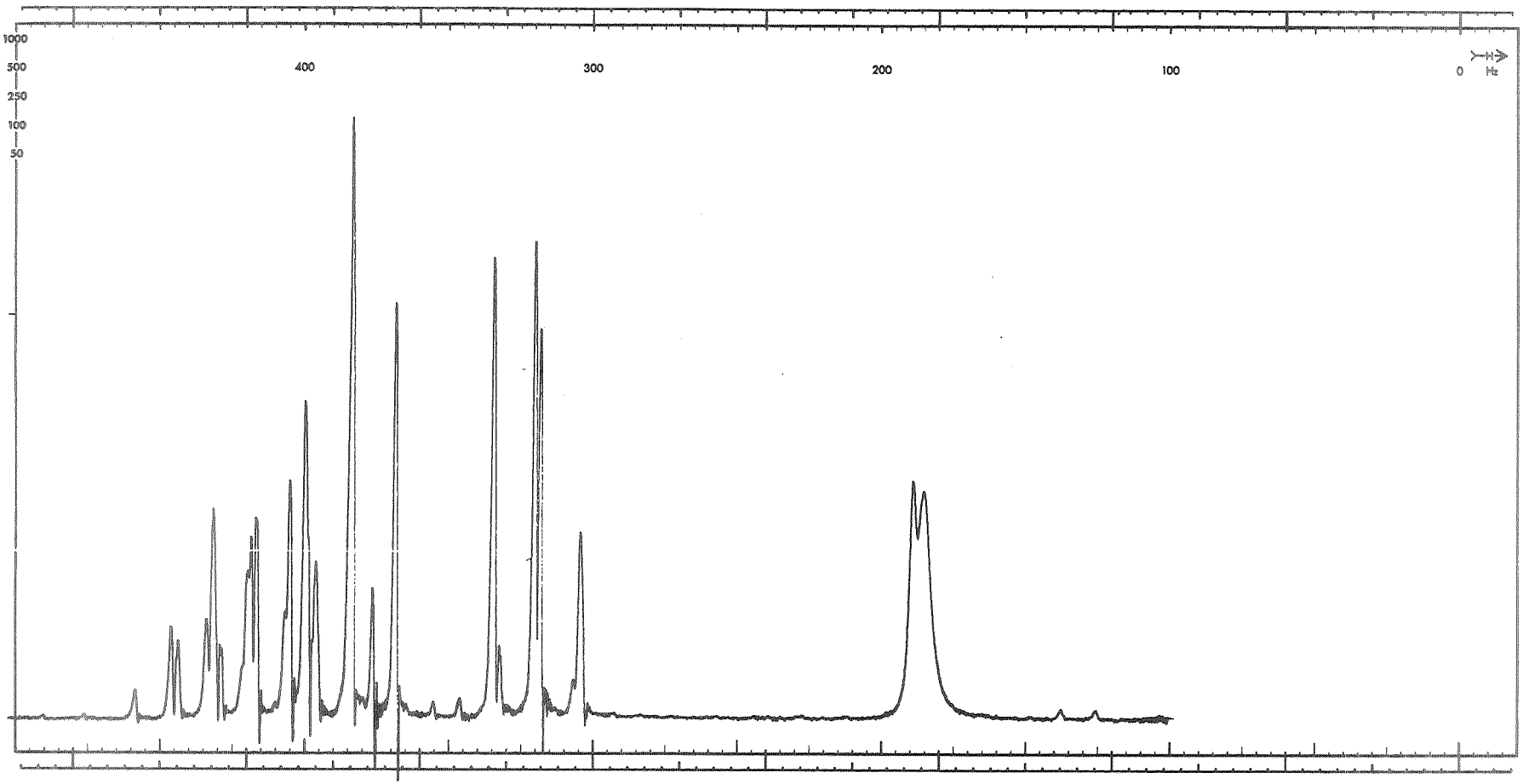

.Fig. 22. ^{1}H NMR Spectra In 1M $AlCl_3$ #4/PC #7-4 & 1.3 M DMSO #1-1

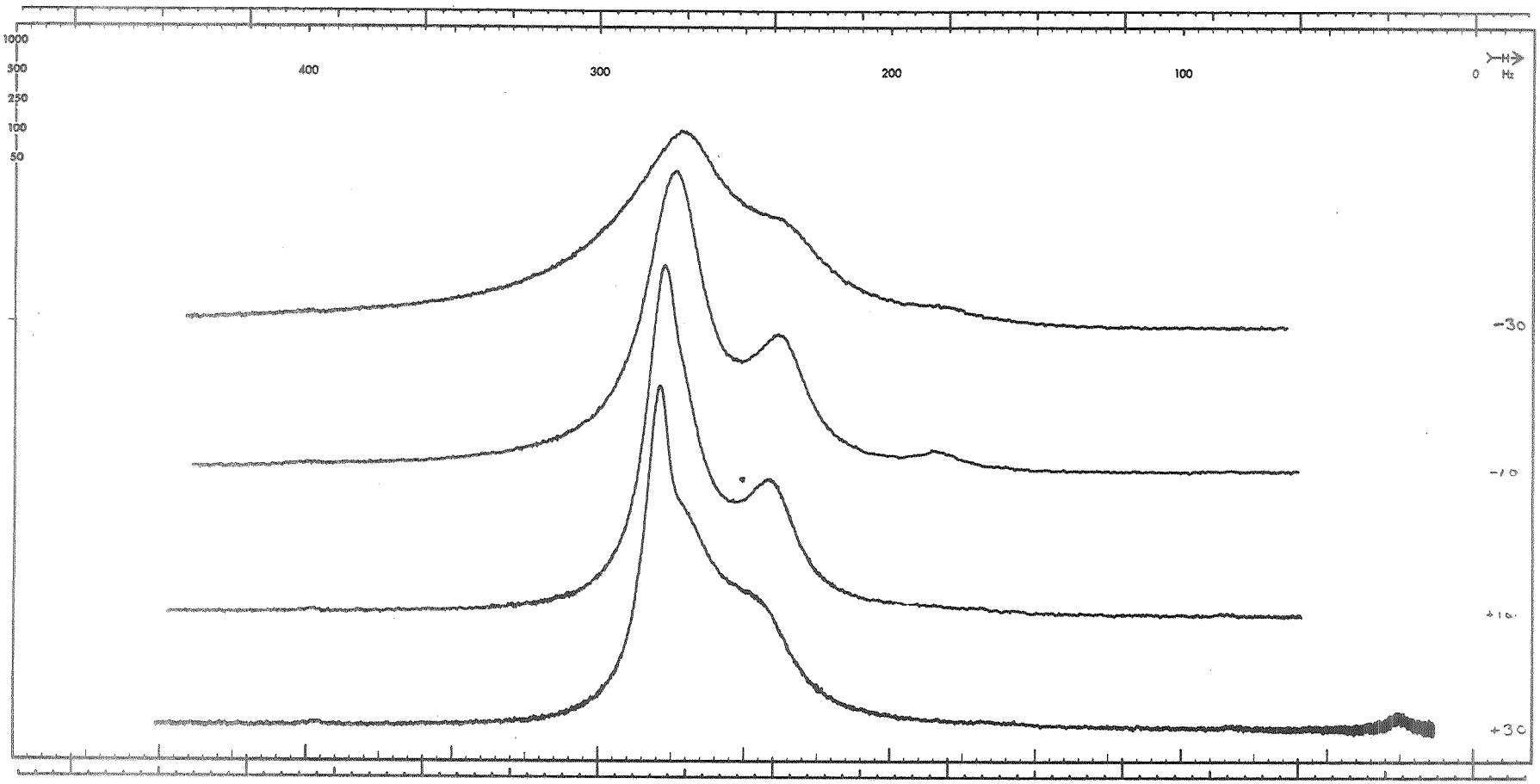

Fig. 23. ^{1}H NMR Spectra In 1M $AlCl_3$ #4/PC #7-4 & 1.3 M DMSO #1-1. Expanded Scale Covering The DMSO Spectra Taken At +30, +10, -10 and -30 C

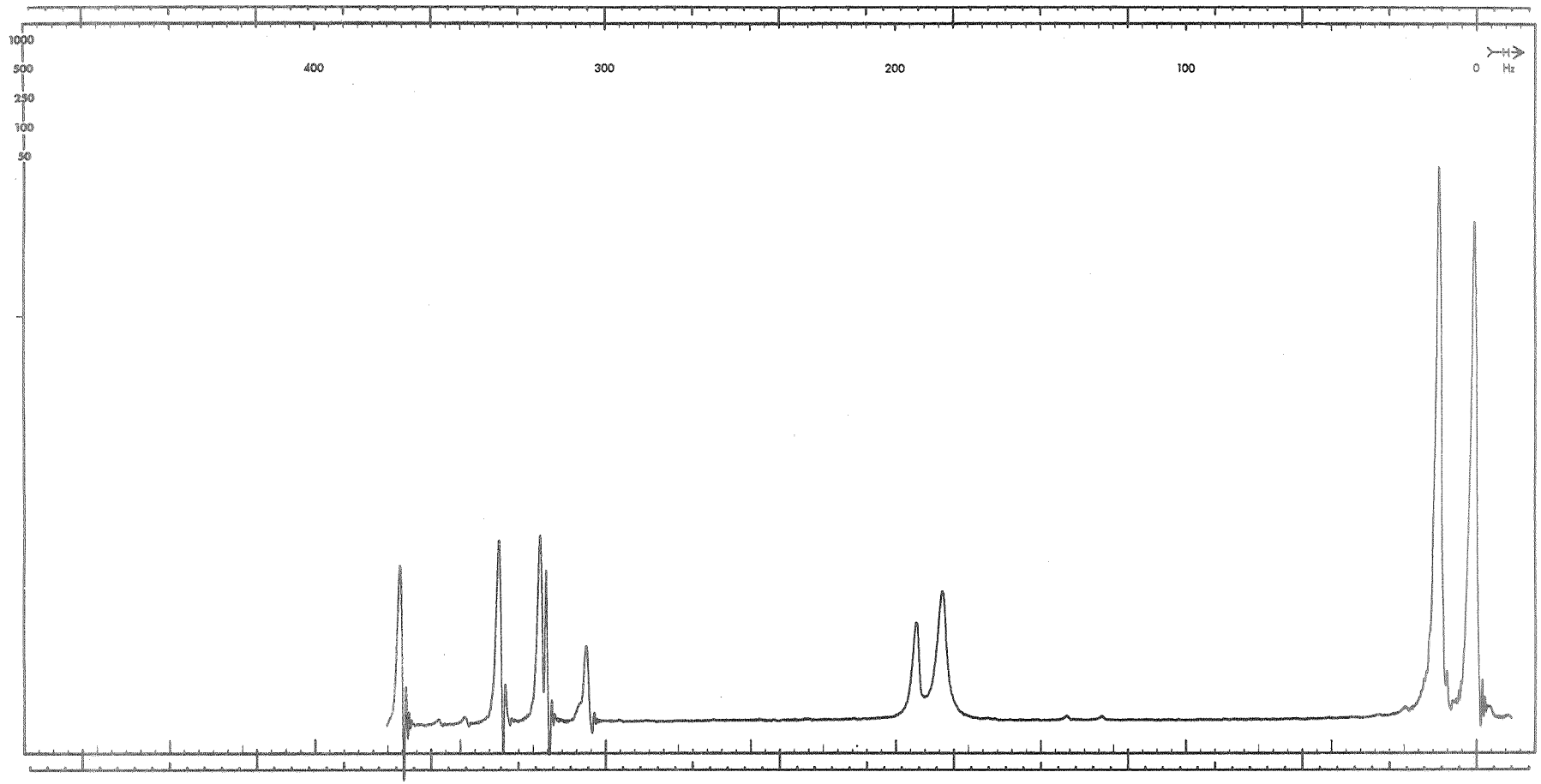

Fig. 24. ^{1}H NMR Spectra In 1M $AlCl_3$ #4/PC #6-6 & 1.5 M DMSO #1-1

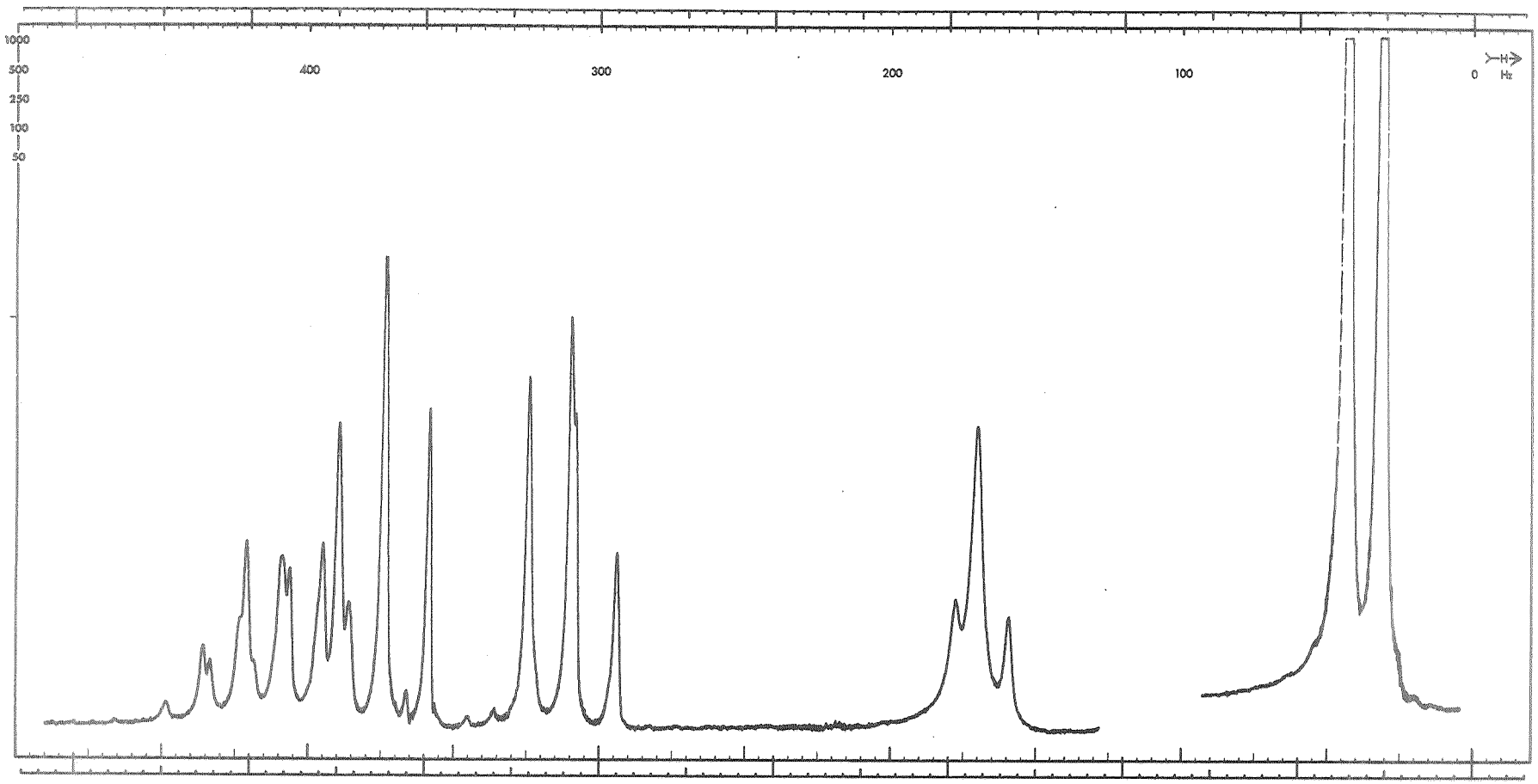

Fig. 25. ^{1}H NMR Spectra In 1M $AlCl_3$ #4/PC #6-6 & 1.5 M DMSO #1-1 Taken at -10 C

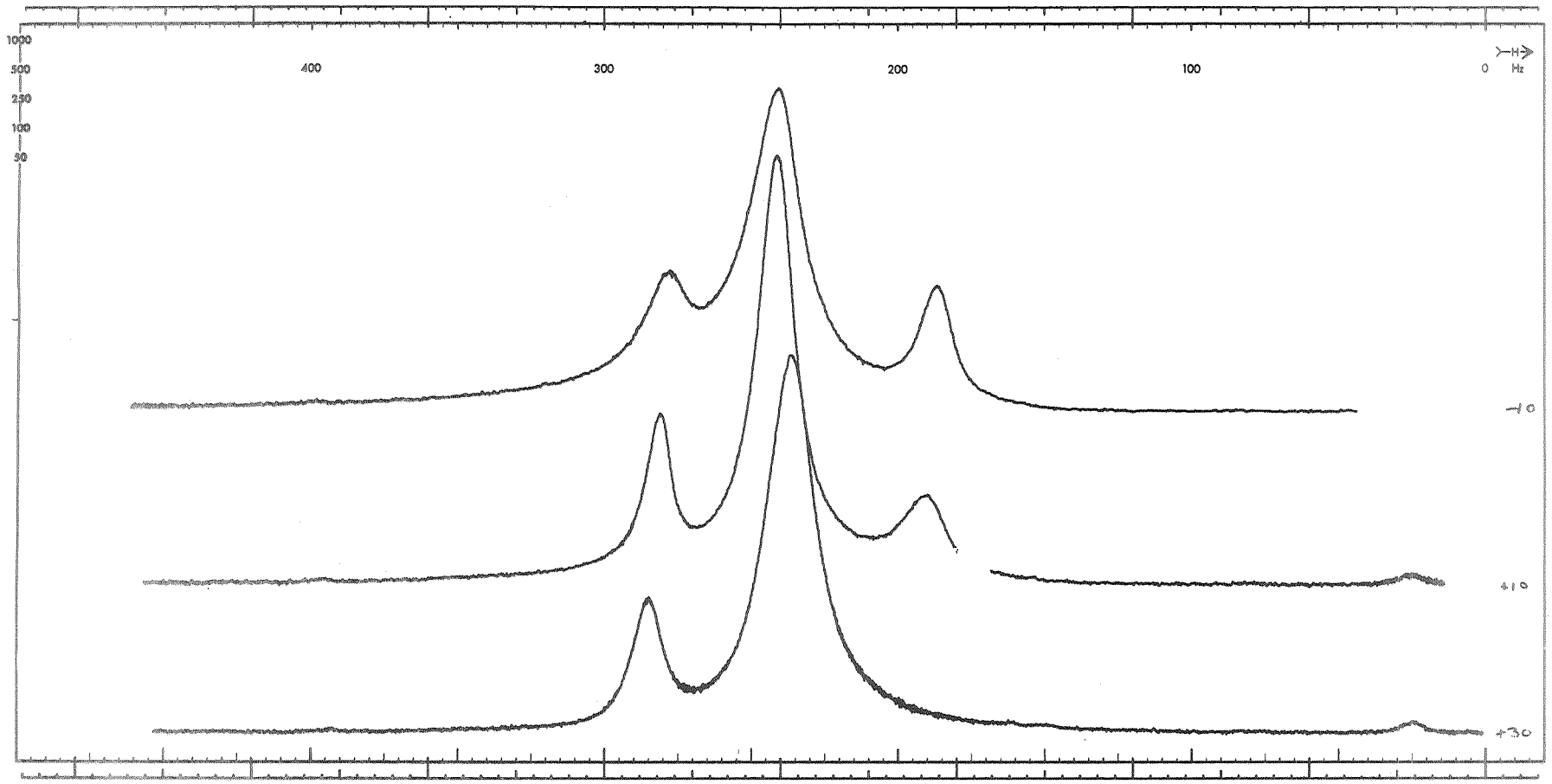

Fig. 26. ^{1}H NMR Spectra In 1M $AlCl_3$ #4/PC #6-6 & 1.5 M DMSO #1-1. Expanded Scale Covering The DMSO Spectra Taken at +30, +10 and -10 C

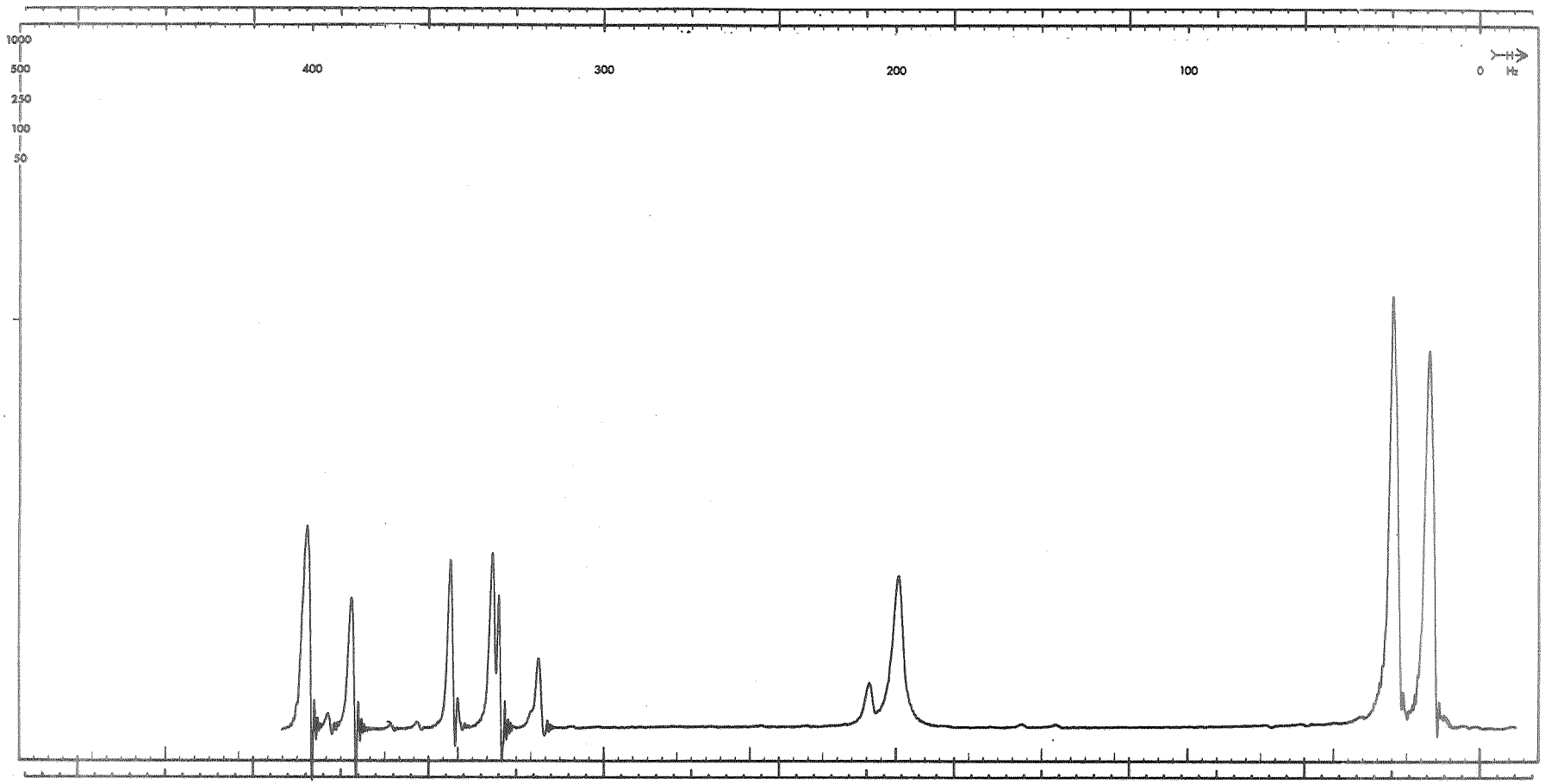

Fig. 27. ^{1}H NMR Spectra In 1M $AlCl_3$ #4/PC #6-6 & 2.0 M DMSO #1-1. White Precipitate In Bottom Of Tube

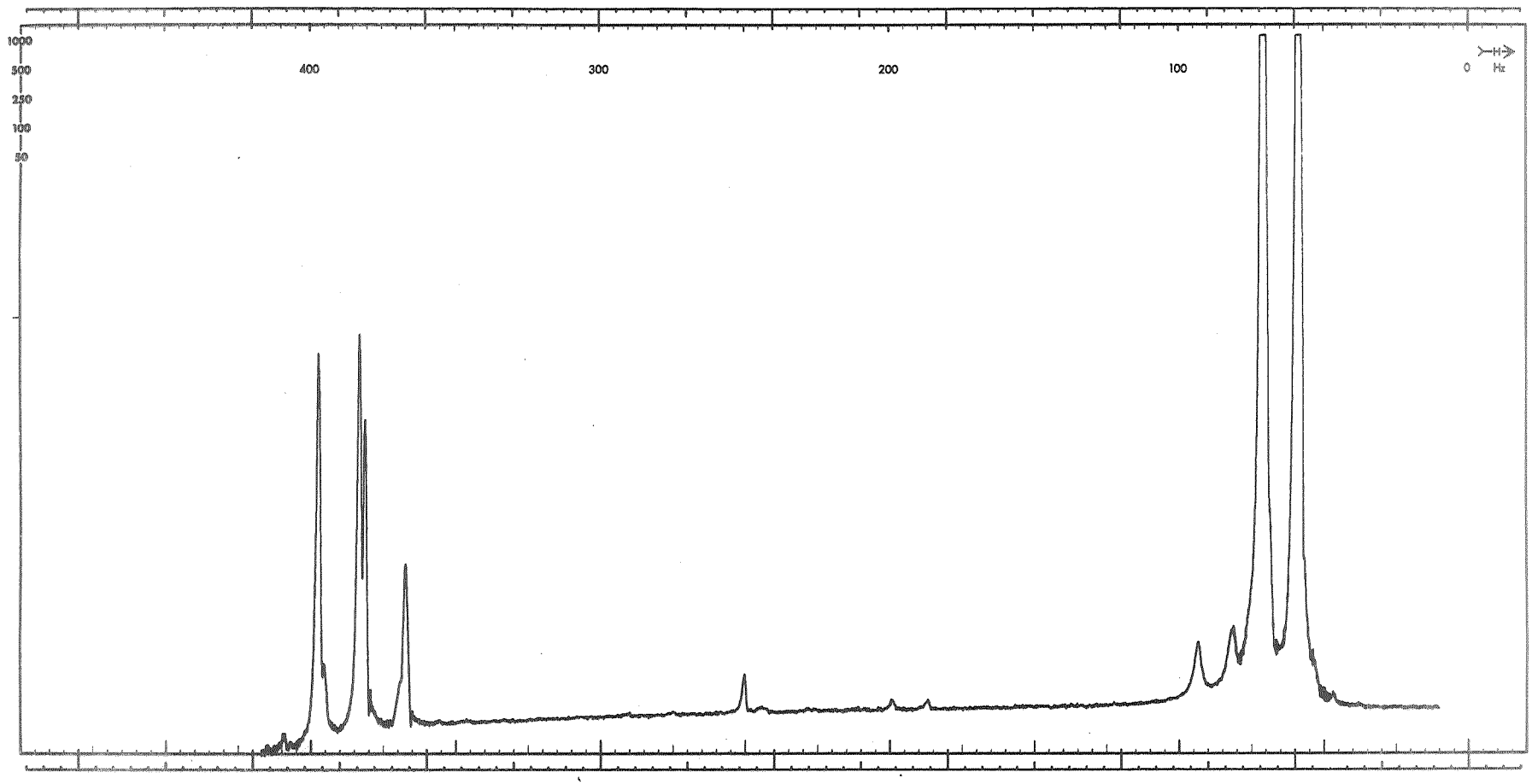

Fig. 28. ^{1}H NMR Spectra In 1M $AlCl_3$ #4 + 0.4 M LiCl #3/PC #7-4 & 0.05 M DMSO #1-1

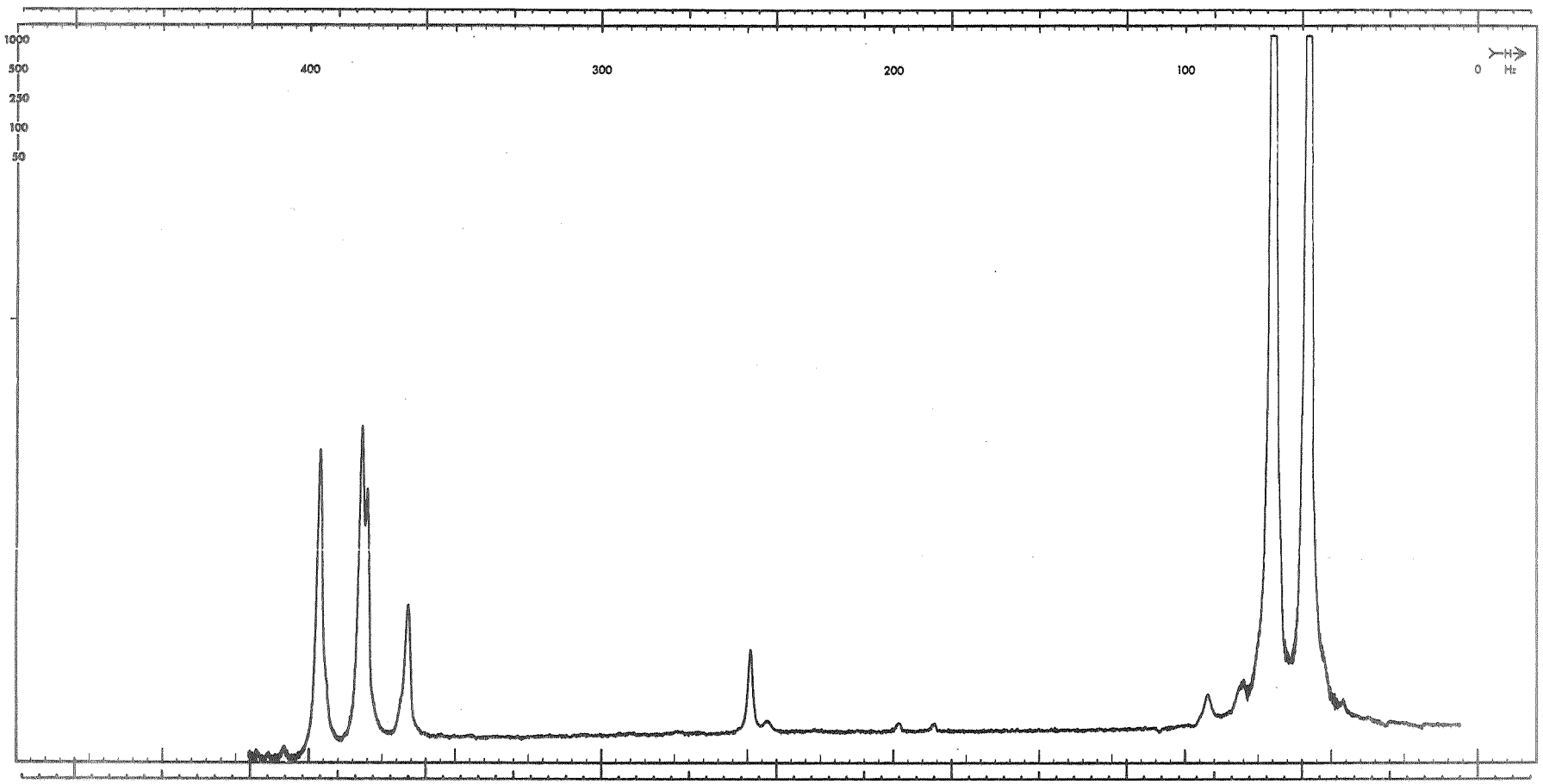

Fig. 29. ^{1}H NMR Spectra In 1M $AlCl_3$ #4 + 0.4 M LiCl #3/PC #7-4 & 0.15 M DMSO #1-1

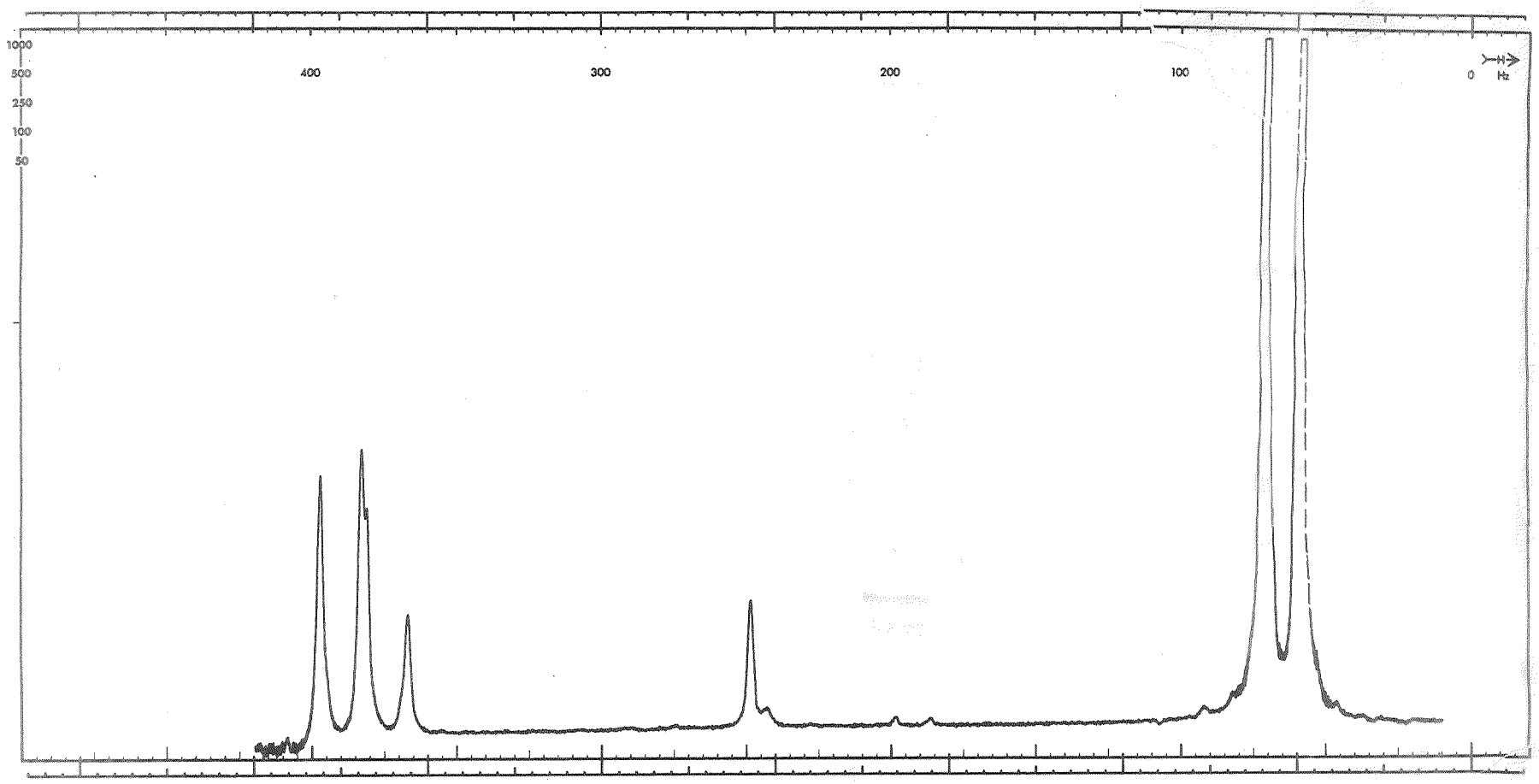

Fig. 30. ^{1}H NMR Spectra In 1M $AlCl_3$ #4 + 0.4 M LiCl #3/ PC #7-4 & 0.3 M DMSO #1-1

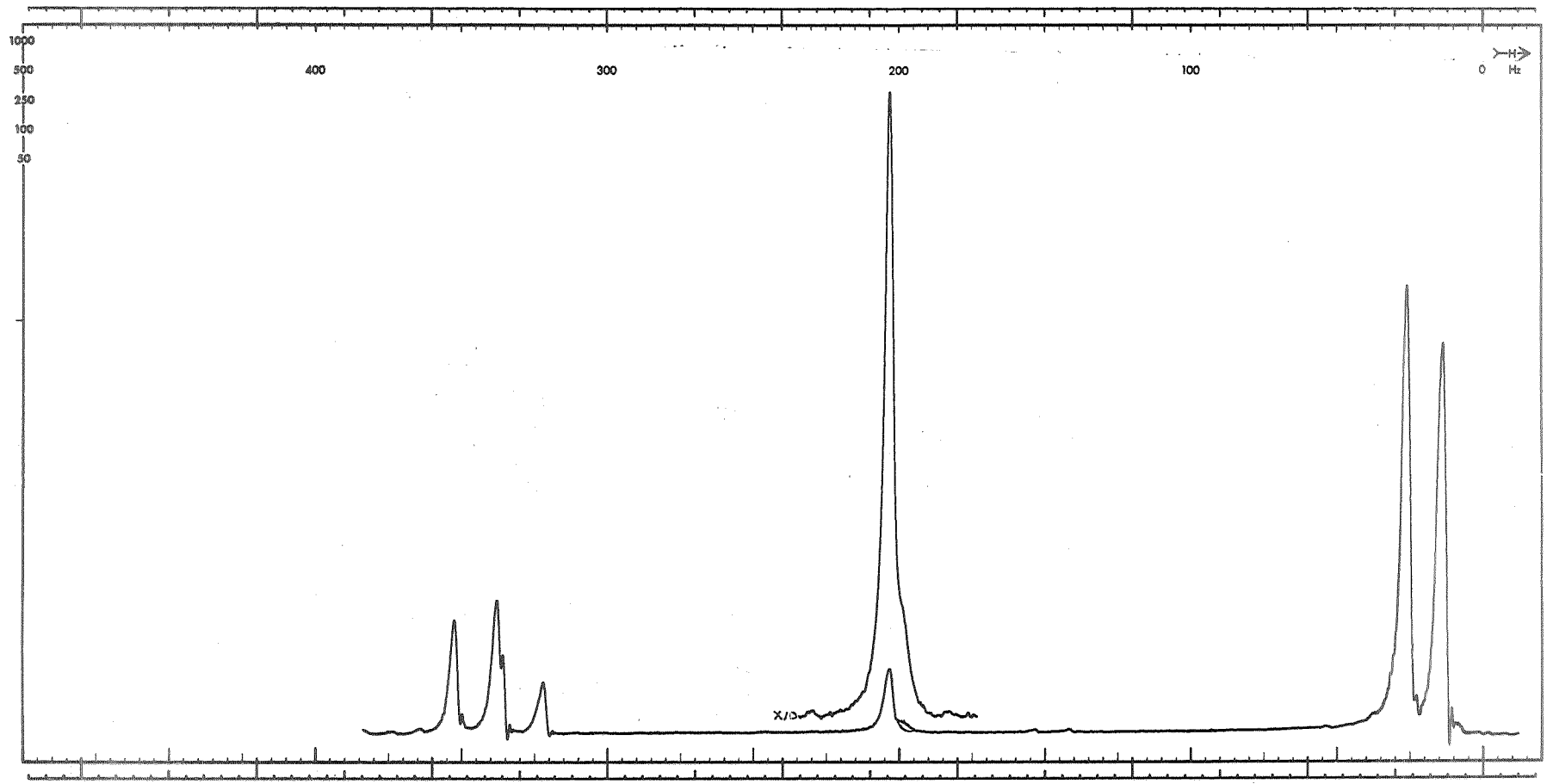

Fig. 31. ^{1}H NMR Spectra In 1M $AlCl_3$ #4 + 0.4 M LiCl #3/PC #6-6 & 0.5 M DMSO #1-1

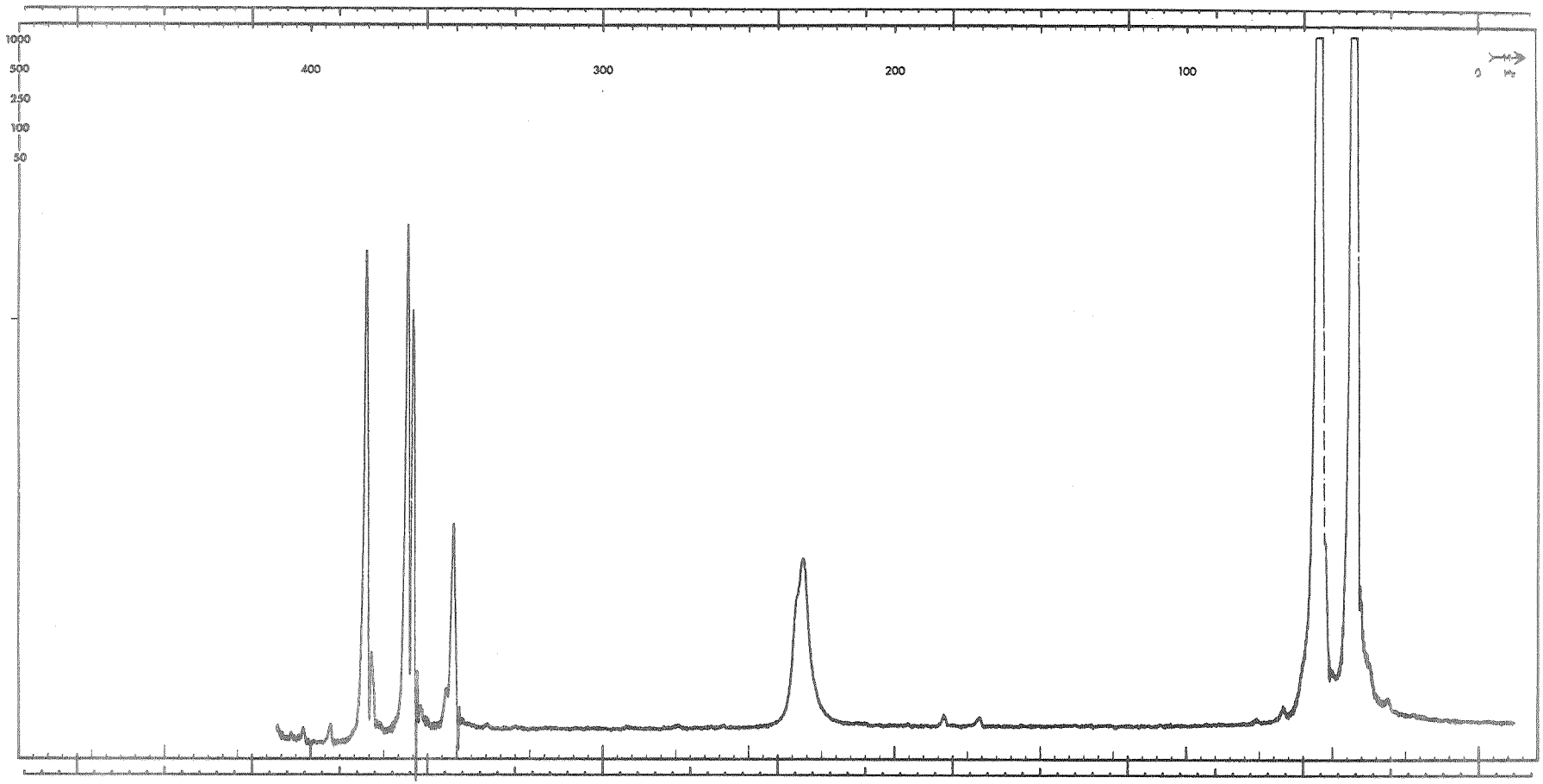

Fig. 32. ^{1}H NMR Spectra In 1M $AlCl_3$ #4 + 0.4 M LiCl #3/PC #7-4 & 0.7 M DMSO #1-1

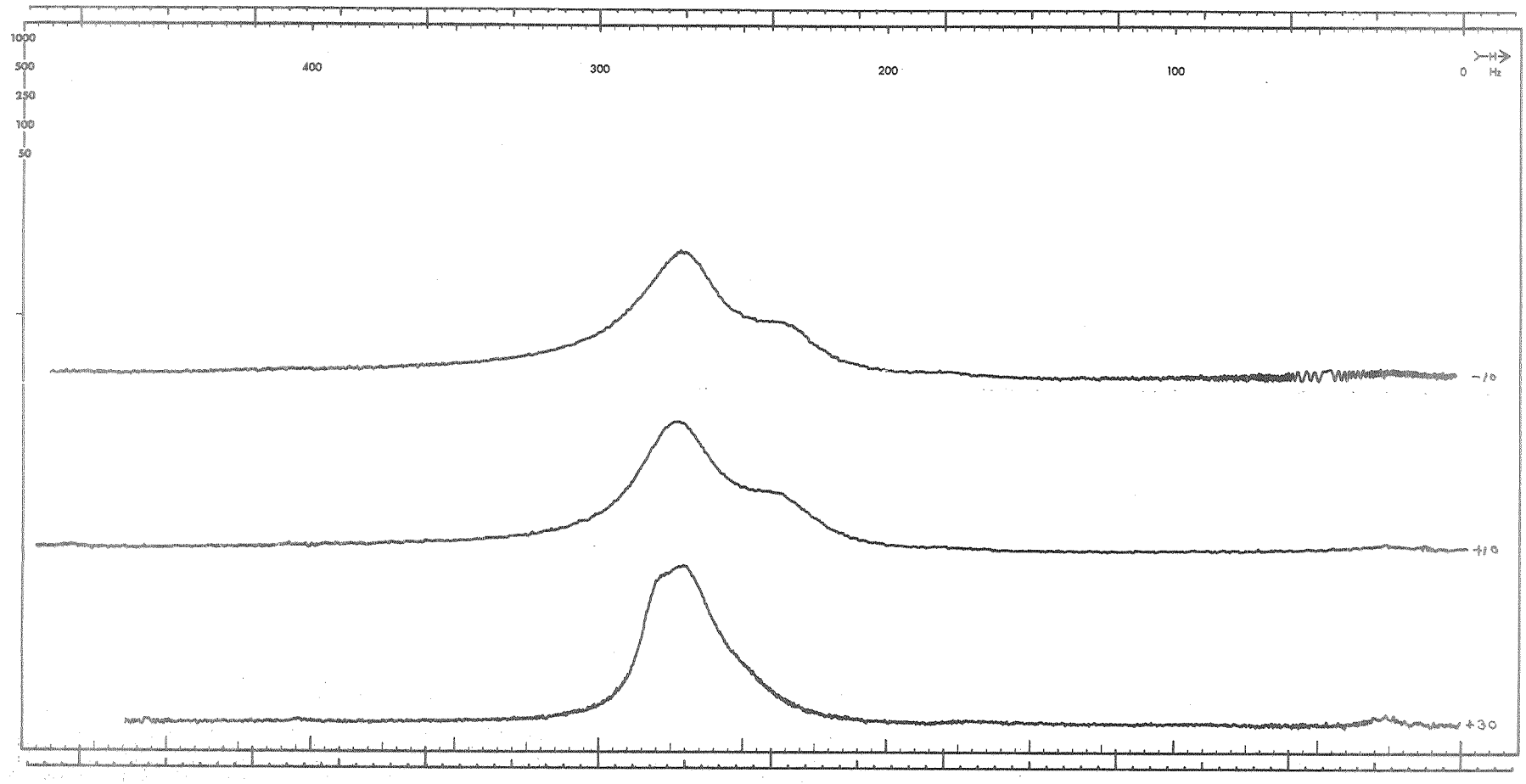

Fig. 33. ^{1}H NMR Spectra In 1M $AlCl_3$ #4 + 0.4 M LiCl #3/PC #7-4 & 0.7 M DMSO #1-1. Expanded Scale Covering The DMSO Spectra Taken at +30, +10 and -10 C

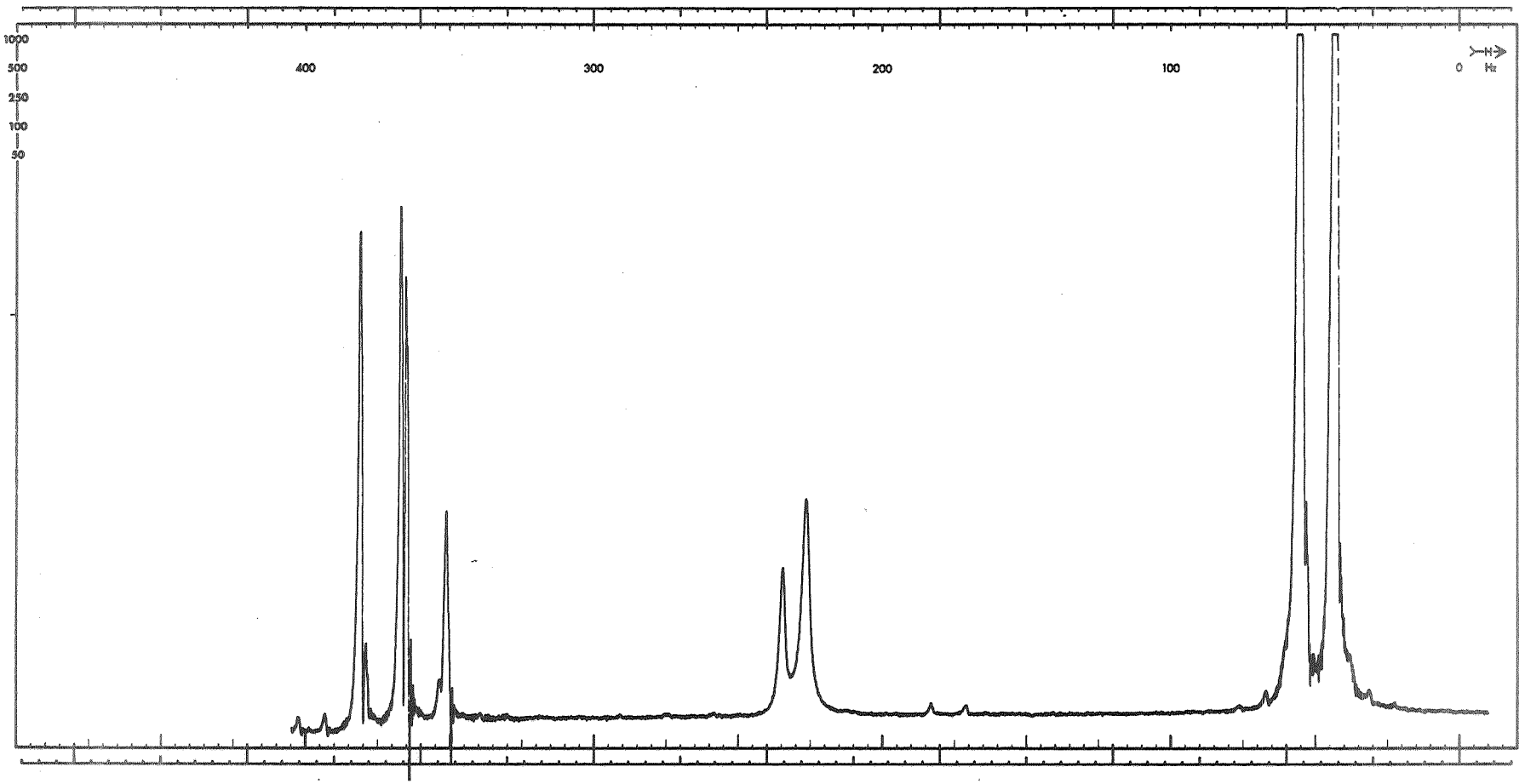

Fig. 34. ^{1}H NMR Spectra In 1M $AlCl_3$ #4 + 0.4 M LiCl #3/PC #7-4 & 0.9 M DMSO #1-1

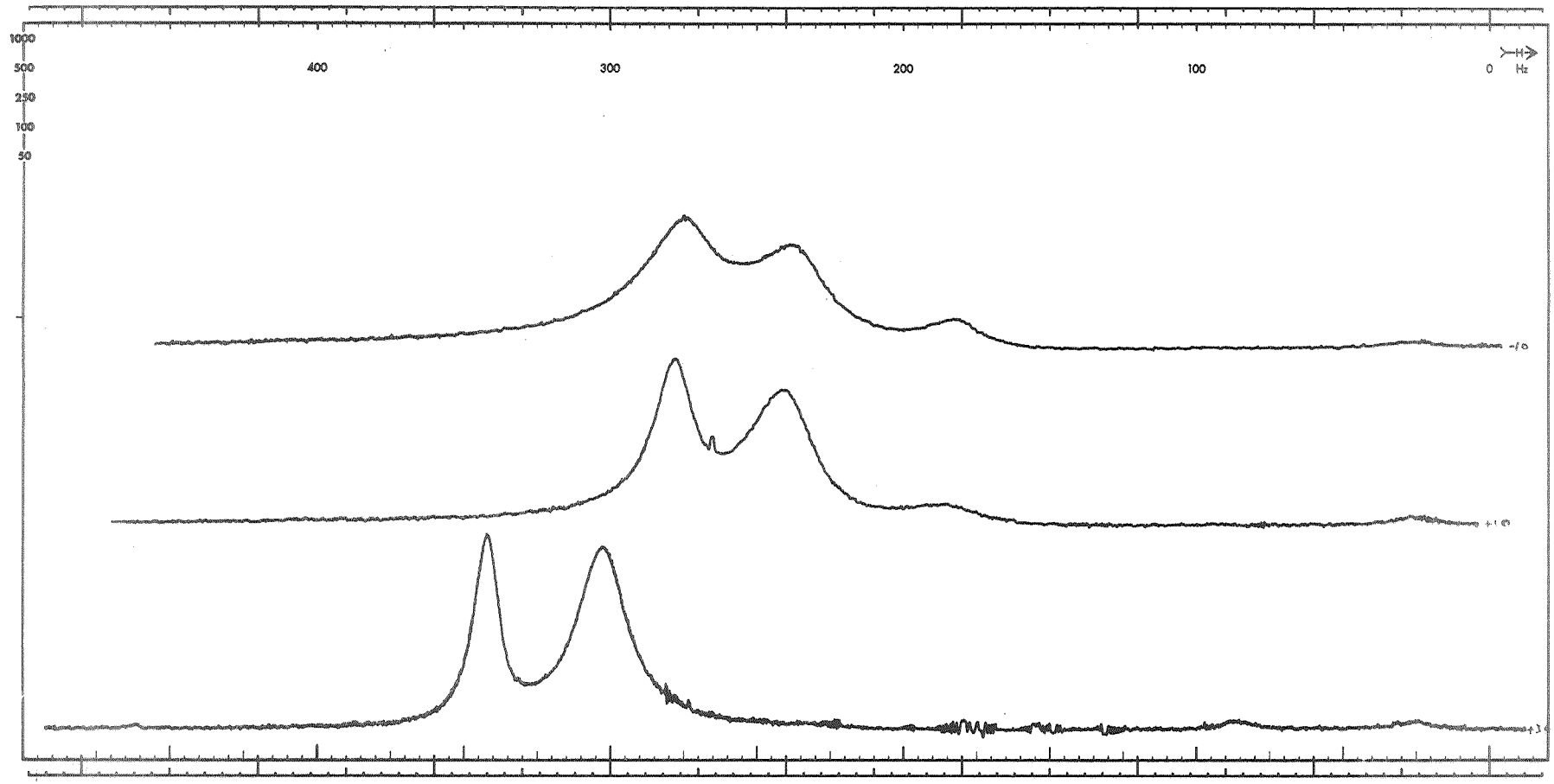

Fig. 35. ^{1}H NMR Spectra In 1M $AlCl_3$ #4 + 0.4 M LiCl #3/PC #7-4 & 0.9 M DMSO #1-1. Expanded Scale Covering the DMSO Spectra Taken at +30, +10 and -10 C

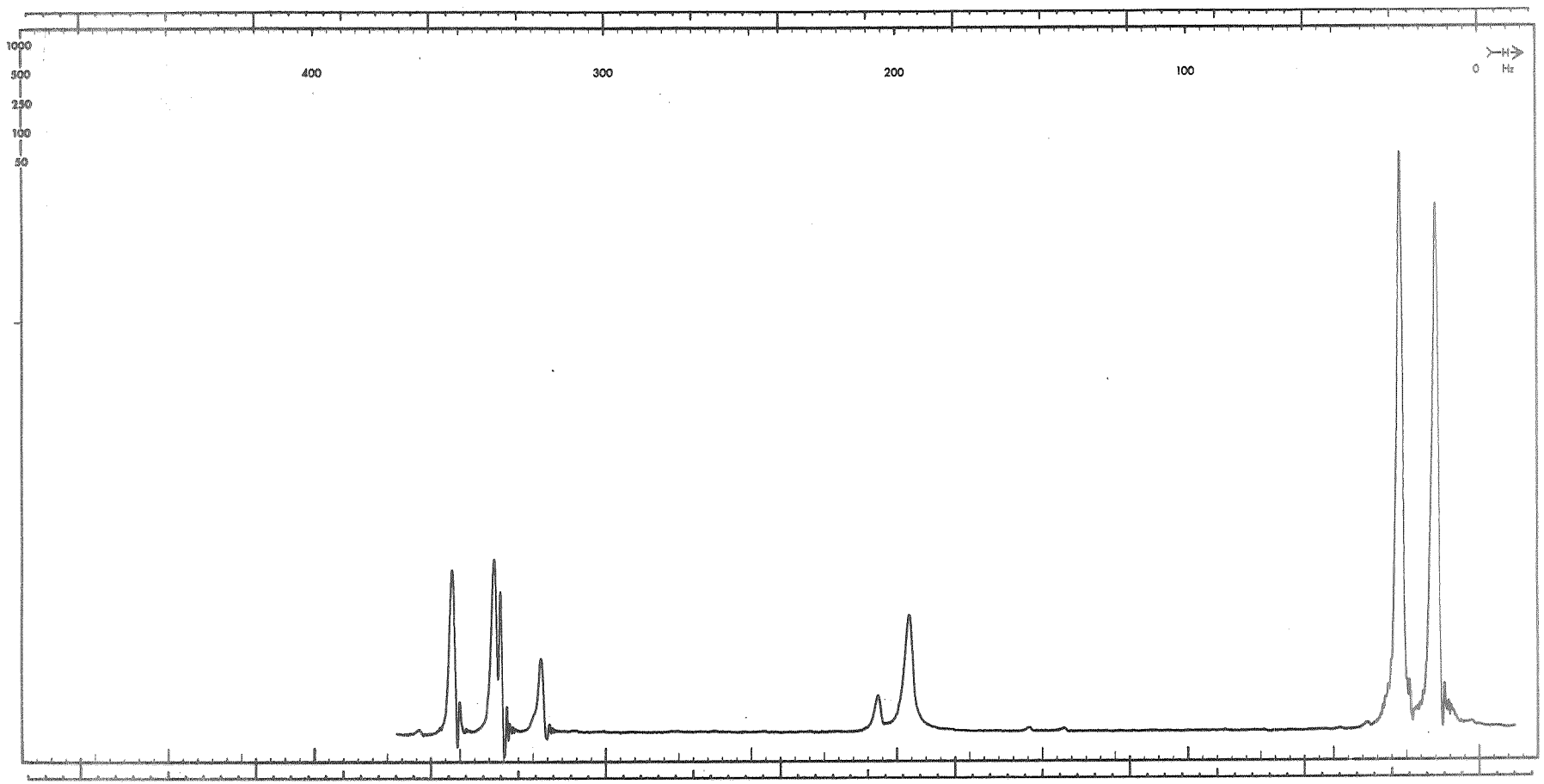

Fig. 36. ^{1}H NMR Spectra In 1M $AlCl_3$ #4 + 0.4M LiCl #3/PC #7-4 & 1.0 M DMSO #1-1

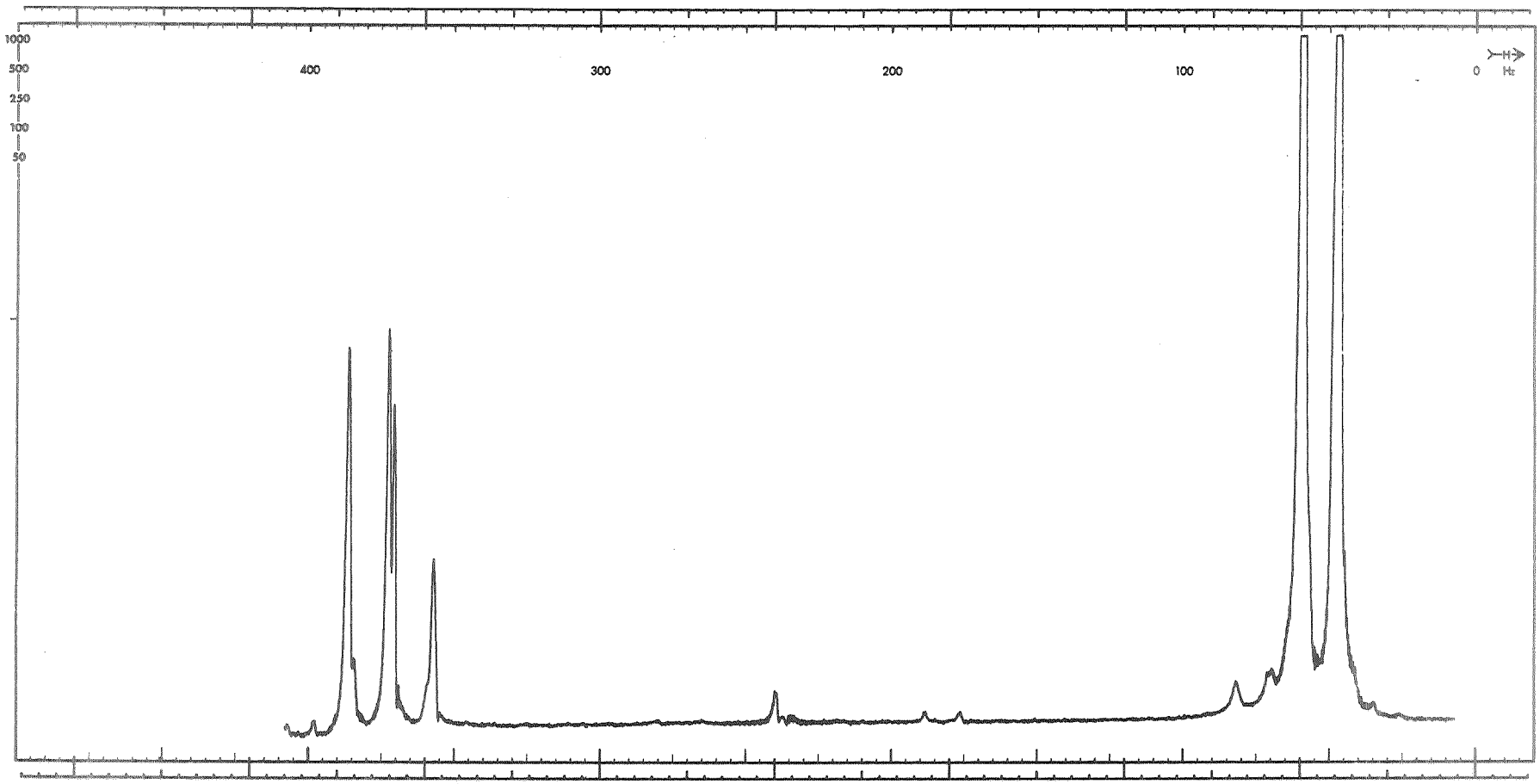

Fig. 37. ^{1}H NMR Spectra In 1M $AlCl_3$ #4 + 0.6 M LiCl #3/PC #7-4 & 0.05 M DMSO #1-1

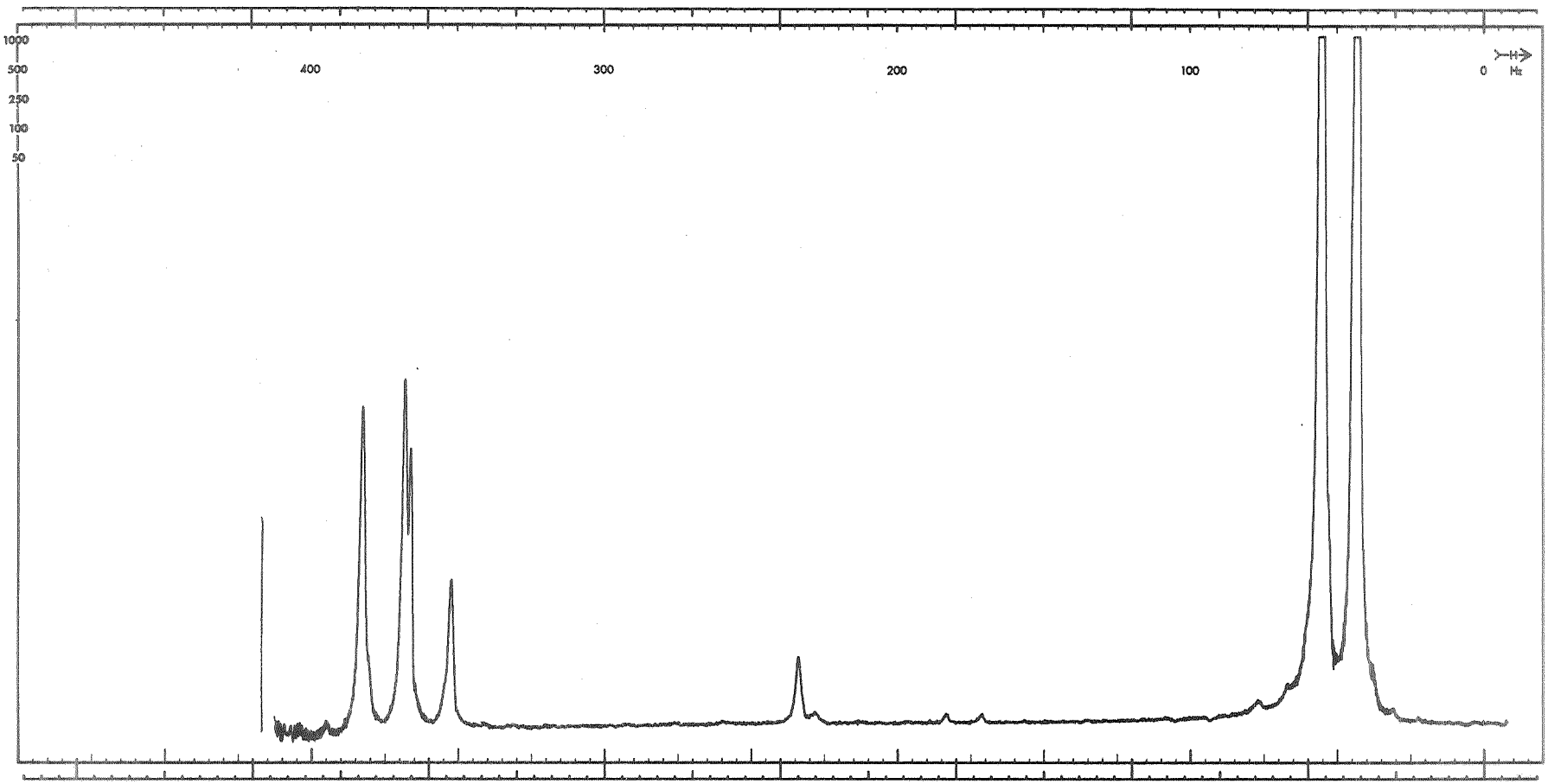

Fig. 38. ^{1}H NMR Spectra In 1M $AlCl_3$ #4 + 0.6 M LiCl #3/PC #7-4 & 0.15 M DMSO #1-1

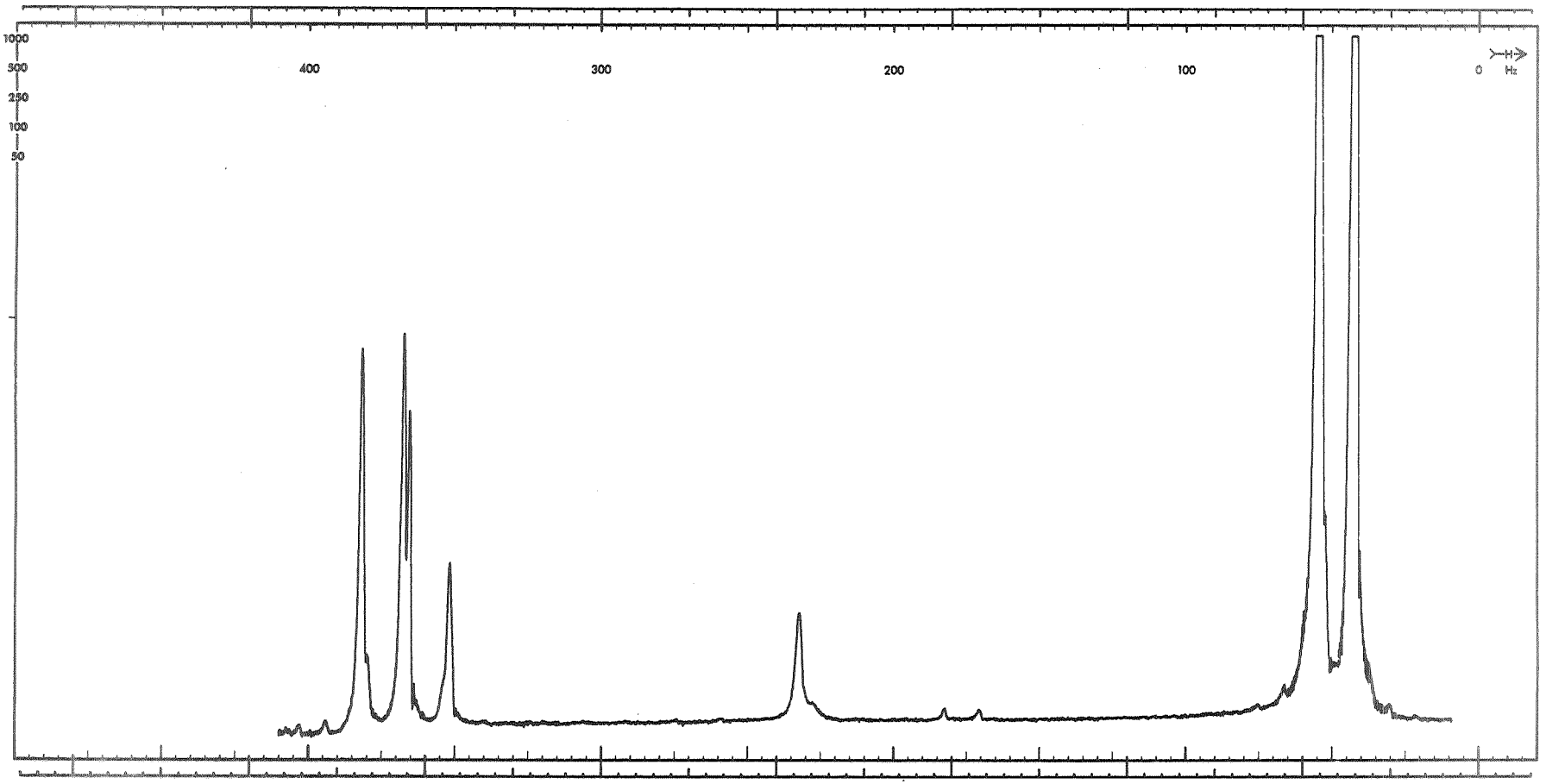

Fig. 39. ^{1}H NMR Spectra In 1M $AlCl_3$ #4 + 0.6 M LiCl #3/PC #7-4 & 0.3 M DMSO #1-1

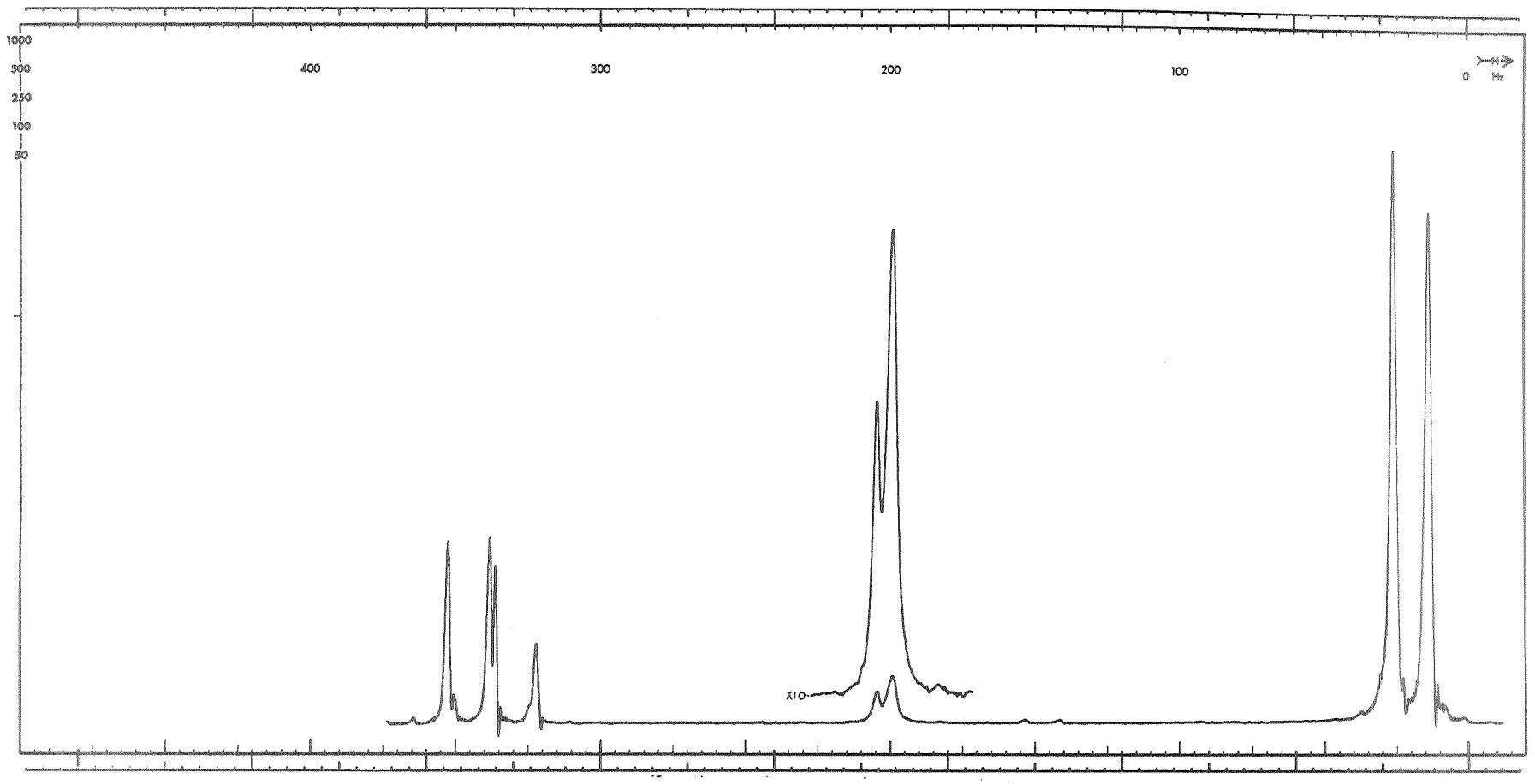

Fig. 40. ^{1}H NMR Spectra In 1M $AlCl_3$ #4 + 0.6 M LiCl #3/PC #7-4 & 0.5 M DMSO #1-1

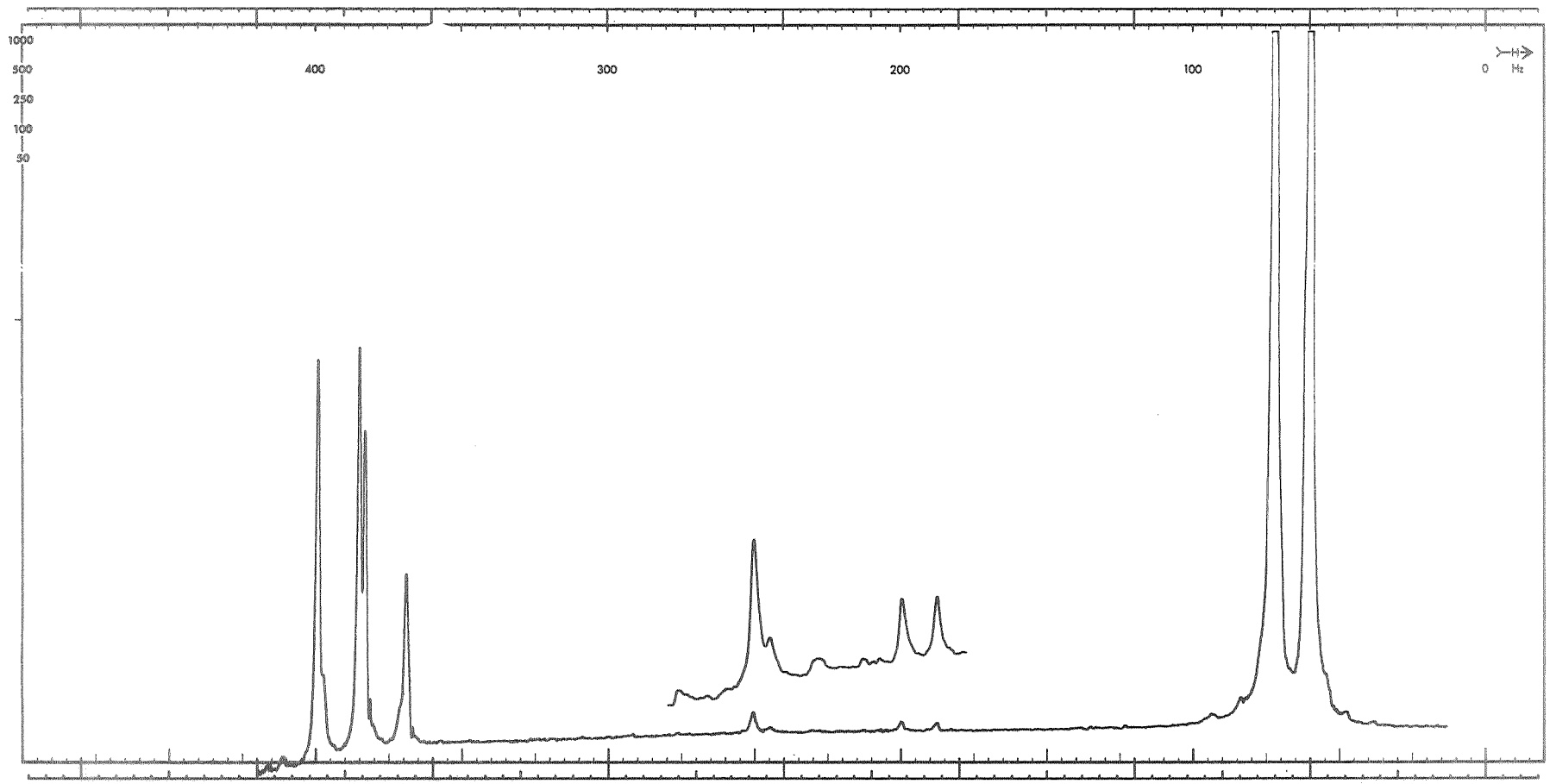

Fig. 41. ^{1}H NMR Spectra In 1M $AlCl_3$ #4 + 0.8 M LiCl #3/PC #7-4 & 0.05 M DMSO #1-1

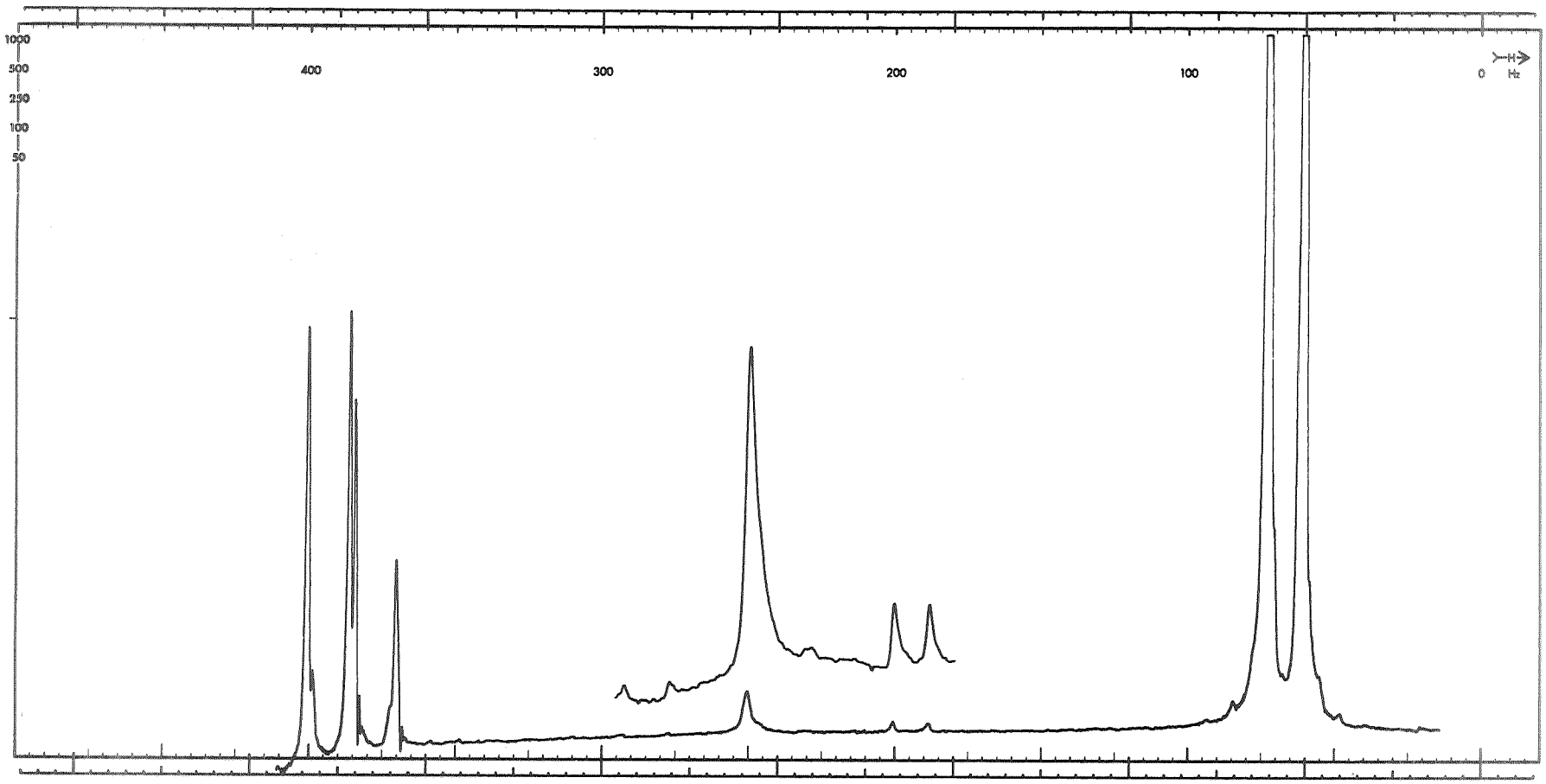

Fig. 42. ^{1}H NMR Spectra In 1M $AlCl_3$ #4 + 0.8 M LiCl #3/PC #7-4 & 0.15 M DMSO #1-1

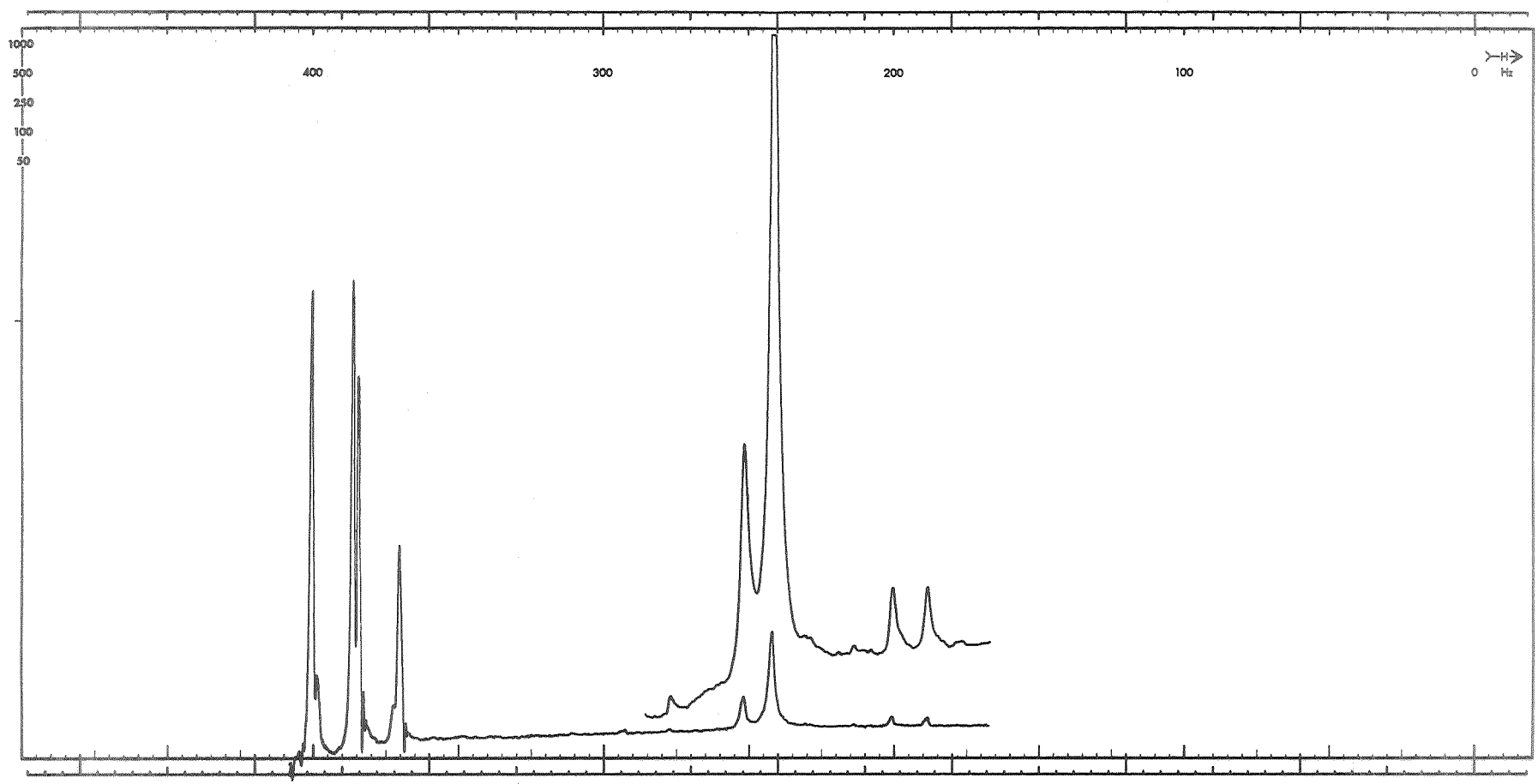

Fig. 43. ^{1}H NMR Spectra In 1M $AlCl_3$ #4 + 0.8 M LiCl #3/PC #7-4 & 0.30 M DMSO #1-1

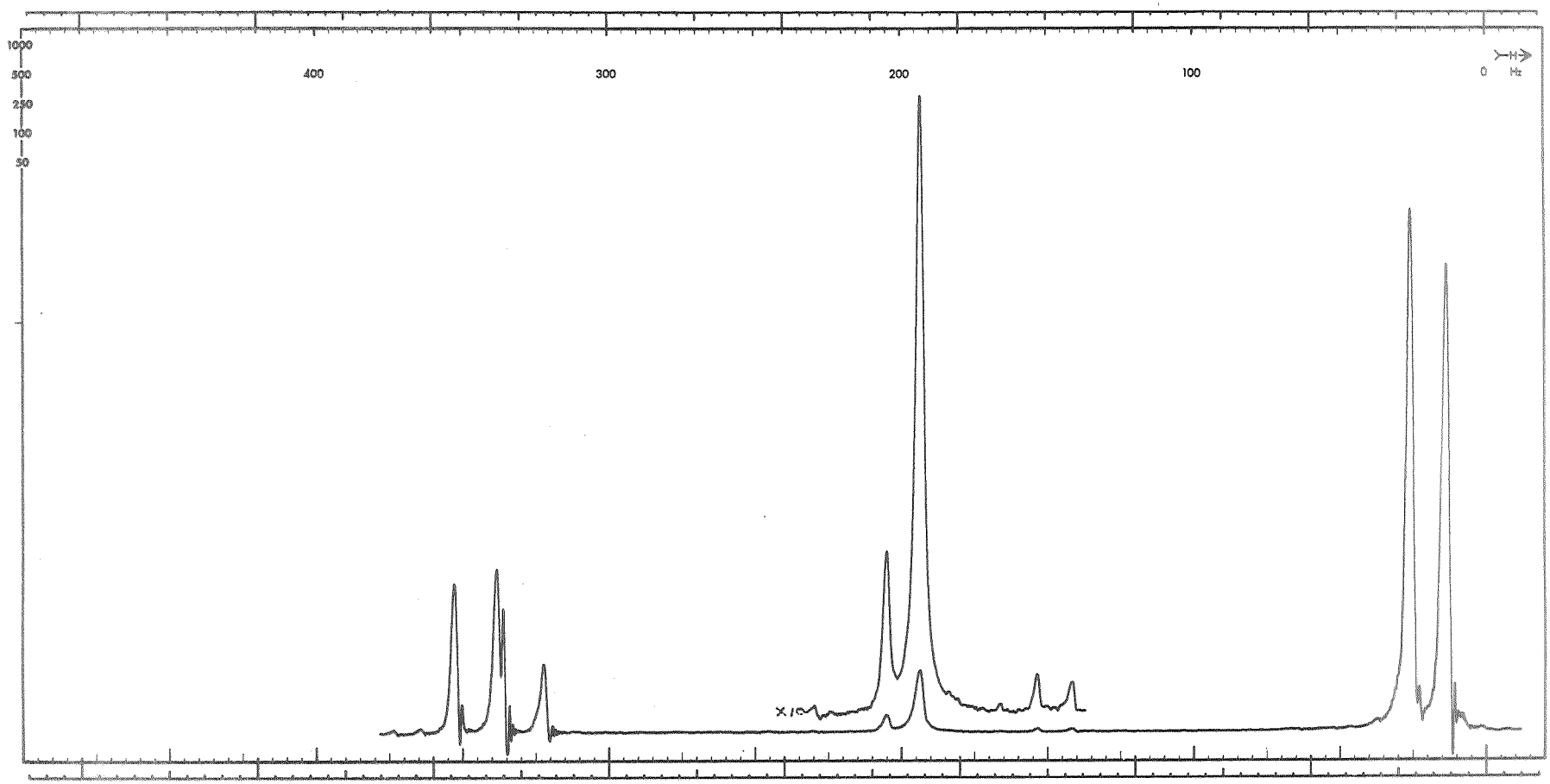

Fig. 44. ^{1}H NMR Spectra In 1M $AlCl_3$ #4 + 0.8 M LiCl #3/PC #6-6 & 0.5 M DMSO #1-1

comparison. Data taken as a function of temperature are also shown. Figures are included in this rather extensive collection of spectra, which are not discussed individually, so that the reader may have available to him additional data for future reference.

Figure 9 shows the proton spectrum obtained from a specimen containing 20% DMSO volume percent in PC to provide a comparative basis for the addition of DMSO to electrolytes. The DMSO peak is the largest peak near the center of the figure. Figures 10, 11, 12, 13, 19, and 24 show the spectra for increasing concentrations of DMSO in 1 M $AlCl_3$/PC. Of note is the decrease in intensity of the peaks due to coordinated PC (these are the two small peaks just downfield to the left from the PC methyl proton peaks which constitute the prominent doublet at the far right of the spectra) and the character of the DMSO peak which is the peak in the center of the spectra. This peak is displaced downfield from its position in pure PC as shown in Figure 9. At all concentrations other than the lowest (0.05 M DMSO) the DMSO proton spectra are complex, consisting of more than one line (in some cases, the lines are not resolved), showing the presence of more than one DMSO species. (uncoordinated DMSO is considered in this discussion to be a separate possible species.) At 0.5 M DMSO, Figure 7, the coordinated PC peaks are no longer observed. This is consistent with the broadline ^{27}Al results described above.

Figure 14 shows the spectrum obtained in the 0.5 M DMSO specimen three months after that shown in Figure 13. The DMSO portion of the spectrum is broadened suggesting that some changes have occurred. Changes with time have been clearly observed when DMF is added, as will be discussed later.

For 0.7 M and 0.9 M DMSO added to 1 M $AlCl_3$/PC, Figures 16 and 18 show the DMSO portion at lower temperatures, of the spectra shown in Figures 15 and 17. The two lines broaden due to increase in viscosity with lower temperatures. Figure 21 shows the DMSO spectra with the scale expanded over that in Figure 20 for 1.1 M DMSO at +30, +10 and -10 C. The sharpening of the lines observed at +10 C compared to the +30 C spectra indicates exchange is occurring. Further reduction of temperature broadens the lines due to viscosity effects. Figure 23 which shows the DMSO spectra with the scale expanded relative to that in Figure 22 shows large variations in the DMSO spectra as the temperature is decreased. There appear to be four different DMSO lines, depending upon the temperature. This could result from exchange effects and/or changes in equilibrium as the temperature is varied. Figures 24, 25, and 26 show the ^1H spectra for 1.5 M DMSO in 1 M $AlCl_3$/PC at ambient temperature, at -10 C, and at +30, +10 and -10 C for the DMSO part of the spectra, in an expanded scale, respectively. This shows that there are at least three DMSO species depending upon temperature due either to changes in exchange rates or changes in equilibria.

Figure 27 shows the ^{1}H spectra for 1 M $AlCl_3$/PC and 2 M DMSO. In this specimen a white precipitate formed so that the actual concentration of DMSO may be less than 2 molar.

Figures 28 through 44 show the ^{1}H spectra for 1 M $AlCl_3$/PC with LiCl in several concentrations, with DMSO added. Qualitatively, these spectra show the same characteristics as those with no LiCl except that as the concentration of LiCl increases, with the resultant decrease in the concentration of $Al[PC]_6^{+3}$; the concentration of DMSO which causes similar change in the spectra decreases accordingly.

The acquisition of another r.f. unit permitted obtaining some high resolution ^{27}Al spectra. In general, the information obtained was the same as that obtained using the broadline spectrometer. The one exception was that of 1 M $AlCl_3$/PC with DMSO added. In 1 M $AlCl_3$/PC with 1.3 M DMSO added, a third ^{27}Al line was observed. This line is low in intensity and has about the same chemical shift as the solvent coordinated ^{27}Al line. It is also found in 1 M $AlCl_3$/PC and 1.5 M DMSO but is reduced in intensity. Thus in these solutions at least three different aluminum containing species are present. The concentration of the third aluminum containing species was only a few percent of that of the solvent coordinated ^{27}Al species; the species was not identified.

The addition of DMSO to LiCl+$AlCl_3$/PC results in the formation of several DMSO containing complexes at intermediate concentration. At high concentrations (>1 M) complexes depleted of PC began to predominate.

DMF As Additive. DMF added to LiCl+$AlCl_3$/PC behaves in a similar fashion as DMSO, at least at times shortly after solution preparation. After long times, other effects were noted which will be discussed later.

The broadline ^{27}Al spectra for a series of solutions containing LiCl and DMF in various concentrations are essentially the same as those shown for DMSO in Figure 7. With increasing DMF concentrations, the line due to $Al[PC]_6^{+3}$ disappears at low DMF concentrations, and at high DMF concentrations a line ascribed to $Al[DMF]_6^{+3}$ appears. The chemical shift difference in this case is just observable, being less than that observed in the case of $Al[DMSO]_6^{+3}$. The rate at which the $Al[PC]_6^{+3}$ line decreases with increasing DMF concentration is less than in the case of DMSO addition, indicating that while DMF readily displaces PC in the Al^{+3} coordination sphere it does not displace PC as readily as does DMSO. Also at high DMF concentrations the rate of appearance of $Al[DMF]_6^{+3}$ with increasing DMF is somewhat slower than that of $Al[DMSO]_6^{+3}$, which further indicates that DMF does not displace PC as readily as DMSO.

Several high resolution ^{1}H spectra are shown in Figures 45 through 54. Figures 45 shows a portion of the spectra obtained from PC containing 0.5 M DMF (the upper trace) and 2.0 M DMF (the lower trace). The pair of peaks near the center* is due to the methyl proton in DMF. The methyl proton line in PC, which is not shown, would be at the extreme right. The DMF formyl proton line is to the left (off the figure) of the large number of PC peaks which are at the left of the figure.

The DMF formyl proton peak is displayed above the group of PC peaks separately by shifting the scan region. Figure 46 shows the complete spectra for 0.5 M DMF in 1 M $AlCl_3$/PC. The two DMF methyl proton peaks are shifted downfield, relative to the PC spectra, from their position in Figure 45 , indicating that the DMF is being coordinated by Al^{+3}. Figure 47 shows the two DMF methyl proton peaks on an expanded scale for several DMF concentrations in 1 M $AlCl_3$/PC. At low concentrations the lines appear to have some structure, suggesting that there is more than one DMF containing species. Figures 48 through 51 show the PC methyl proton peaks in 1 M $AlCl_3$/PC for DMF concentrations of 0.05 M, 0.15 M, 0.30 M and 0.50 M. In the 0.05 M DMF scan, the two peaks to the left of the large peaks are the peaks due to PC coordinated by Al^{+3}. These peaks decrease in intensity as the DMF concentration increases. At 0.50 M DMF these peaks have almost disappeared showing that DMF displaces PC from Al^{+3}. The monotonically increasing (from left to right) curve in these figures is the integral of the spectrum.

Figure 52 shows the spectrum obtained from 1 M $AlCl_3$/PC with 2 M DMF added. There are two noteworthy features. First, the large group of PC lines are sharper which indicates a lack of interaction of PC with Al^{+3} and there is structure on the DMF methyl proton doublet lines. The DMF methyl proton doublet lines are shown in Figure 53 with an expanded scale. This shows that at this DMF concentration there is more than one DMF species.

Spectra were run on a series of 1 M $AlCl_3$/PC electrolytes containing various concentrations of LiCl and DMF. These spectra were consistent with the picture that as LiCl is added the concentration of $Al[PC]_6^{+3}$ is diminished and as a result less DMF was required to displace PC from $Al[PC]_6^{+3}$.

The above discussion relates to the LiCl+$AlCl_3$/PC electrolytes containing DMF, shortly after the specimens were prepared. Several spectra were re-run about 4 months later. At that time the distribution of species containing DMF had appreciably changed. It was observed that the ^{27}Al spectrum no longer consisted of a narrow $AlCl_4^-$ line and a smaller somewhat broader $Al[PC]_6^{+3}$ line as shown in Figure 7, but instead there was just one rather broad line. This indicates a lack of $AlCl_4^-$. The high resolution proton spectra had changed as well. Figure 54 shows the spectra for 1 M $AlCl_3$/PC and

*These peaks are indicated with a dot above them.

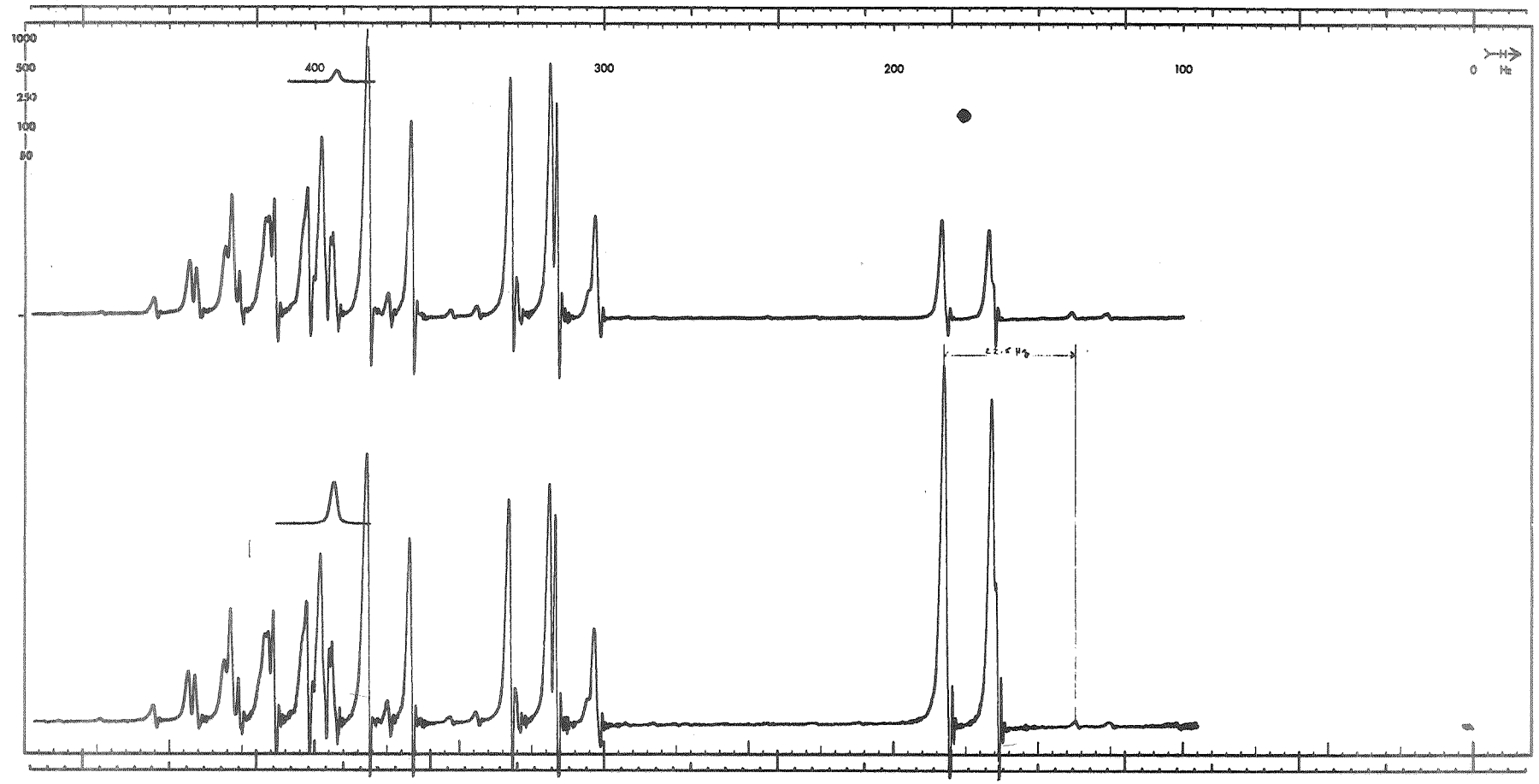

Fig. 45. ^{1}H NMR Spectra in PC #6-5 With 0.5 M and 2.0 M DMF #7-3 Added

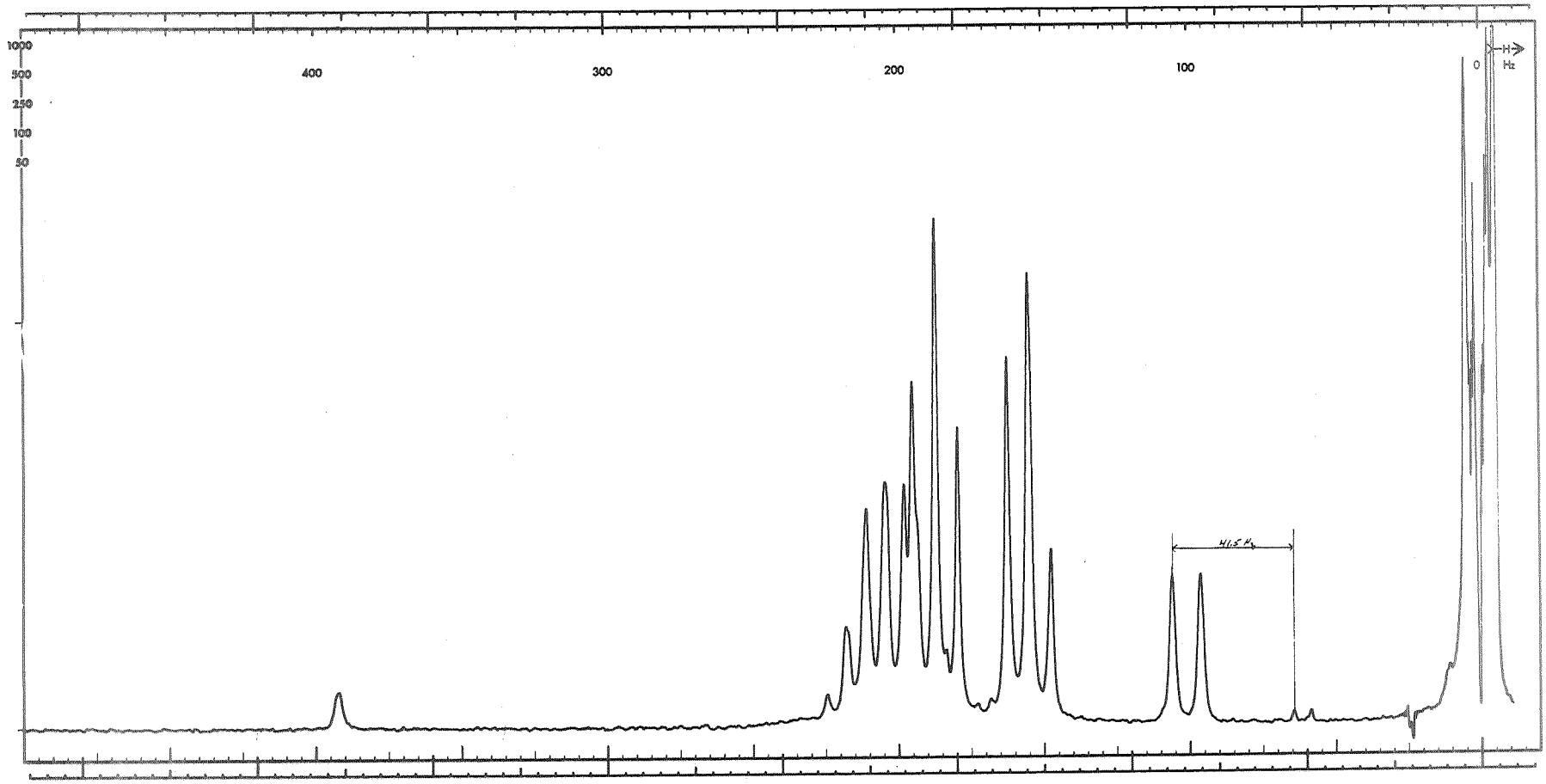

Fig. 46. ^{1}H NMR Spectrum in 1M $AlCl_3$ #4/PC #6-5 & 0.50 M DMF #7-3

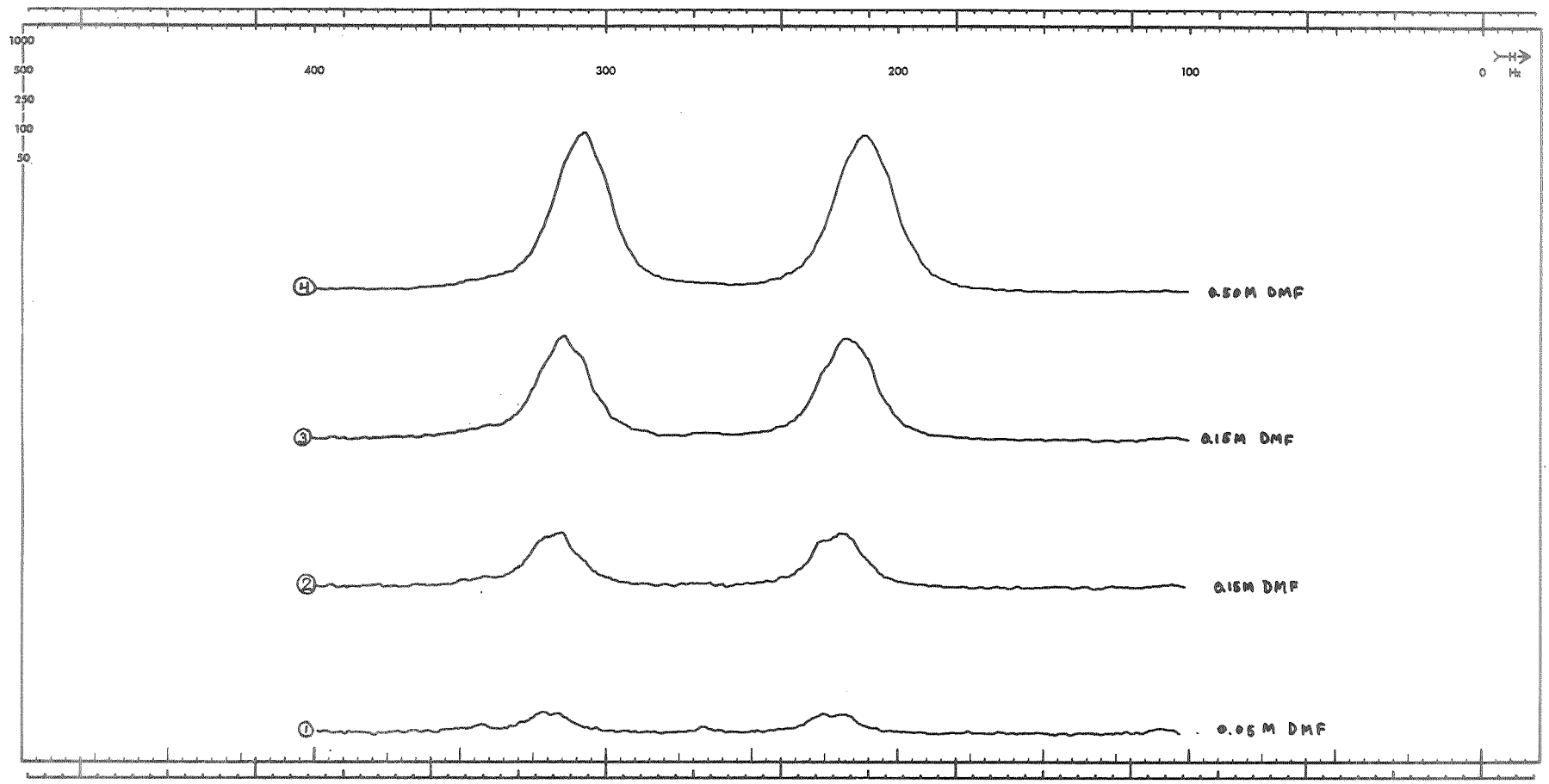

Fig. 47. ^{1}H NMR Spectra in 1M $AlCl_3$ #4/PC #6-5 & Several Concentrations of DMF #7-3. Expanded Scale at DMF Methyl Proton Doublet

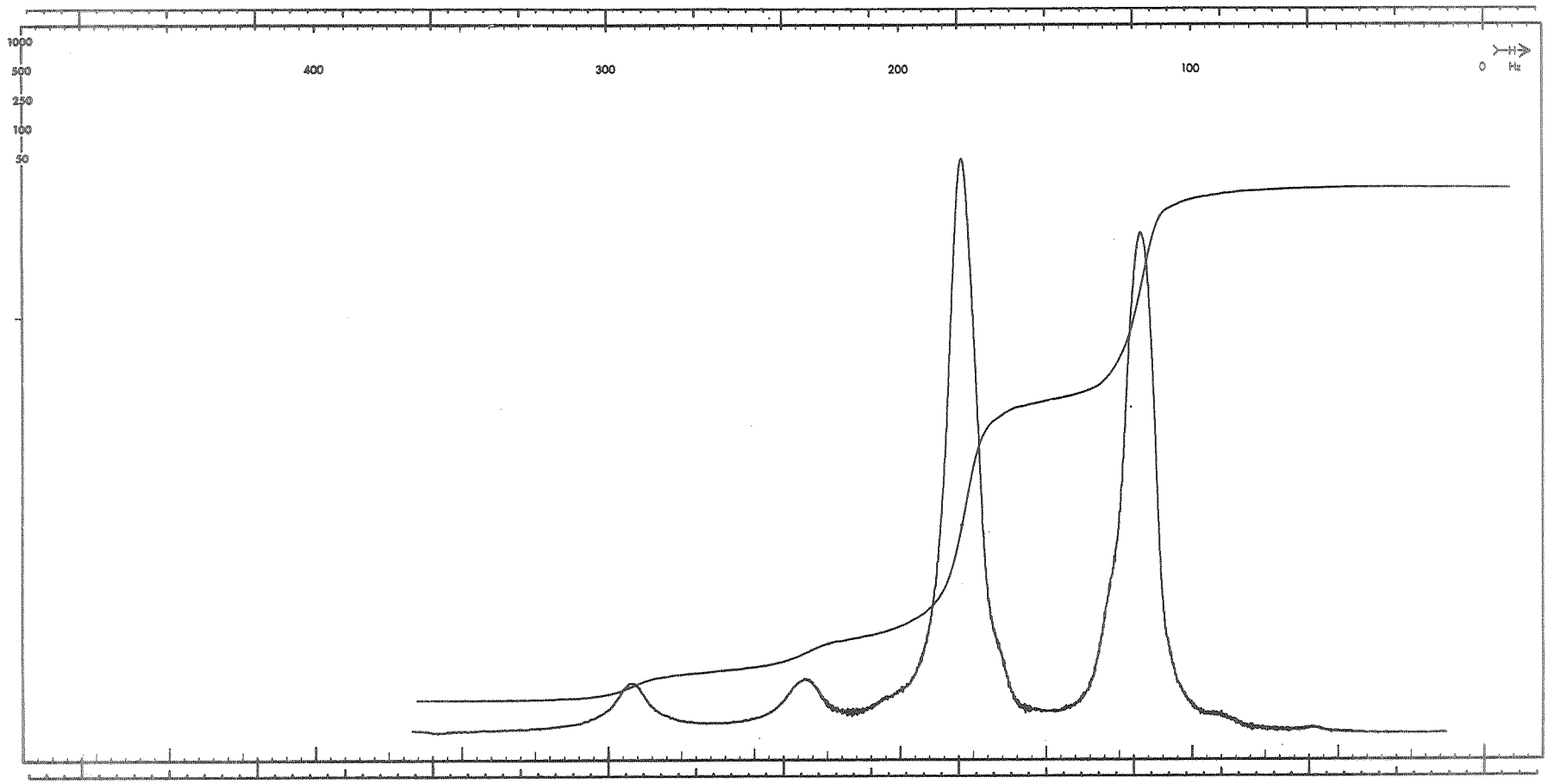

Fig. 48. ^{1}H NMF Spectrum in 1M $AlCl_3$ #4/PC #6-5 & 0.05 M DMF #7-3. Expanded Scale at PC Methyl Proton Doublet

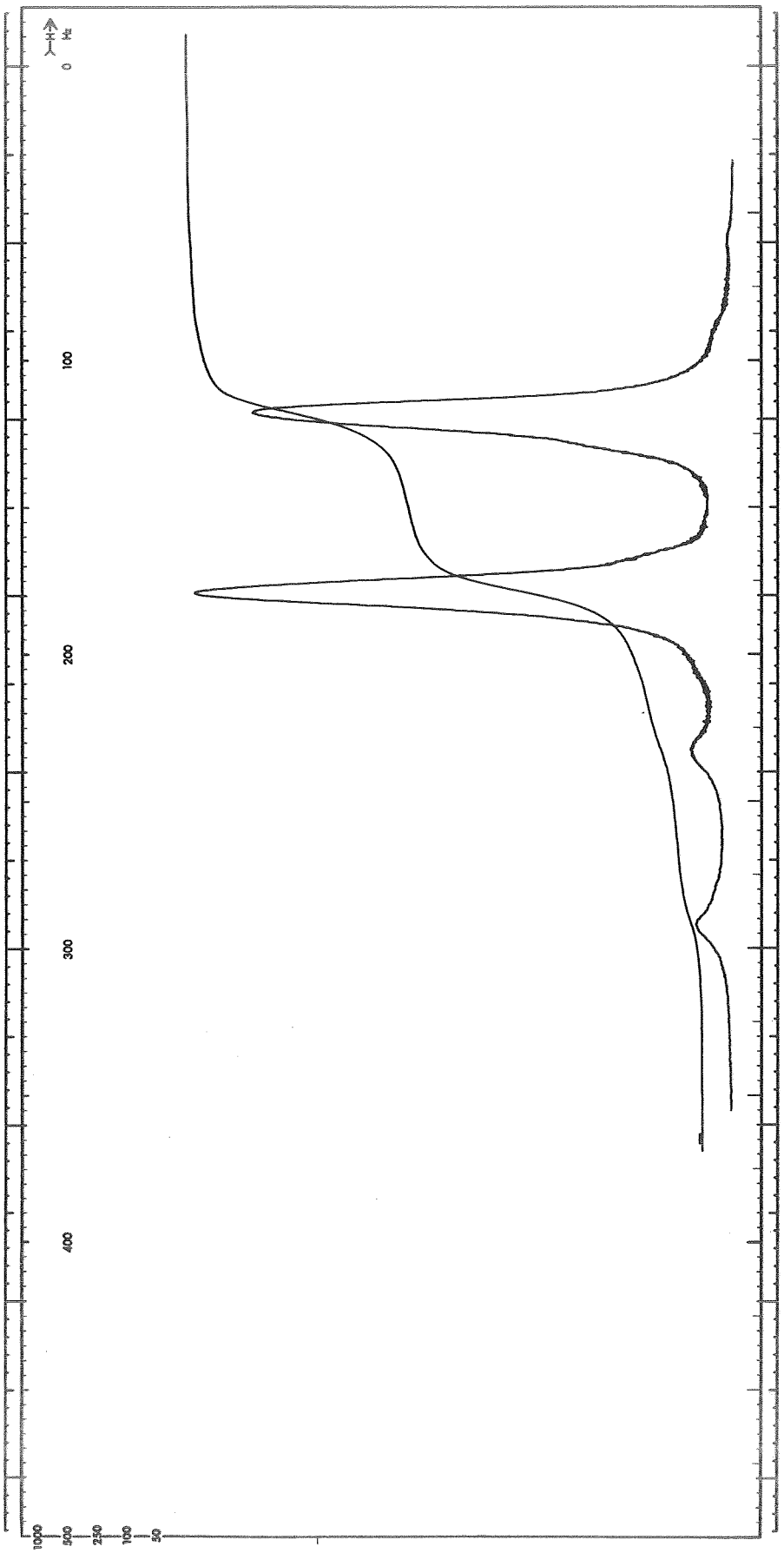

Fig. 49. ^{1}H NMF Spectrum in 1M $AlCl_3$ #4/PC #6-5 & 0.15 M DMF #7-3.
Expanded Scale at PC Methyl Proton Doublet

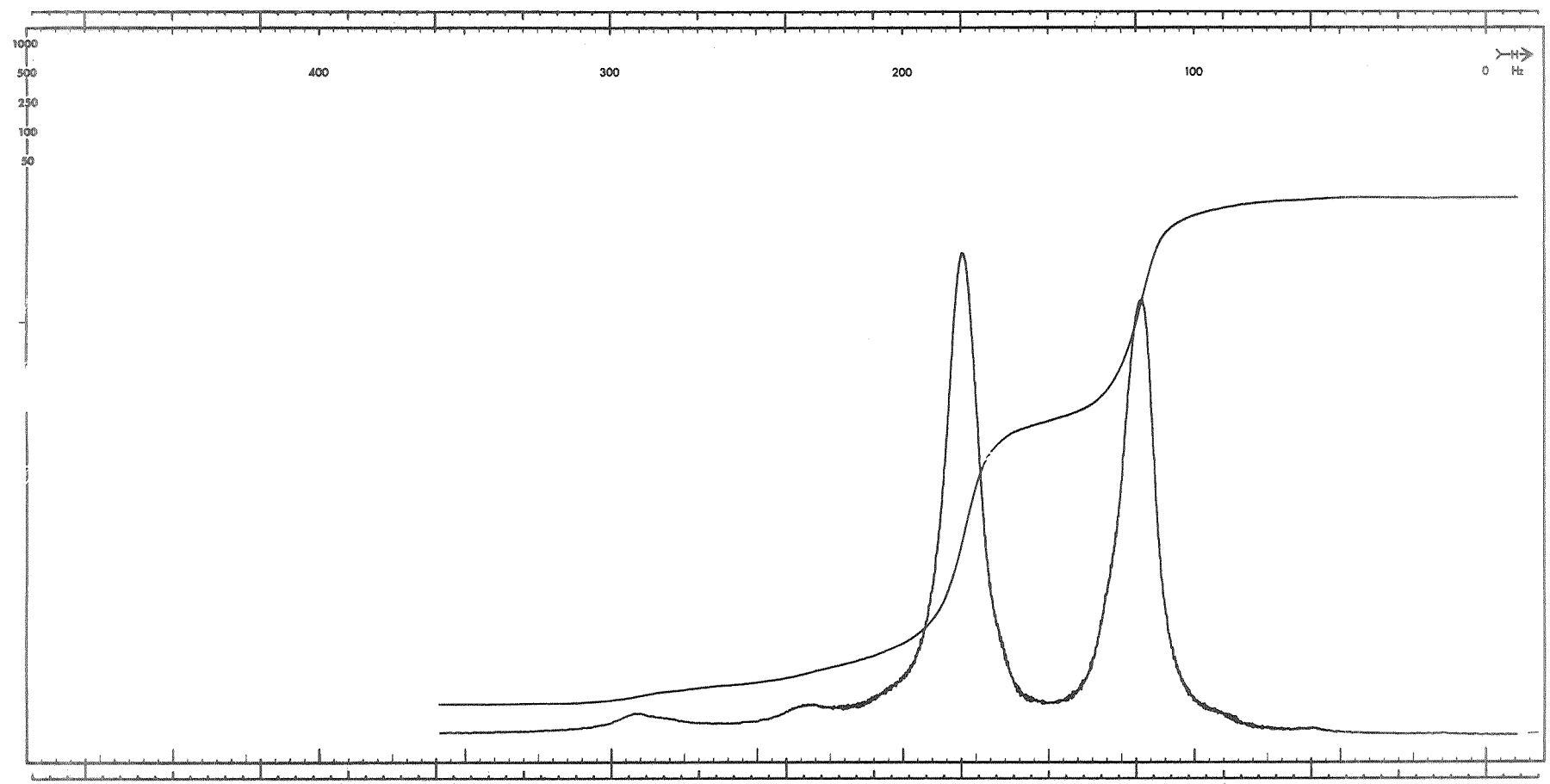

Fig. 50. ^{1}H NMR Spectrum in 1M $AlCl_3$ #4/PC #6-5 & 0.30 M DMF #7-3. Expanded Scale at PC Methyl Proton Doublet

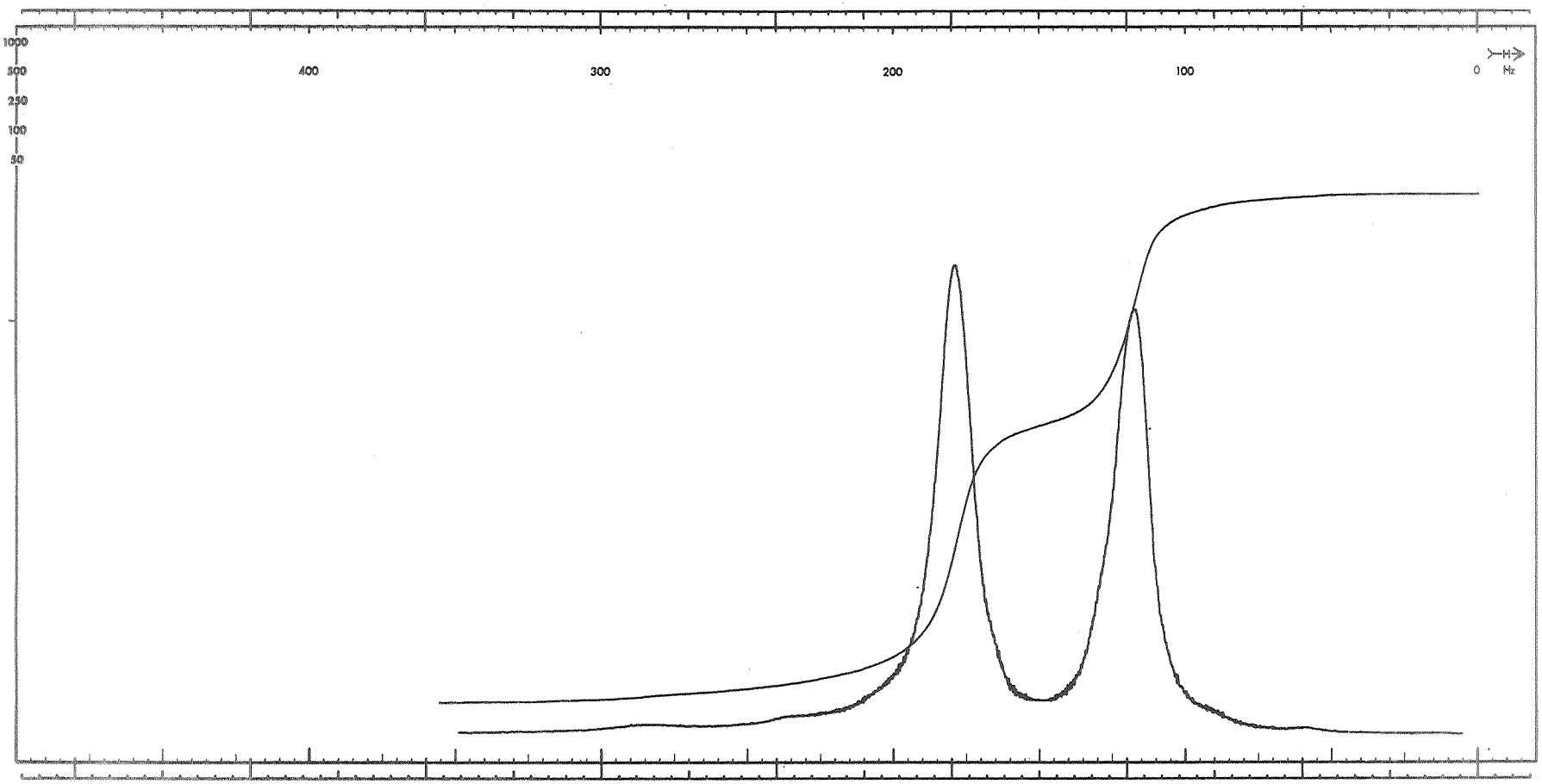

Fig. 51. ^{1}H NMR Spectrum in 1M $AlCl_3$ #4/PC #6-5 & 0.50 M DMF #7-3. Expanded Scale at PC Methyl Proton Doublet

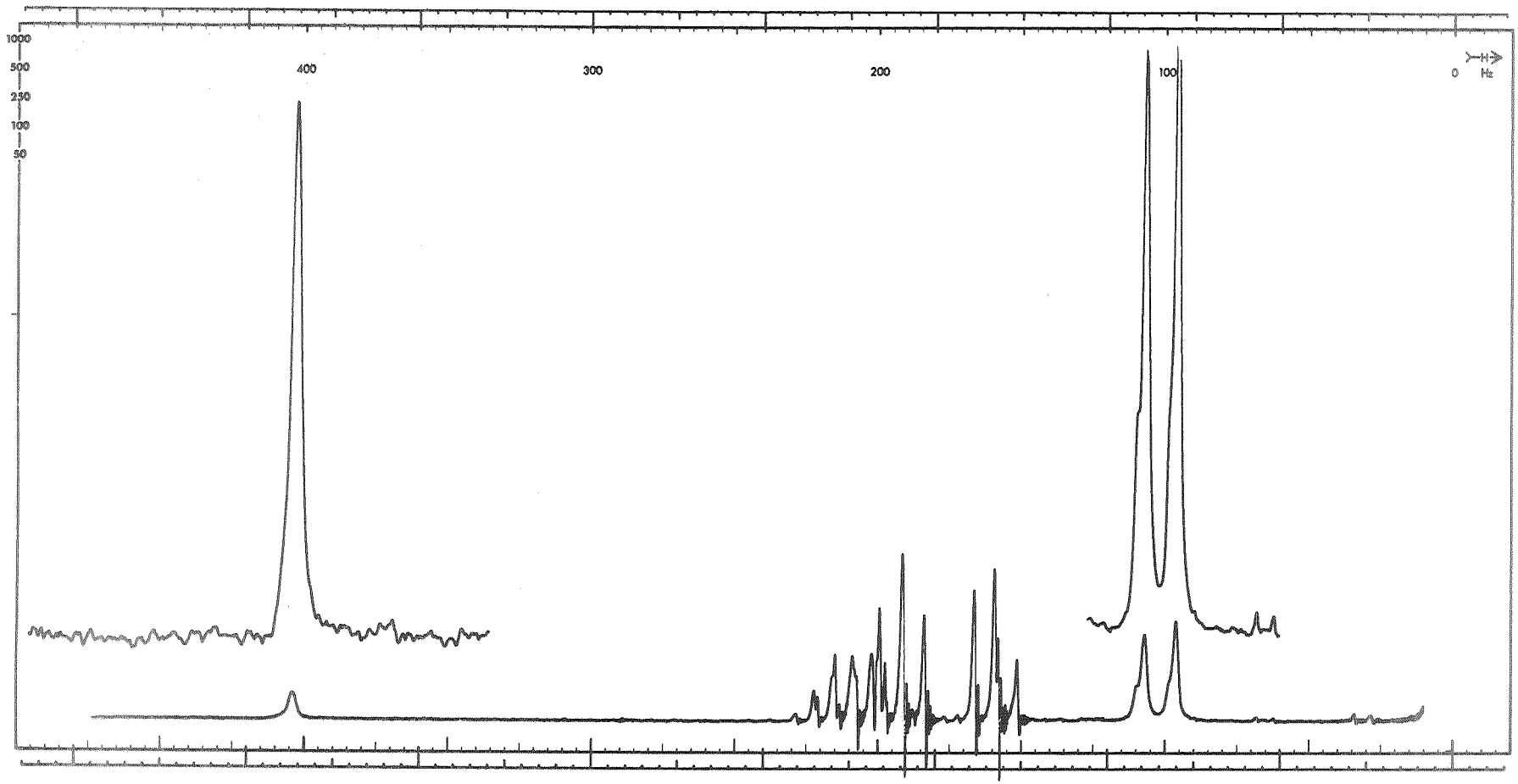

Fig. 52. ^{1}H NMR Spectrum in 1M $AlCl_3$ #4/PC #6-5 & 2.0 M DMF #7-3

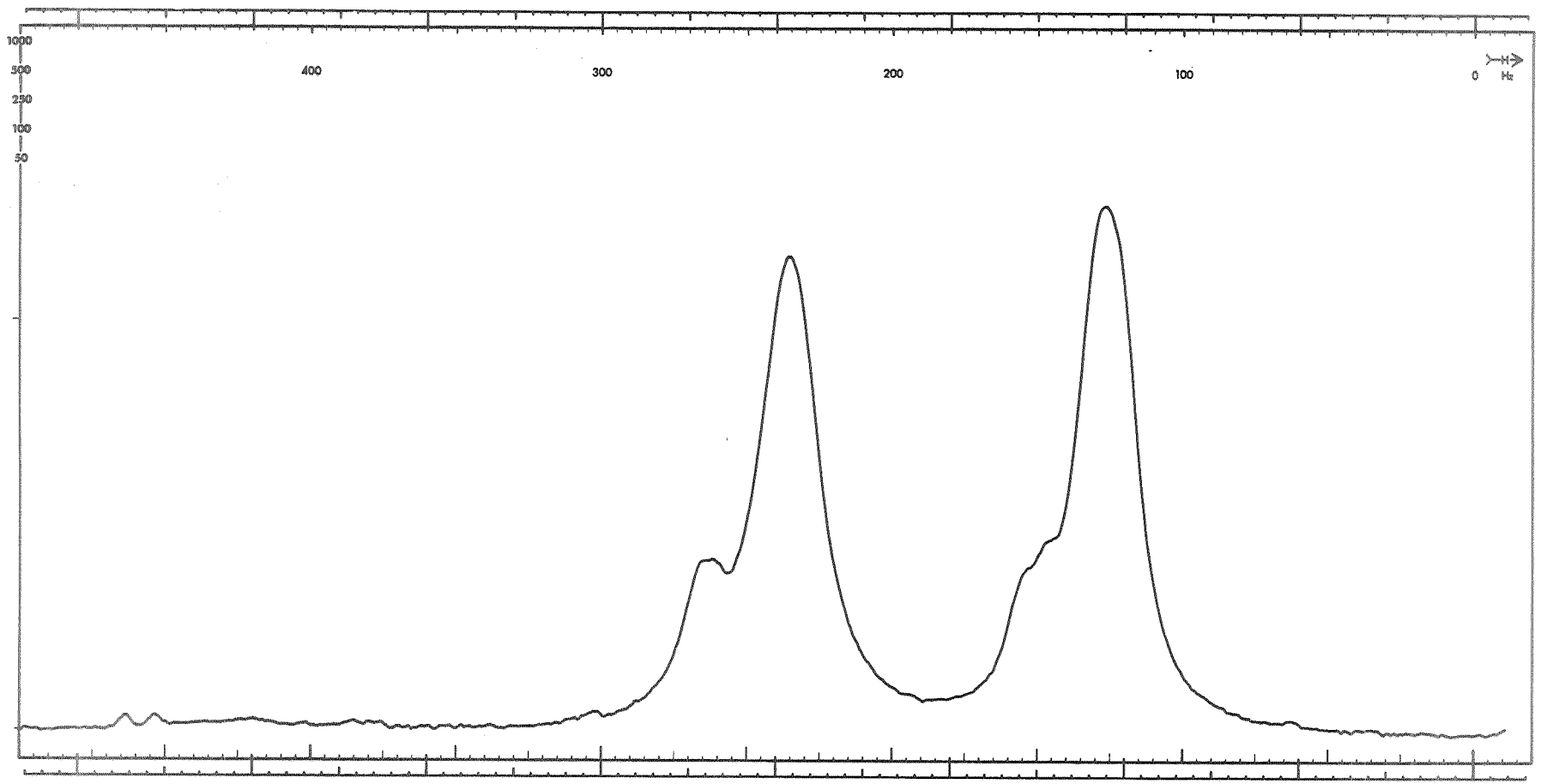

Fig. 53. ^{1}H NMR Spectrum in 1M $AlCl_3$ #4/PC #6-5 & 2.0 M DMF #7-3. Expanded Scale at DMF Methyl Proton Doublet

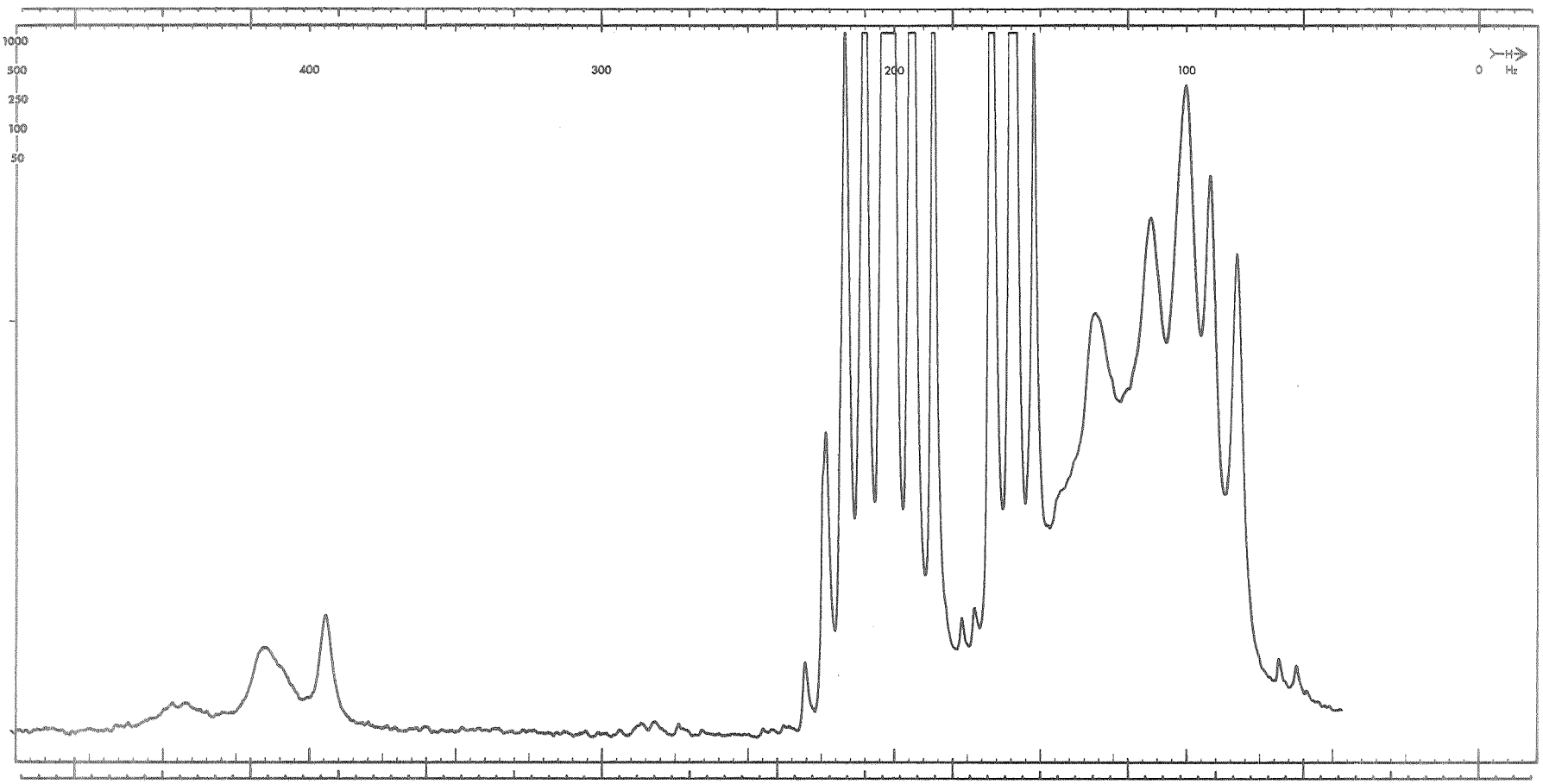

Fig. 54. ^{1}H NMR Spectrum in 1M $AlCl_3$ #4/PC #6-4 & 2.0 M DMF #7-3

2 M DMF. In particular, note the spectrum of the DMF formyl proton at the left of the scan. There are clearly three peaks, a narrow peak at the right, a large broader peak in the center and a smaller broader peak to the left. This shows that there are at least three different DMF containing species. Figure 55 shows the spectra from the same specimen with attention to the region of the DMF methyl proton peaks. Spectra are shown for several specimen temperatures of +30, +20, +10, 0 and -10 C. At the lowest temperature (the top spectrum) the two sharp DMF methyl proton peaks have the same chemical shift relative to PC as they exhibit with no $AlCl_3$ present as in Figure 45. To the left of the sharp doublet is a broad doublet which has a downfield chemical shift somewhat larger than that of DMF coordinated by Al^{+3}. Further downfield (to the left) is a broad line that appears to be a broad doublet at +30 C, and that broadens further at low temperatures. This broadening is probably a viscosity effect. These data have been given the following interpretation. When such specimens are first prepared, the DMF displaces the PC from the $Al[PC]_6^{+3}$ complex forming $Al[DMF]_6^{+3}$ complexes at high DMF concentrations. There are other complexes namely the mixed complexes, $Al\left[(PC)_x(DMF)_y\right]^{+3}$, as well. However, there is a slow equilibrium of these complexes with $AlCl_4^-$ towards the formation of bridged complexes such as

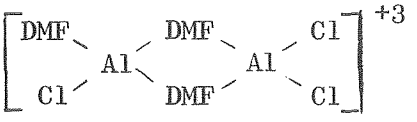

having the general composition

$$Al_2(DMF)_{6-x}(Cl)_x^{+(6-x)}$$

This reduces the stoichiometric concentration of DMF required to complex Al and thus produces bulk non-coordinated DMF which gives rise to the sharp doublet. DMF at an end position can exchange with bulk DMF so that the sharp doublet and the broad doublet broaden and begin to merge as the temperature increases. The bridged DMF is not free to exchange and therefore gives rise to the broad peak that gets broader as the temperature is lowered. Furthermore, the doublet character of the DMF methyl protons is due to hindered rotation about the C-N bond with the two possible positions having different chemical shifts. It is hypothesized that in the bridge position the methyl proton groups have been "frozen" in positions that have essentially the same chemical shift, thus giving rise to essentially a single broad line.

In summary, the addition of DMF to $AlCl_3$/PC changes the species in a rather complex fashion with the species distribution being time dependent. At early times there is simple displacement of coordinated PC by DMF. This distribution is then further changed by a slow

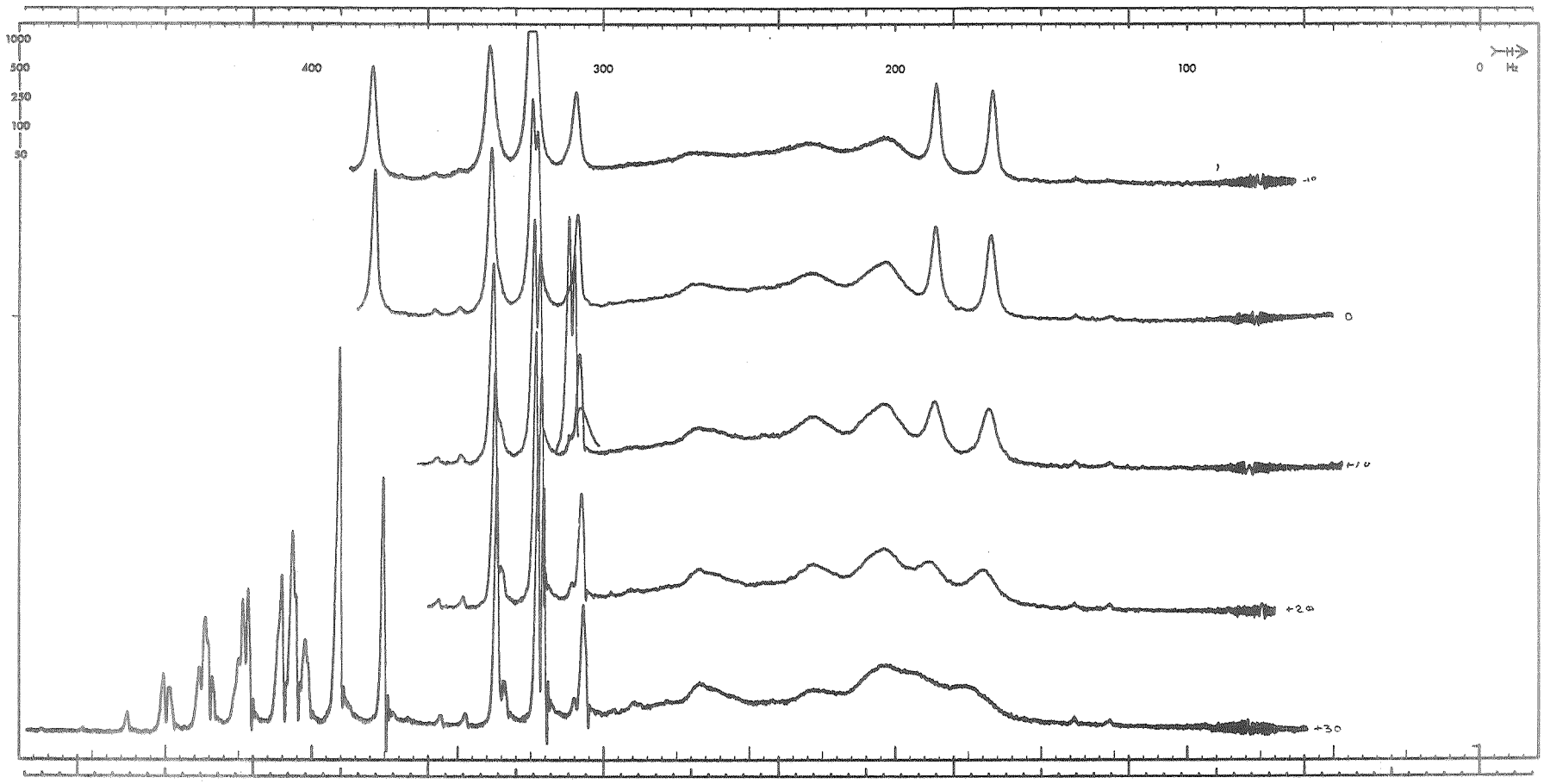

Fig. 55. ^{1}H NMR Spectrum in 1M $AlCl_3$ #4/PC #6-4 & 2.0 M DMF #7-3, Taken at +30, +20, +10, 0 and -10 C

equilibrium to another species. Both the ^{27}Al and the ^{1}H spectra are consistent with the types of species as described above.

AN As Additive. The broadline ^{27}Al spectra of $LiCl+AlCl_3/PC$ electrolyte containing 0.5 M, 1.5 M and 3 M AN were essentially the same as those without AN indicating that AN does not readily displace PC from $Al[PC]_6^{+3}$. Figure 56 shows the ^{1}H NMR reference spectrum in PC and 20 v/o AN. The two large peaks on the right are the PC methyl proton doublet. The AN peak is to the left of these peaks. Figure 57 shows the ^{1}H NMR spectrum for 1 M $AlCl_3/PC$ and 0.5 M AN. The coordinated PC peaks are the two small peaks to the left of the large PC methyl proton doublet. The next peak to the left is the AN peak which is at the same position as in Figure 56 showing no interaction with Al^{+3}. Figure 58 shows the ^{1}H NMR spectrum for 1 M $AlCl_3/PC$ and 1.5 M AN. The coordinated PC peaks are essentially the same. There is a large AN peak as before. Downfield from the bulk AN peak is a weak group of several peaks. Figure 59 shows the ^{1}H NMR spectrum for 1 M $AlCl_3/PC$ and 3 M AN. This spectrum is much like that in Figure 58 ; the most important feature is that coordinated PC peaks are still observed, though perhaps somewhat less intense, and the group of small lines downfield from the bulk AN peak is observed again. The group of weak lines observed in the 1.5 M and 3.0 M AN specimens just downfield from the large AN line is ascribed to mixed complexes $Al[(PC)_{6-x}(AN)_x]^{+3}$. There appear to be at least three such species. The intensity of these lines is low. It thus appears that AN does not readily displace PC from $Al[PC]_6^{+3}$ but can compete so that as the concentration of AN is increased some mixed species are produced. The effect of the addition of LiCl is not changed by the presence of AN.

MF As Additive. The ^{27}Al spectra for 1 M $AlCl_3/PC$ with up to 2 M MF added were not changed from that obtained from 1 M $AlCl_3/PC$ as shown in Figure 7a. This indicates that MF does not readily displace PC from $Al[PC]_6^{+3}$. The high resolution reference ^{1}H spectra for PC with 10 v/o MF added is shown in Figure 60. There are two peaks due to MF, the peak further to the left which is a quartet and the peak which is a doublet just to the right of the PC group. As MF is added to 1 M $AlCl_3/PC$, no change is noted in the PC portion of the spectra. As 2 M MF is added, the coordinated PC peaks remain essentially the same. At 2 M MF there is an additional small peak, as shown in Figure 61, which is downfield (to the left) of the MF quartet which appears as a single line in this figure. These two peaks are shown on an expanded scale in Figure 62. The gain for the right hand peak is, as noted, 1/10 of that for the peak on the left. The peak on the left is ascribed to MF in mixed $Al[(PC)_{6-x}(MF)_x]^{+3}$ species. This peak is shown again in Figure 63 on a further expanded scale and shows structure. This could be due to the occurrence of several mixed species or to the fact that in a mixed species the quartet nature of this line, which had been obscured by line broadening, is again observed. MF behaves, then, in a similar manner to AN. It does not displace PC readily but it does produce mixed complexes at higher concentrations. The effect of the addition of LiCl is not affected by the presence of MF.

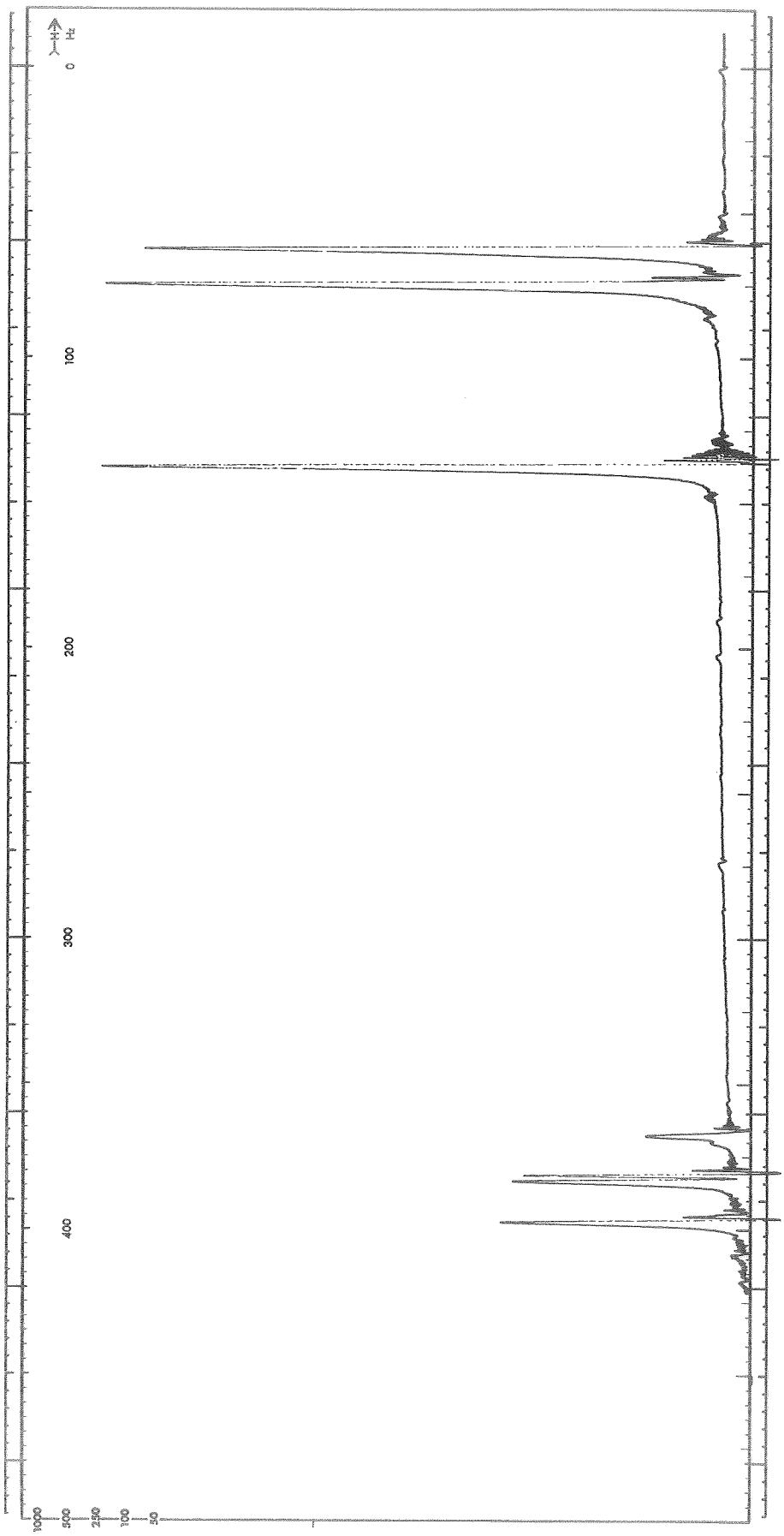

Fig. 56. ^{1}H NMR Spectrum In 20 $^{v}/o$ AN Added To PC #6-7

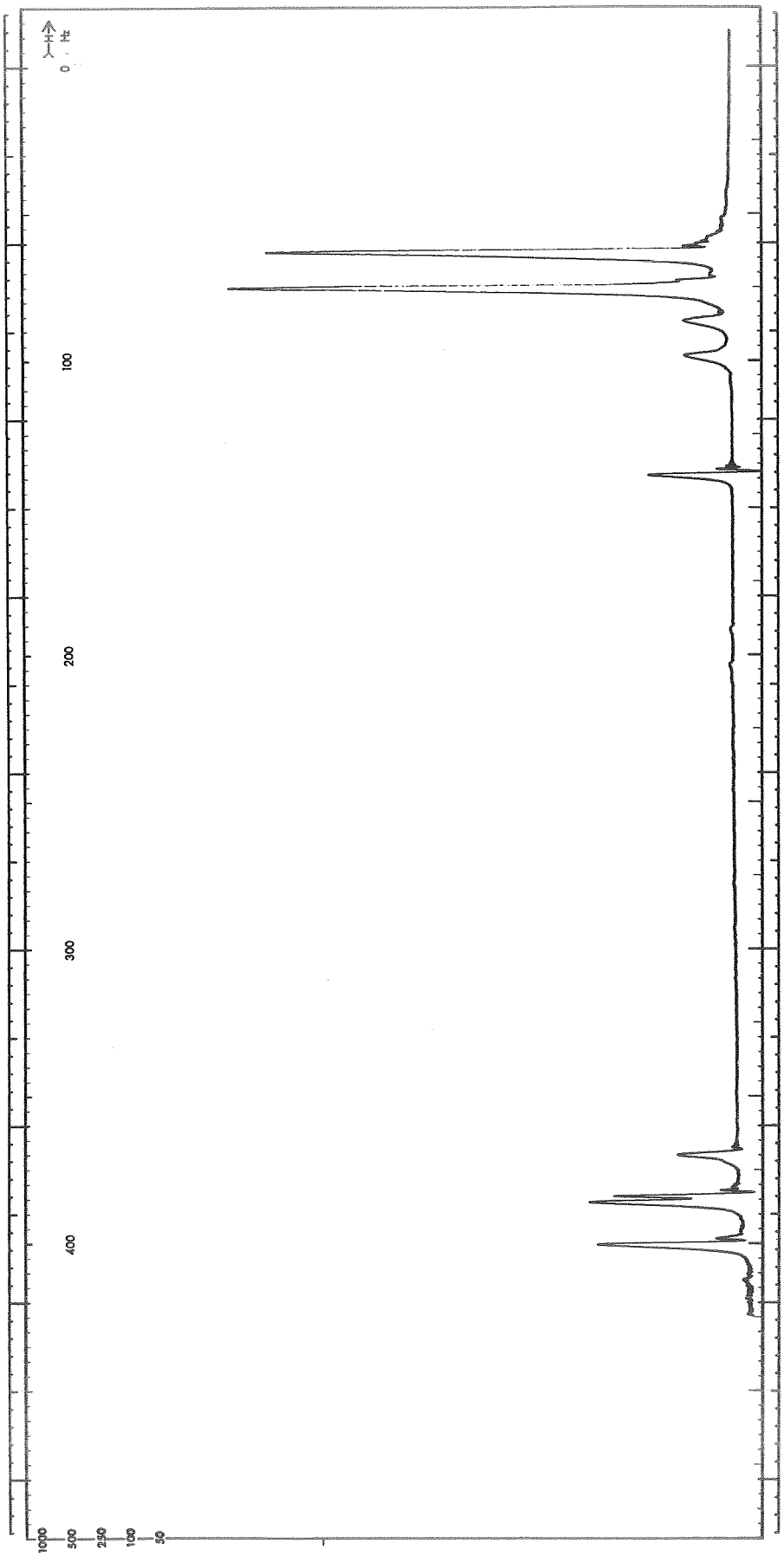

Fig. 57. ^{1}H NMR Spectrum In 1M $AlCl_3$ #4/PC #6-7 & 0.5 M AN #6-1

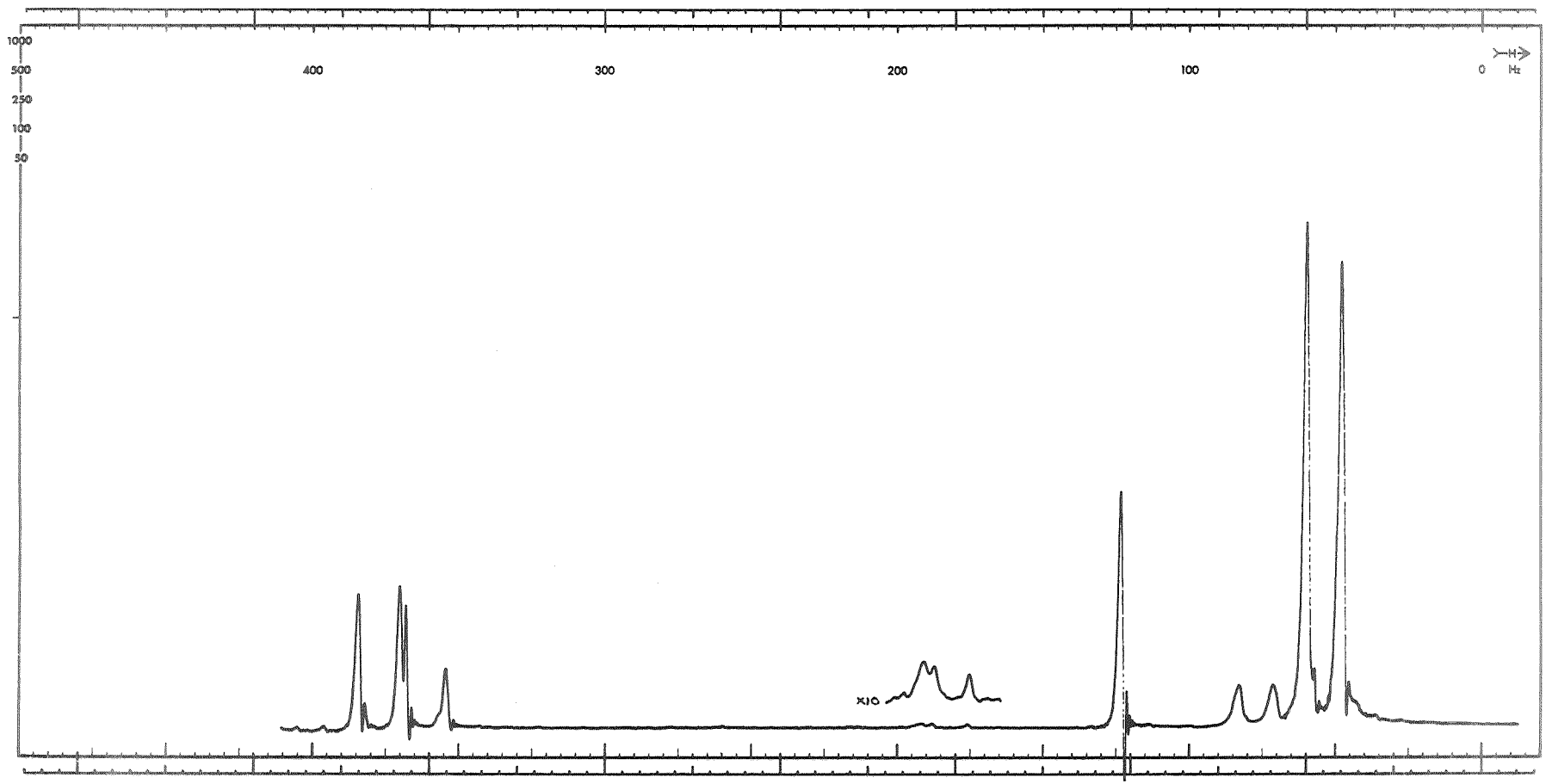

Fig. 58. ^{1}H NMR Spectrum In 1M $AlCl_3$ #4/PC #6-7 & 1.5 M AN #6-1

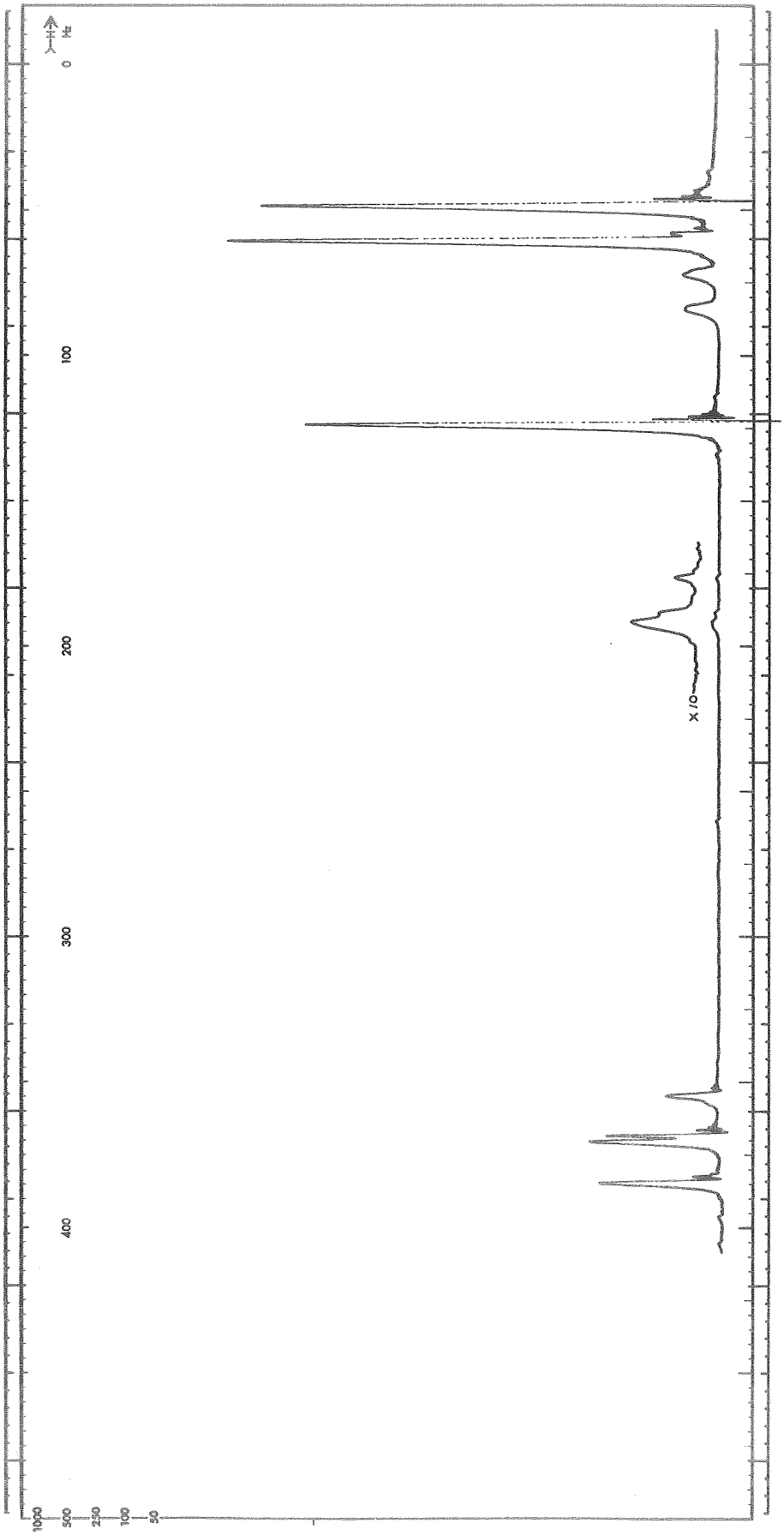

Fig. 59. ^{1}H NMR Spectrum In 1M $AlCl_3$ #4/PC #6-7 & 3.0 M AN #6-1

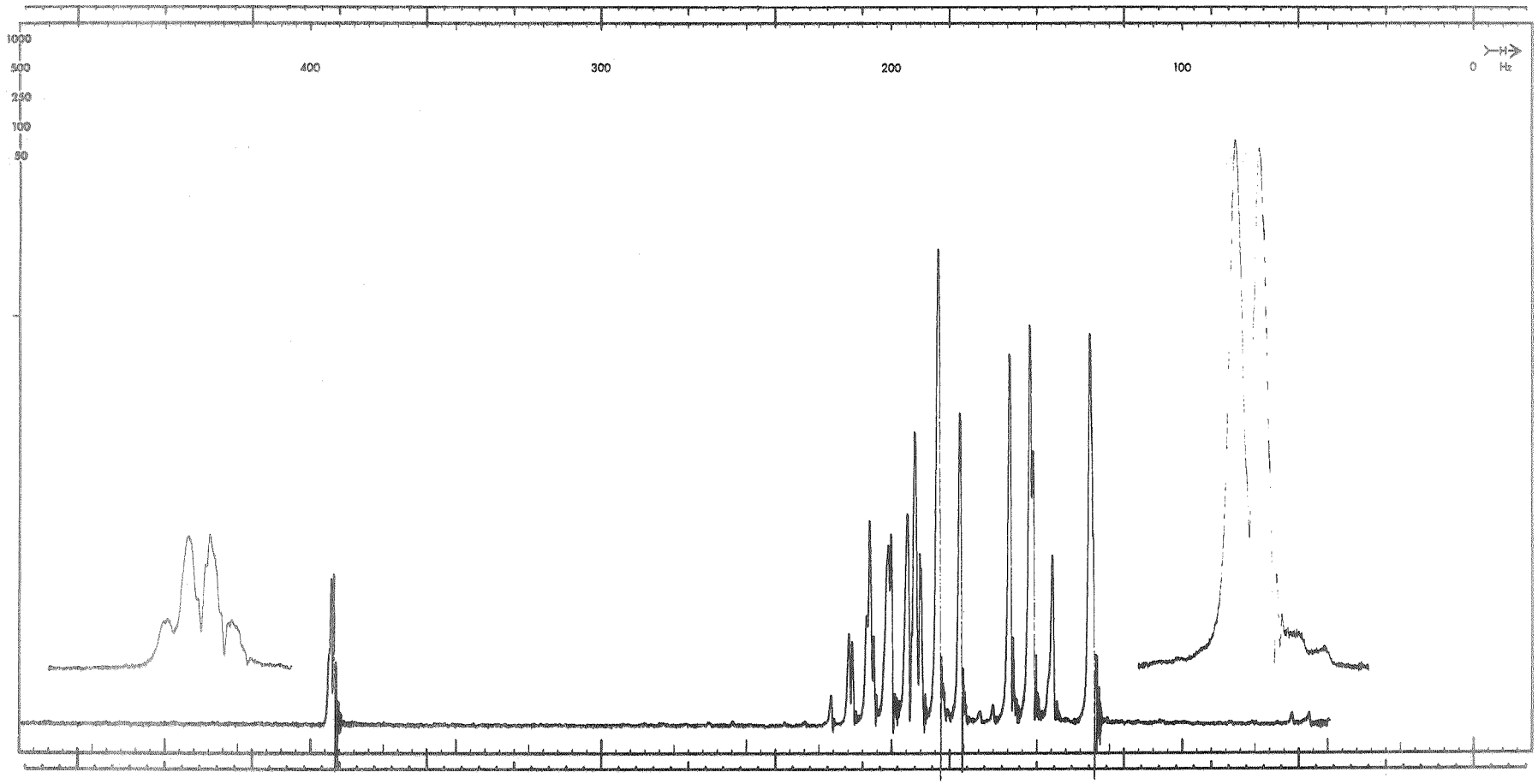

Fig. 60. ^{1}H NMR Spectrum In 10 $^{v}/_{o}$ MF #2-11 Added To PC #3-1

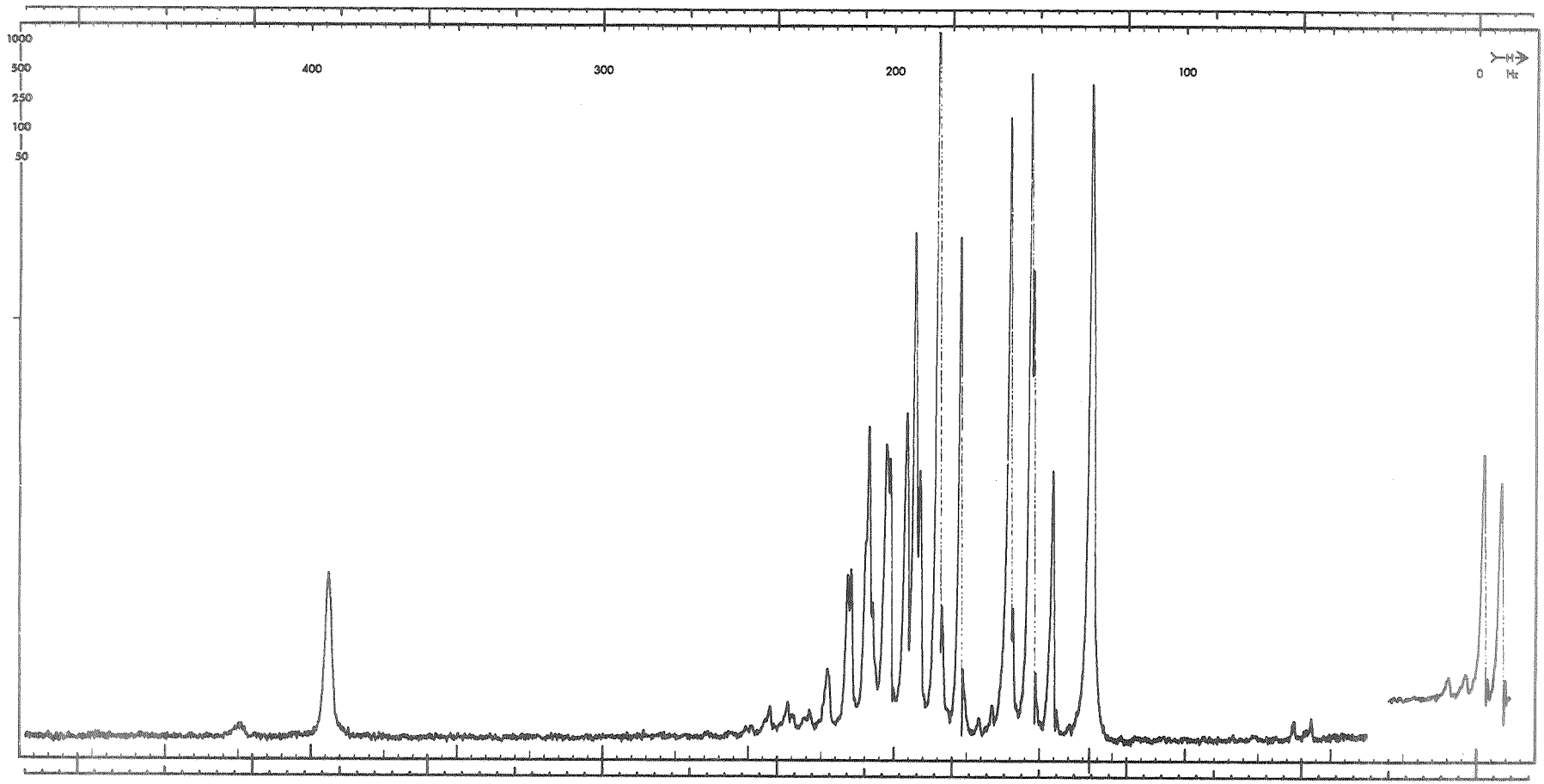

Fig. 61. ^{1}H NMR Spectrum In 1M $AlCl_3$ #4/PC #3-1 & 2M MF #2-11

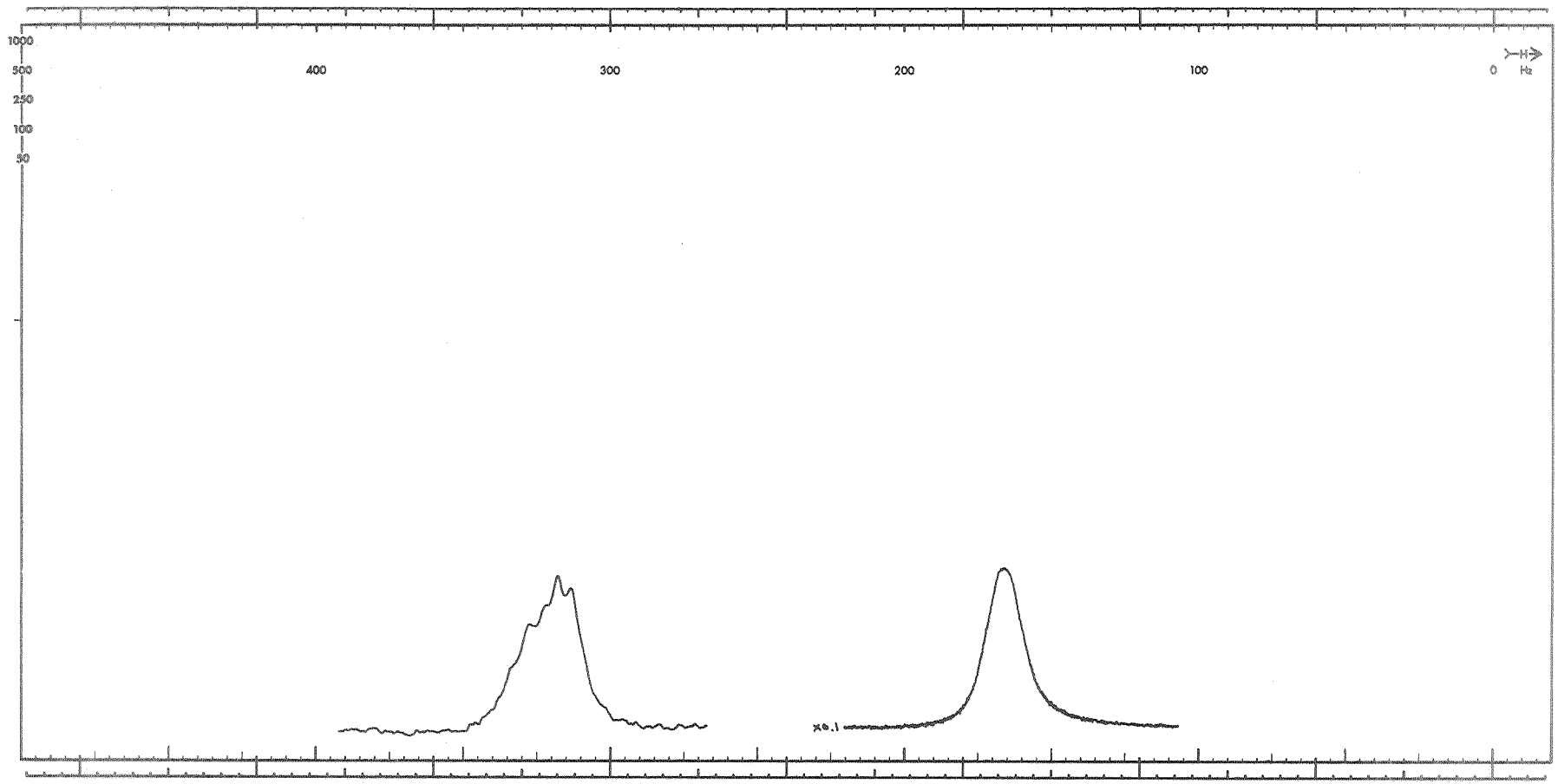

Fig. 62. ^{1}H NMR Spectrum In 1M $AlCl_3$ #4/PC #3-1 & 2M MF #2-11
Expanded Scale In Region of MF Quartet

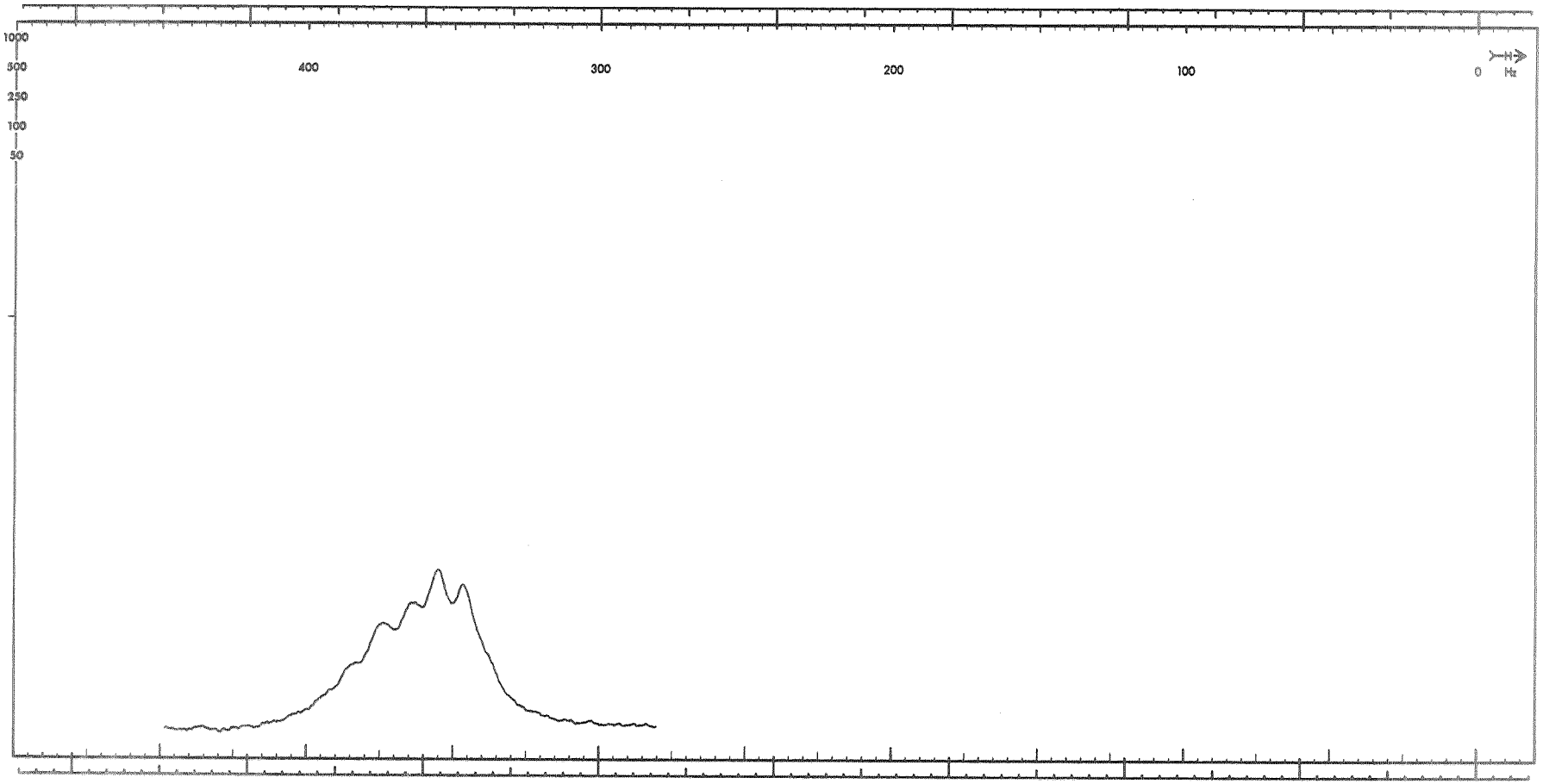

Fig. 63. ^{1}H NMR Spectrum In 1M $AlCl_3$ #4/PC #3-1 & 2M MF #2-11 Expanded Scale in Region of Coordinated (Mixed Complex) MF Quartet

NM As Additive. The ^{27}Al spectra for 1 M $AlCl_3$/PC with up to 3 M NM added are essentially the same as that for 1 M $AlCl_3$/PC . This indicates that NM does not displace PC in the $Al[PC]_6^{+3}$ complex. The lines were somewhat narrower which can be attributed to the decrease in viscosity produced by the addition of NM. Figure 64 shows the reference ^1H NMR spectrum for 20 v/o NM in PC. The large peak in the in the midst of the PC group marked with a dot above is due to NM. Figure 65 and 66 show the ^1H spectra for 1 M $AlCl_3$/PC with 1.5 M and 3.0 M NM added, respectively. In each case the peaks due to coordinated PC are unchanged, showing that NM does not displace PC from the $Al[PC]_6^{+3}$ complex. Again, the peak marked with a dot above it in the PC group is due to the added NM. Inspection of the 3 M NM spectrum indicates that there are no small peaks showing coordinated NM; because of the proximity of the PC group, however, this cannot be certain.

The NM peak in these two spectra is shifted slightly upfield relative to the PC spectra from its position in the reference spectra. This may be due to some small interaction with the PC.

The effects of the addition of LiCl is not changed by the presence of NM. Thus, all the data indicate that NM acts only as a diluent and does not affect species.

THF As Additive. The ^{27}Al spectra of 1 M $AlCl_3$/PC with THF show the same lines as 1 M $AlCl_3$/PC. They are somewhat broader, indicating some interaction with THF. The saturation characteristic of the $AlCl_4^-$ line was observed qualitatively to be different. (Saturation effects with addition of THF will be discussed in greater detail later.) Similar bheavior was observed in 1 M $AlCl_3$/MF electrolytes containing THF. As will be discussed later, this is evidence of a species different from those discussed previously. This new species is thought to be a $AlCl_3$·THF etherate.

Figure 67 shows the ^1H reference spectra from 20 v/o THF in PC. The part of the spectrum due to THF is the pair of quite similar complex peaks denoted by the arrows. (The response on the far right of the spectrum is due to one of the PC methyl proton peaks which is distorted because it is being utilized for a lock signal.) The THF peaks are not as well resolved as they are in neat THF, indicating an interaction between THF and PC or effects of viscosity. Figure 68 shows the ^1H spectrum for 1 M $AlCl_3$/PC and 1 M THF. The peaks due to coordinated PC are still observed. The THF peaks have been broadened, which suggests some interaction of THF with $AlCl_3$. Figures 69 through 72 show the ^1H spectrum for 1 M $AlCl_3$/PC and 1 M THF for increasing concentration of LiCl. As the LiCl concentration increases, the peaks due to coordinated PC disappear, as was the case with no THF present. Also noticeable is the fact that the peaks due to THF sharpen up and become like those in PC containing no $AlCl_3$ (see Figure 67). This

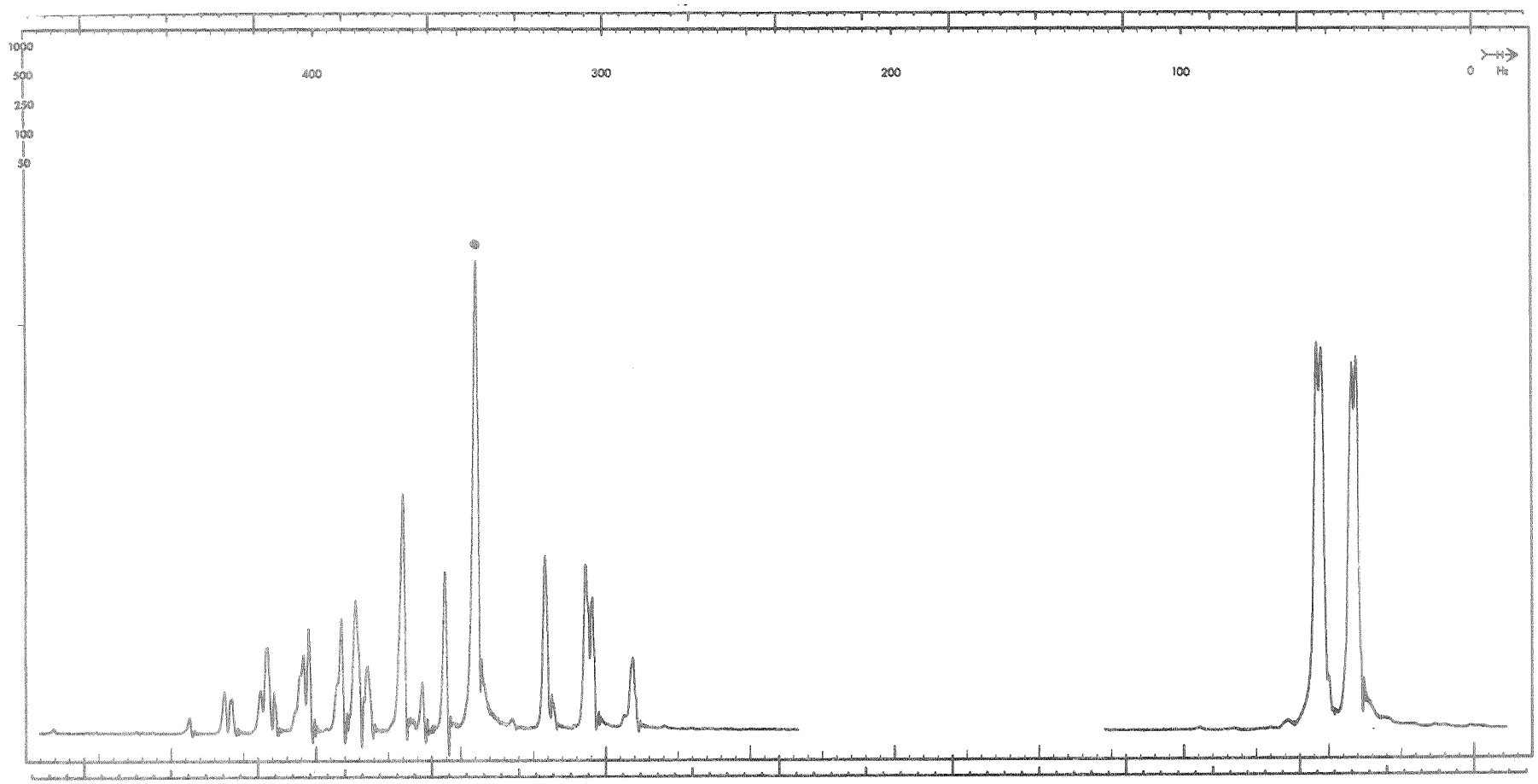

Fig. 64. ^{1}H NMR Spectrum of 20 $^{V}/o$ NM #1-2 in PC #7-4

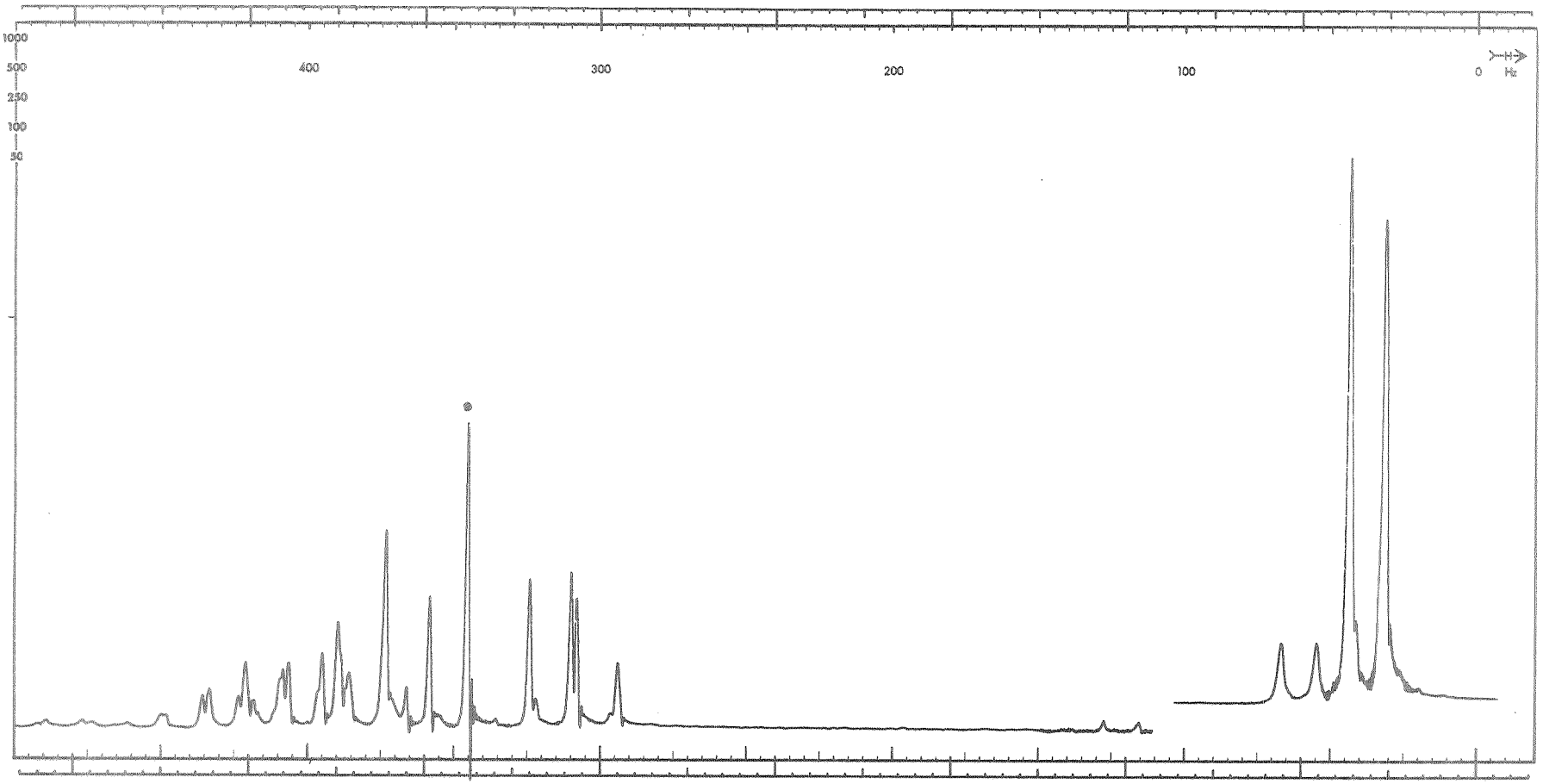

Fig. 65. ^{1}H NMR Spectrum of 1M $AlCl_3$ #4/PC #7-1 & 1.5 M NM #1-2

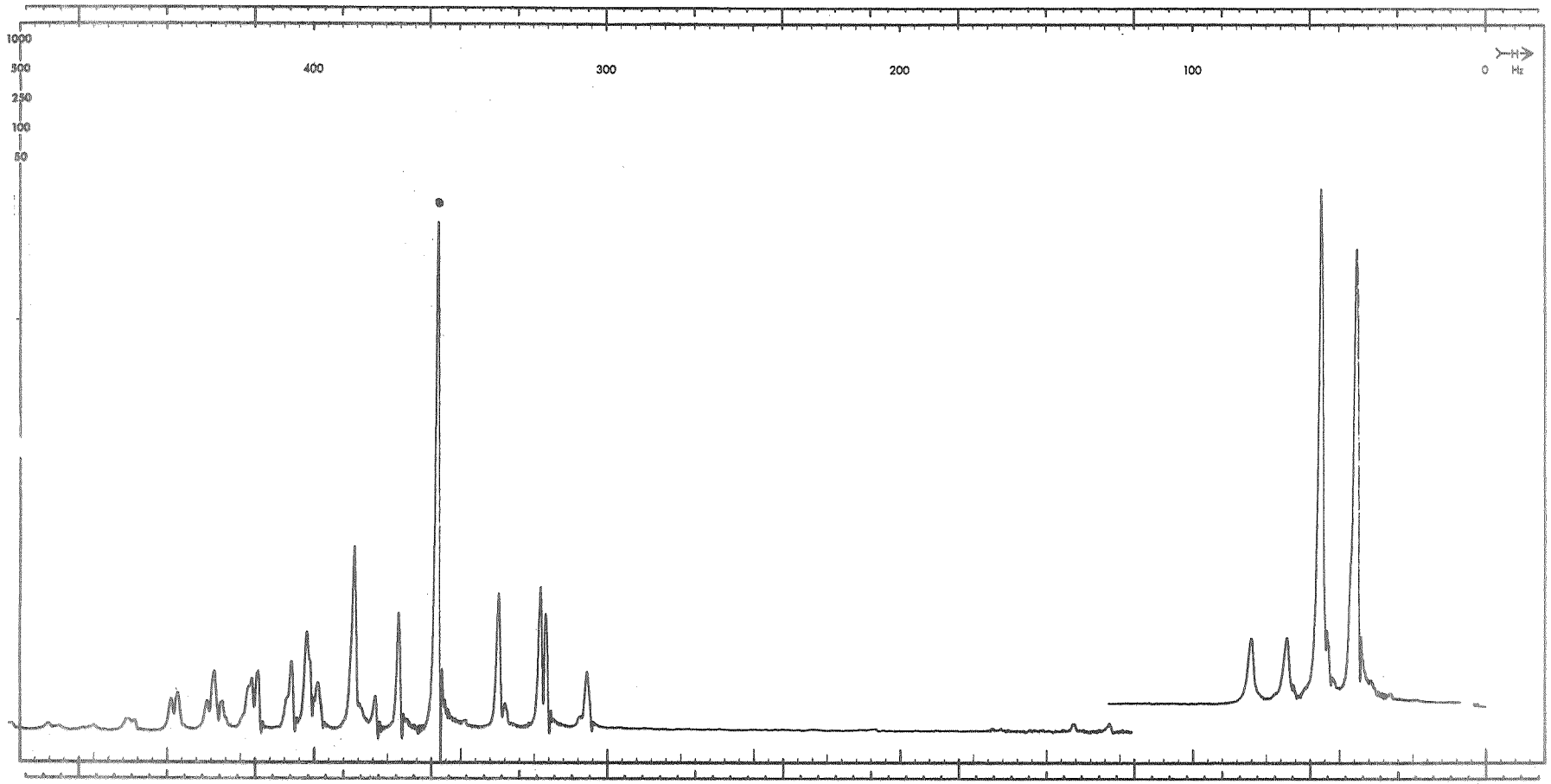

Fig. 66. ^{1}H NMR Spectrum of 1M $AlCl_3$ #4/PC #7-1 & 3.0 M NM #1-2

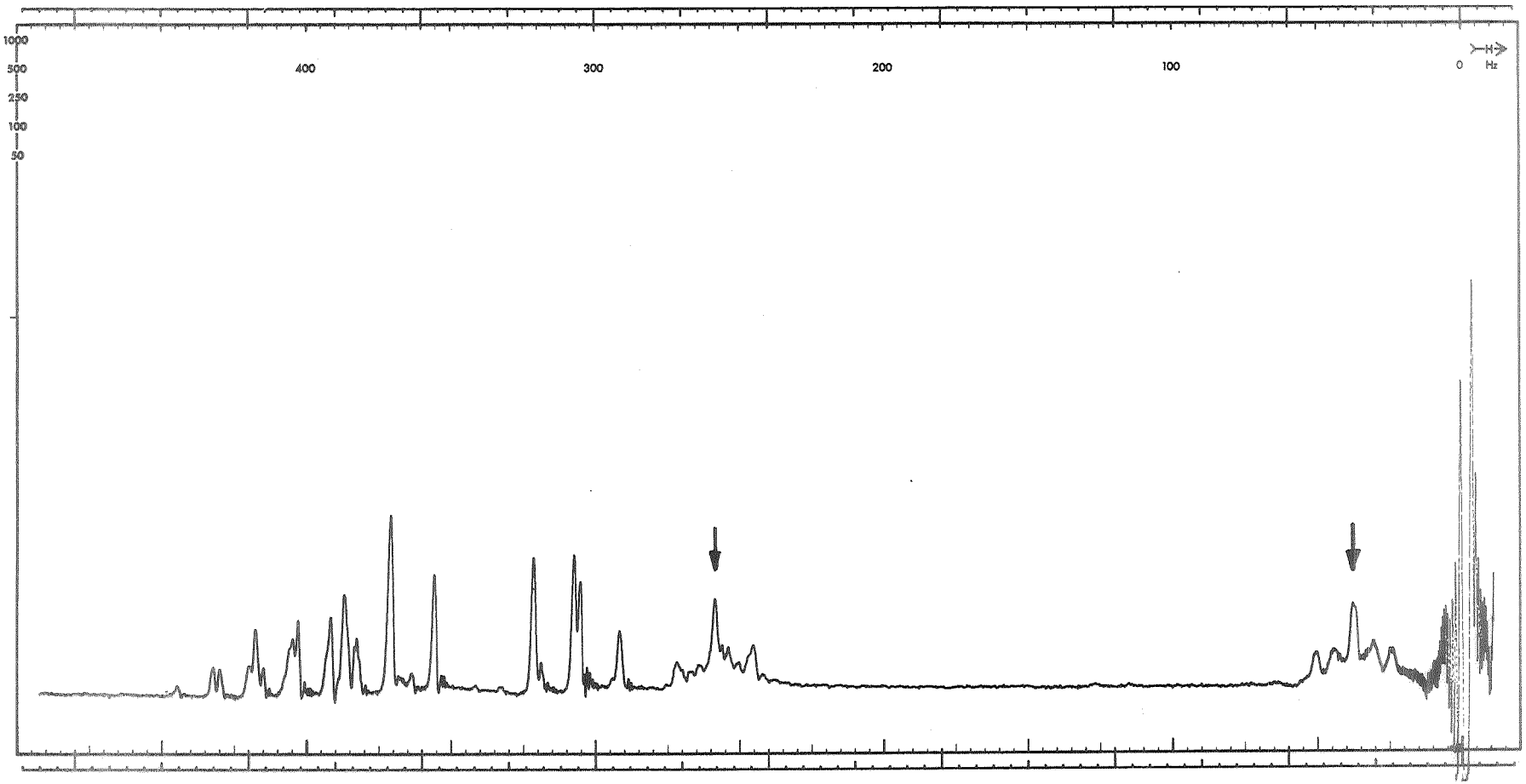

Fig. 67. ^{1}H NMR Spectrum of 20 $^{V}/o$ THF #1 in PC #6-6

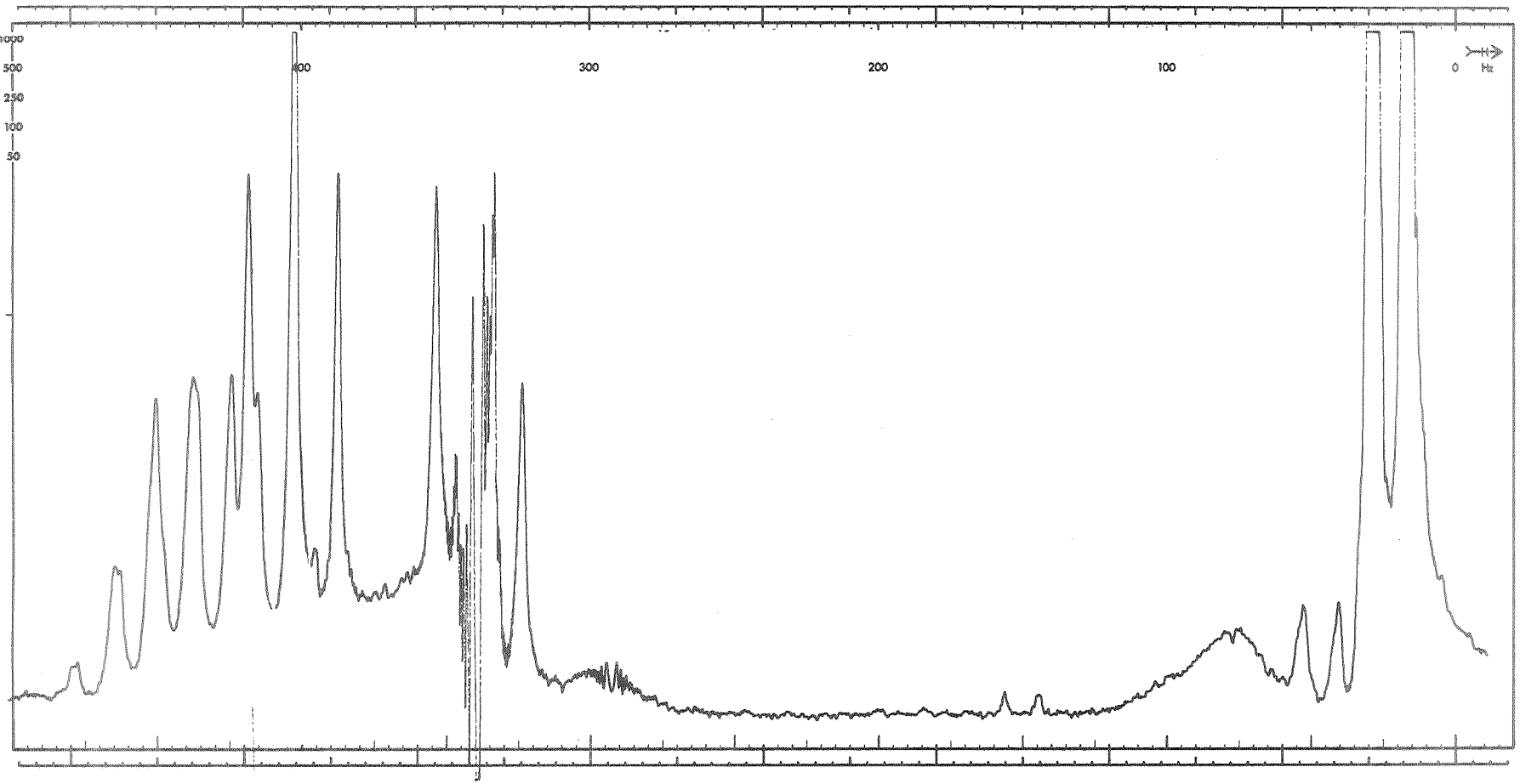

Fig. 68. ^{1}H NMR Spectrum of 1M $AlCl_3$ #4/PC #6-6 & 1M THF #1

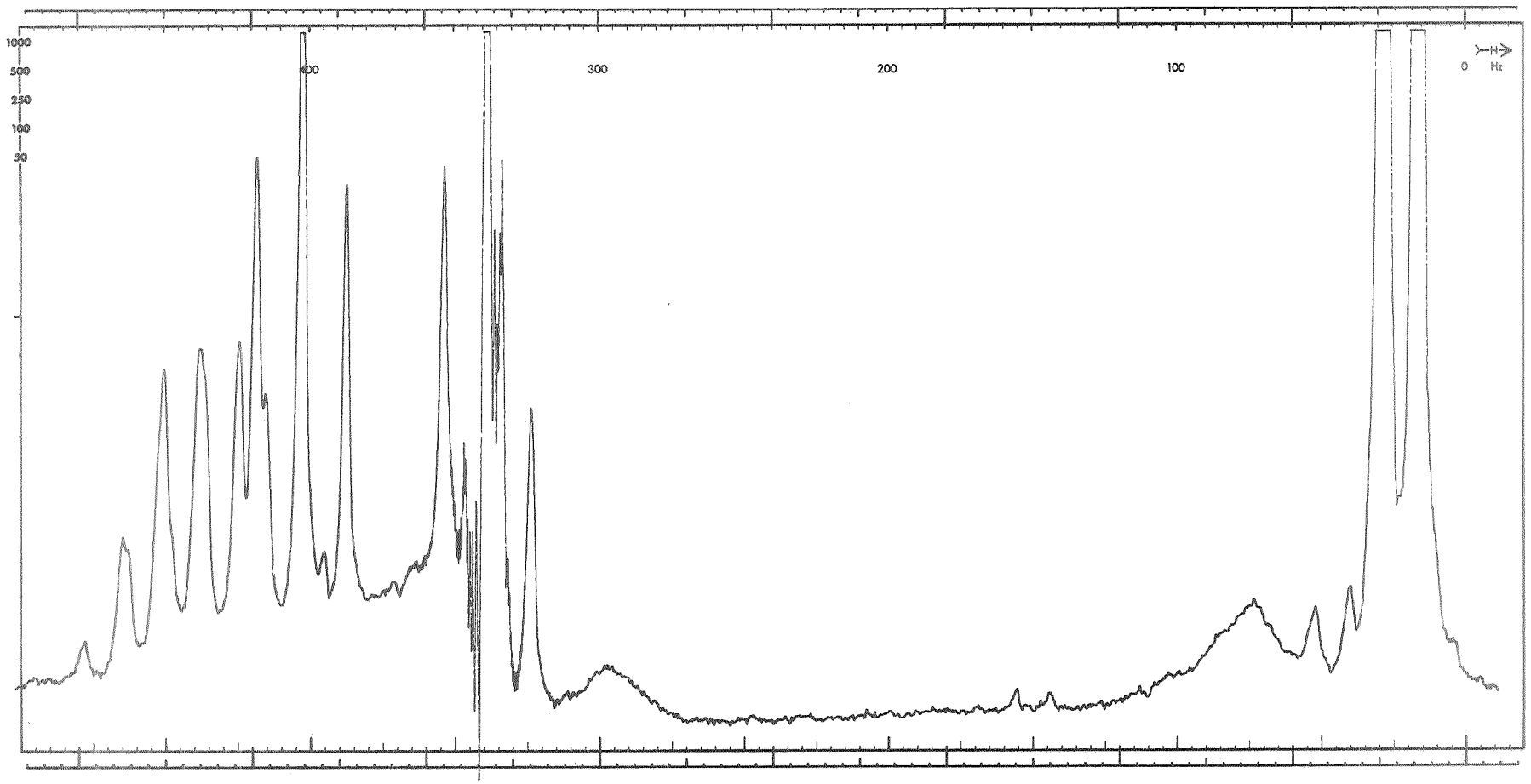

Fig. 69. ^{1}H NMR Spectrum of 1M $AlCl_3$ #4 + 0.2 M LiCl #3/PC #6-6 & 1M THF #1

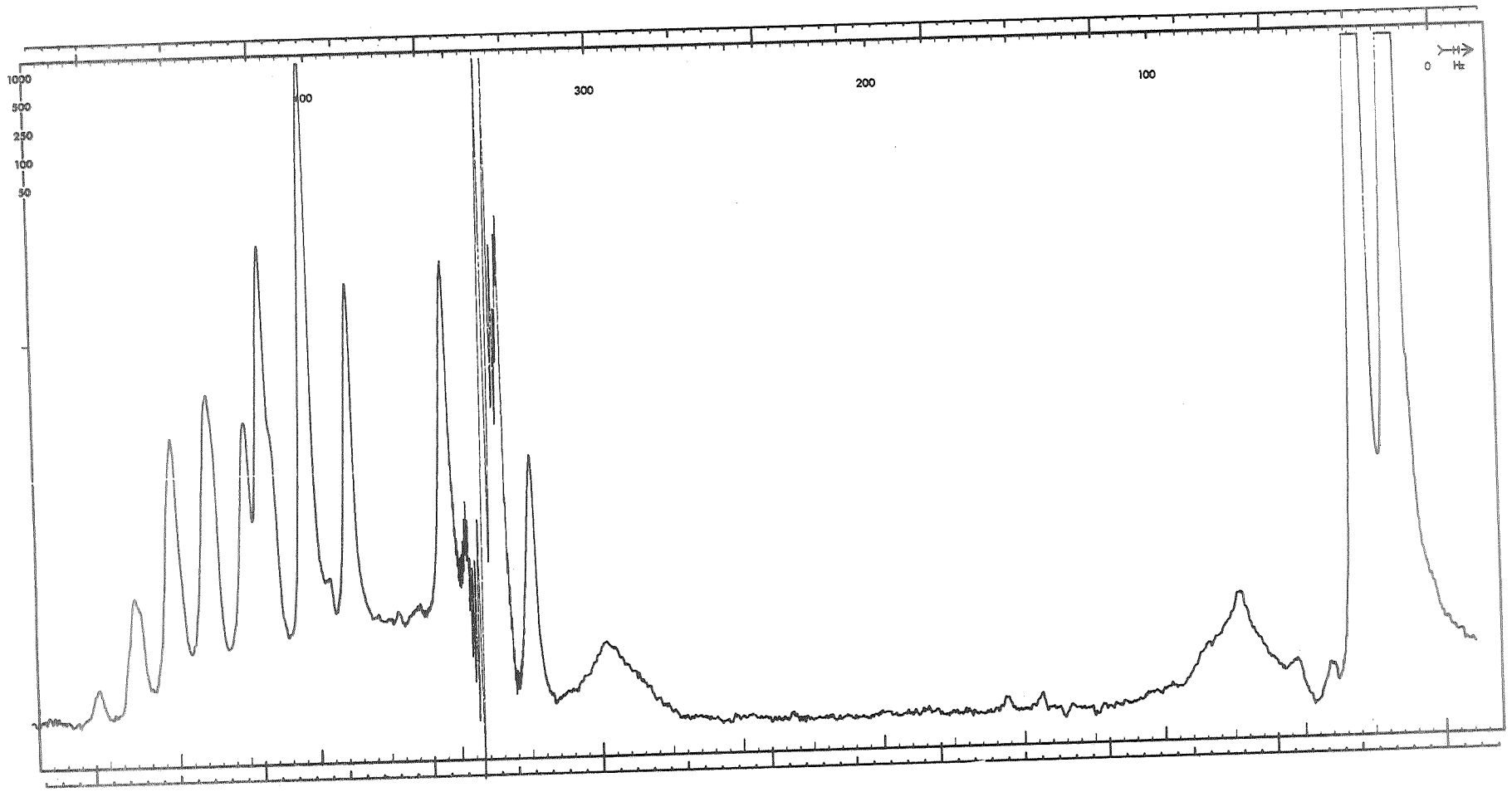

Fig. 70. ^{1}H NMR Spectrum of 1 M $AlCl_3$ #4 + 0.4 M LiCl #3/PC #6-6 & 1M THF #1

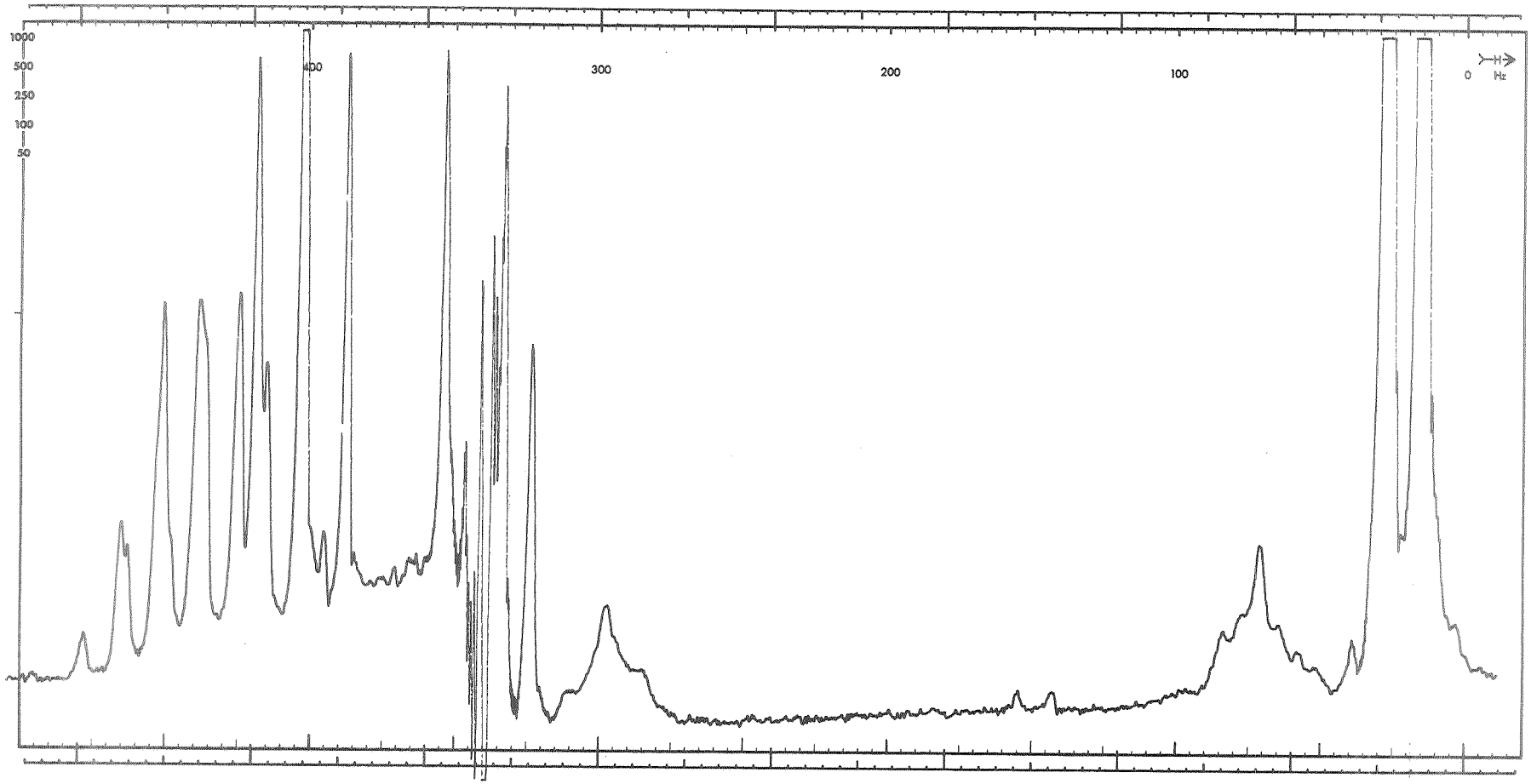

Fig. 71. ^{1}H NMR Spectrum of 1M $AlCl_3$ #4 + 0.6 M LiCl #3/PC #6-6 & 1M THF #1

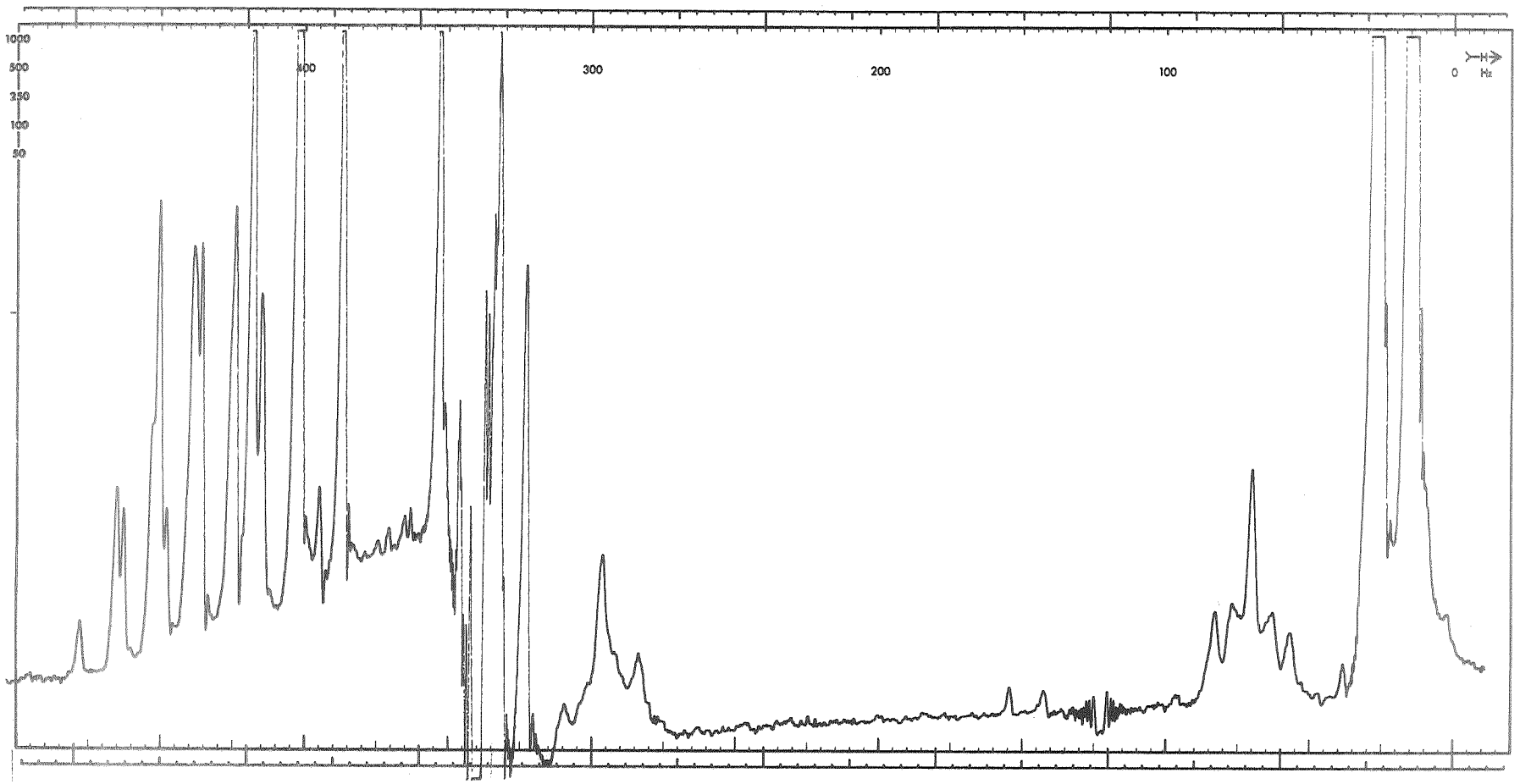

Fig. 72. ^{1}H NMR Spectrum of 1M $AlCl_3$ #4 + 0.8 M LiCl #3/PC #6-6 & 1M THF #1

indicates that the interaction that broadens the THF is with Al^{+3} or $Al[PC]_6^{+3}$ or both. Another possibility is that there is some neutral $AlCl_3 \cdot THF$, as suggested earlier, and which will be discussed again in a later discussion.

$LiClO_4$ As Additive. The results of broadline ^{27}Al spectra run for 1 M $AlCl_3$/PC with several concentrations of $LiClO_4$ are summarized in Figure 73. In this figure, the ratio of the approximate relative intensity of the $Al[PC]_6^{+3}$ line to the sum of the $AlCl_4^-$ line and the $Al[PC]_6^{+3}$ line is plotted as a function of the concentration of $LiClO_4$. The same ratio is shown for the addition of LiCl (from Ref. 1). This data indicates that the addition of $LiClO_4$ affects the $Al[PC]_6^{+3}$ species. Because 1 M $LiClO_4$ does not remove all $Al[PC]_6^{+3}$ as does LiCl, the formation of the species $Al(ClO_4)_4^-$ is apparently not highly favored over $Al[PC]_6^{+3}$. It is more likely that the competition between PC and ClO_4^- for sites in the Al^{+3} coordination sphere is relatively even. Figure 74 shows the ^1H spectra of 1 M $AlCl_3$/PC on an expanded scale in the region of the PC methyl proton doublet. The two small peaks to the left are due to coordinated PC. Figures 75 through 77 show the same lines for different concentrations of $LiClO_4$. The coordinated PC peaks appear to decrease in intensity which is in agreement with the ^{27}Al NMR data. At high $LiClO_4$ concentration, both the coordinated and the bulk PC line are considerably broadened. This may be due to increased viscosity. However, at 1.5 M $LiClO_4$ the coordinated PC peaks are still observable. The effects of the addition of LiCl are not changed by the presence of $LiClO_4$.

The data above indicate that addition of $LiClO_4$ to LiCl+$AlCl_3$/PC electrolytes produces mixed species of $Al[(PC)_x(ClO_4^-)_y]^{+3-y}$ at the expense of $Al[PC]_6^{+3}$ rather than $Al(ClO_4)_4^-$.

^{35}Cl NMR spectra were also run on 1 M $AlCl_3$/PC containing several concentrations of $LiClO_4$. The line widths, $\Delta\nu$, of the ^{35}Cl line in ClO_4^- are shown in Figure 78 as a function of $LiClO_4$ concentration. The purpose of these measurements was to determine if some information could be obtained regarding the solvation of Li^+. Direct collisions of Li^+ with ClO_4^- would decrease the relaxation time which could be observed as an increase in line width. Thus, the line width would be expected to increase with the increase in Li^+ concentration. Data in Figure 78 show an increase in line width with increase in $LiClO_4$ concentration. However, it is known that the viscosity, η, of these solutions increases with $LiClO_4$ concentration as well. This increase in viscosity could also produce an increased line width. Viscosities have been estimated on the basis of data from Ref. 1. If the line width increase is caused by viscosity effects, the ratio of $\Delta\nu/\eta$ would remain constant. A plot of $\Delta\nu/\eta$ as a function of $LiClO_4$ concentration, Figure 79, indicates that this ratio is not constant, suggesting that the line width change is due to some other interaction. If this interaction is with Li^+ ions, it suggests that PC does not solvate Li^+ strongly.

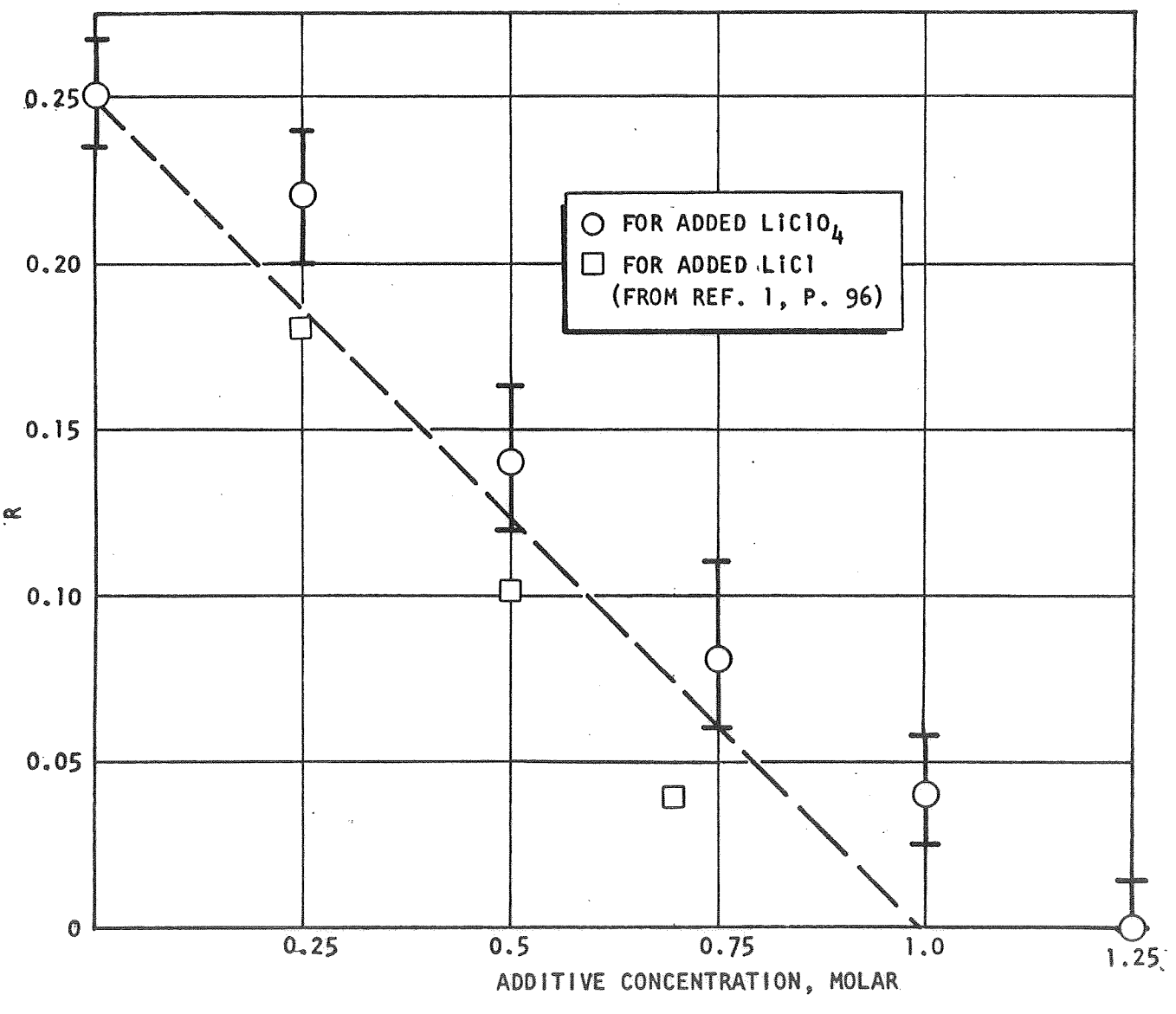

Fig. 73 . Ratio R, of Intensity of Coordinated Al^{+3} Resonance to Sum of Al^{+3} Resonance Plus $AlCl_4^-$ Resonance in 1 M $AlCl_3$/PC, as a Function of Added $LiClO_4$ and LiCl.

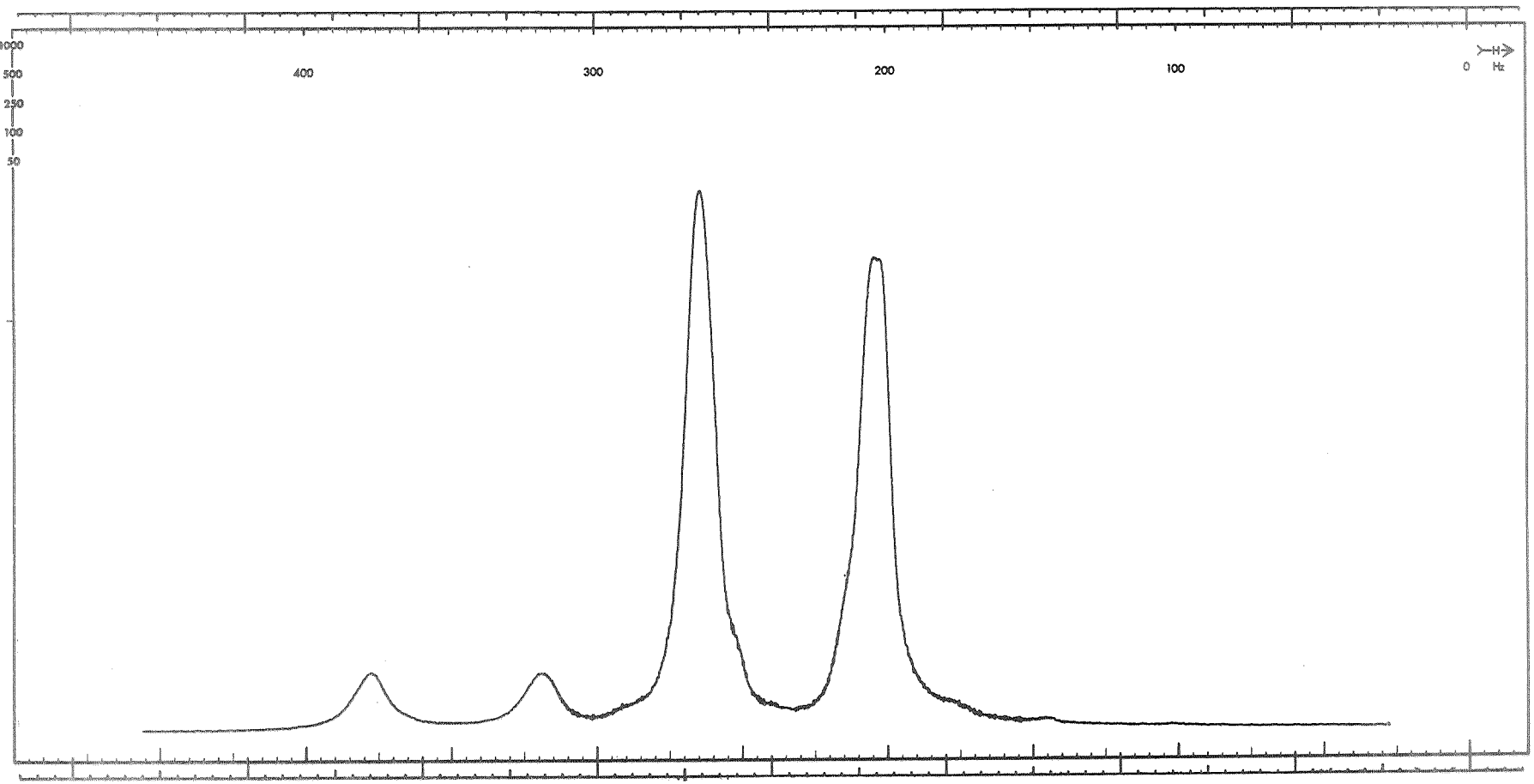

Fig. 74. ^{1}H NMR Spectrum in 1M $AlCl_3$ #4/PC #6-4. Expanded Scale in Region of PC Methyl Proton Doublet

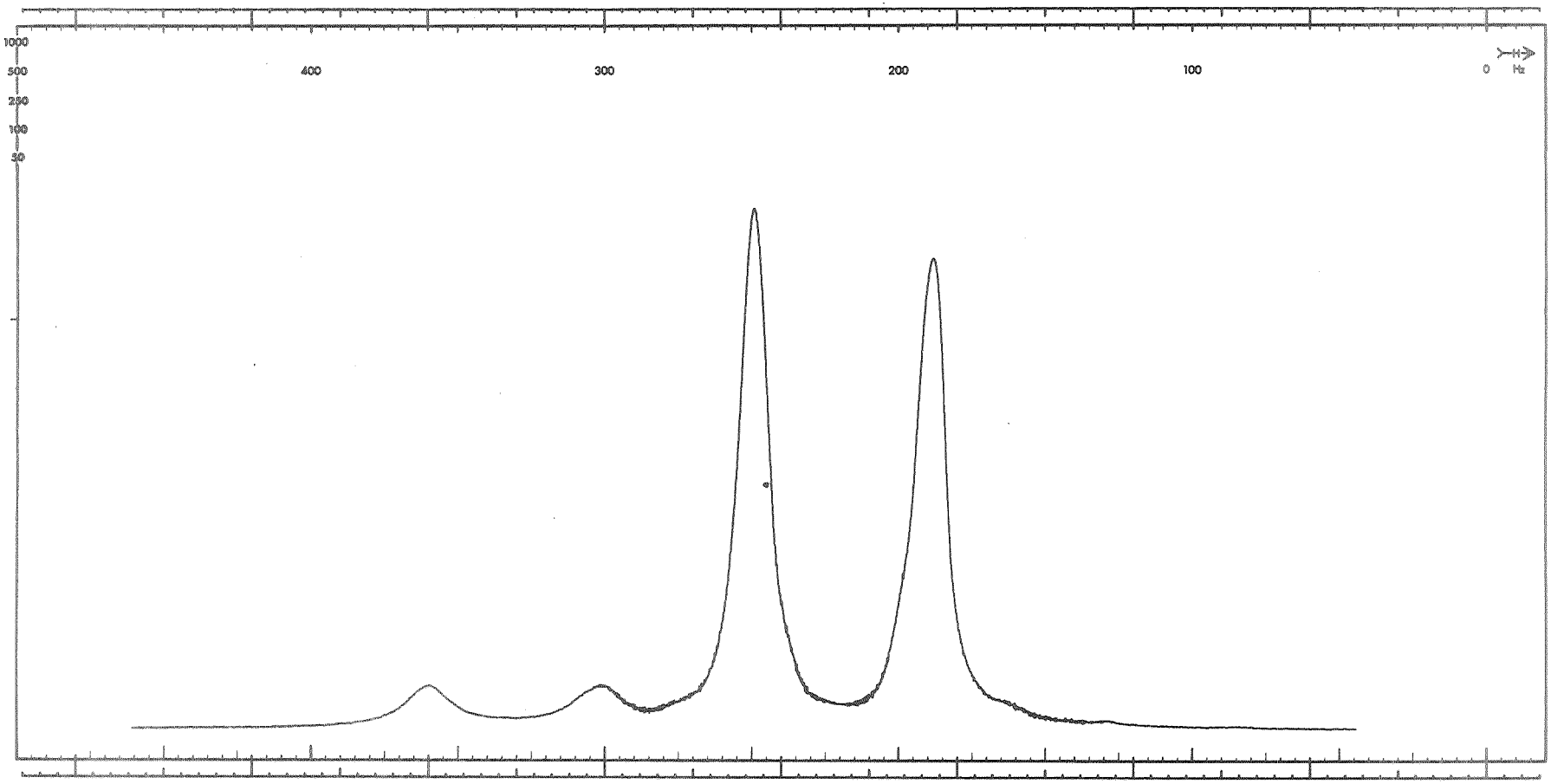

Fig. 75. ^{1}H NMR Spectrum in 1M $AlCl_3$ #4/PC #6-4 & 0.5 M $LiClO_4$ #3. Expanded Scale in Region of PC Methyl Proton Doublet

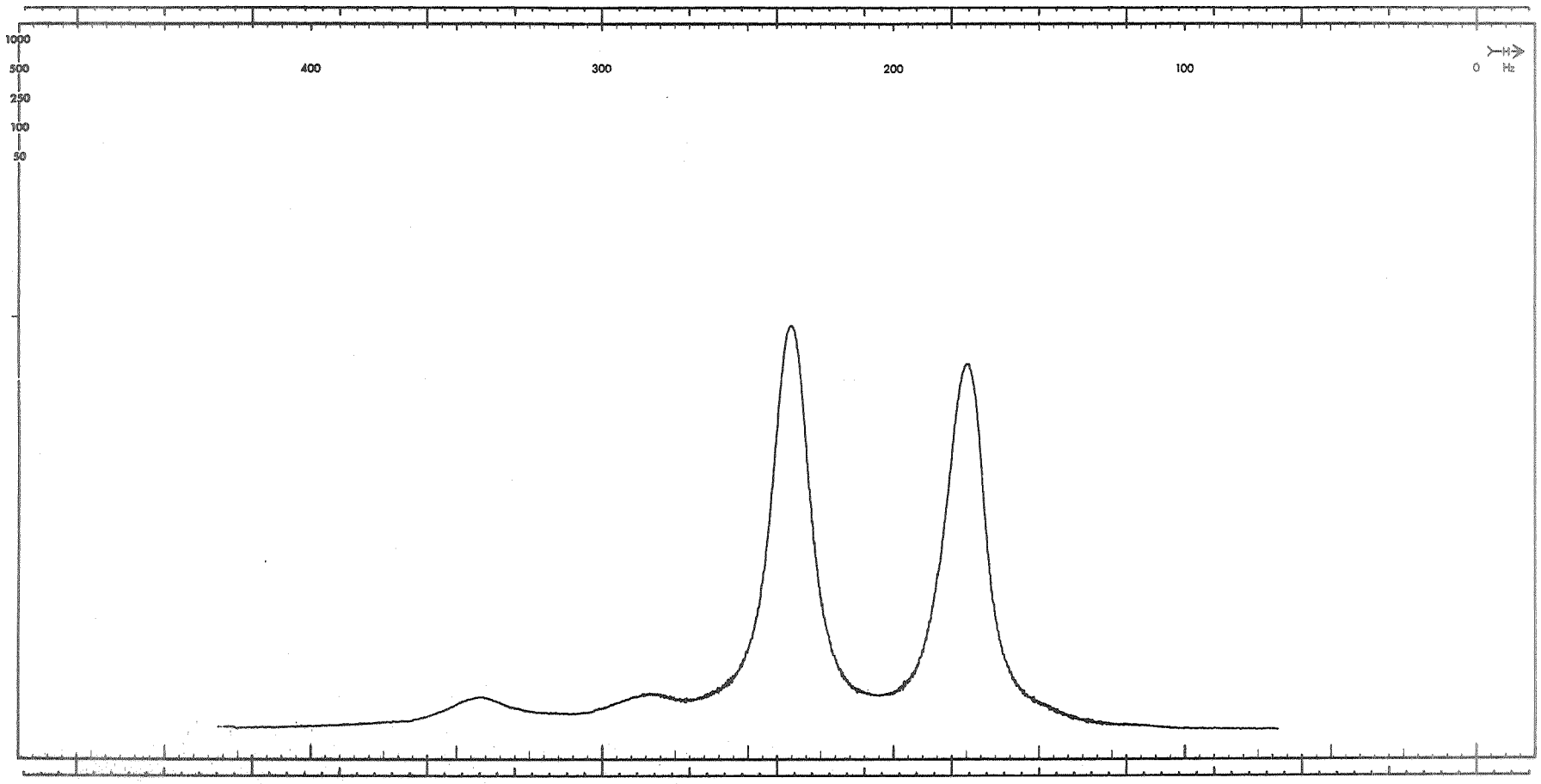

Fig. 76. ^{1}H NMR Spectrum in 1M $AlCl_3$ #4/PC #6-4 & 1.0 M $LiClO_4$ #3. Expanded Scale in Region of PC Methyl Proton Doublet

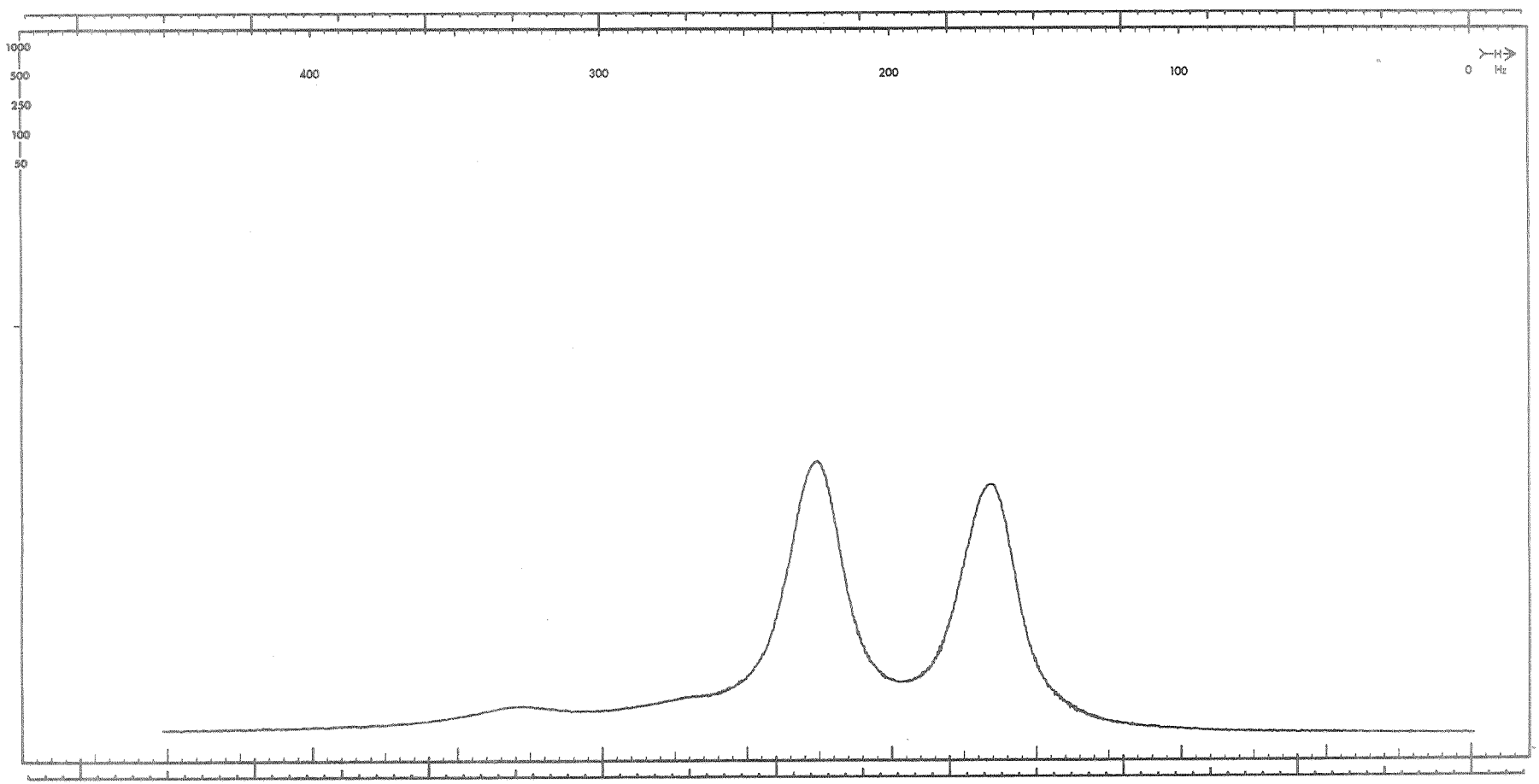

Fig. 77. ^{1}H NMR Spectrum in 1M $AlCl_3$ #4/PC #6-4 & 1.5 M $LiClO_4$ #3. Expanded Scale in Region of PC Methyl Proton Doublet

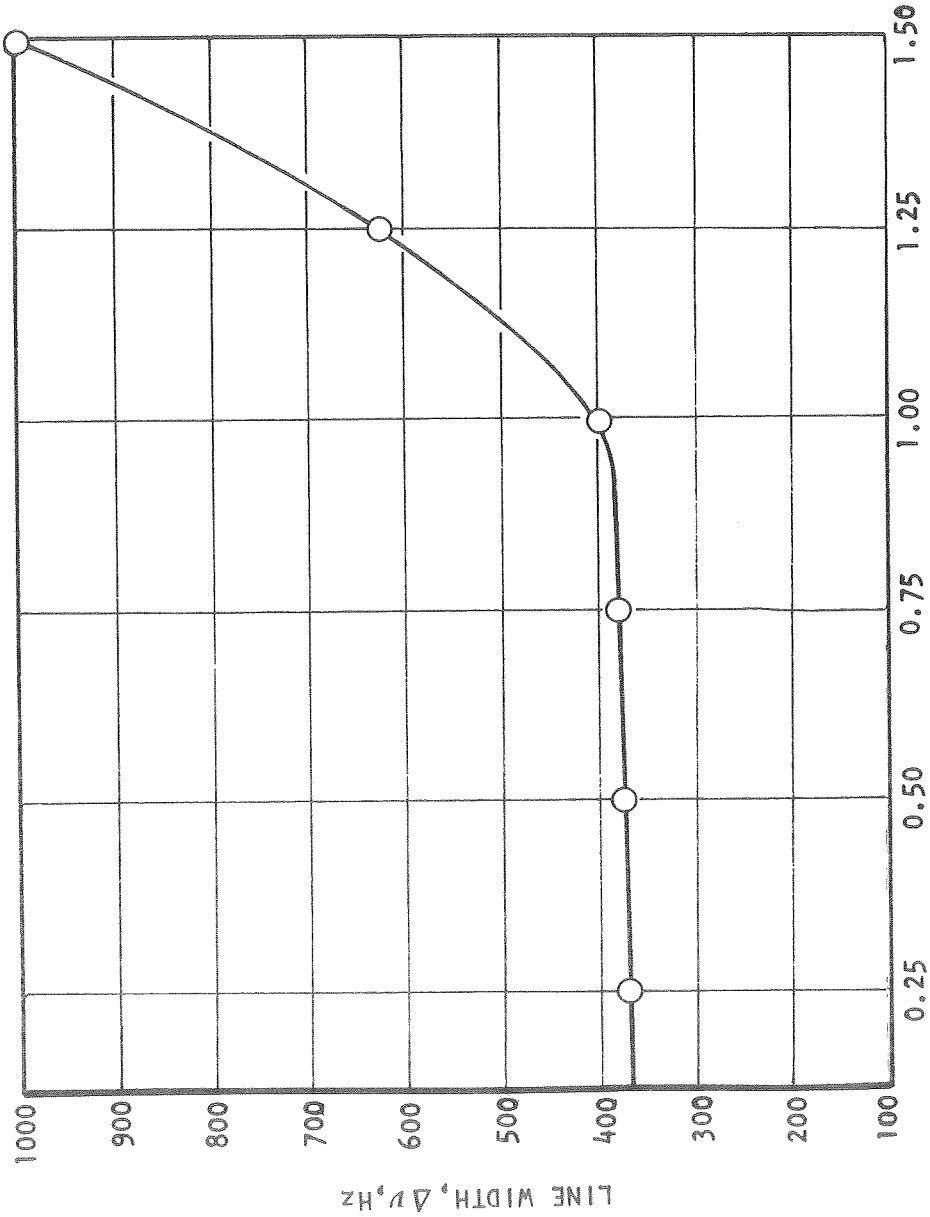

Fig. 78. Line Width of the ^{35}Cl Line from ClO_4^- in 1 M $AlCl_3$/PC as a Function of the Concentration of Added $LiClO_4$

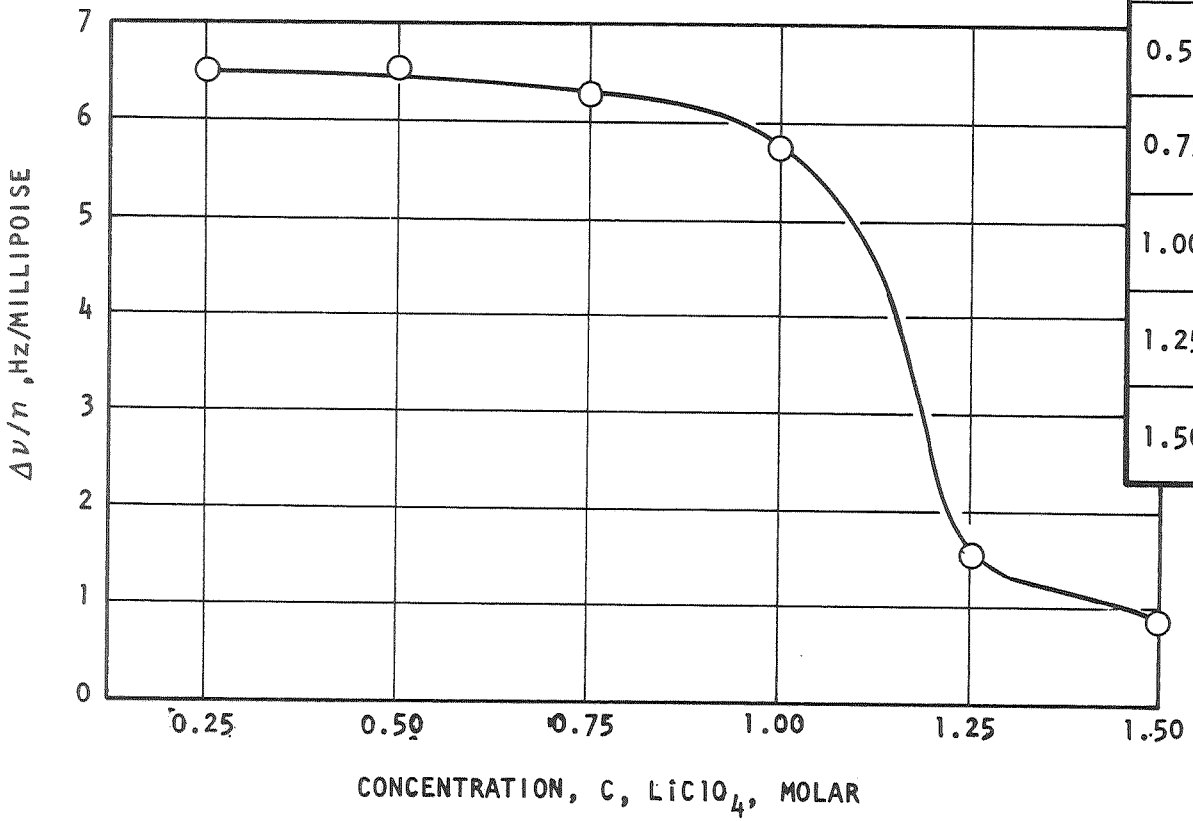

C	Δν	η	Δν/η
0.25	370Hz	(MILLI POISE) 57	6.50
0.50	370	57	6.50
0.75	385	60	6.42
1.00	400	70	5.71
1.25	625	400	1.56
1.50	1000	1100	0.91

Fig. 79 . Ratio of Line Width of the ^{35}Cl Line from ClO_4^- to Viscosity in 1 M $AlCl_3$/PC as a Function of the Concentration of Added $LiClO_4$.

LiBr As Additive. Neither ^{27}Al NMR spectra nor ^{1}H spectra showed any evidence of $Al[PC]_6^{+3}$ in 1 M $AlCl_3$/PC to which 0.5 M and 1.0 M LiBr had been added; the same applied to 0.5 M LiCl + 1.0 M $AlCl_3$/PC and 0.5 M LiBr. This would be consistent with the displacement of PC by Br^- in the Al^{+3} coordination sphere. However, these specimens contained solid precipitates and showed rapid decomposition so that these results cannot be taken with certainty.

H_2O As Additive. High resolution proton spectra were run for 1 M $AlCl_3$ 0.5 M LiCl/PC to which 2000, 500 and 100 ppm H_2O had been added. For comparison, high resolution spectra were also run for pure PC containing 2000, 500 and 100 ppm H_2O. Portions of the spectra for the latter solutions are shown in Figures 80 through 82. All three spectra were run under the same instrumental conditions. The water proton line was easily observed in the specimen containing 2000 ppm H_2O. In the 500 ppm specimen the line is still readily observed but the line width has increased, from 7.2 Hz in the 2000 ppm H_2O specimen to about 13 Hz in the 500 ppm H_2O specimen. The water peak in the 100 ppm specimen is not observable under these conditions, probably due to further line broadening. Spectra run under these conditions for the 1 M $AlCl_3$ + 0.5 M LiCl/PC nominally containing 2000 ppm, 500 ppm, and 100 ppm H_2O, respectively, showed no water peaks. This is consistent with the observation that when the samples were prepared, a precipitate formed upon water addition. It is thought that the precipitate is aluminum hydroxide. Inspection of the peaks of the PC spectra due to Al^{+3} coordinated PC shows that the intensity of these peaks has been reduced. Assuming that the precipitate is $Al(OH)_3$, the intensity reduction is nearly quantitative. The coordinated PC peak intensity in the 2000 ppm H_2O specimen is reduced by about 24%. Quantitative precipitation of 2000 ppm H_2O as $Al(OH)_3$ would reduce the peak by 32%.

$LiClO_4$/PC

DMF, MF and AN As Additives. All broadline ^{7}Li and ^{35}Cl spectra that have been obtained in these electrolytes are consistent with the ionic species Li^+ and ClO_4^-. Chemical shifts of the ^{1}H spectra were determined for several electrolytes. The results of these measurements are shown in Table 13. σ_{PC} is the chemical shift of the PC methyl proton relative to the group of PC lines (see Figure 3), while $\sigma_{additive}$ is the chemical shift of the methyl doublet relative to the aldehyde proton in DMF or the chemical shift between the methyl and formyl proton peaks in MF. For comparison, σ_{DMF} in neat DMF is 305 Hz, σ_{MF} in 1 M $LiClO_4$/MF is 263 Hz, and when DMF is coordinated by Al^{+3} σ_{DMF} for the coordinated DMF is 319 Hz. Furthermore, in a solution of 2.0 M DMF in PC, σ_{DMF} is 302 Hz.

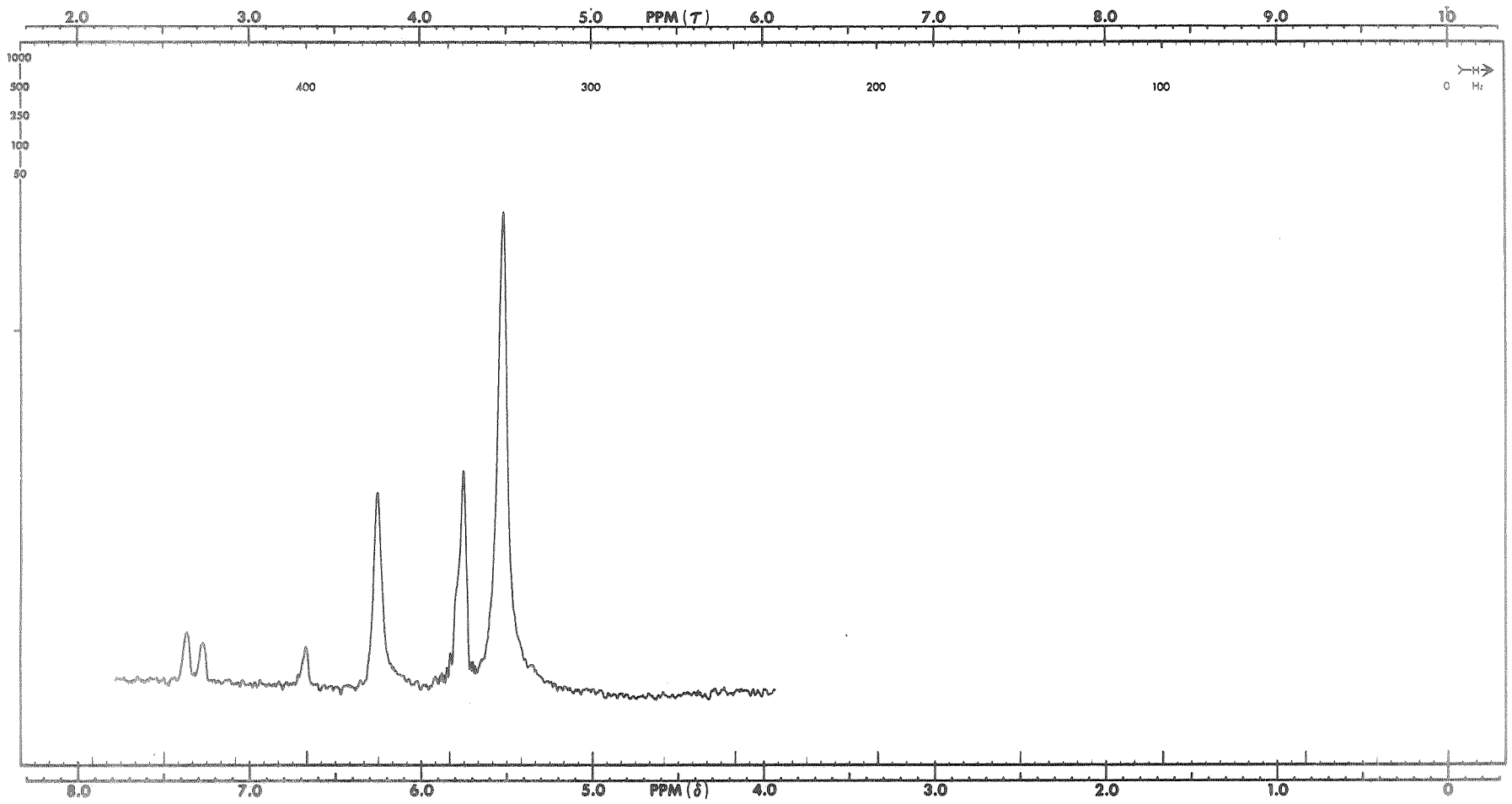

Fig. 80. ^{1}H NMR Spectra in PC #7-8 With 2000 ppm H_2O Added. Expanded Scale in Region of Water Proton Peak

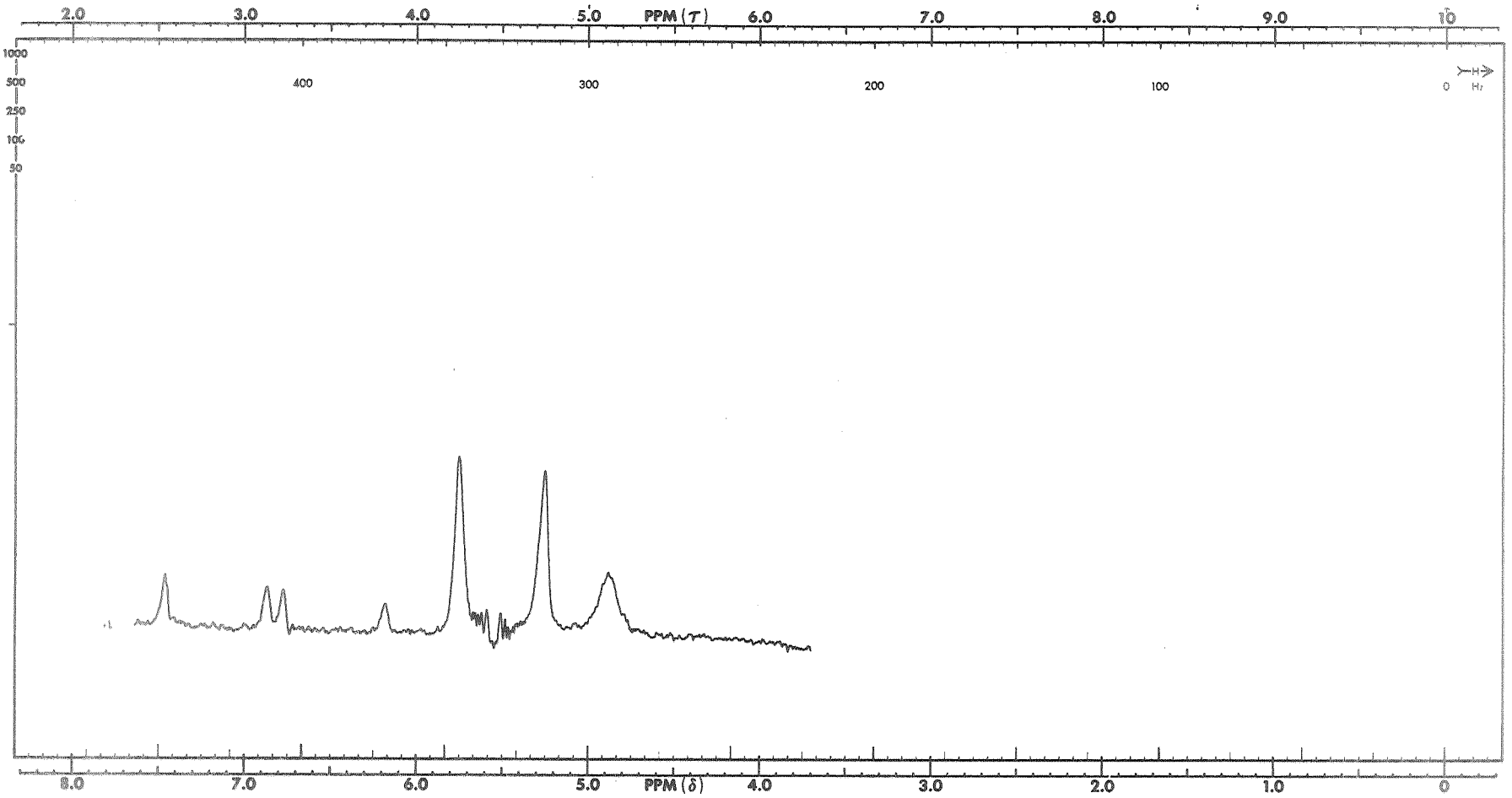

Fig. 81. ^{1}H NMR Spectra in PC #7-8 With 500 ppm H_2O Added. Expanded Scale in Region of Water Proton Peak

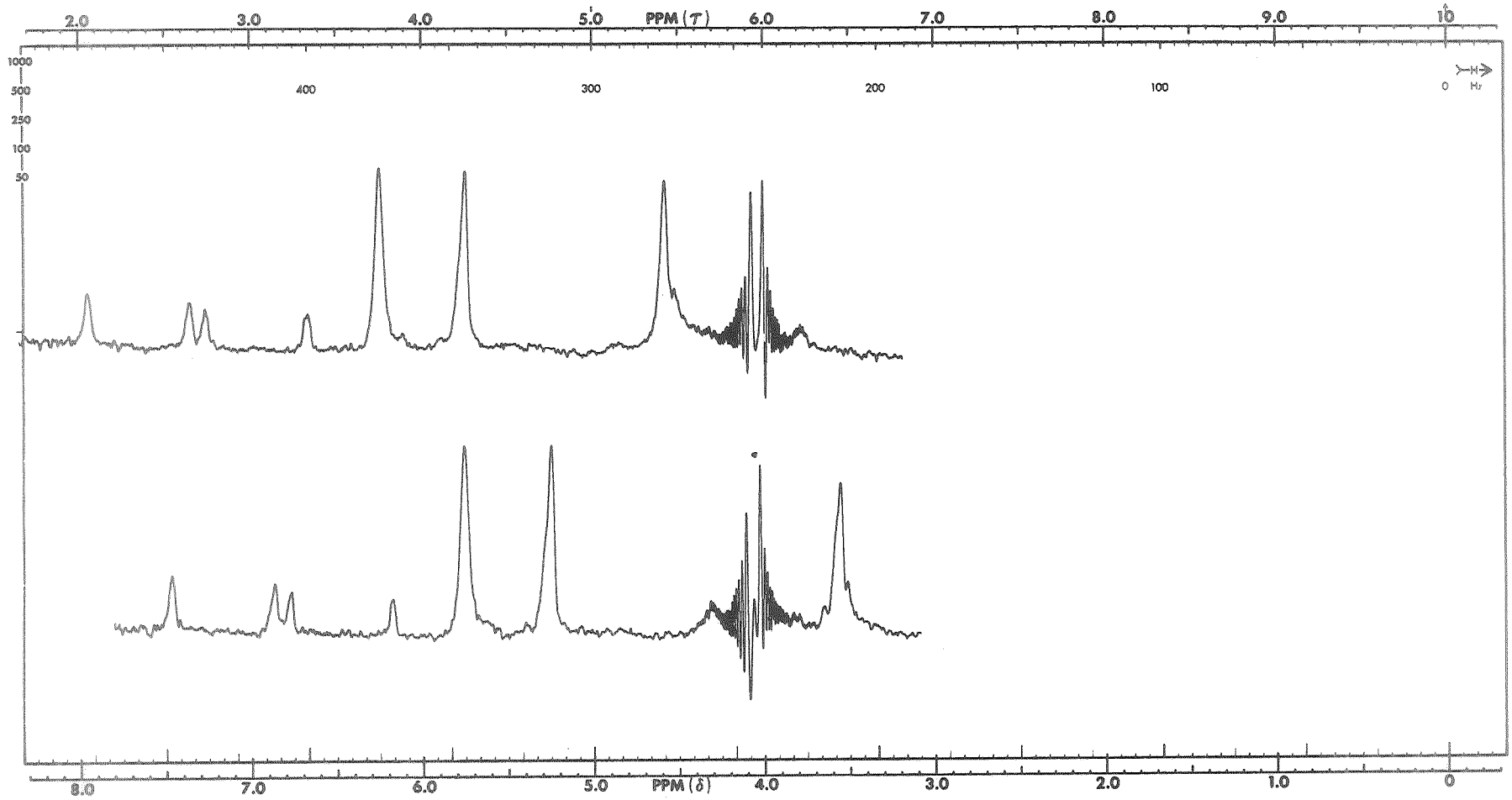

Fig. 82. ^{1}H NMR Spectra in PC #7-8 With 100 ppm H_2O Added. Expanded Scale in Region of Water Proton Peak

TABLE 13

CHEMICAL SHIFTS, σ, 1 M $LiClO_4$/PC WITH ADDITIVES

Additive	σ_{PC} (Hz)	$\sigma_{Additive}$ (Hz)
0.25 M DMF	161 ± 2	294 ± 2
1.0 M DMF	161 ± 2	295 ± 2
2.0 M DMF	161 ± 2	296 ± 2
4.0 M DMF	161 ± 2	298 ± 2
0.25 M MF	164 ± 2	263 ± 2
1.0 M MF	164 ± 2	--
2.0 M MF	164 ± 2	--
4.0 M MF	164 ± 2	263 ± 2

According to the results in Table 13, the PC chemical shift is not affected by the presence of $LiClO_4$. The chemical shift of DMF as an additive shows some interaction depending upon its concentration and some change in 1 M $LiClO_4$/PC compared to its addition to PC. But the change is not consistent with a model based upon solvation of Li^+. If DMF were to solvate Li^+ in 1 M $LiClO_4$/PC, it would be expected that σ_{DMF} in this electrolyte would be larger than σ_{DMF} in PC or in neat DMF because solvation of Al^{+3} increases σ_{DMF}. The reverse is observed, namely, that σ_{DMF} in 1 M $LiClO_4$/PC is less than for both neat DMF and DMF in PC. From the measurements in Table 13 it is indicated that neither PC, MF or DMF solvate Li^+ strongly but there may be some interaction of DMF with Li^+ of a different nature than with Al^{+3}. Data taken with NM as an additive also indicate no interaction of NM with Li^+. Thus, the ionic species present in the 1 M $LiClO_4$/PC electrolyte with the additives studied are primarily Li^+ and ClO_4^- as with no additives.

<u>$AlCl_3$ As Additive</u>. $LiClO_4$/PC with $AlCl_3$ added is a system that was picked for initial study. This has been covered previously in the $LiCl+AlCl_3$/PC section with $LiClO_4$ as an additive.

<u>$LiAsF_6$/PC</u>

<u>DMSO, DMF, MF, THF and MF As Additives</u>. Because of the use of a different NMR technique for $LiAsF_6$, the discussion of this electrolyte with these additives is included in the MF section.

METHYL FORMATE ELECTROLYTES

It was believed that a high dielectric constant was a necessary characteristic of a good solvent for nonaqueous electrolytes. A high dielectric constant depresses the formation of ion pairs and thus promotes conductivity for a given solute concentration. A low dielectric constant medium is favorable to ion pair formation because attraction of an anion for a cation is not attenuated. Since methyl formate has a low dielectric constant, it was therefore unexpected that it would be a good solvent for nonaqueous electrolytes.

Dielectric constant measurements, made on pure MF and a 1.1 M $LiAsF_6$/MF electrolyte, reported in Ref. 1, provide the basis for an answer to the exceptional behavior of MF. Usually the addition of a salt to a solvent results in a decrease in dielectric constant as a result of the dielectric saturation of the solvent in the immediate vicinity of the ions in solution. Measurements reported in Ref. 1 showed that the dielectric constant of 1.1 M $LiAsF_6$/MF was 27.4 as compared to a value of 8.4 for neat MF. For some reason not known, the addition of 1.1 M $LiAsF_6$ to MF resulted in an increase in dielectric constant. With this data, it is less surprising that $LiAsF_6$/MF is a good (high conductivity) electrolyte, though the increase in dielectric constant is a surprise.

The most probable reason for the increase in dielectric constant is that there are species formed when $LiAsF_6$ is dissolved in MF that have effective dipole moments. A strongly bound ion pair for example would exhibit a large dipole moment. A weakly bound ion pair may exhibit a dipole-like nature. A higher order cluster, such as a triplet, may also exhibit a dipole-like nature if sufficiently well defined. Dielectric effects due to ion pairs has been discussed for aqueous solutions in Ref. 7.

This section, like the previous one, is subdivided according to the solute(s) added to MF to produce the electrolyte, and then by solvents and/or solutes added to the electrolyte.

LiCl + $AlCl_3$/MF

Aluminum chloride dissolved in MF produces the same type of ^{27}Al broadline spectra as does $AlCl_3$ in PC, a narrow peak ascribable to $AlCl_4^-$, and a broader, less intense peak upfield which is ascribable to solvated Al^{+3}. Addition of LiCl also has the same effect, reducing the intensity of the solvated Al^{+3} peak.

The ^1H spectrum of 1 M $AlCl_3$/MF shows a downfield peak due to coordinated MF as in the case of 1 M $AlCl_3$/PC. In MF, however, the downfield peak is noticeably broadened. This indicates that the residence time of MF in

the first coordination sphere of Al^{+3} is less than that of PC which suggests a weaker interaction. The bulk MF peaks are also somewhat broadened for essentially the same reason. Addition of 1 M LiCl results in a spectrum essentially like that of neat MF, showing that Cl^- displaces MF from the first coordinated sphere of Al^{+3} as was the case for PC.

Because of the extensive broadening of the coordinated MF peak, an accurate measure of the coordination number of MF by Al^{+3} could not be made. An estimate of the coordination number based upon the integration of the bulk and coordinated MF peaks by "counting squares" yielded a value of 6.4. In view of the results with Al^{+3} in other solvents, which give a value of 6, and this estimate, it is reasonable to assume that the coordinated species in 1 M $AlCl_3$/MF is $Al[MF]_6^{+3}$ at the temperature at which the spectrum utilized for this estimate was taken, which was 30 C. Thus, for LiCl and $AlCl_3$ in MF the dominant species are Li^+, $AlCl_4^-$ and $Al[MF]_6^{+3}$, the relative population depending upon the concentration of LiCl. This parallels the results obtained for acetonitrile (Ref. 1) and propylene carbonate.

Although this was not pursued further, it should be noted here that in the ^1H spectra taken of 1 M $AlCl_3$/MF at low temperatures the peak due to coordinated MF showed structure. This structure suggests that there is more than one type of MF complex or that there are possibly clusters such as ion pairs or higher mulitplets which have a "life" time comparable to the NMR time scale.

DMSO As Additive. The ^{27}Al spectrum from 1 M $AlCl_3$/MF with 1 M DMSO added was similar to that obtained from 1 M $AlCl_3$/MF except that the intensity of the $Al[MF]_6^{+3}$ peak was decreased, which is attributed to displacement of MF by DMSO in the first coordination sphere of Al^{+3}. 1 M DMSO added to 1 M LiCl + 1 M $AlCl_3$/MF resulted in an ^{27}Al spectrum which had two peaks, the $AlCl_4^-$ peak and a solvated Al^{+3} peak. Because the ^{27}Al spectrum obtained from 1 M LiCl + 1 M $AlCl_3$/MF displays only the $AlCl_4^-$ peak, this is direct evidence that DMSO displaces Cl^- from $AlCl_4^-$ to produce DMSO solvated Al^{+3}.

The ^1H spectra obtained from these specimens yield results in complete agreement with the broadline ^{27}Al results. The addition of 1 M DMSO to 1 M $AlCl_3$/MF gave a bulk solvent spectrum identical to the neat solvent and a complexed DMSO resonance shifted approximately 30 Hz downfield

from that observed in a mixed solvent system (DMSO and MF). No residual bulk DMSO resonance was observed but the complexed species spectrum appeared to consist of at least two components. In an electrolyte containing LiCl, 1 M LiCl + 1 M $AlCl_3$/MF & 1 M DMSO, the MF proton spectrum was still that of the neat solvent, but the DMSO resonance consisted of two separate sharp peaks separated by about 8 Hz with the small downfield member at the position of the resonance observed without LiCl (as reported on page 206, formation of a precipitate was observed in this system, and the composition was different from that nominally given). The above results again show that DMSO displaces Cl^- in this system, although the exact species formed cannot be determined on the basis of the two samples studied.

PC As Additive. Addition of 2 M PC to 1 M $AlCl_3$/MF produced no gross change in the ^{27}Al spectrum, except that the solvated peak appeared to broaden somewhat; and addition of 2 M PC to 1 M LiCl + 1 M $AlCl_3$/MF produced no gross change in the ^{27}Al spectrum, except that the saturability of the $AlCl_4^-$ peak was decreased somewhat. This latter result will be discussed further under the next heading (THF As Additive).

The ^1H spectra obtained from these specimens provide some additional information. In the presence of 2 M PC, 1 M $AlCl_3$/MF showed both bulk and coordinated species resonances for this additive. Only a slight decrease in the coordinated MF resonance upon addition of PC was observed. All of the proton resonances in this system, however, appeared to be quite broad and any attempt at a quantitative determination of species present would require variable temperature studies. This data indicates that PC displaces MF from the first coordination sphere of Al^{+3}. Again the presence of 1 M LiCl caused the proton spectra to approximate that observed in the neat mixed solvent system. A slight broadening of all of the lines was observed (probably due to viscosity effects) and the intramolecular chemical shift between the ring protons and the methyl protons of PC was slightly larger in the presence of the added solutes.

THF As Additive. Addition of 2 M THF to 1 M $AlCl_3$/MF resulted in a two peak ^{27}Al spectrum similar to that obtained from 1 M $AlCl_3$/MF. However, the chemical shift between the two peaks was reduced, the relative intensity of the two lines was changed (the solvated peak showing less intensity), and the saturation behavior of the $AlCl_4^-$

peak was considerably changed. Addition of 2 M THF to 1 M LiCl + 1 M $AlCl_3$/MF produced no change in the ^{27}Al spectrum except for some decrease in the saturatability of the $AlCl_4^-$ peak.

Because the addition of THF to 1 M $AlCl_3$/MF so noticeably affects the saturation behavior of the $AlCl_4^-$ line, this characteristic was investigated somewhat further. Fig. 83 shows the saturation behavior of the ^{27}Al line from $AlCl_4^-$ in 1 M $AlCl_3$/MF and in 1 M LiCl + 1 M $AlCl_3$/MF with several additions. The ratio of the peak to peak intensity of the derivative of the $^{27}AlCl_4^-$ line at some higher r.f. power level to the intensity of the derivative at a quite low r.f. is plotted. If no saturation is occurring, this intensity should increase with r.f. power. When saturation occurs, the intensity decreases with r.f. power. Before discussing these data, it should be noted that the most efficient relaxation mechanism is quadrupolar interactions. The species $AlCl_4^-$ which is tetrahedral would be expected to relax poorly because the intraspecies quadrupole interaction is zero. A species such as $Al[MF]_6^{+3}$ would also be expected to relax poorly except that the rapid exchange of bulk solvent with coordinated solvent provides a fluctuating environment for the ^{27}Al nucleus which tends to promote relaxation. It is interesting to first note that the greatest saturation occurs for 1 M LiCl + 1 M $AlCl_3$/MF, which is expected if the predominant species is $AlCl_4^-$, as has been deduced previously. That the $AlCl_4^-$ line in 1 M $AlCl_3$/MF saturates less readily indicates the dynamic nature of the system, namely, that there is some (eventual) exchange between Al in $AlCl_4^-$ and Al in $Al[MF]_6^{+3}$. That the addition of DMSO to 1 M LiCl + 1 M $AlCl_3$/MF produces a saturation curve much like that of 1 M $AlCl_3$/MF is further evidence of the displacement of Cl^- by DMSO. That the addition of THF to 1 M LiCl + 1 M $AlCl_3$/MF produces little change in the saturation curve is consistent with the inability of THF to displace Cl^-. Addition of DMSO and PC to 1 M $AlCl_3$/MF produces no large change relative to the saturation curve of 1 M $AlCl_3$/MF, which again indicates the dynamic nature of the system. In this case there is some exchanging of Al in $AlCl_4^-$ with Al in $Al[S]_6^{+3}$ where S designates solvent and need not be MF. It is clear that the addition of THF to 1 M $AlCl_3$/MF produces a large change in the saturation curve. This can be explained by the presence of some asymmetric Al species, which, as a result of the asymmetry, displays rapid quadrupolar relaxation. Exchange of the Al in $AlCl_4^-$ with this species then provides the enhanced relaxation (reduced

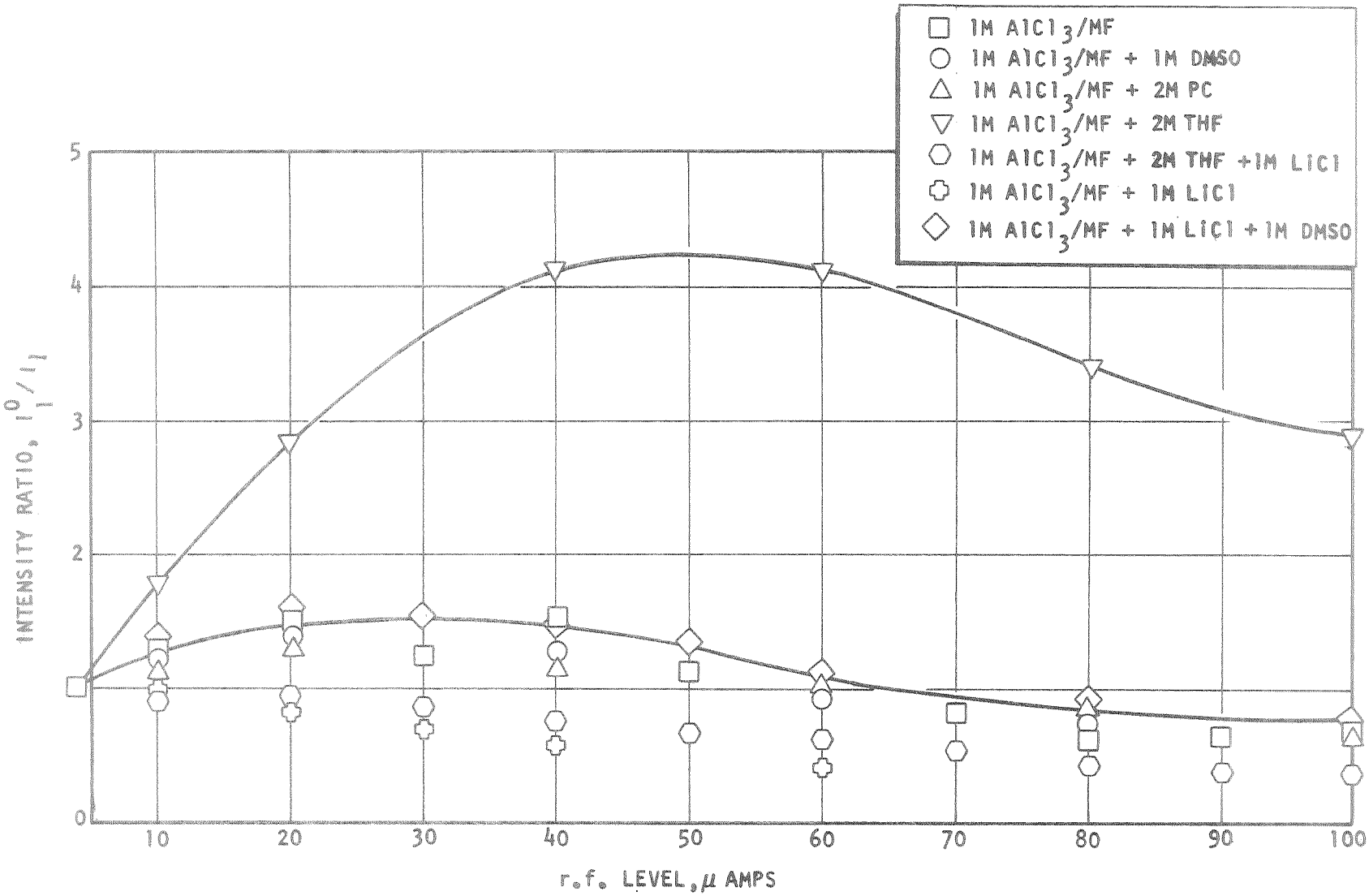

Fig. 83 . Saturation Curves for ^{27}Al Line from $AlCl_4^-$ in 1 M $AlCl_3$/MF with Additives as Noted.

saturation) of the $AlCl_4^-$ line. Because THF is an ether and other Al etherates have been reported, it is reasonable to assume that the species obtained when THF is added to 1 M $AlCl_3$/MF is the etherate $AlCl_3$·THF. This species provides an asymmetrical environment for the Al, thus promoting quadrupolar relaxation and greatly reduced saturation.

^1H spectra obtained for 1 M $AlCl_3$/MF & 2 M THF indicate a complete displacement of complexed MF. However, the THF spectrum consists of only a single sharp resonance pattern with a shift indicative of a complexed molecule, rather than of two patterns, as would be expected for bulk and complexed species. In 1 M LiCl + 1 M $AlCl_3$/MF & 2 M THF a spectrum characteristic of THF in the mixed solvent was not observed, but rather a THF pattern which is intermediate between the bulk and complexed species. This intermediate pattern still retains the sharp line character of a non-exchanging species. These results can also be explained on the same basis as the broadline ^{27}Al data.

$LiClO_4$/MF

DMF As Additive. Because DMF has been shown to be a much stronger agent than MF in solvating Al^{+3}, it seems reasonable to assume that DMF would also solvate Li^+ more strongly than MF. Several specimens of $LiClO_4$/MF containing DMF were investigated to determine if Li^+ solvation by DMF could be observed. The results obtained from ^1H spectra are shown in Table 14. The chemical shifts σ in this table have the same designation as in Table 13. σ_{DMF} does not change, though σ_{MF} does. The data do not show a trend which can be attributed to solvation effects only. Solvation of Li^+ by DMF would be expected to produce a change σ_{MF-DMF} as observed but the change in σ_{MF} coupled with no change in σ_{DMF} can account for this. The lack of observable Li^+ solvation effects indicates that solvation is weak, giving rise to a very small chemical shift, that an interaction of DMF with ClO_4^- is also occurring, that the relative solvating properties of solvents may be different for different ions, or that some other unknown interaction is cancelling out solvation effects.

Broadline ^{35}Cl spectra were run on 1 M $LiClO_4$/MF containing 1 M, 2 M and 4 M DMF. The line observed is relatively narrow and attributable to the ClO_4^- ion. As the concentration of DMF added is increased, the line width decreased indicating an increase in the relaxation time. This is in qualitative accord with the results discussed in the next section for 1 M $LiAsF_6$/MF with DMF added. However, in the 1 M $LiClO_4$/MF and DMF system the changes noted are apparently much smaller. While the line width decreased, the maximum change was less than a factor of two which would correspond to less than a factor of two change in relaxation time. This could be due to an increase in viscosity with the addition of DMF or could be the result of the breaking up of ion pairs.

TABLE 14

CHEMICAL SHIFTS IN $LiClO_4$/MF ELECTROLYTES WITH DMF ADDED

Conc. $LiClO_4$ (M)	Conc. DMF (M)	σ_{MF}(Hz)	σ_{DMF}(Hz)	σ_{MF-DMF}(Hz)
1	6	265	298	8.97
1	4	263	298	7.12
1	4	263	299	7.12
1	1	260	298	3.53
2	2	252	298	8.59
2	4	--	--	8.58
2	4	252	297	8.58
10% MF/DMF		261	303	15

PC and THF As Additives. Neither the addition of 2 M PC or 2 M THF to 1 M $LiClO_4$/MF altered the ^1H spectrum from that obtained from 1 M $LiClO_4$/MF.

$LiAsF_6$/MF*

High resolution ^1H spectra obtained at ambient temperature from a variety of $LiAsF_6$/MF electrolytes with various concentrations of additives did not yield information regarding the solvation of Li^+. Small changes in chemical shifts were observed in some systems but no data were sufficiently consistent to permit any conclusions in this regard. Because of this, more effort was put into broadline NMR experiments which were rendered more informative because of unique characteristics of the NMR of the AsF_6^- ion. Furthermore, because the measurements and their interpretation are unique to AsF_6^-, this discussion includes all electrolytes containing $LiAsF_6$ and represents a deviation (the only major one) from the general organization of this section of the report.

It is anticipated that $LiAsF_6$ dissolved in MF would yield Li^+ and AsF_6^- ions. Theoretically, the ^{19}F spectrum for the AsF_6^- ion should be an equal intensity quartet by virtue of the spin-spin splitting produced by interaction with the ^{75}As nucleus which has a spin, I, of 3/2. The ^{19}F NMR of AsF_6^-, in a different electrolyte has been discussed in the

*$LiAsF_6$/PC electrolytes are discussed in this section also.

literature (Ref. 8). The ^{75}As spectrum should be a seven line pattern with the lines having intensity ratios of 1:6:15:20:15:6:1 by virtue of the interaction with the six equivalent ^{19}F nuclei having spin I = 1/2. These theoretical patterns can be altered, of course, by other effects.

A parameter that has a great effect on the NMR line shape in the case of the patterns mentioned above is the spin lattice relaxation time, T_1. In fact, this parameter for the ^{75}As nucleus can be obtained from the ^{19}F line shape (Ref. 8, 9, and 10), and this parameter is determined by the local environment of the AsF_6^- ion.

It has generally been reported in the literature (there are some exceptions) that a linear correlation exists between T_1^{-1} and the solution viscosity, even though there is considerable debate as to the actual relaxation mechanism. It has been suggested that the primary modes of relaxation are a result of rotational motion of the neighboring solvent molecules, which have electric dipole moments, "collisions" with diffusing ions, and exchange, which is fast compared to T_1, with a highly asymmetric species.

In the case of the AsF_6^- ion changes in T_1^{-1} due to the cations or the solvent molecules in the immediate vicinity of the AsF_6^- ions have been discussed in several papers by Arnold and Packer (Ref. 8, 11, and 12) and other workers referred to in these papers. It is the contention of Arnold and Parker that the major contribution to T_1 is the effect of cations, and they suggest that only some of the AsF_6^- ions need to be in an environment with short T_1 to obtain a net short T_1 for the system.

Because variations in the relaxation times, with different solvents and different additives in a given solvent, are determined by, (1) solvation of the anion (AsF_6^-) and liquid properties, such as viscosity, and (2) solvation of the cation (Li^+) and liquid properties such as viscosity, and (3) changes in chemical equilibria with other species, particularly asymmetric species, T_1 is generally a useful parameter for monitoring changes in the electrolyte structure produced by additives; and because of the ease in determining T_1 for the AsF_6^- ion, this method is also quite convenient for electrolytes containing this ion.

^{19}F broadline NMR spectra were obtained for several electrolytes containing $LiAsF_6$ as listed in Table 15. These spectra are shown in Figures 84 through 98.

For the specimens listed in Table 15, T_1's were estimated by comparing the line shape with curves shown in Ref. 9, and interpolation when the line shapes were between those displayed in Ref. 9 using Figure 99. Figure 99 is a plot of T_1 vs the line shape defining parameter, $X = 2\pi JT_1$, where J is the spin-spin coupling constant between ^{75}As and ^{19}F. J was taken as 933 Hz (Ref. 8). (When comparing the spectra shown in Figures 84 through 98 with the curves on Figure 99, one should recall that the spectra are first derivatives of the absorption curves, while absorption curves are shown on Figure 99).

TABLE 15

^{75}As RELAXATION TIMES IN $LiAsF_6$ ELECTROLYTES

Electrolyte	Additive	η_{est} (millipoise)	$\bar{\mu}$ (Debyes)	T_1 (10^{-3} sec.)
1 M $LiAsF_6$/MF	0	8.00	1.77	0.20
1 M $LiAsF_6$/MF	6 M DMF	12.1	2.51	1.4
1 M $LiAsF_6$/MF	4 M DMF	10.6	2.28	1.4
1 M $LiAsF_6$/MF	2 M DMF	9.2	2.02	0.6
1 M $LiAsF_6$/MF	1 M DMF	8.4	1.91	0.4
1 M $LiAsF_6$/MF	2 M PC	11.1	1.95	0.3
1 M $LiAsF_6$/PC	0	86.3	4.98	0.14
1 M $LiAsF_6$/PC	2 M MF	58.2	4.19	0.16
1 M $LiAsF_6$/PC	4 M NM	47.3	4.38	0.15
1 M $LiAsF_6$/PC	4 M NM	47.3	4.38	0.15
1 M $LiAsF_6$/PC	4 M THF	46.2	3.91	0.18
1 M $LiAsF_6$/PC	4 M DMSO	35.2	4.62	0.80
1 M $LiAsF_6$/DMF	6 M MF	14.5	2.90	1.6

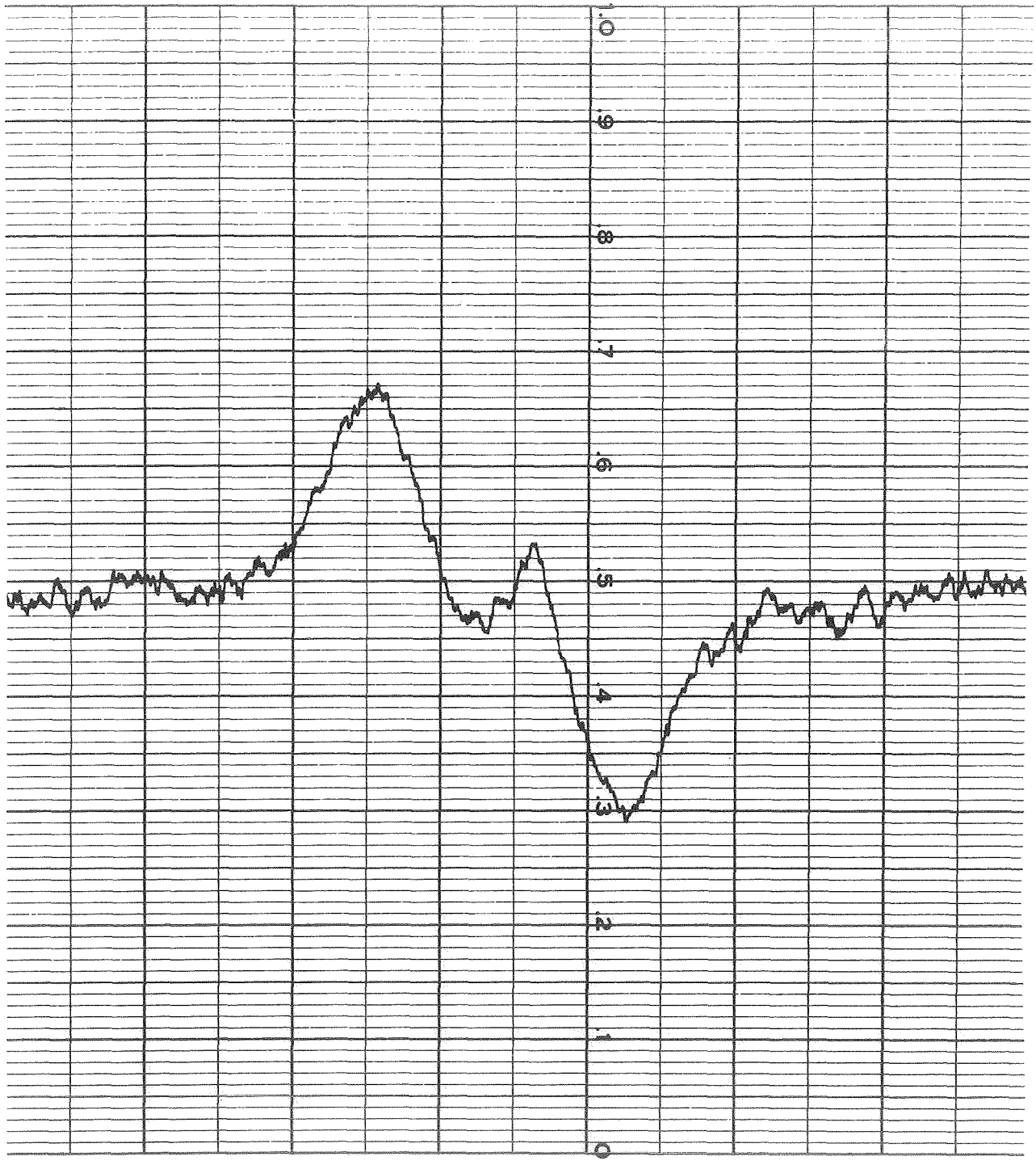

Fig. 84. Broadline ^{19}F Resonance in 1 M $LiAsF_6$ #1/MF #2-11. One Division, Left to Right, is 1 Gauss.

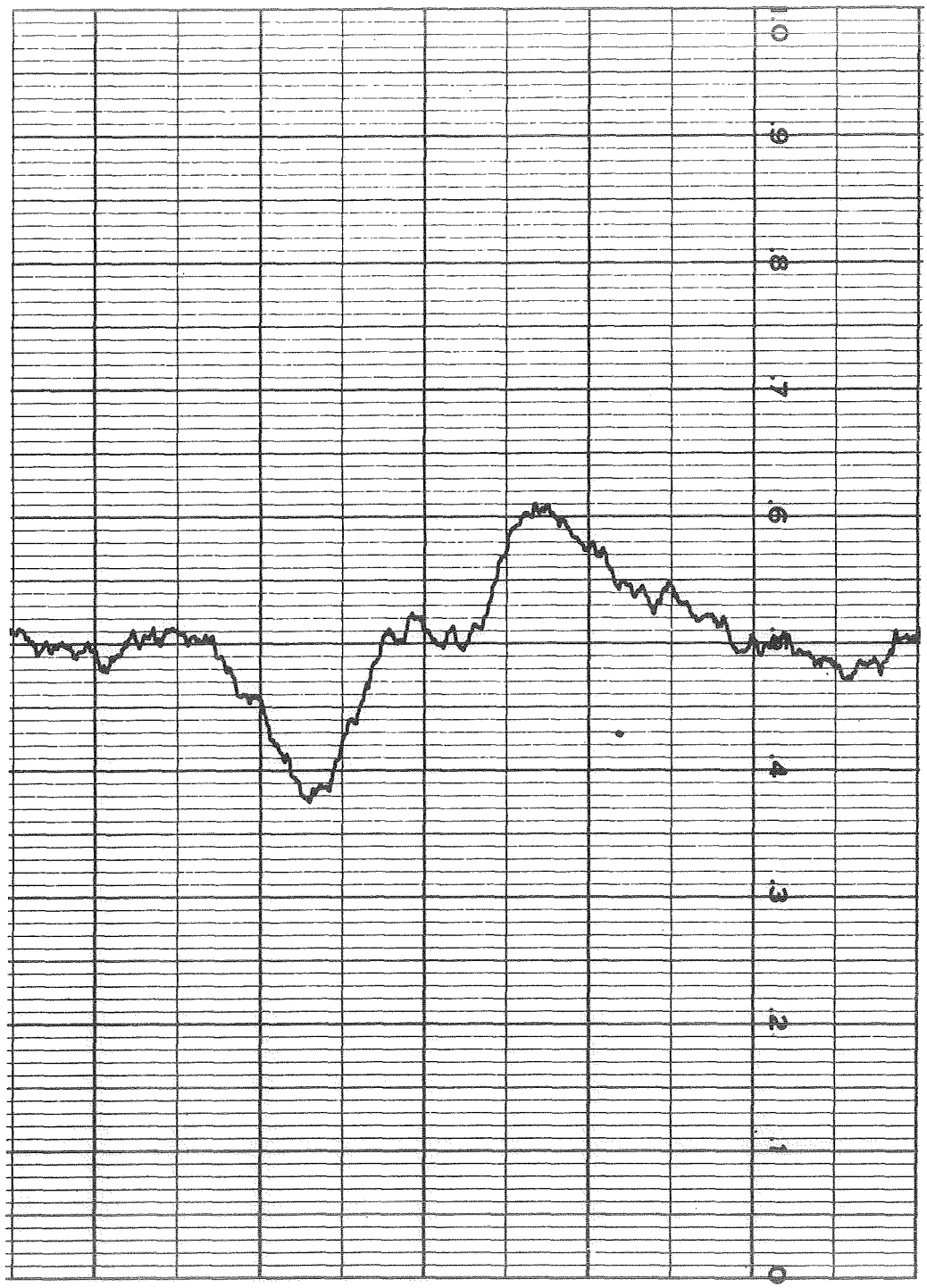

Fig. 85. Broadline ^{19}F Resonance in 1 M $LiAsF_6$ #2/MF #3-2. One Division, Left to Right, is 1 Gauss.

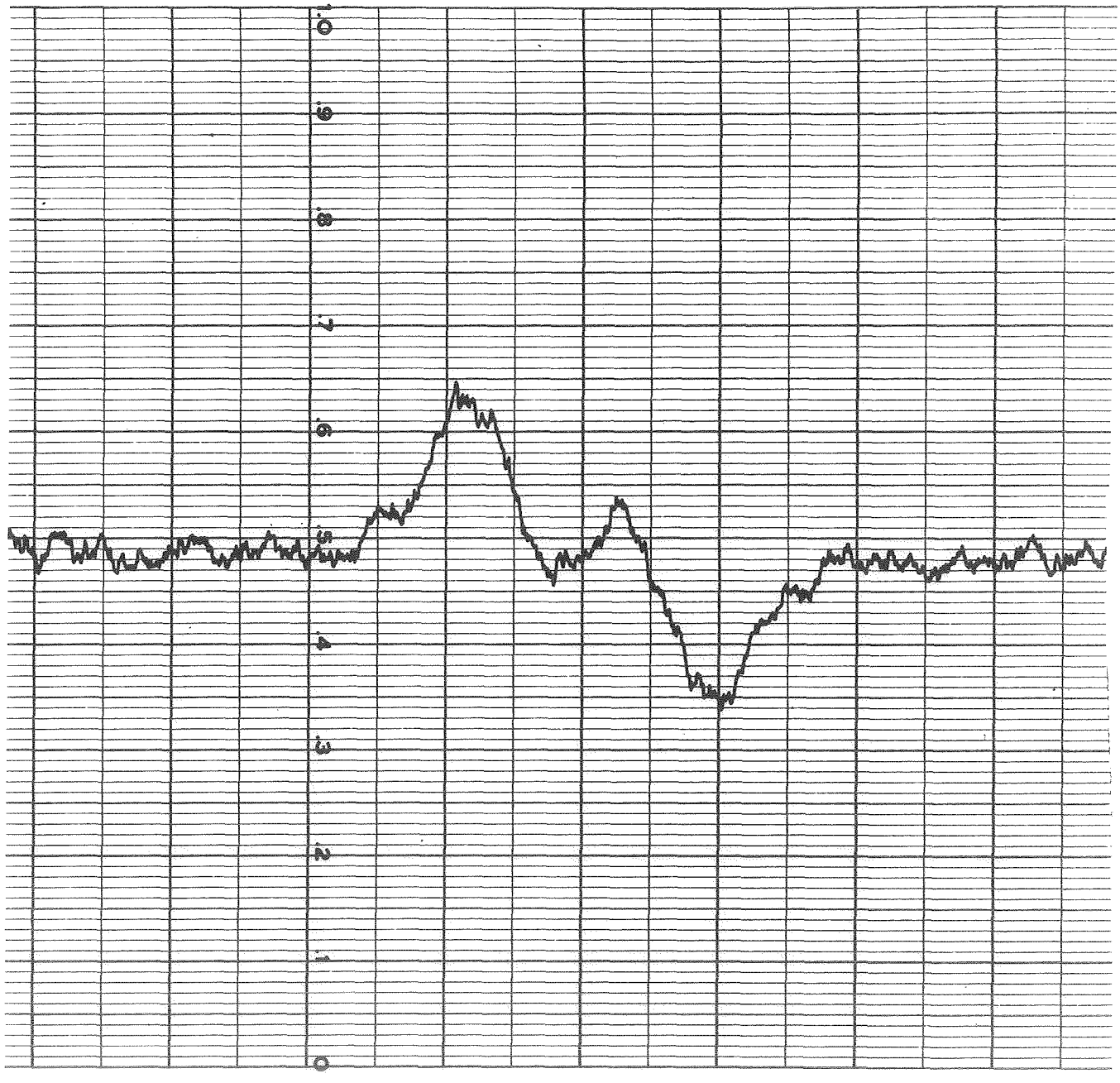

Fig. 86. Broadline ^{19}F Resonance in 1 M $LiAsF_6$ #1/MF #2-11 & 1 M DMF #7-3. One Division, Left to Right, is 1 Gauss.

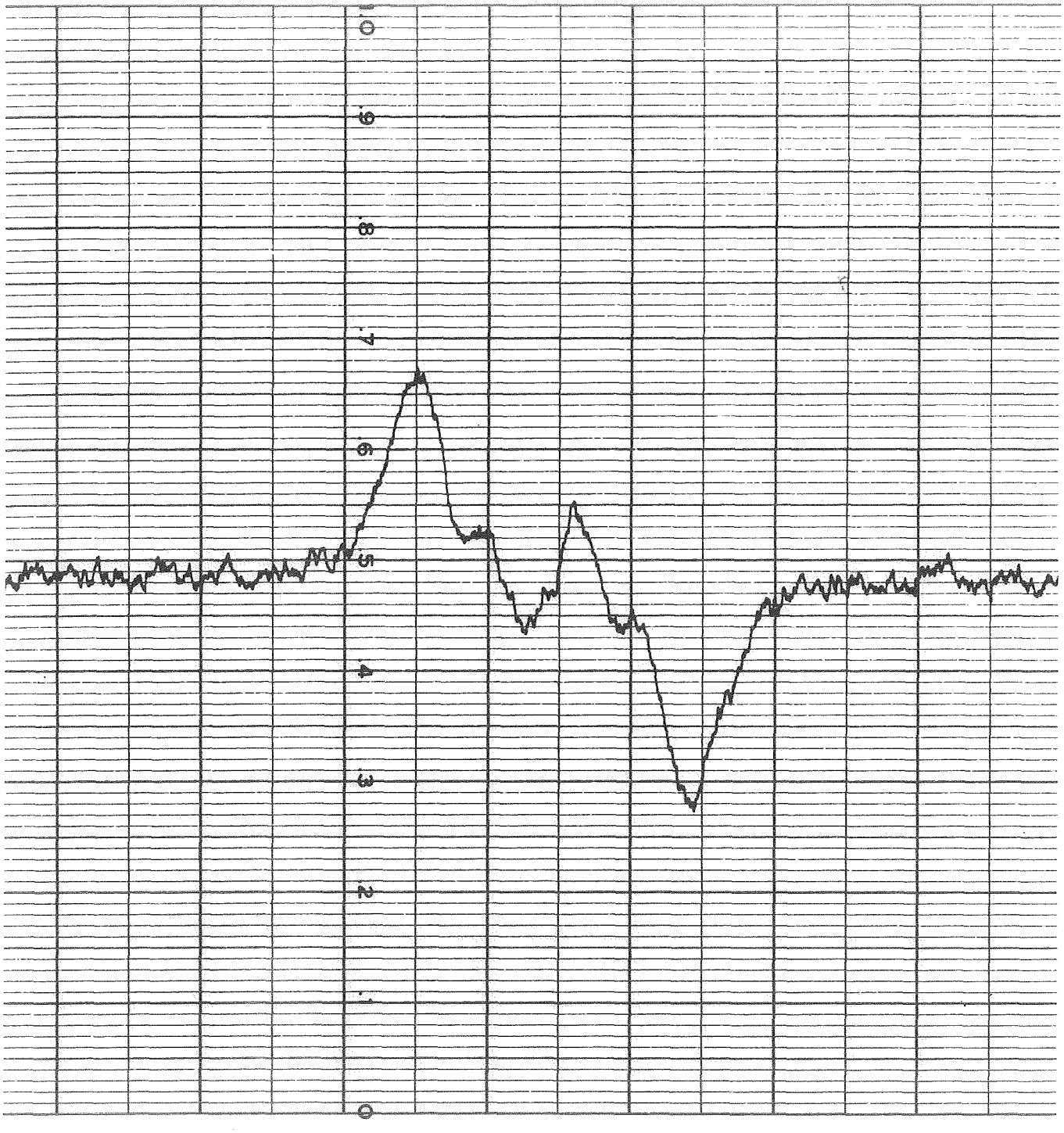

Fig. 87. Broadline ^{19}F Resonance in 1 M $LiAsF_6$ #1/MF #2-11 & 2 M DMF #7-3. One Division, Left to Right, is 1 Gauss.

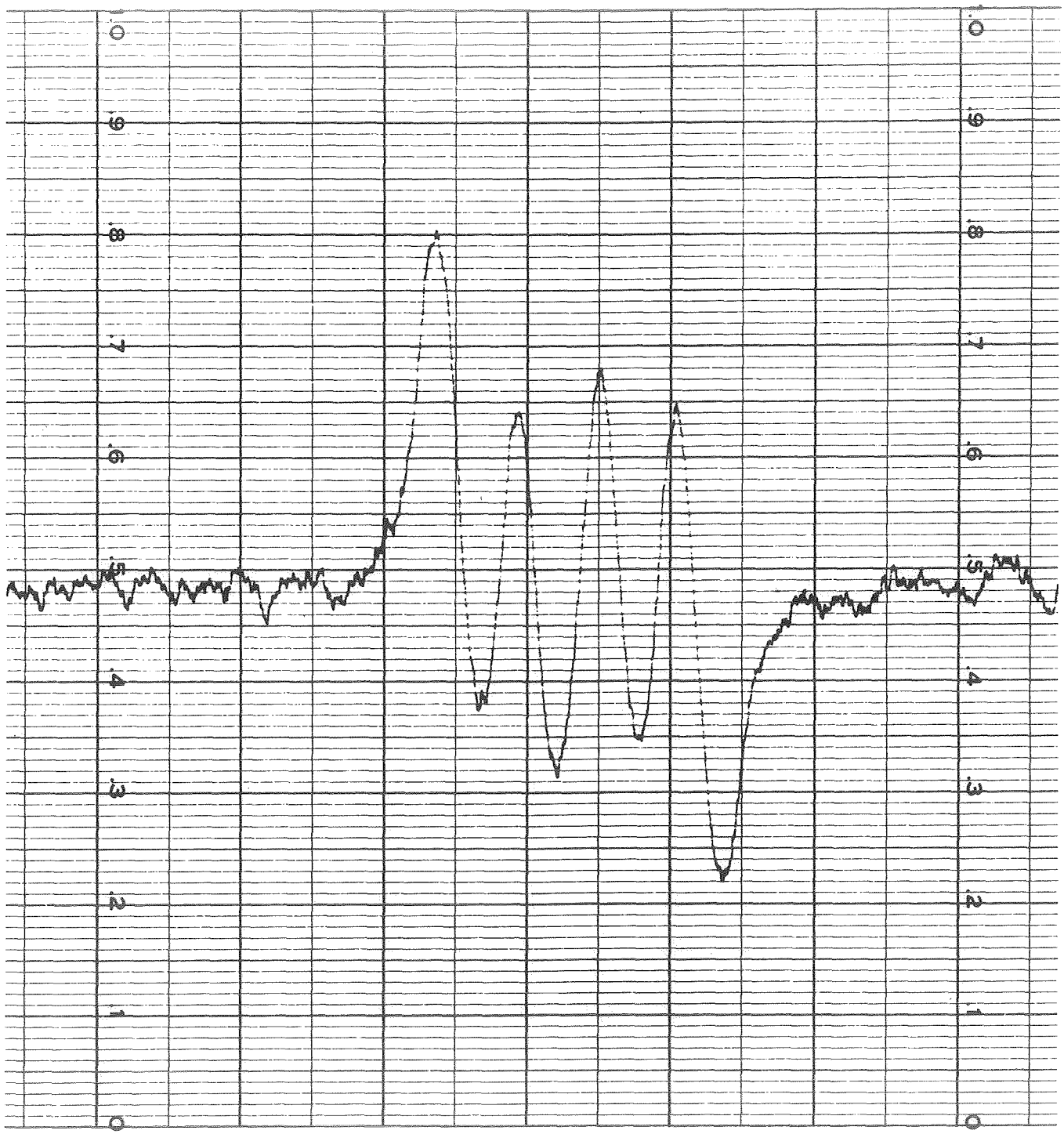

Fig. 88. Broadline ^{19}F Resonance in 1 M $LiAsF_6$ #1/MF #2-11 & 4 M DMF #7-3. One Division, Left to Right, is 1 Gauss.

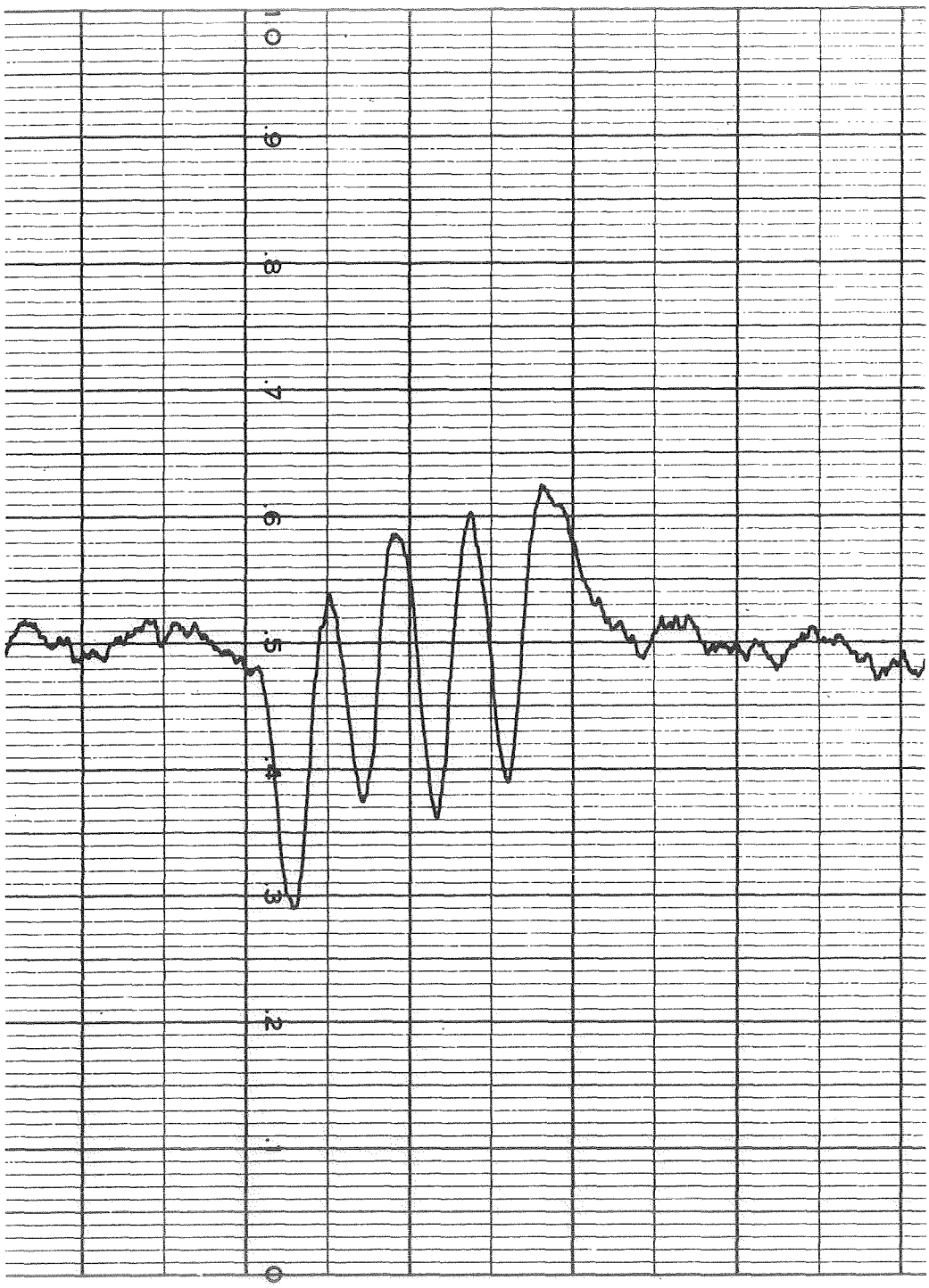

Fig. 89. Broadline ^{19}F Resonance in 1 M $LiAsF_6$ #2/MF #3-3 & 6 M DMF #7-3. One Division, Left to Right, is 1 Gauss.

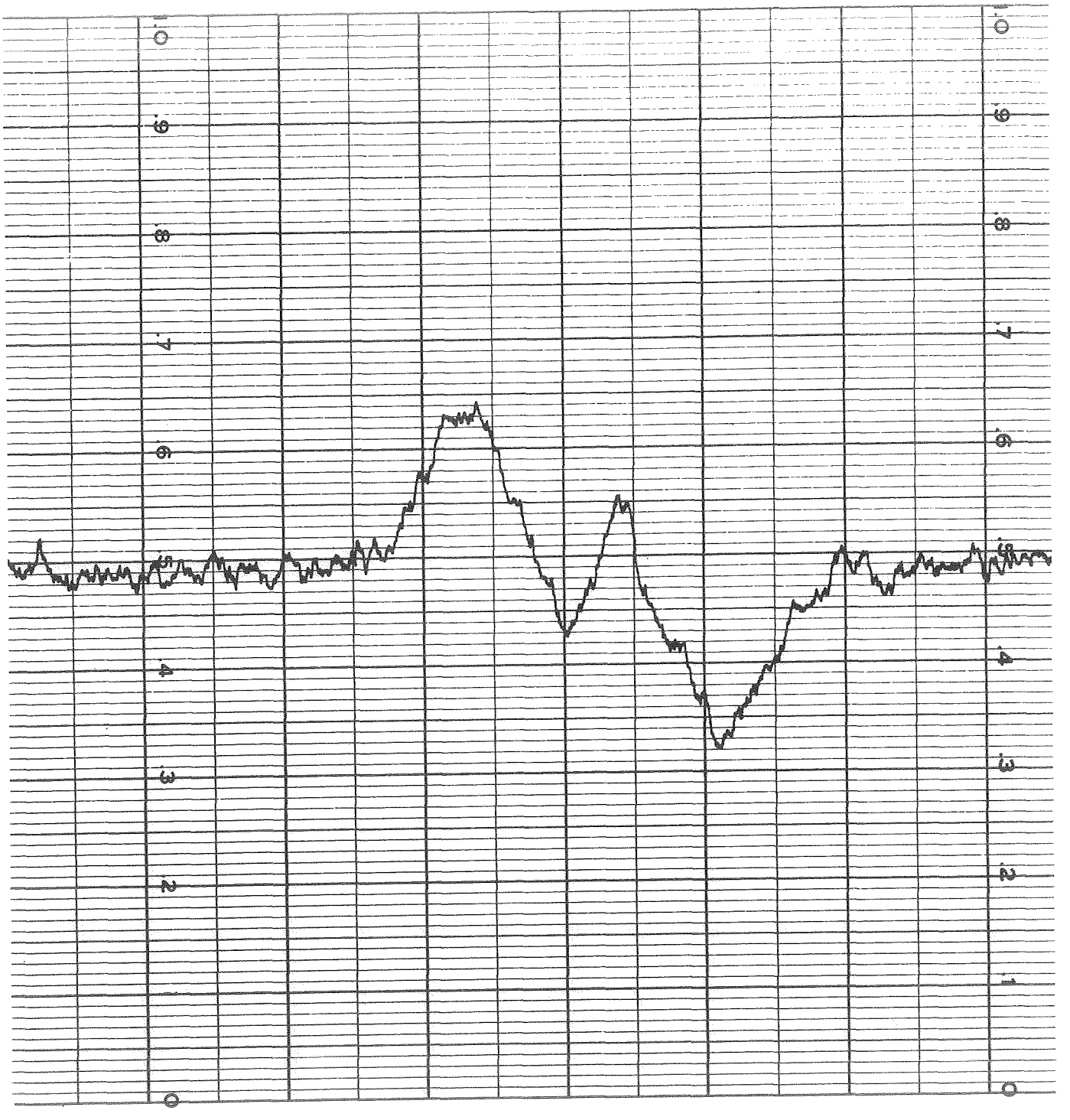

Fig. 90. Broadline ^{19}F Resonance in 1 M $LiAsF_6$ #1/MF #2-11 & 2 M PC #7-1. One Division, Left to Right is 1 Gauss.

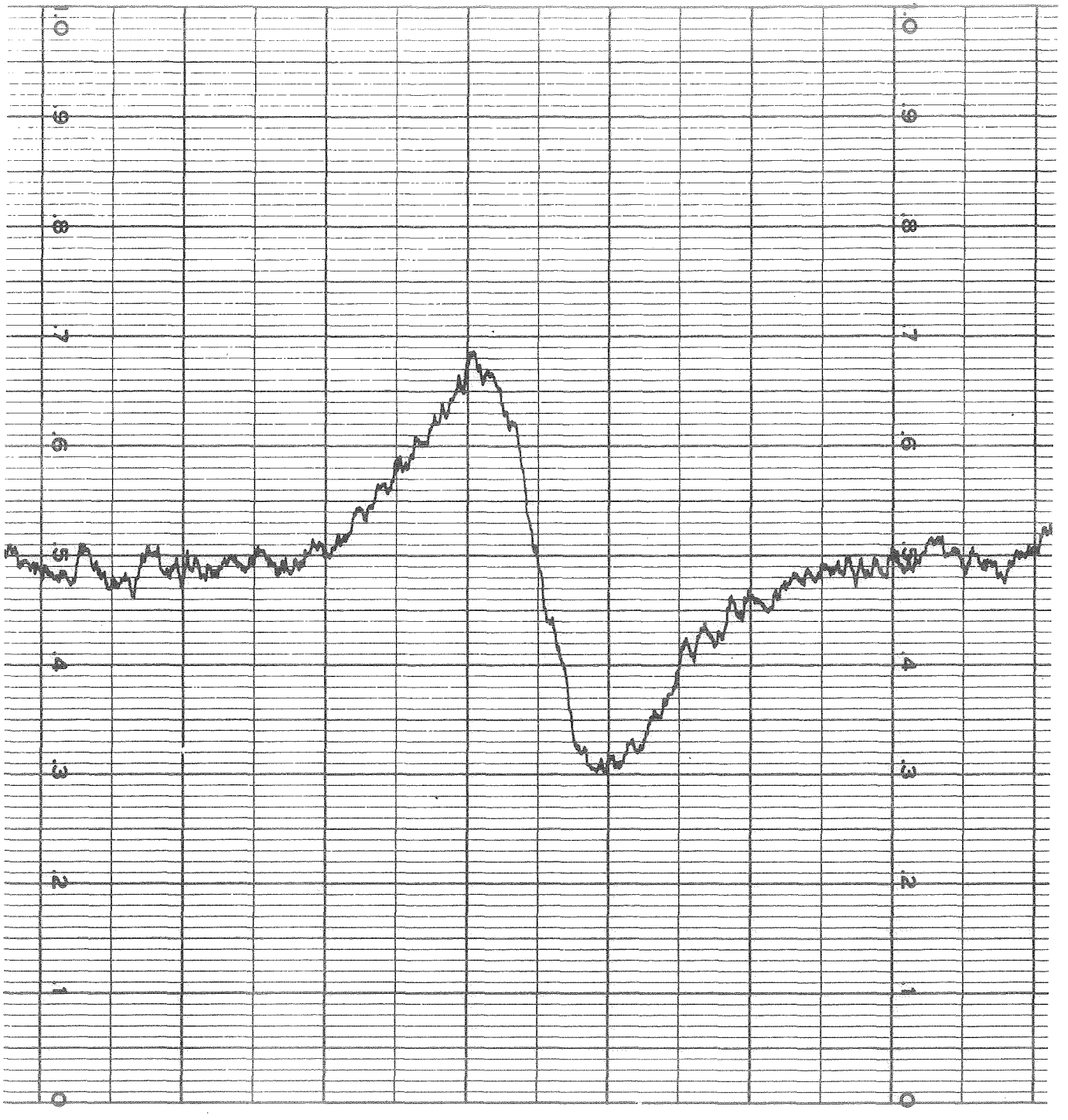

Fig. 91. Broadline ^{19}F Resonance in 1 M $LiAsF_6$ #2/PC #7-5. One Division, Left to Right is 1 Gauss.

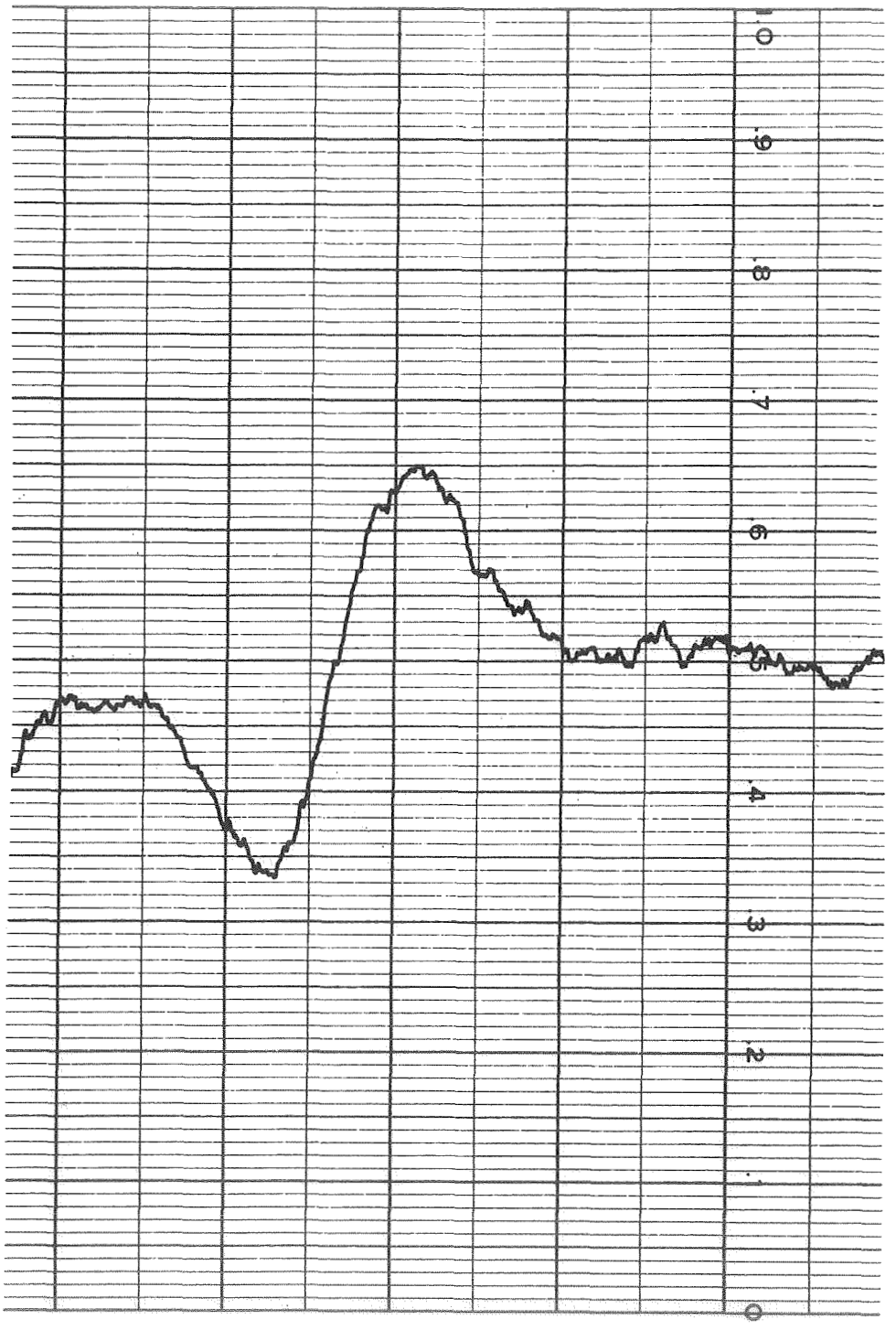

Fig. 92. Broadline ^{19}F Resonance in 1 M $LiAsF_6$ #4/PC #7-8. One Division, Left to Right is 1 Gauss.

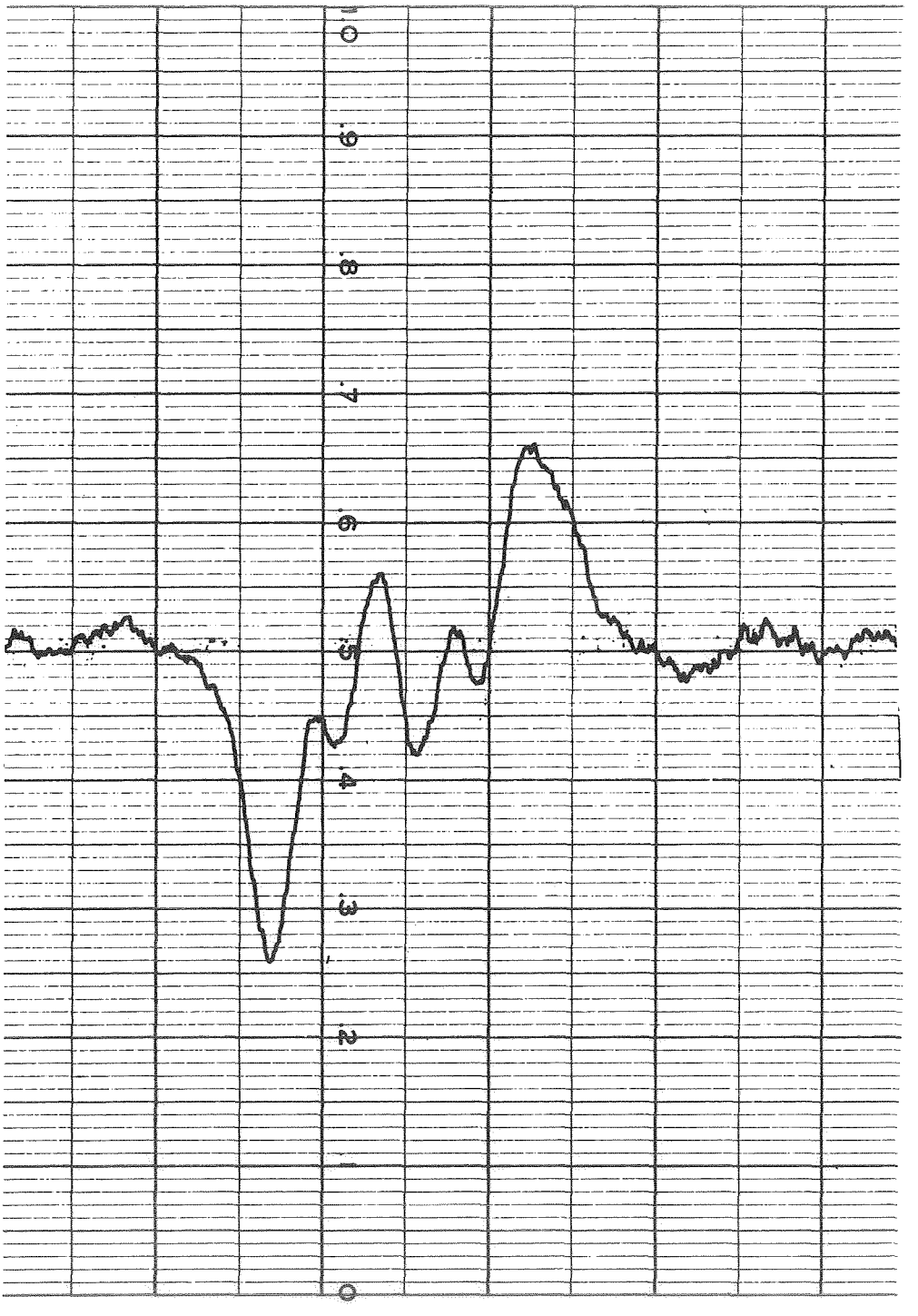

Fig. 93. Broadline ^{19}F Resonance in 1 M $LiAsF_6$ #4/PC #7-8 & 4 M DMSO #1-1. One Division, Left to Right, is 1 Gauss.

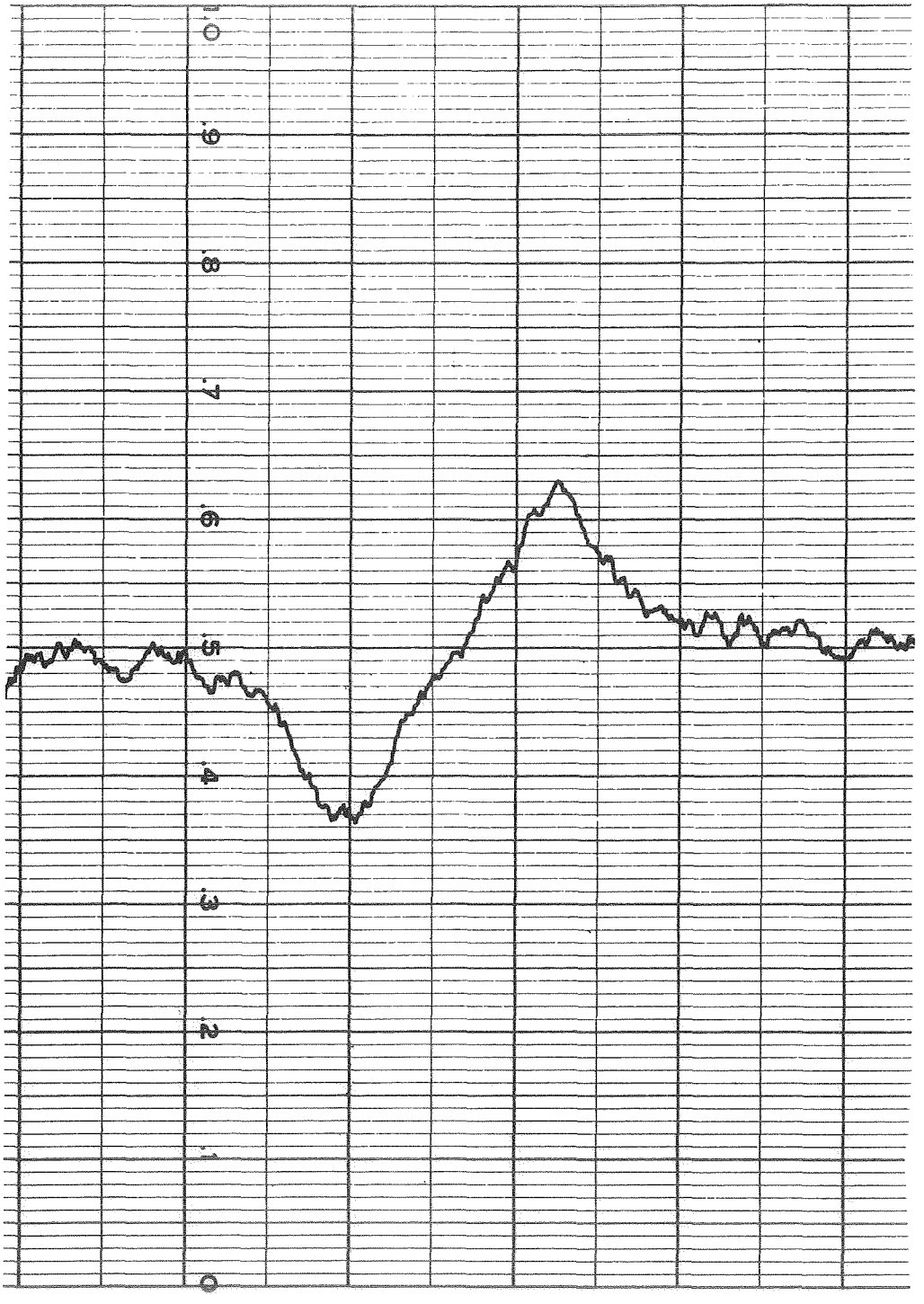

Fig. 94. Broadline ^{19}F Resonance in 1 M $LiAsF_6$ #2/PC #7-5 & 2 M MF #2-14. One Division, Left to Right, is 1 Gauss.

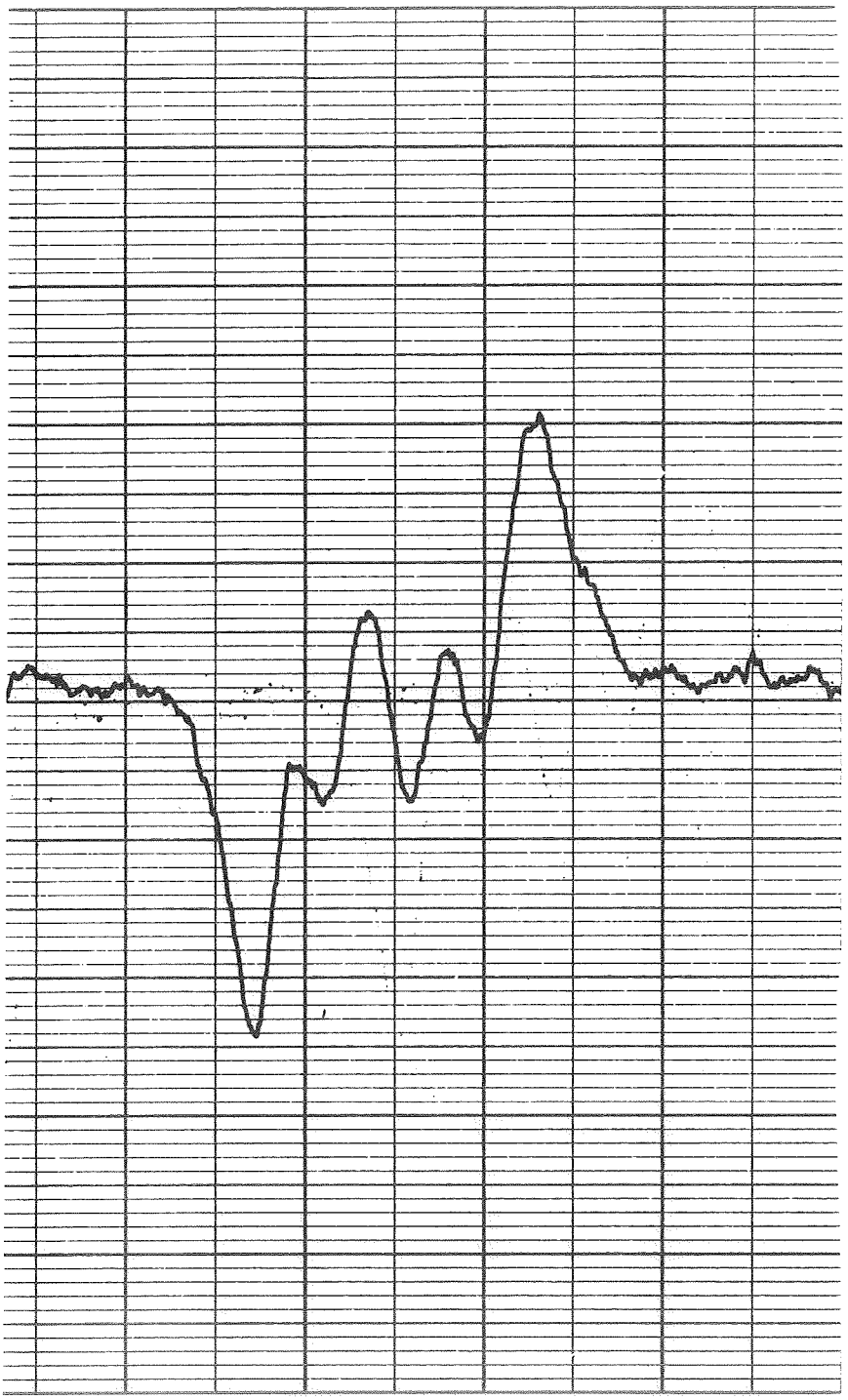

Fig. 95. Broadline ^{19}F Resonance in 1 M $LiAsF_6$ #4/PC #7-8 & 4 M DMF #7-3. One Division, Left to Right is 1 Gauss.

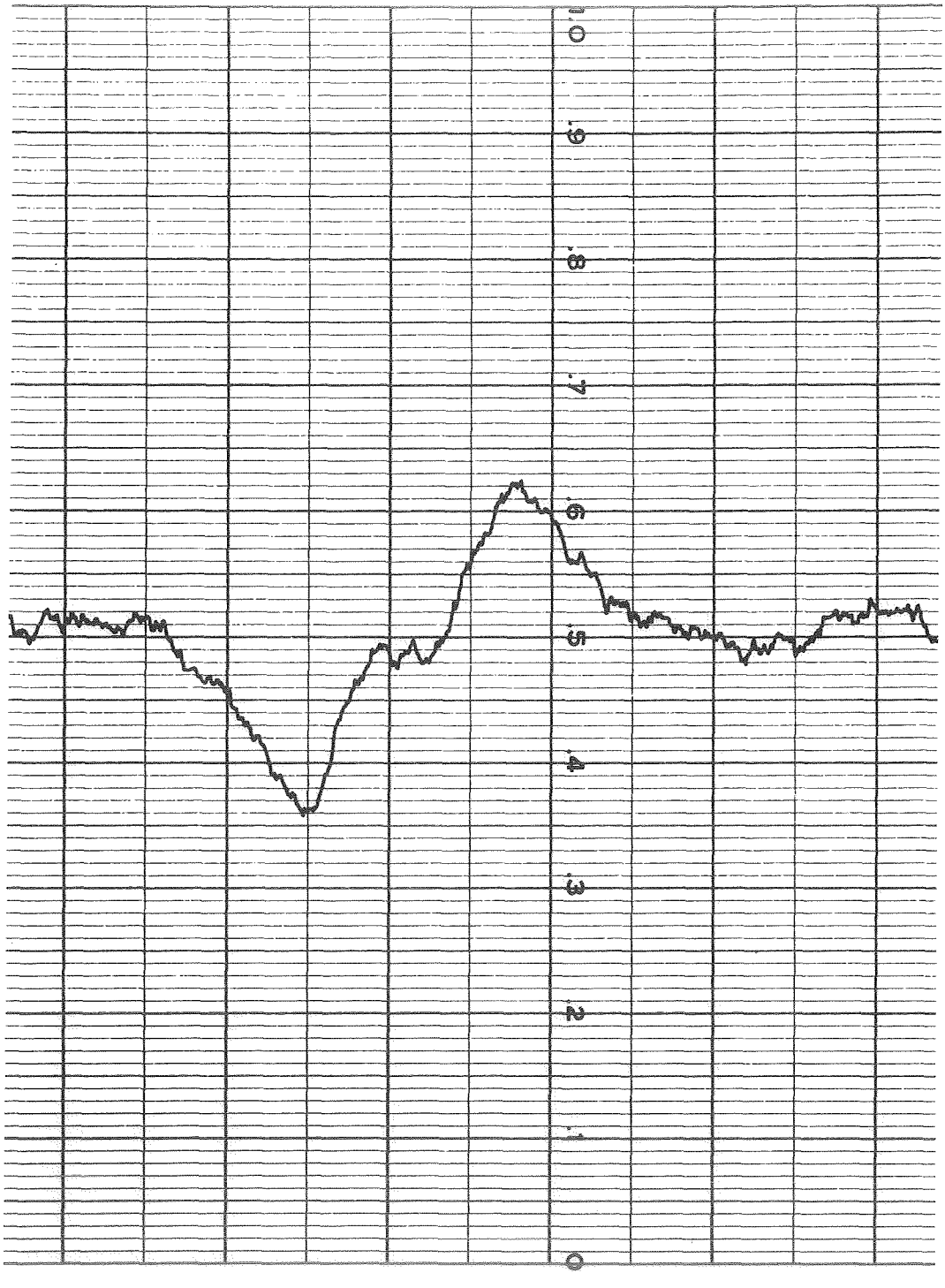

Fig. 96. Broadline ^{19}F Resonance in 1 M $LiAsF_6$ #4/PC #7-8 & 4 M THF #1. One Division, Left to Right, is 1 Gauss.

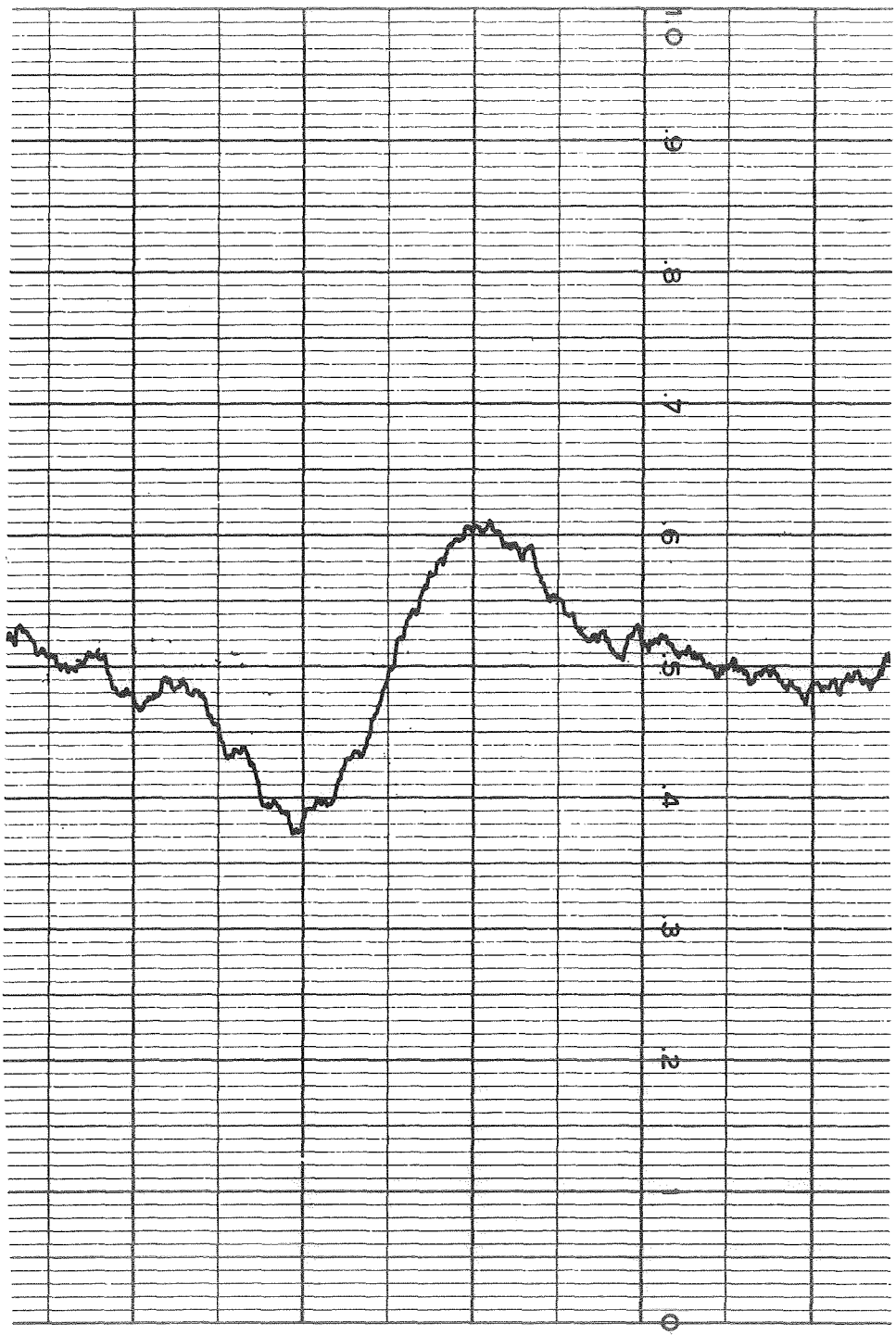

Fig. 97. Broadline ^{19}F Resonance in 1 M $LiAsF_6$ #4/PC #7-8 & 4 M NM #1-2. One Division, Left to Right, is 1 Gauss.

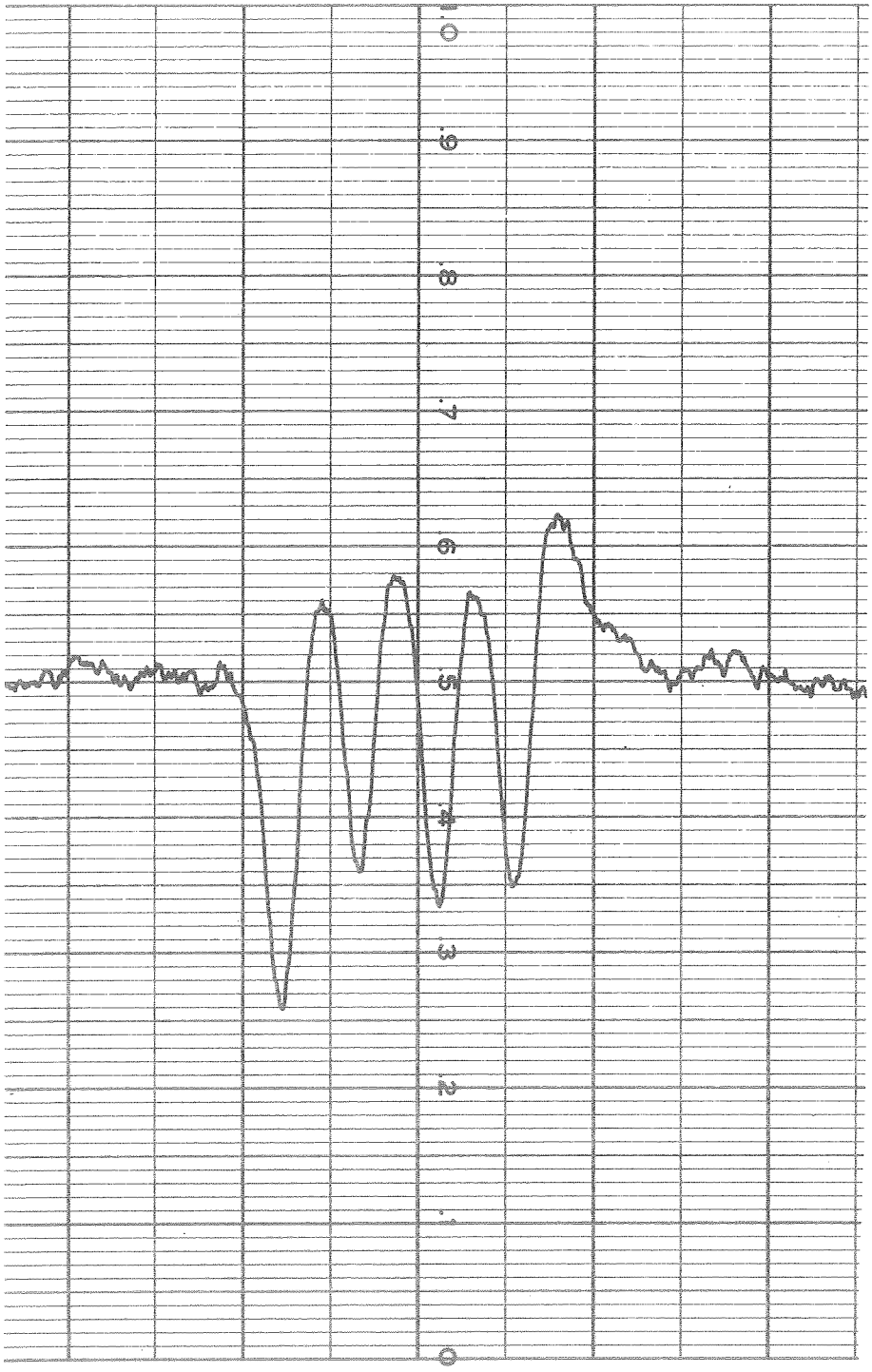

Fig. 98. Broadline ^{19}F Resonance in 1 M $LiAsF_6$ #2/DMF #7-3 & 6 M MF #3-3. One Division, Left to Right, is 1 Gauss.

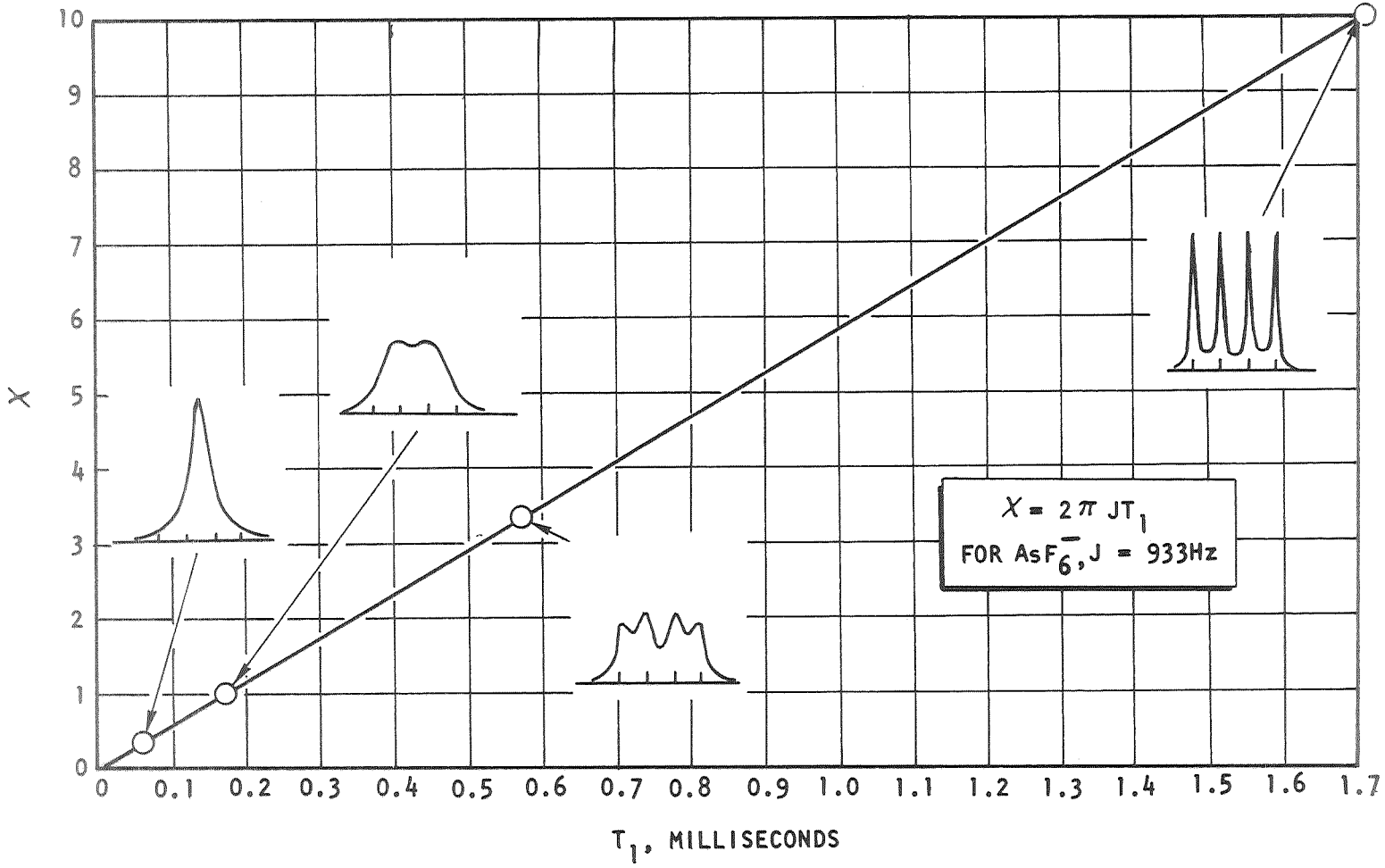

Fig. 99. Plot of T_1 vs $\chi = 2\pi JT_1$, with Line Shapes as Determined in Ref. 9.

As a preliminary test of the possible relaxation method, it is desirable to plot T_1^{-1} as a function of solution viscosity. Because the solution viscosities have not been measured, they were estimated assuming ideal solutions. For a solvent mixture containing solvent A and solvent B with viscosities η_A and η_B, respectively, the mixed solvent viscosity η_M is given by

$$\eta_M = \eta_B \left(\frac{\eta_A}{\eta_B} \right)^{m_A}$$

where m_A is the molar fraction of solvent A. When known, the viscosity with the salt added was used; when not known, the viscosity increase upon salt addition was estimated by comparison with measured solutions. All η_M's are based upon either known or estimated η_A's and η_B's with salt added. The estimated viscosity is also shown in Table 15 and a plot of T_1^{-1} vs η_M is shown in Figure100. Clearly, even taking into account errors in estimation of viscosities and approximations in T_1's, there is not a linear correlation between T_1^{-1} and the viscosity.

Because one of the postulated mechanisms of relaxation is through interaction with the local solvent dipole moments, an average (arithmetic) dipole moment is also indicated in Table 15. Relaxation via solvent dipole moments should result in a decrease in T_1 as the average dipole moment increases. However, as can be seen from the results for MF based electrolytes, the opposite trend is observed.

Based upon these results, it is apparent that the relaxation times are dependent upon some phenomena other than the ion-solvent interaction. Furthermore, because the relaxation times do not correlate with viscosity,* and because they all have the same salt concentration (1 M), relaxation via ion-ion interactions also appears not to be the dominant mechanism. However, another possibility not noted in the literature is that some of the solvent additives may preferentially solvate cations making the distance of closest approach in anion (AsF_6^-) cation (Li^+) collisions effectively larger and thus increasing the ion-ion induced relaxation time. At this juncture, though, it seems that the most likely of the three mechanisms listed above is that based upon rapid exchange between the AsF_6^- ion and another species having asymmetry relative to the arsenic site, the asymmetric species then providing the relaxation. The asymmetric species could be a "chemical" species such as AsF_5 or a relatively long lived charge multiplet, such as an ion pair or triplet, having AsF_6^- as one of the participants. Changes in T_1 as a function of additives would then be incurred, provided the additives can change the equilibrium between AsF_6^- and one or more asymmetric species.

---

*The lack of correlation is with T_1^{-1}.

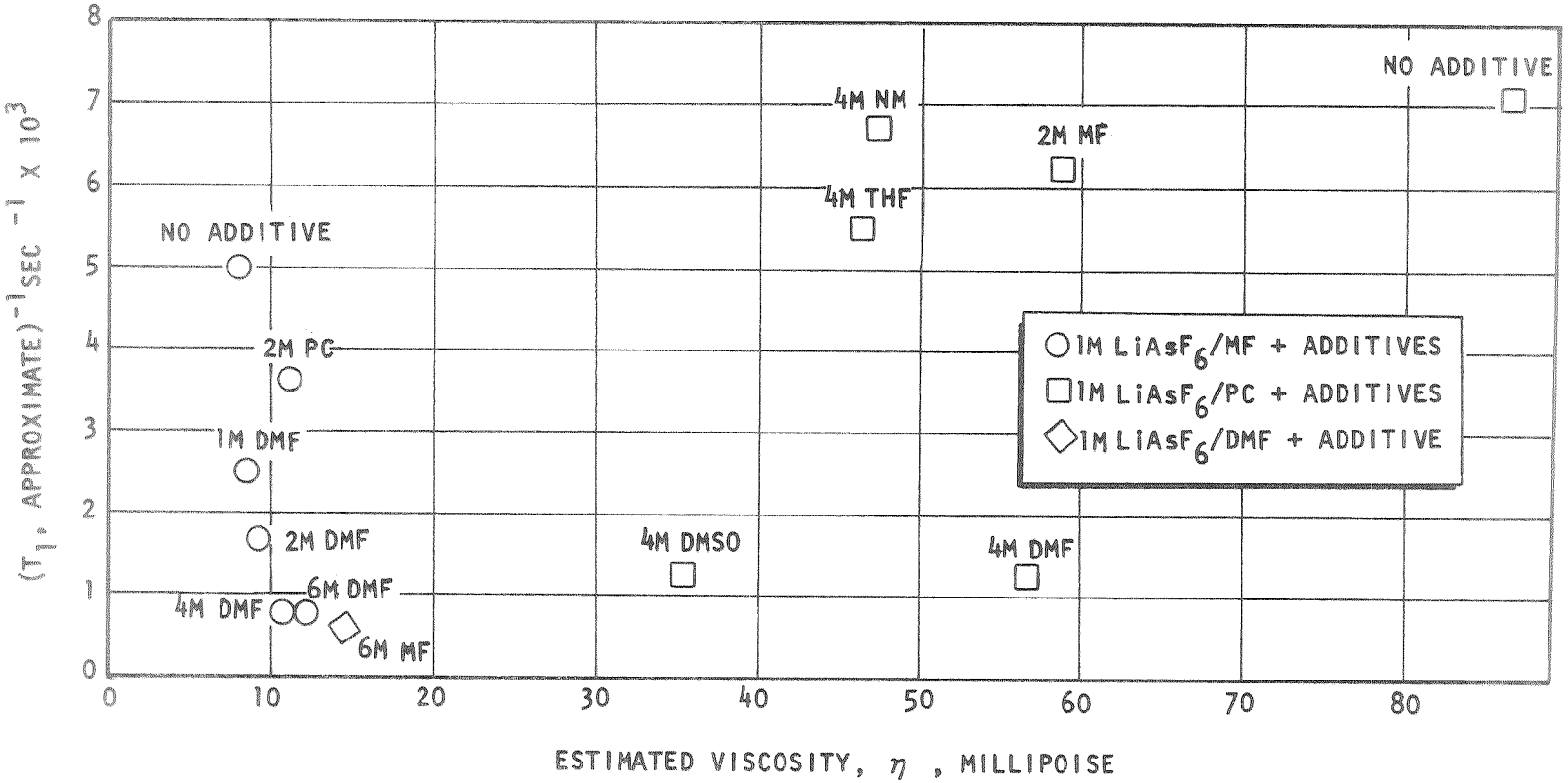

Fig.100. Plot of Reciprocal T_1's vs Estimated Viscosities for the AsF_6^- Ion, in Solutions, As Noted, Containing $LiAsF_6$.

Figures 101 through 105 show the ^{75}As line for $LiAsF_6$/MF electrolytes. The change in line shape noted here is in accord with the changes in the ^{19}F line shape in the same specimens.

From these results the major species in electrolytes with $LiAsF_6$ are Li^+ and AsF_6^- as expected. The unexpected results is the evidence of an asymmetric As containing species. This species was not observed directly, so little can be said regarding its concentration.

$AlCl_3$

$LiAsF_6$/MF with $AlCl_3$ added was originally planned to be studied. However, an attempt to prepare a sample was unsuccessful when a gel was formed rather than a solution.

H_2O As Additive. High resolution proton spectra were run on a variety of specimens to investigate the effect of small amounts of water in $LiAsF_6$/MF electrolytes. The amount of water involved has no affect on the ^{19}F or ^{75}As broadline spectra. For comparison, ^1H spectra were recorded for pure MF with water added (no $LiAsF_6$). Specimens consisting of pure MF with 2000, 500 and 100 ppm H_2O added show the water proton peak as displayed in Figures 106, 107, and 108. In the 100 ppm specimen the water peak is barely perceptible at the instrument conditions used to record the proton line in the 2000 and 500 ppm specimen. As the water concentration is reduced, the line width increases rendering the line in the 100 ppm water added specimen more difficult to observe. In the initial survey of 1 M $LiAsF_6$/MF, with 2000, 500 and 100 ppm water added, the water proton line could not be observed immediately (about one hour) after sample preparation. In fact, no evidence could be found for the water added. A day later, a peak shown in Figure 109, was observed in the 1 M $LiAsF_6$/MF and 2000 ppm H_2O at the position that corresponds to the methyl protons in methanol; no other peaks were observed. After another day, peaks appeared at essentially the same position in the 500 ppm H_2O and 100 ppm H_2O specimens, as shown in Figures 110 and 111. By comparison with the nearby ^{13}C sideband of the methyl protons in MF, it can be concluded that essentially all of the water in the 2000 ppm specimen has been converted to CH_3OH. It is presumed that the presence of $LiAsF_6$ catalyzes the deesterification reaction

$$HCOOCH_3 + HOH \rightarrow CH_3OH + HCOOH$$

because in the pure MF the water proton line was still observed two days after preparation. An old (about 2 years) specimen of MF with 1% water added was investigated and both the CH_3 and an OH line were observed.

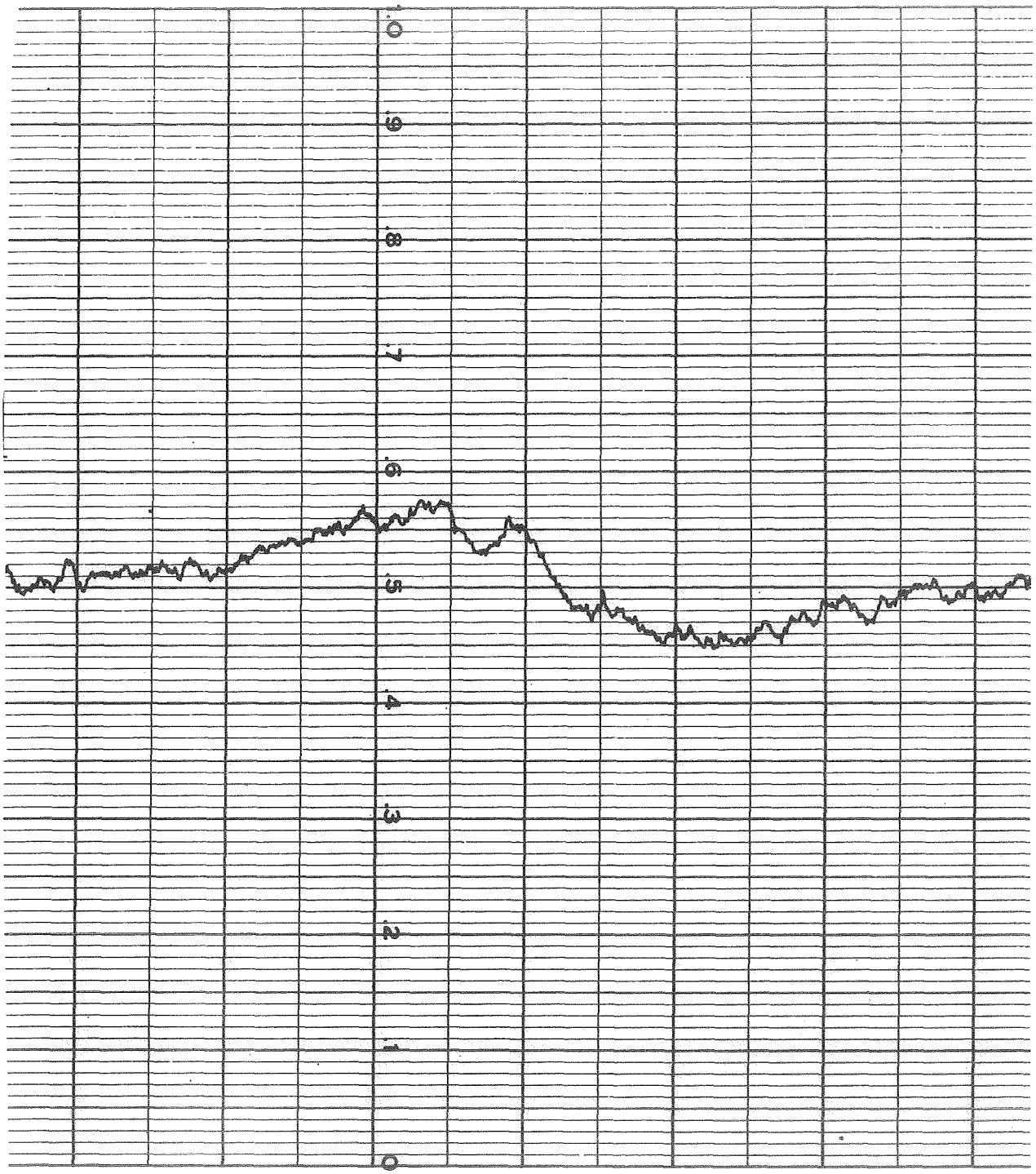

Fig. 101. Broadline ^{75}As Resonance in 1 M $LiAsF_6$ #1/MF #2-11.
One Division, Left to Right, is 1 Gauss.

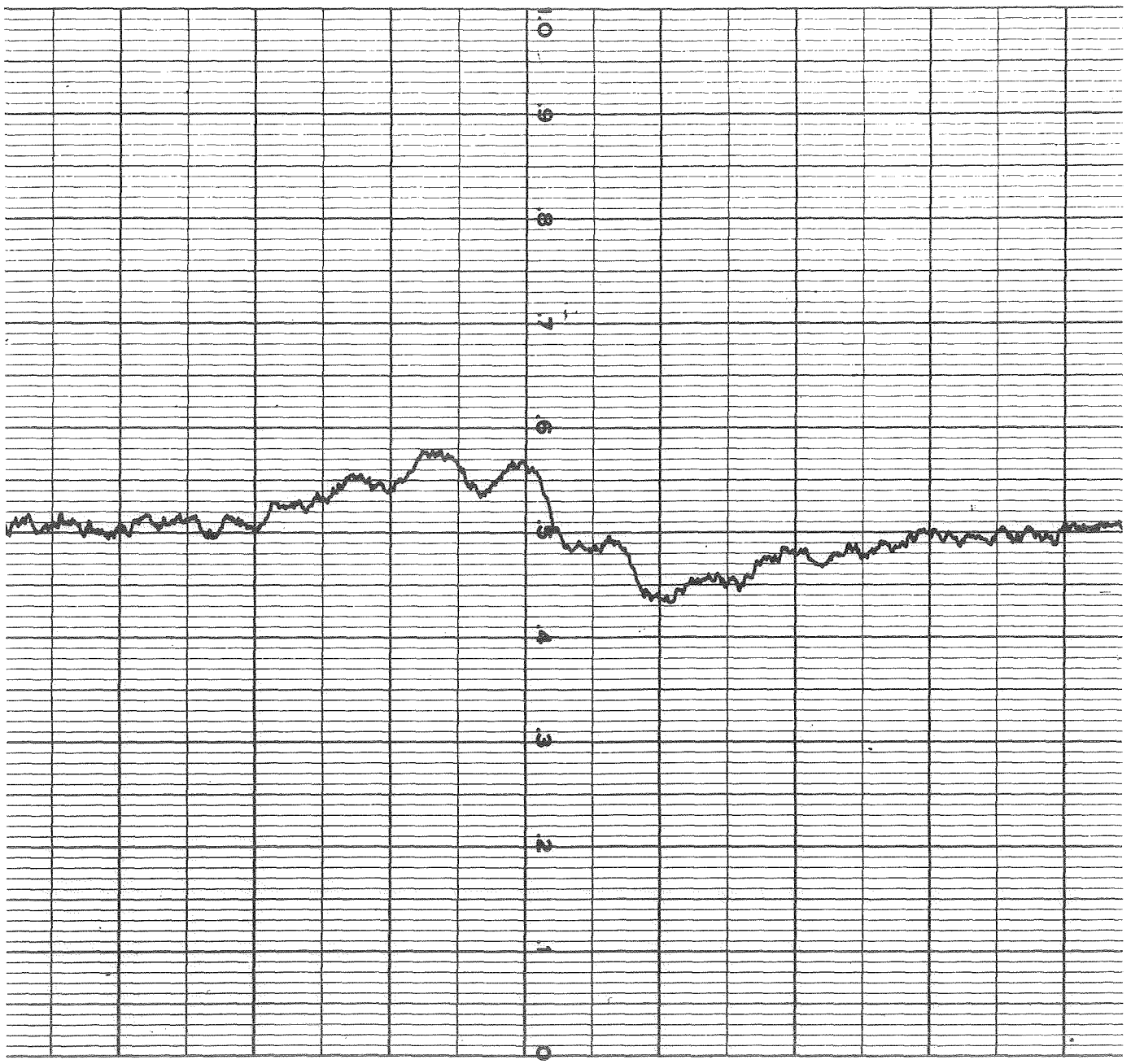

Fig. 102. Broadline ^{75}As Resonance in 1 M $LiAsF_6$ #1/MF #2-11 & 1 M DMF #7-3. One Division, Left to Right, is 1 Gauss.

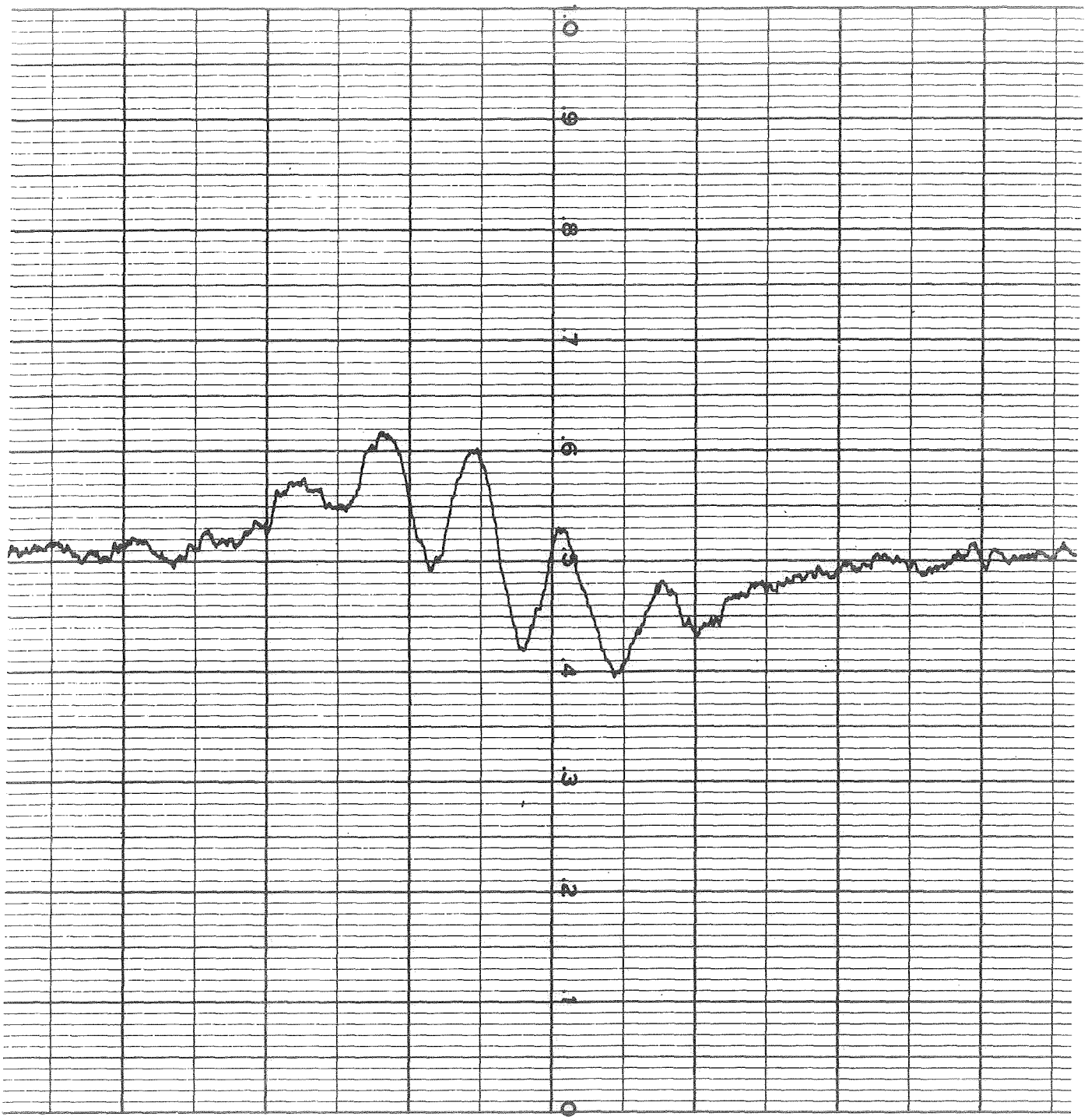

Fig. 103. Broadline ^{75}As Resonance in 1 M $LiAsF_6$ #1/MF #2-11 with 2 M DMF #7-3. One Division, Left to Right, is 1 Gauss.

Fig. 104. Broadline ^{75}As Resonance in 1 M $LiAsF_6$ #1/MF #2-11 & 4 M DMF #7-3. One Division, Left to Right, is 1 Gauss.

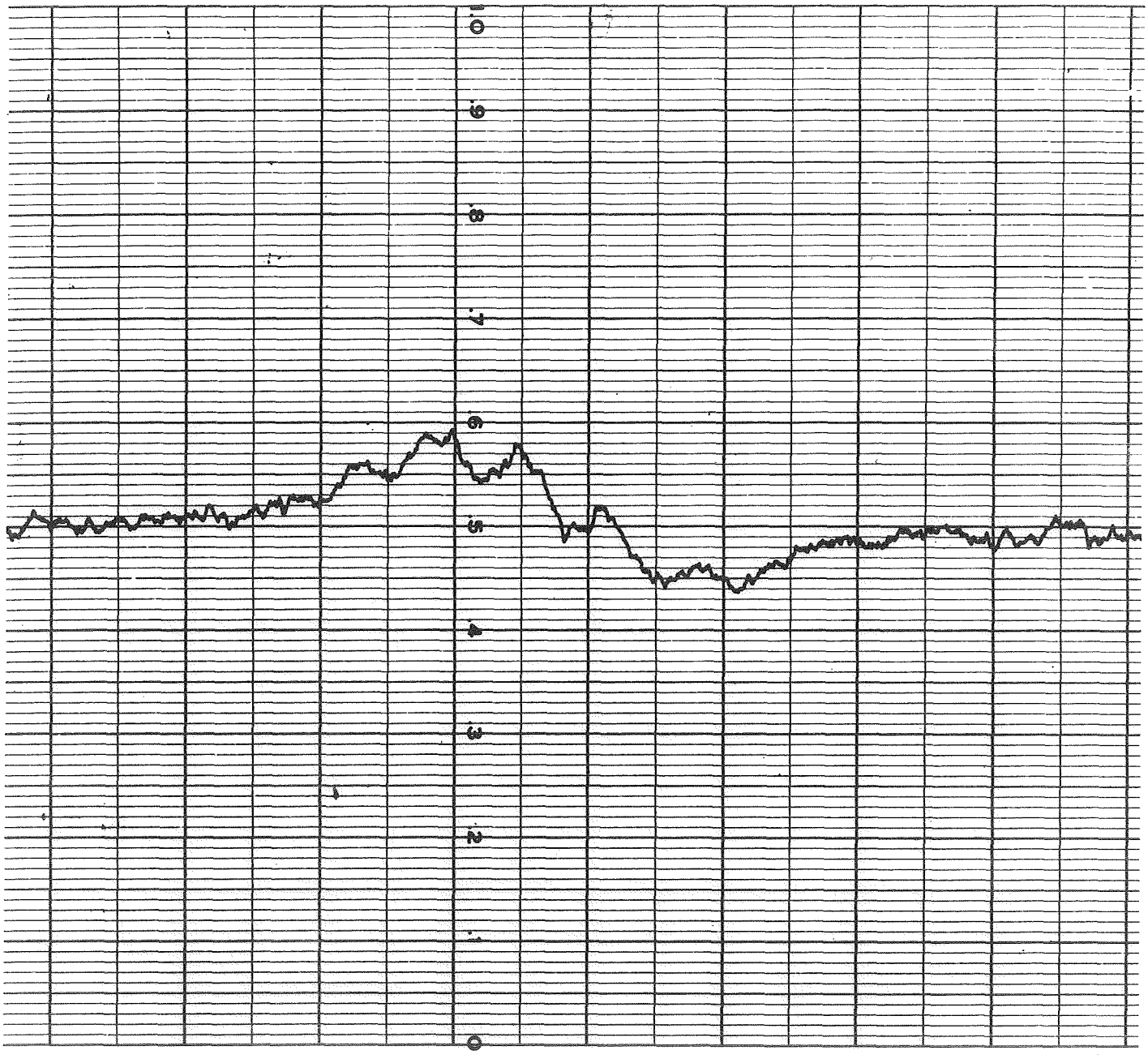

Fig. 105. Broadline ^{75}As Resonance in 1 M $LiAsF_6$ #1/MF #2-11 & 2 M PC #7-1. One Division, Left to Right, is 1 Gauss.

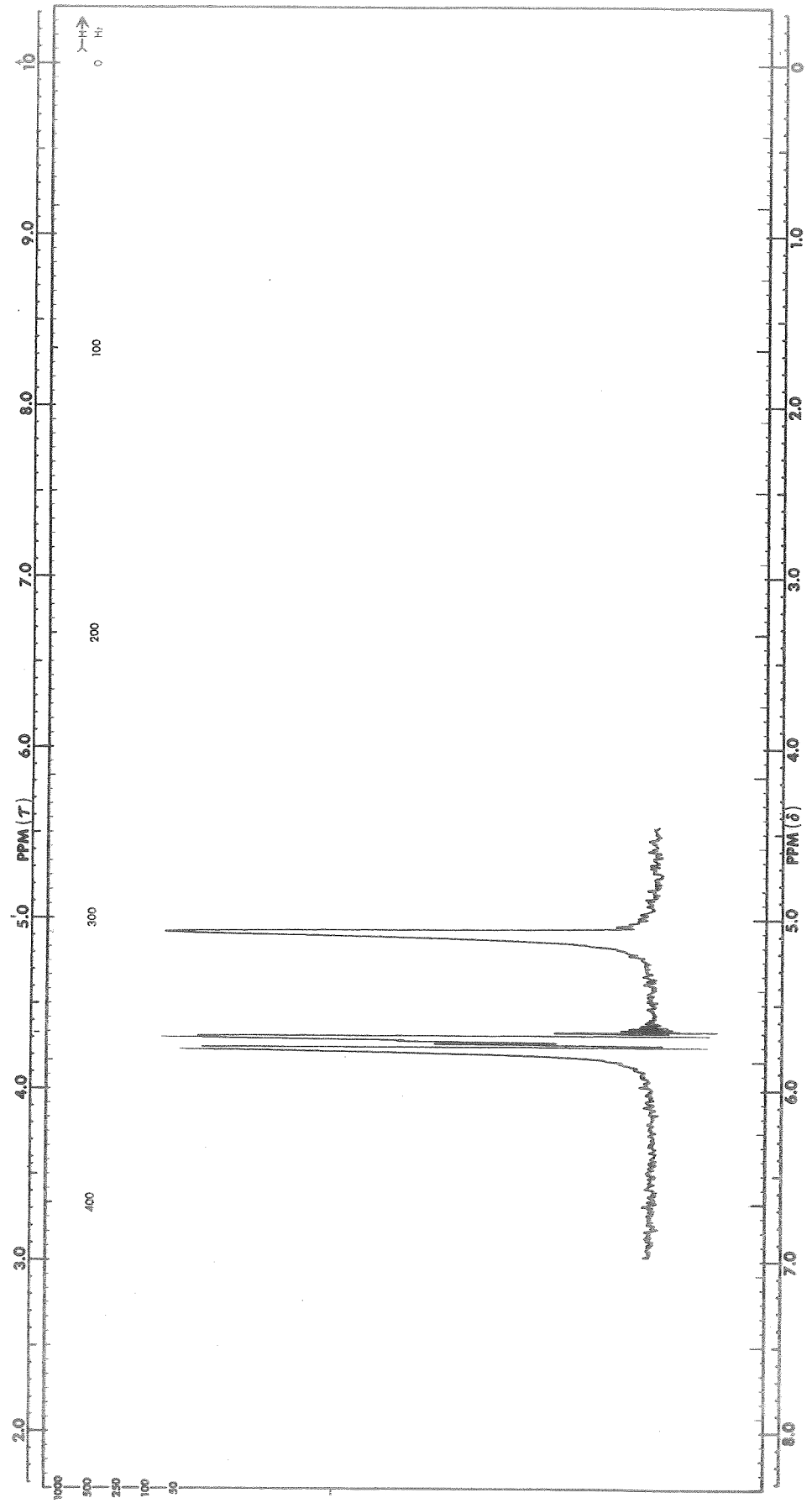

Fig. 106. ^{1}H NMR Spectra in MF #3-7 With 2000 ppm H_2O Added. Expanded Scale in Region of Water Proton Peak

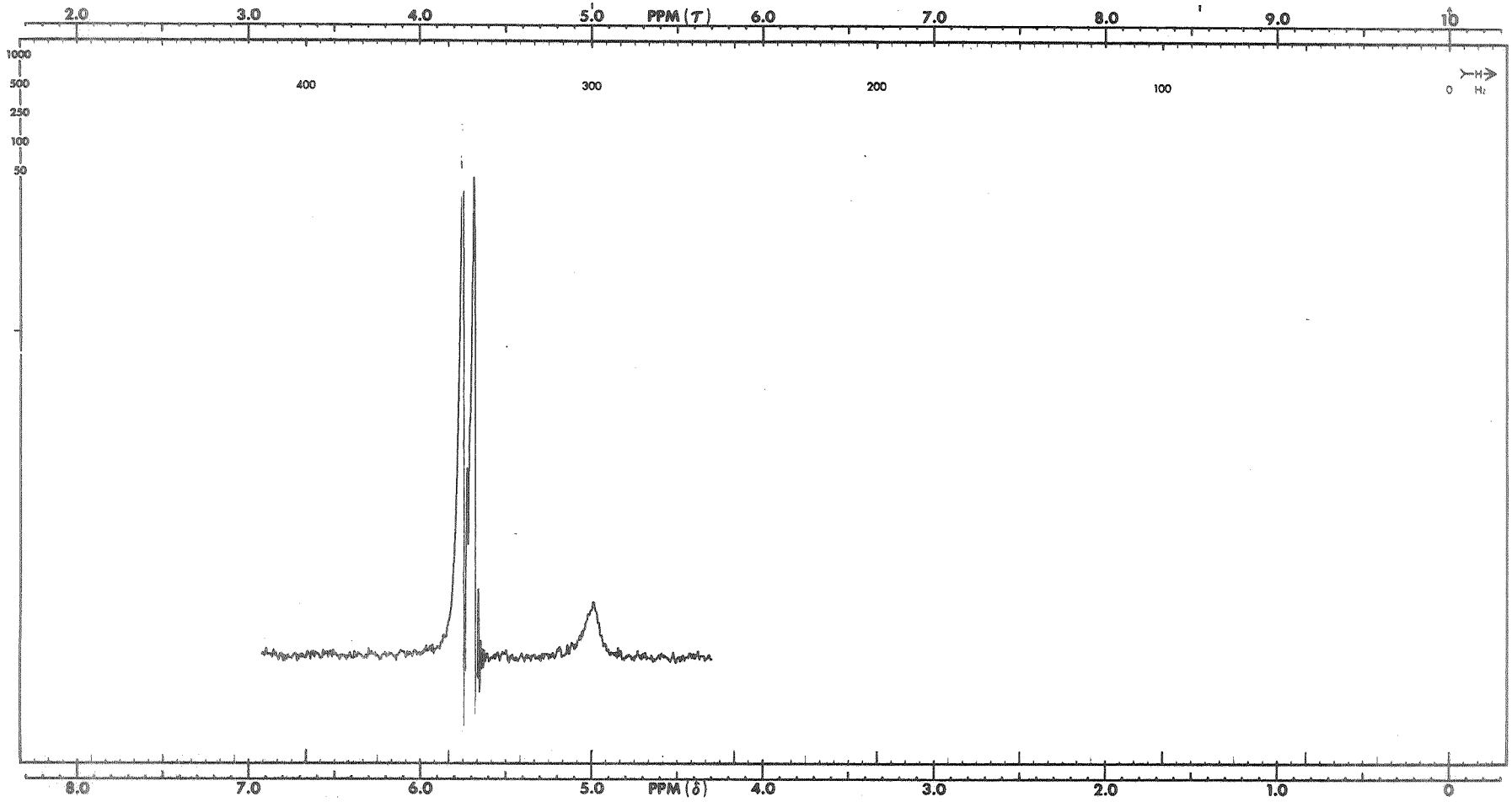

Fig.107. ^{1}H NMR Spectra in MF #3-7 With 500 ppm H_2O Added. Expanded Scale in Region of Water Proton Peak

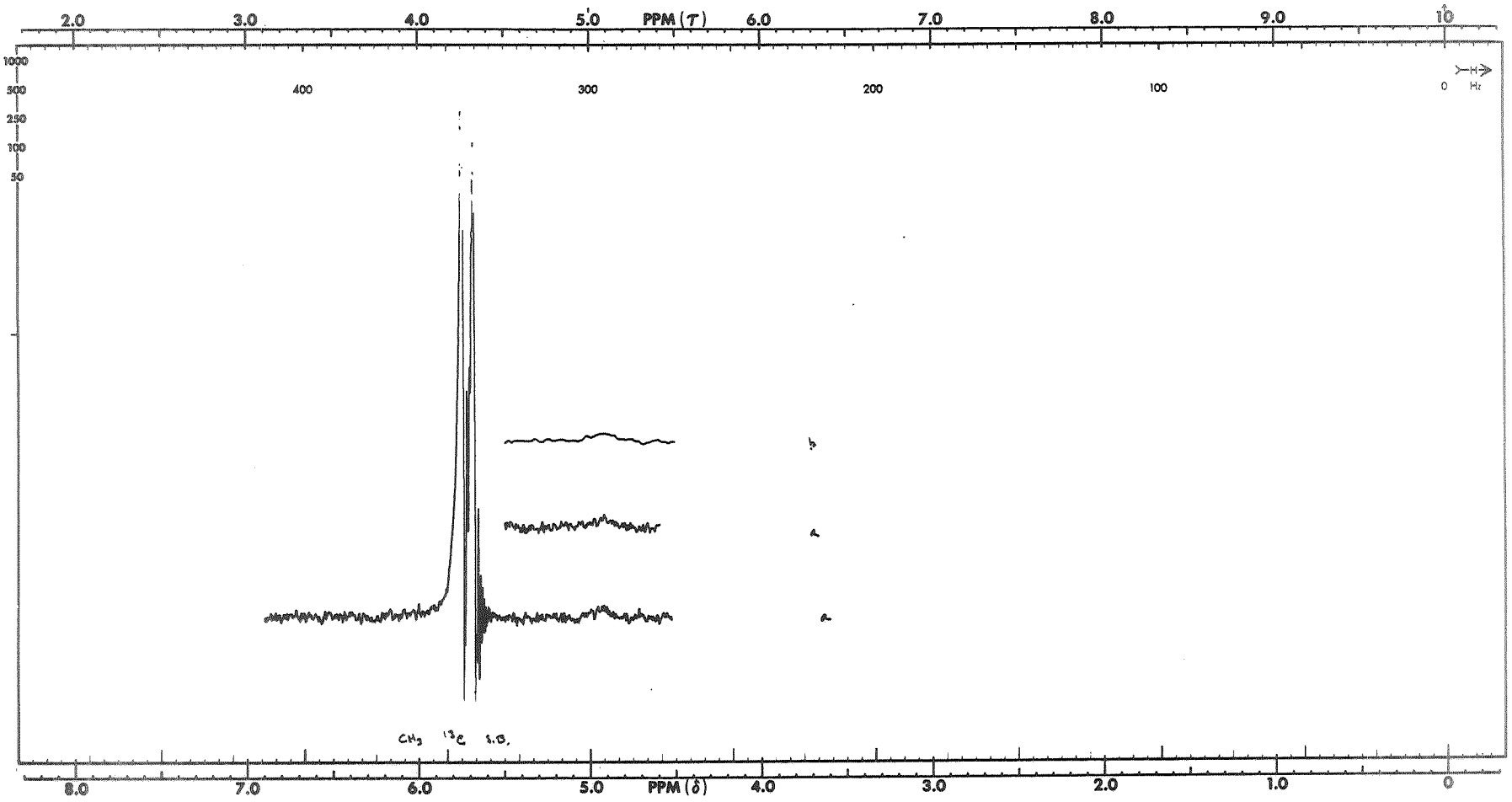

Fig. 108. ^{1}H NMR Spectra in MF #3-7 With 100 ppm H_2O Added. Expanded Scale in Region of Water Proton Peak

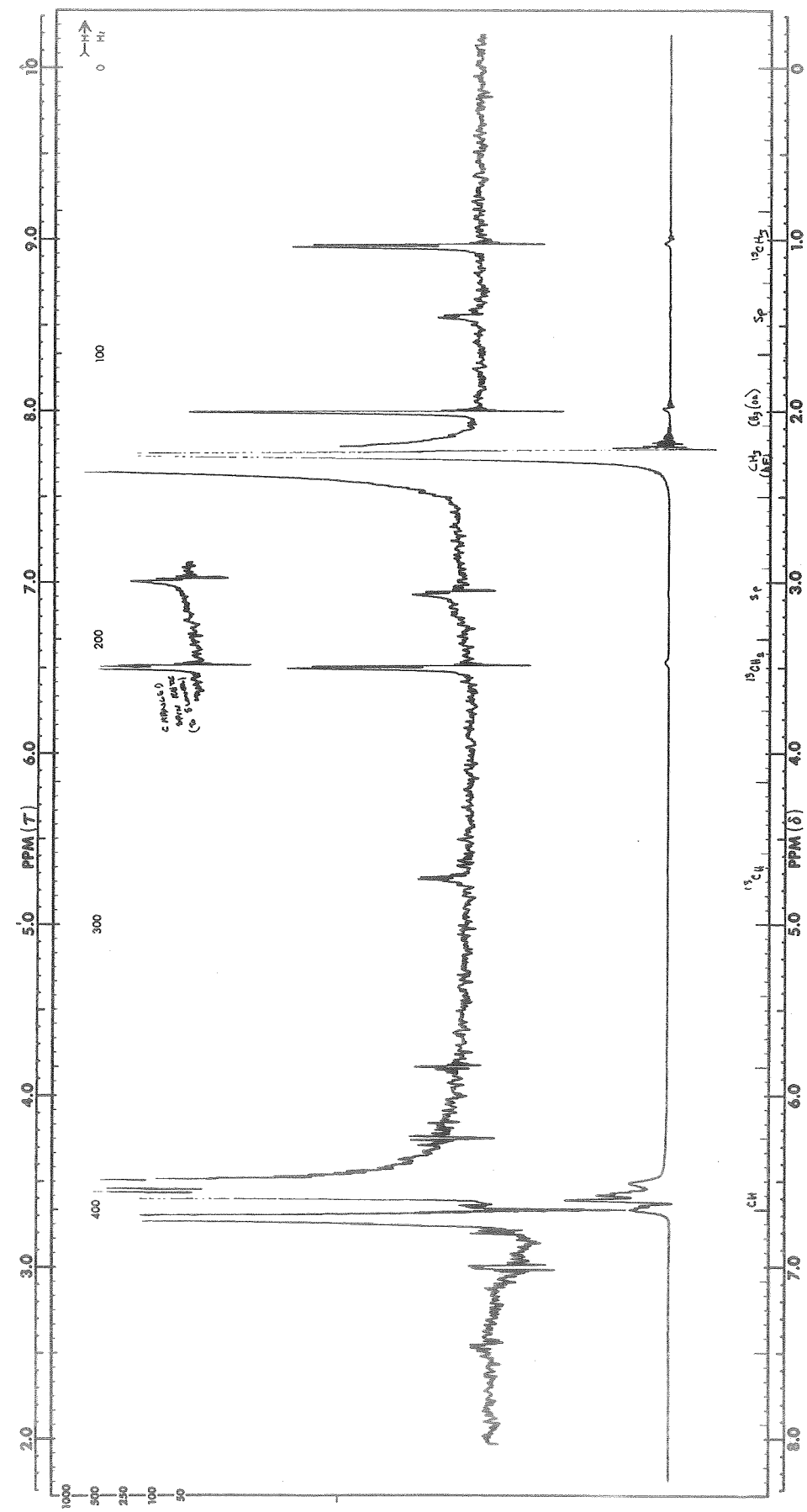

Fig. 109. ^{1}H NMR Spectra in 1M $LiAsF_6$ #5/MF #3-4 @ 2000 ppm H_2O

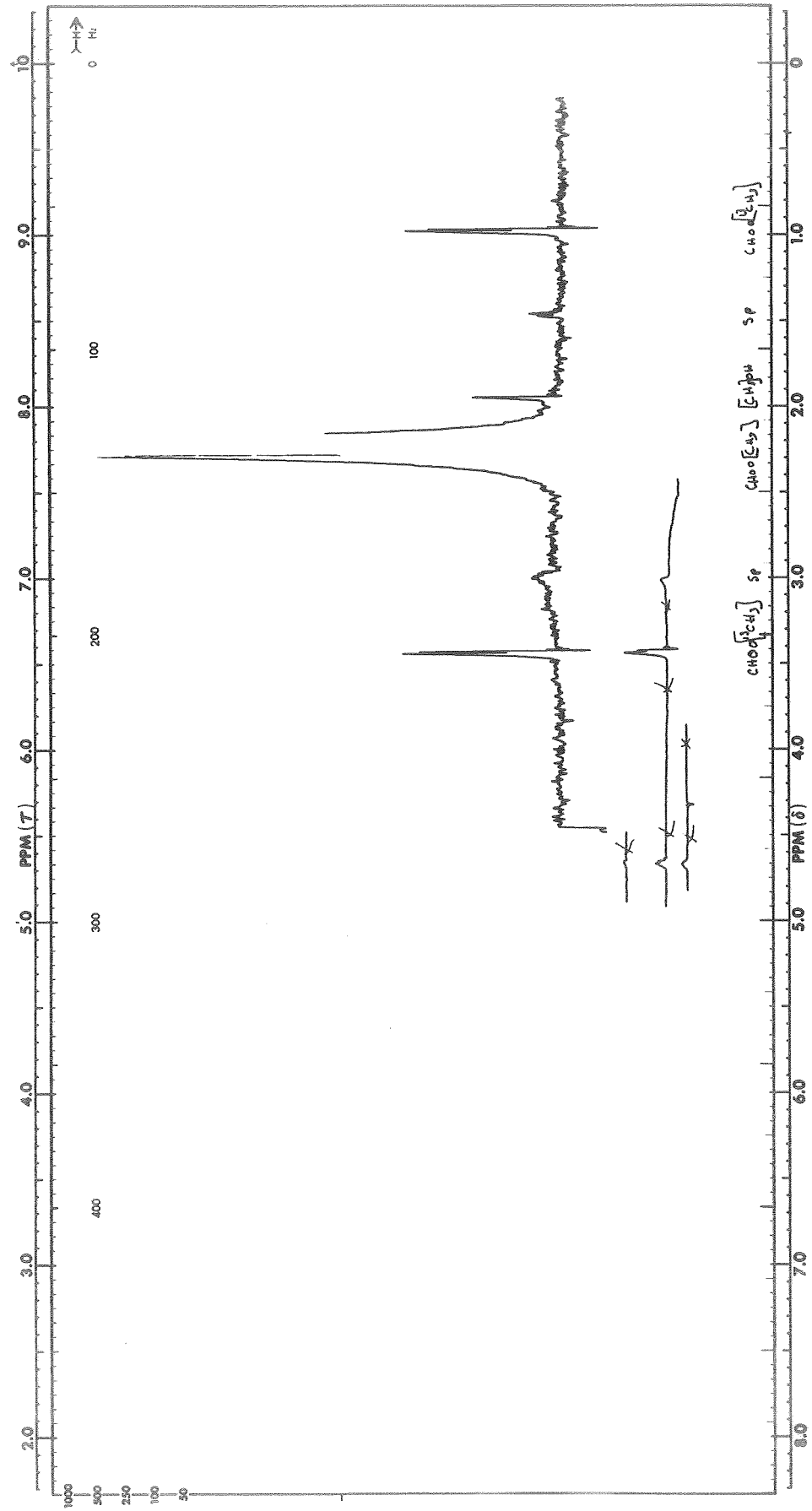

Fig. 110. ^{1}H NMR Spectra in 1M $LiAsF_6$ #5/MF #3-4 & 500 ppm H_2O

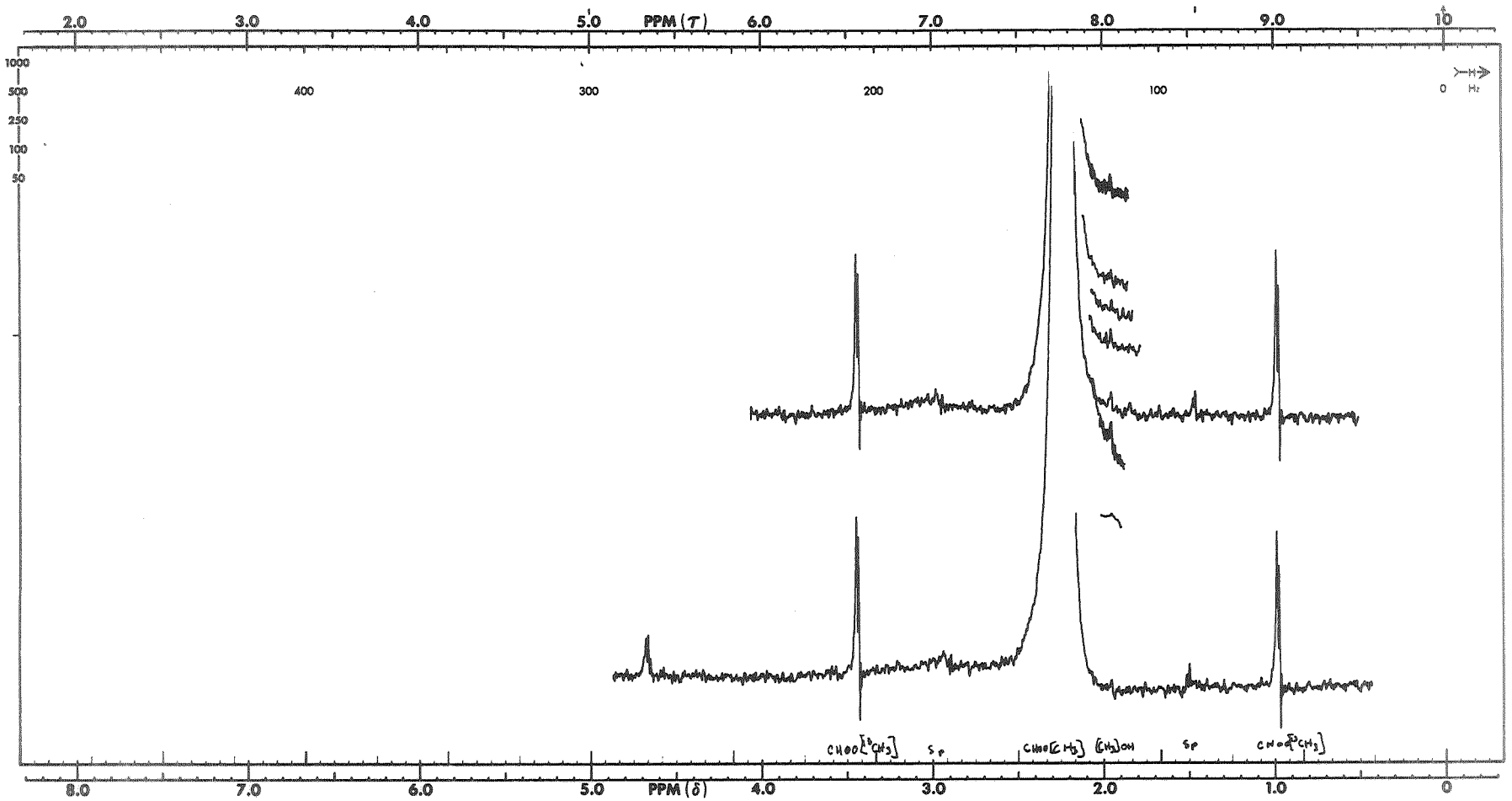

Fig. 111. ^{1}H NMR Spectra in 1M $LiAsF_6$ #5/MF #3-4 & 100 ppm H_2O

Several days later, a small peak was also observed in the 2000 ppm H_2O specimen at the position of the CH proton in HCOOH, thus substantiating the presumption of the above reaction.

Essentially the same thing occurs with water in 3 M $LiAsF_6$/MF (the stock solution supplied by Livingston Electronic Laboratory). However, in a spectrum run on this specimen several days after the water addition, the MeOH methyl proton line was found to be considerably broader than when first observed.

Because the deesterification reaction in the 3 M $LiAsF_6$/MF appears to be completed after an over-night period, a second specimen was kept refrigerated over-night at -15 C to delay the reaction so that it could be followed. However, after a subsequent period of exposure to room temperature which was considerably longer than the time it took for the reaction to go to completion in the non-refrigerated specimen, only a very small peak had appeared.

Because of the observation that the peak ascribed to the methyl proton in methanol resulting from hydrolysis of methyl formate was broader a couple of days after it appeared, the high resolution proton spectra for 3 M $LiAsF_6$/MF (stock solution supplied by Livingston Electronic Laboratory) with 2000 ppm water added was rerun several times. These runs showed the continuation of the broadening and a decrease in intensity until the line was no longer observable, about two weeks after preparation. Spectra were run concurrently on the 1 M $LiAsF_6$/MF and 2000 ppm H_2O specimen. No change was observed in the methanol methyl proton peak for this specimen. A dark, somewhat gelatinous substance has appeared on the bottom of the tube of 3 M $LiAsF_6$/MF and 2000 ppm H_2O (this glass tube was sealed by fusing the top of the tube after sample preparation). No such substance is observed in the 1 M $LiAsF_6$/MF and 2000 ppm H_2O specimen.

The 3 M $LiAsF_6$/MF used in the above specimen was the solution recently provided by Livingston Electronic Laboratory. Some time ago an NMR specimen had been prepared from the solution previously supplied by Livingston Electronic Laboratory. This specimen came from the "tail end" of the solution and contained some greyish suspension. The high resolution proton spectrum did not show a methanol methyl proton peak, whereas a specimen prepared from the same solution shortly after it arrived (a couple of years ago) did show a methanol methyl proton peak. Thus, it appears that after methanol is formed by hydrolysis of methyl formate in 3 M $LiAsF_6$/MF electrolytes obtained from the Livingston Electronic Laboratory a further reaction occurs which involves the methanol. Further, the evidence suggests that the grey-black precipitate formed in these solutions may be a result of this reaction.

Because of some inconsistencies noted in these preliminary specimens, high resolution proton spectra were run on several more 1 M $LiAsF_6$/MF specimens (see Figs. 112, 113 and 114 for identification of specimens):

(1) 1 M $LiAsF_6$/MF

(2) 1 M $LiAsF_6$/MF and 2,000 ppm H_2O

(3) 1 M $LiAsF_6$/MF

(4) 1 M $LiAsF_6$/MF and 2,000 ppm H_2O

(5) 1 M $LiAsF_6$/MF and 2,000 ppm H_2O

(6) 1 M $LiAsF_6$/MF and 2,000 ppm H_2O

(7) 1 M $LiAsF_6$/MF and 2,000 ppm H_2O

Specimens numbered (5) and (6) above were repeats of specimens numbered (2) and (4) above which were scanned shortly after preparation. Figures 112 and 113 show the proton spectra in the vicinity of the large MF doublet (from the CH_3 group in $CHOOCH_3$) for specimens (1), (2), (3), and (4). The lines at the extreme left and right are the ^{13}C side bands of the MF methyl proton doublet. In both figures, the upper spectrum is the neat solution, and the spectrum at the bottom is that with 2,000 ppm H_2O added. In both spectra of specimens containing water, an additional peak is observed which is ascribed to the addition of water. This peak is appreciably downfield from the location of the water proton peak in pure MF, and could be due to ionic solvation or exchange effects.

The preparation of these specimens was changed in one respect relative to those used in the preliminary work. Previously, specimen tubes were sealed off with the specimen tube immersed in liquid nitrogen, a procedure which froze the solution. Because previous work showed that lowering the sample temperature apparently increased the induction period, the specimens were sealed off with immersion in granulated dry ice. These specimens were the first to show a water peak when run shortly after preparation. Figure 114 shows the first spectra taken for specimens (5), (6), and (7) from the list above plus a spectra of the 1 M $LiAsF_6$/MF and 2,000 ppm H_2O, which had been investigated previously by running spectra during the day, and then letting the specimen sit in a freezer at -20 C when not being run. A MeOH peak is observed now in the specimen which had been at low temperature for a couple of weeks. Note that the two repeat specimens did not show a water proton peak as was found in the first specimens, whereas the MF specimen did show a water proton peak. This inconsistency is compounded by the results of kinetic studies which follow.

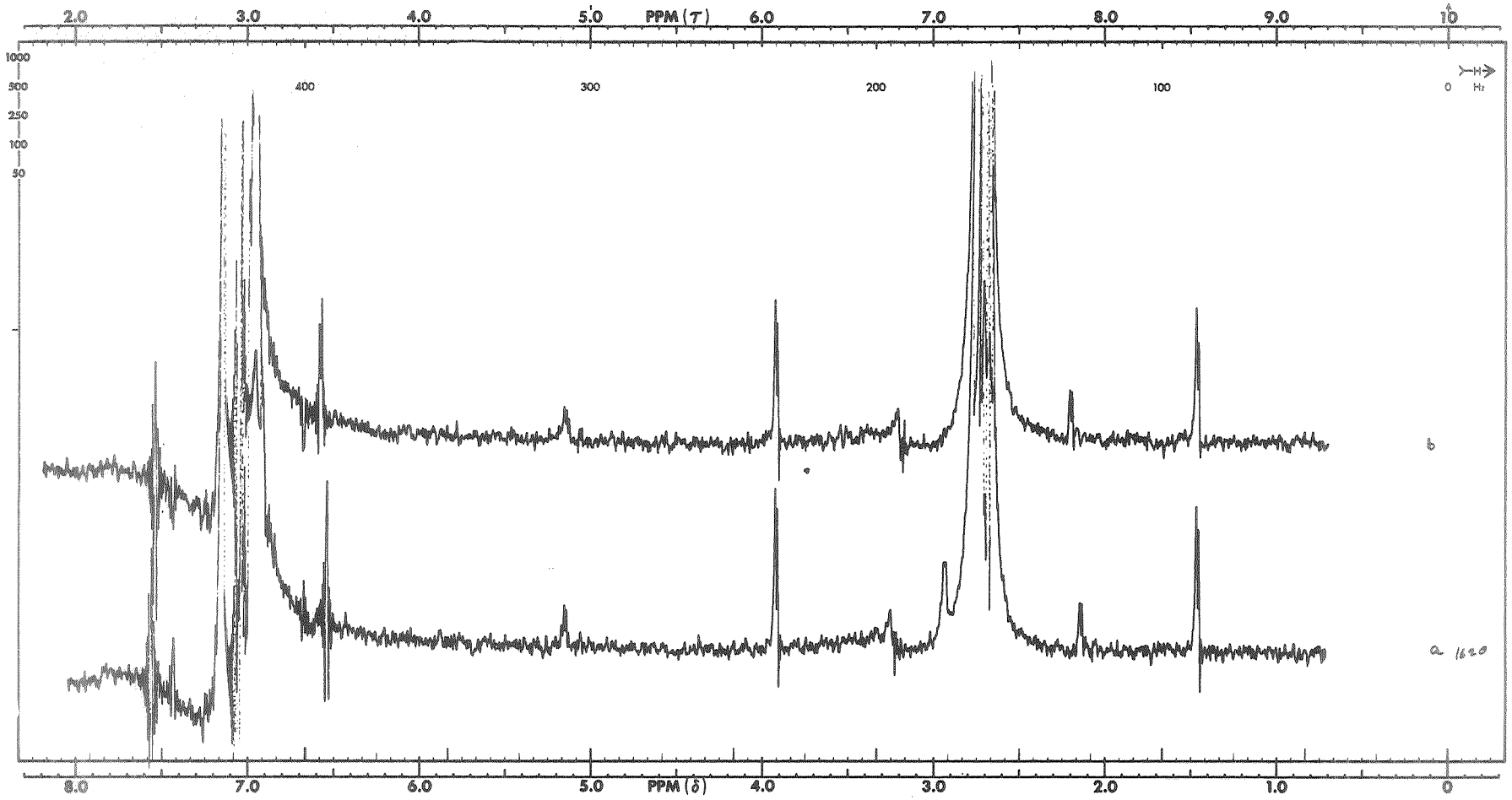

Fig. 112. ^{1}H NMR Spectra in 1M $LiAsF_6$ #6/MF #4 (Upper Trace) and 1M $LiAsF_6$ #6/MF #4 & 2000 ppm H_2O (Lower Trace)

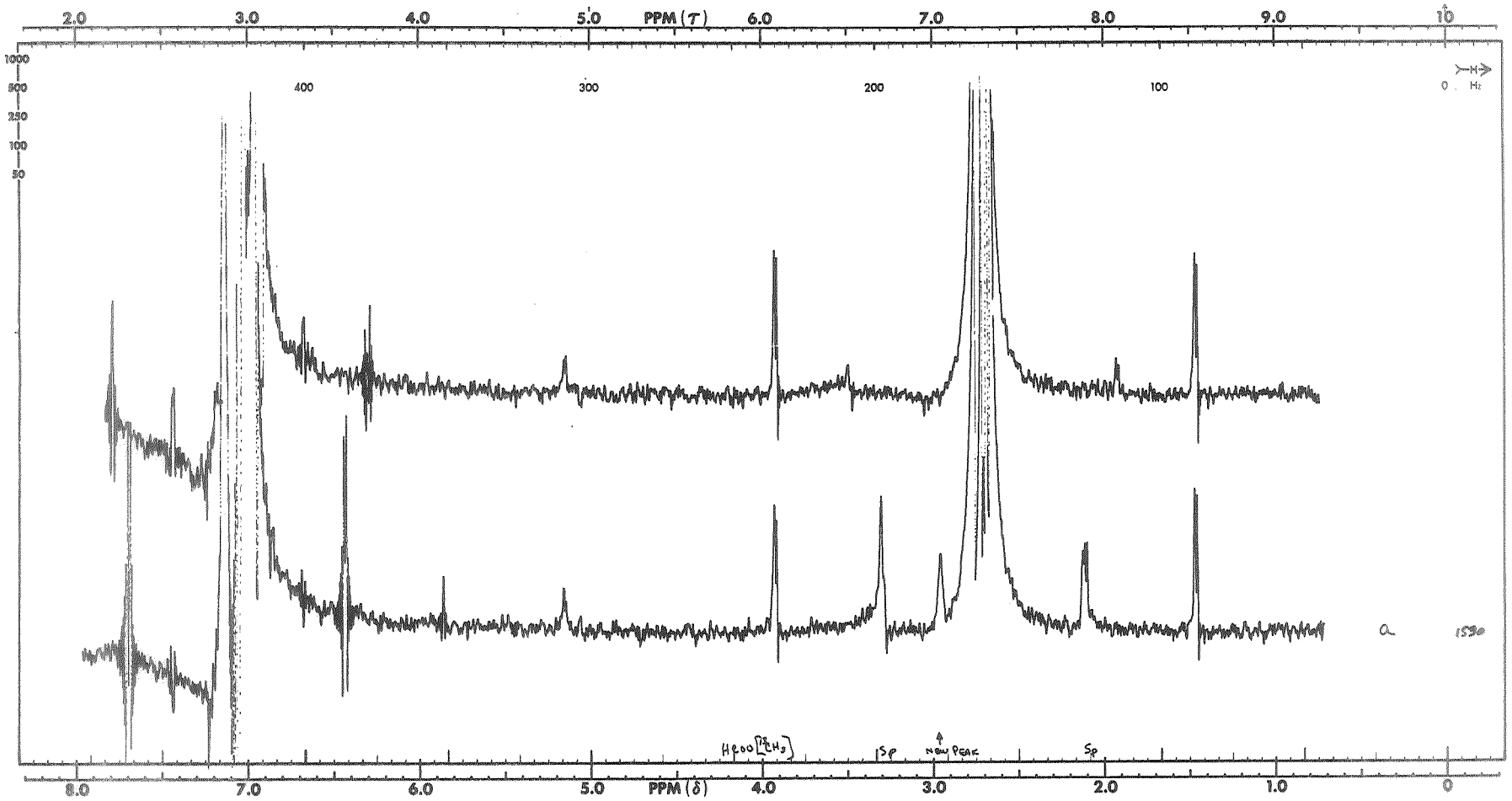

Fig. 113. ^{1}H NMR Spectra in 1M $LiAsF_6$ #7/MF #4 (Upper Trace) and 1M $LiAsF_6$ #7/MF #4 and 2000 ppm H_2O (Lower Trace)

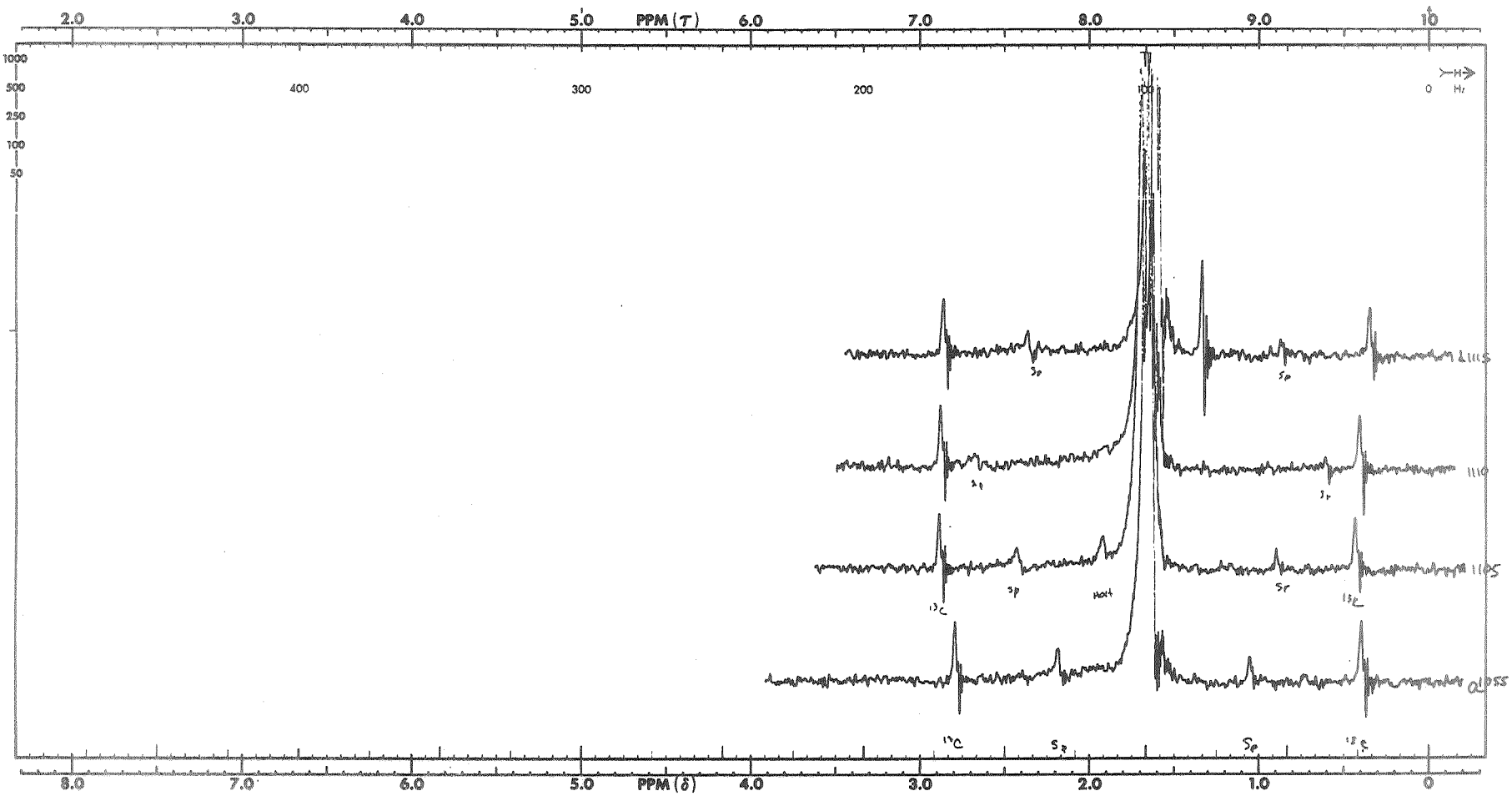

Fig. 114. ^{1}H NMR Spectra in (From Top to Botton) Aged 1M $LiAsF_6$ #7/MF #4 & 2000 H_2O, 1M $LiAsF_6$ #6/MF #4 & 2000 ppm H_2O, 1M $LiAsF_6$ #7/MF #3-8 & 2000 ppm H_2O and 1M $LiAsF_6$ #7/MF #4 & 2000 ppm H_2O

The considerable interest in $LiAsF_6$/MF electrolytes stems from the apparent stability of lithium in these electrolytes. Initially, some differences in stability were thought to have been observed in the Livingston electrolyte, prepared by metathesis, compared to $LiAsF_6$/MF electrolytes prepared by dissolving pure $LiAsF_6$ in pure MF. Because no difference could be observed by ^1H NMR, i.e., no proton containing impurities were found, it was hypothesized that such impurities that might be responsible for this stability might be present in quite small quantities. They could nevertheless successfully act as catalysts for the hydrolysis. Differences in impurities could then cause differences in the rate of hydrolysis. Therefore, measurements of the rate of formation of MeOH were made.

Specimens (5), (6), and (7) were run repeatedly over an extended period of time. Fig. 115 shows the actual spectra recorded for specimen (7). This was chosen because it shows the general nature of the observations. First the water proton line, if it is observed initially, "disappears" in a couple of hours; it can be seen that it broadens and then disappears. No MeOH line is observed until some time after the water proton line is no longer observed. The intensity of the MeOH line then increases with time after this initial appearance. Figure 120 shows plots of the intensity of the MeOH peak as a function of time. The error bars on the points were estimated from the noise level only. Other errors arise because over a long period of time the best magnetic field homogeneity varies, which changes the peak height. This was at least partially compensated for by using the ratio of the MeOH peak to the nearer ^{13}C side band, as an arbitrary measure of relative signal intensity.

All three plots indicate a linear increase of intensity with increasing time until the reaction nears stoichiometric completion. However, the rates are quite different, with the specimen showing the water proton peak initially proceeding much slower than the other two.

In all the specimens investigated, the linear reaction rate with time is the only consistent feature. Why some specimens show a water proton peak initially but others do not, and why the reaction rate is different in those solutions studied as a function of time is not known. Furthermore, no correlation was found, in the results of all of these measurements, with whether the specimen was prepared from a Livingston electrolyte or from mixing of pure $LiAsF_6$ and methyl formate.

To verify that $LiAsF_6$ is perhaps unique in its ability to catalyze the hydrolysis of MF to methanol and formic acid, 2000 ppm H_2O were added to 1 M $LiClO_4$/MF and the ^1H spectra recorded over several days. The water proton line, a sharp peak, was observed immediately after specimen preparation slightly downfield from the water proton line as in Figure 121. After several days the water proton peak had not changed in position. The water proton resonance is considerably downfield from its position in neat MF, which may be due to solvation of Li^+.

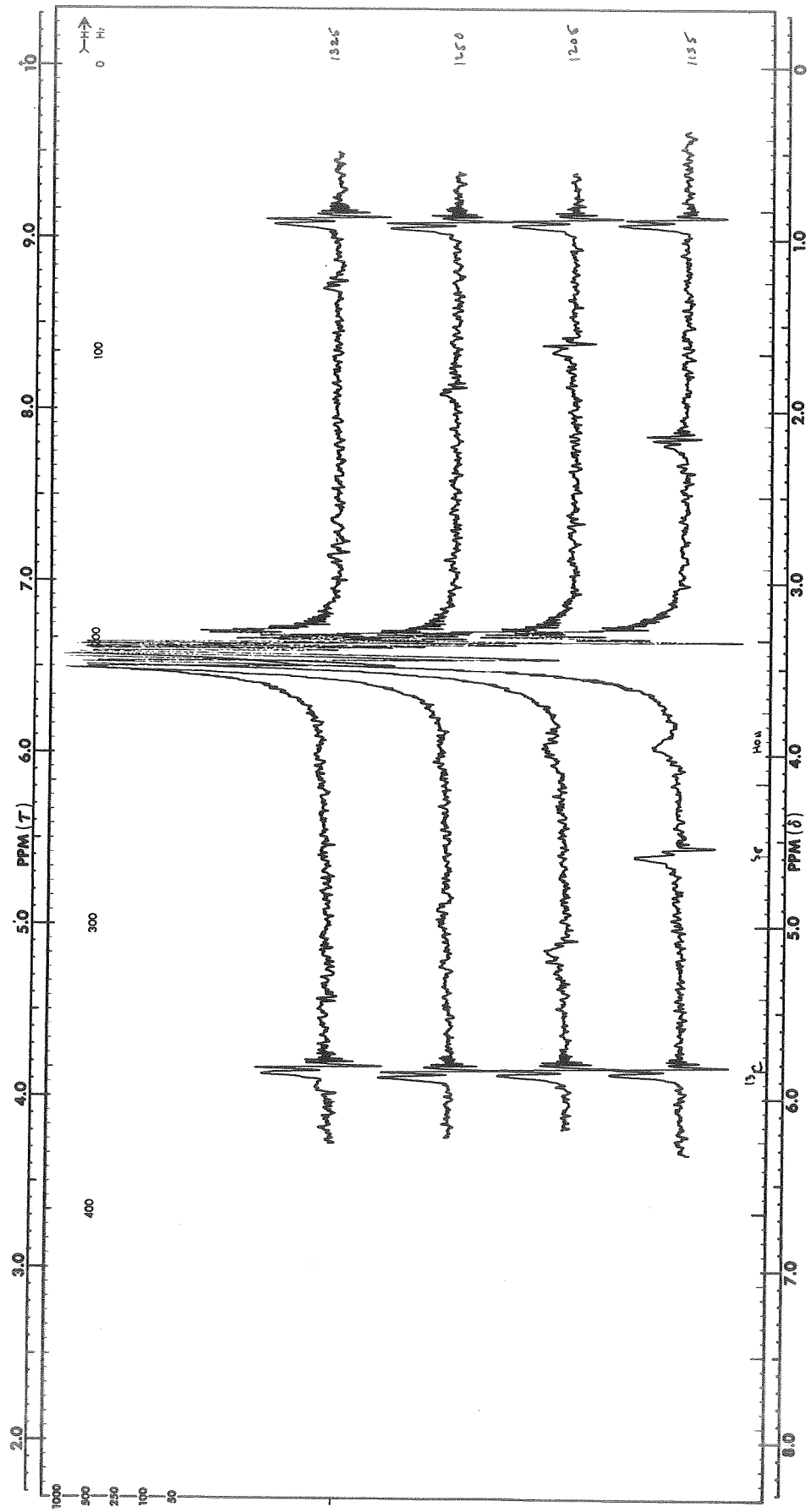

Fig. 115. ^{1}H NMR Spectra in 1M $LiAsF_6$ #7/MF #3-8 & 2000 ppm H_2O.
Time Increases From Bottom to Top

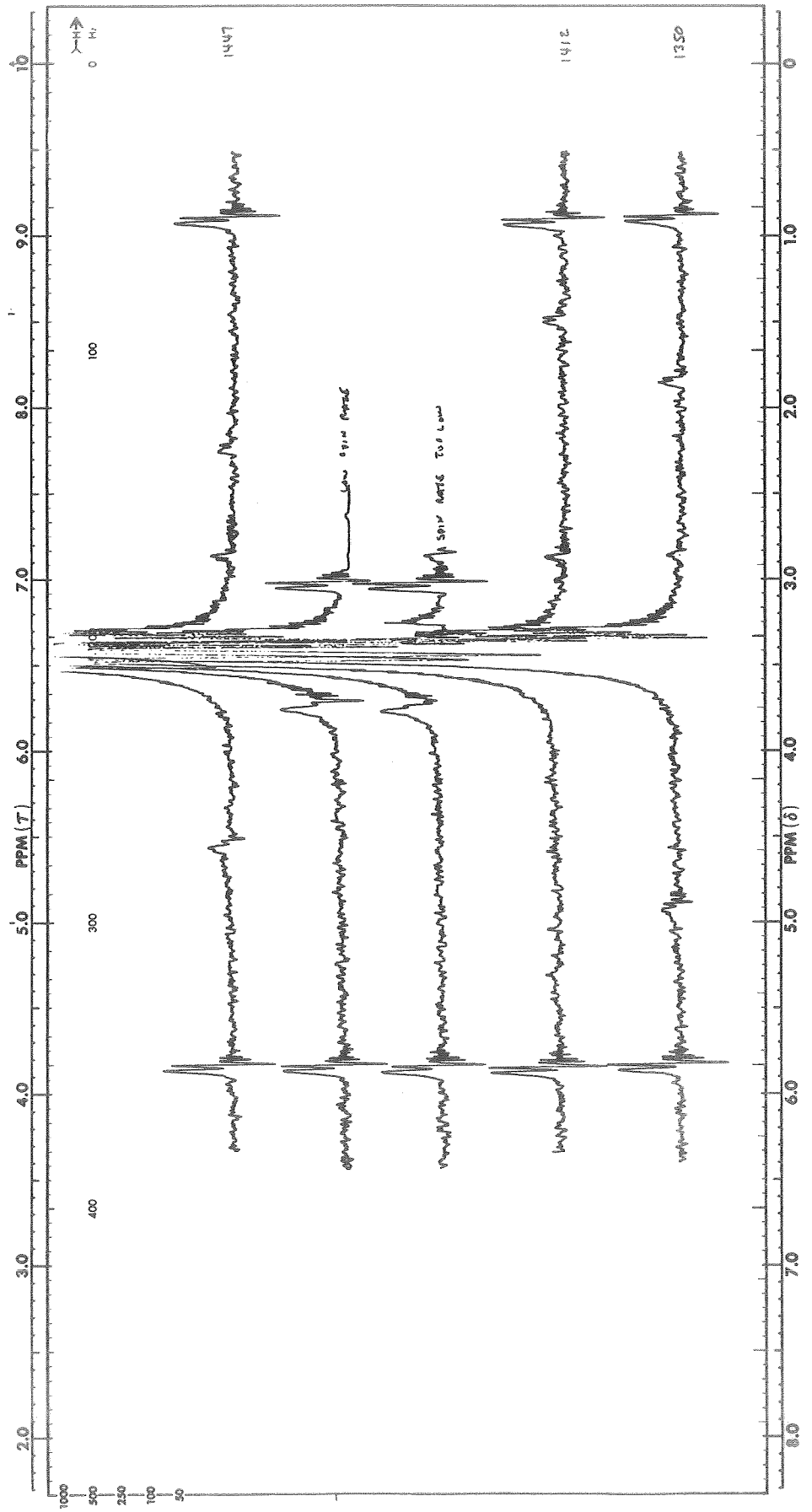

Fig. 116. Figure 115 Continued

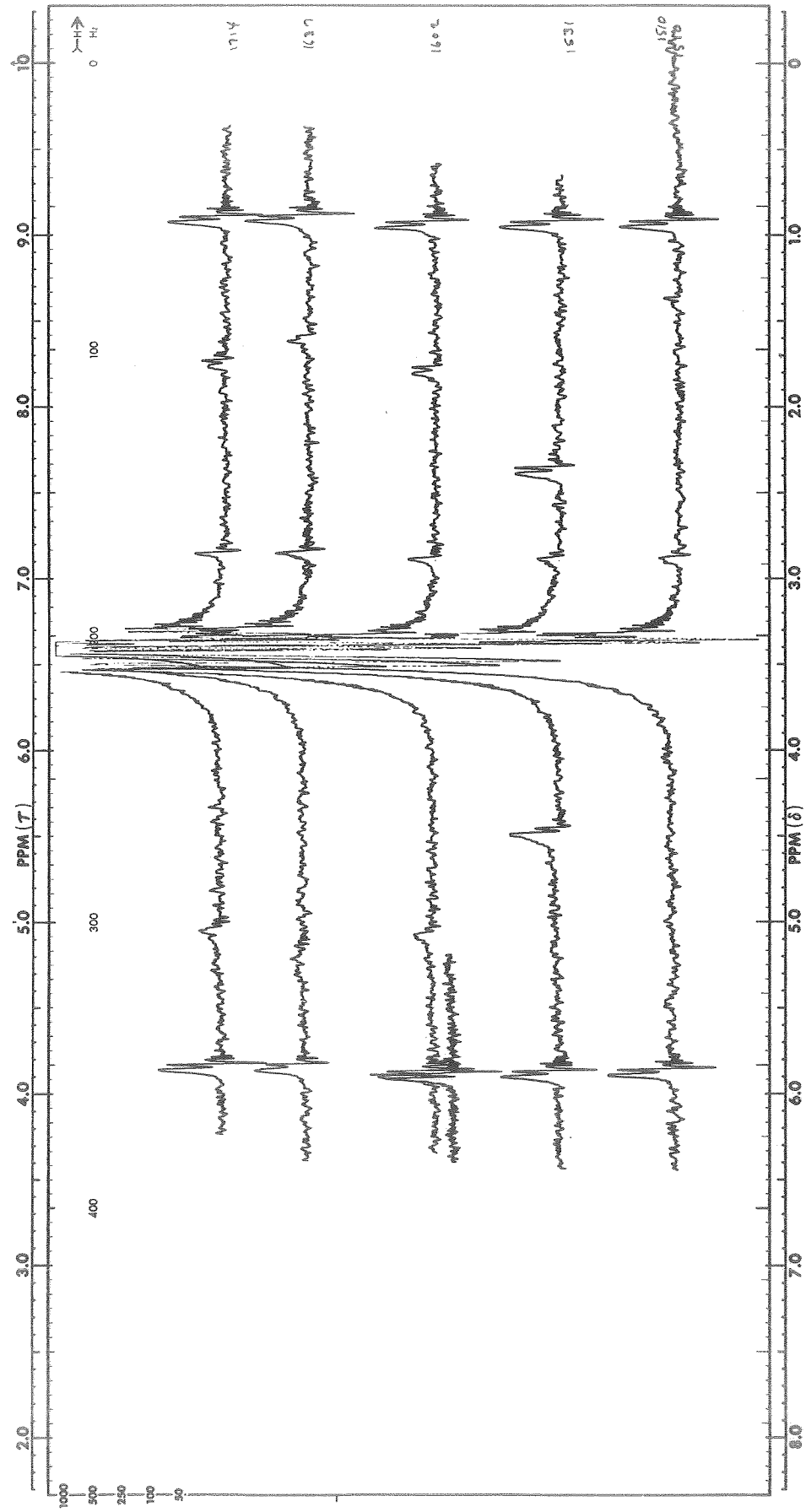

Fig. 117 Figure 115 Continued

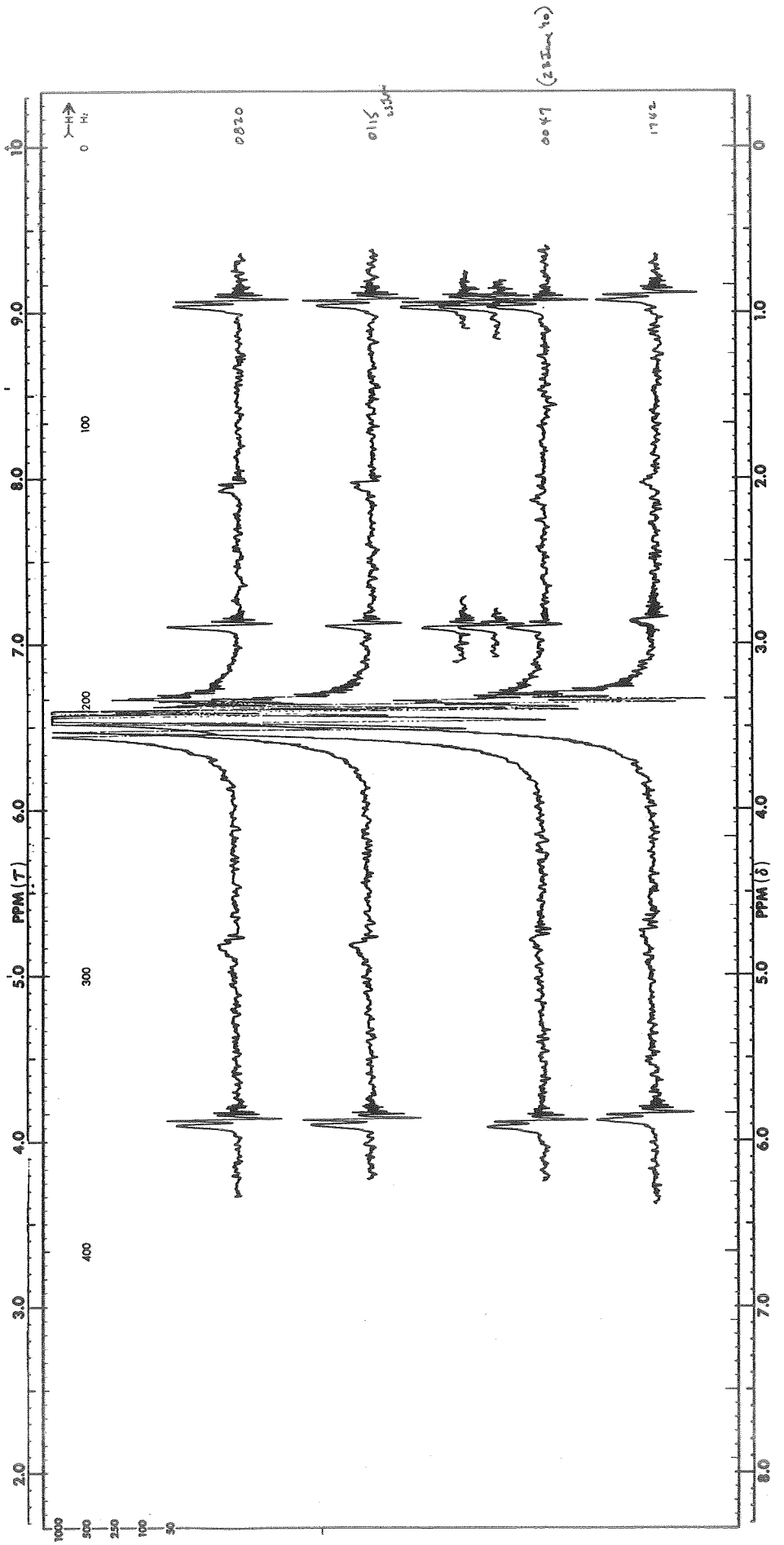

Fig. 118 Figure 115 Continued

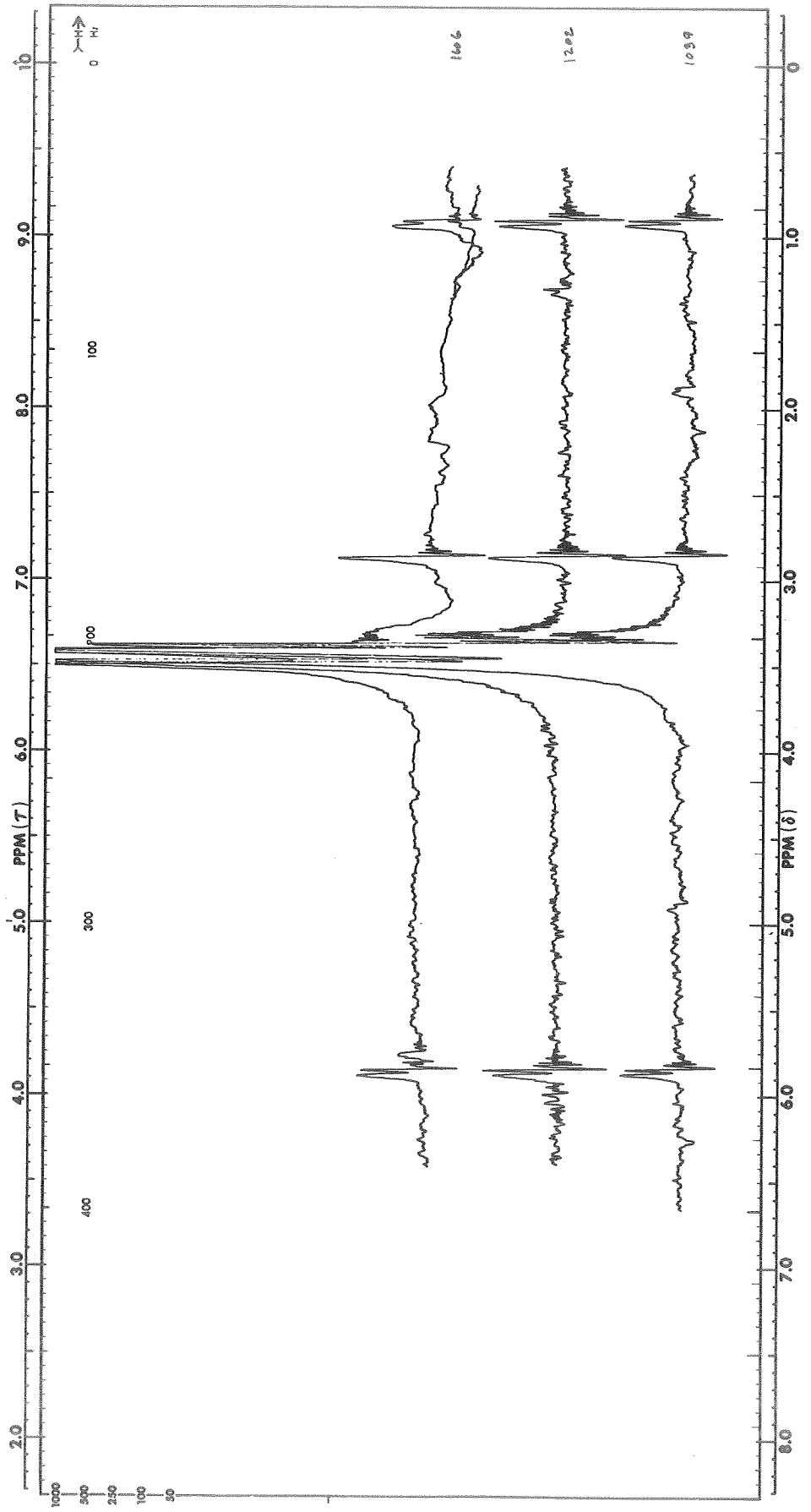

Fig. 119 Figure 115 Continued

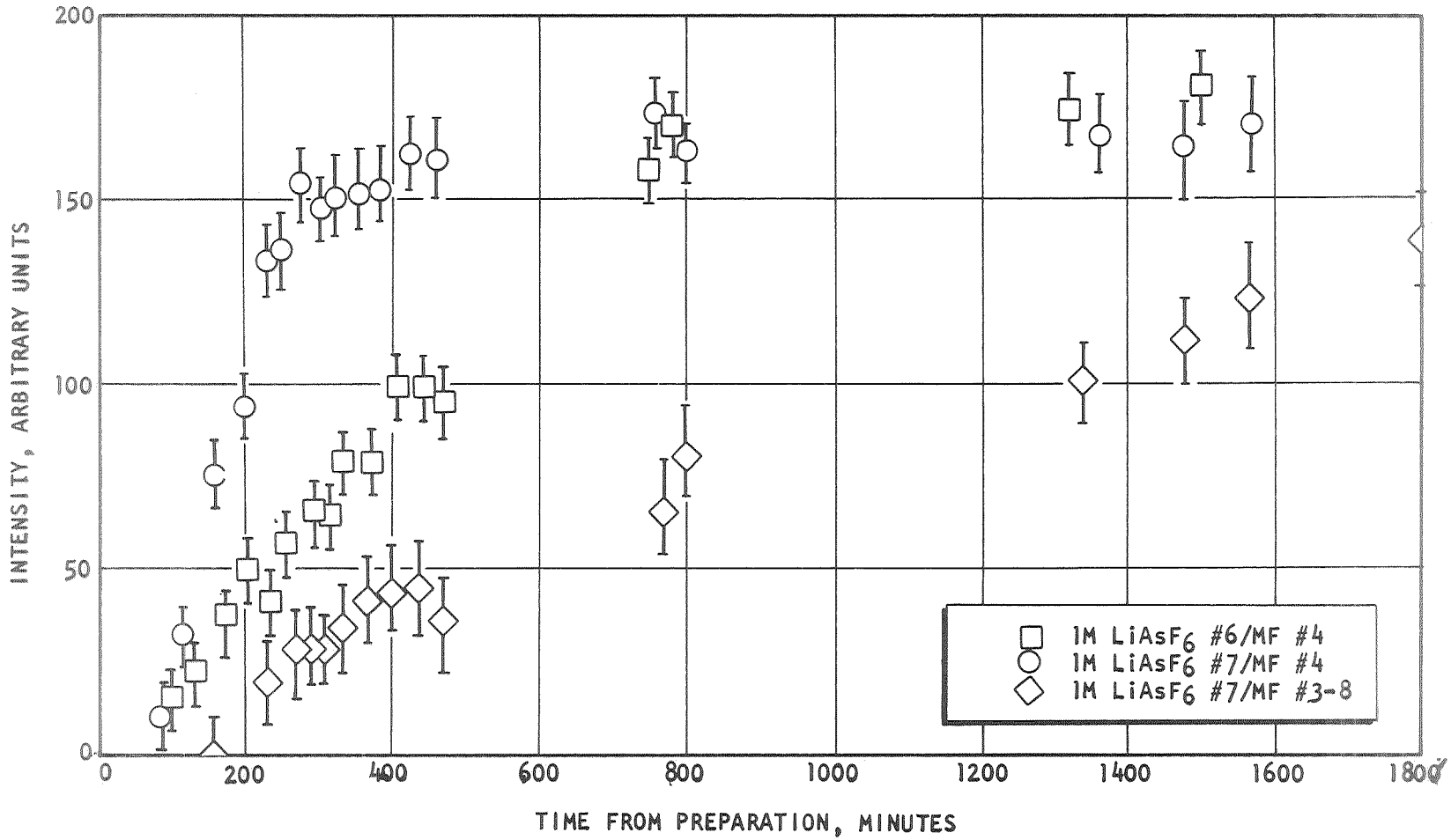

Fig. 120. Intensity, in Arbitrary Units, of Methyl Proton Peak from CH_3OH as a Function Of Time, in Specimens Noted, From Time of Preparation.

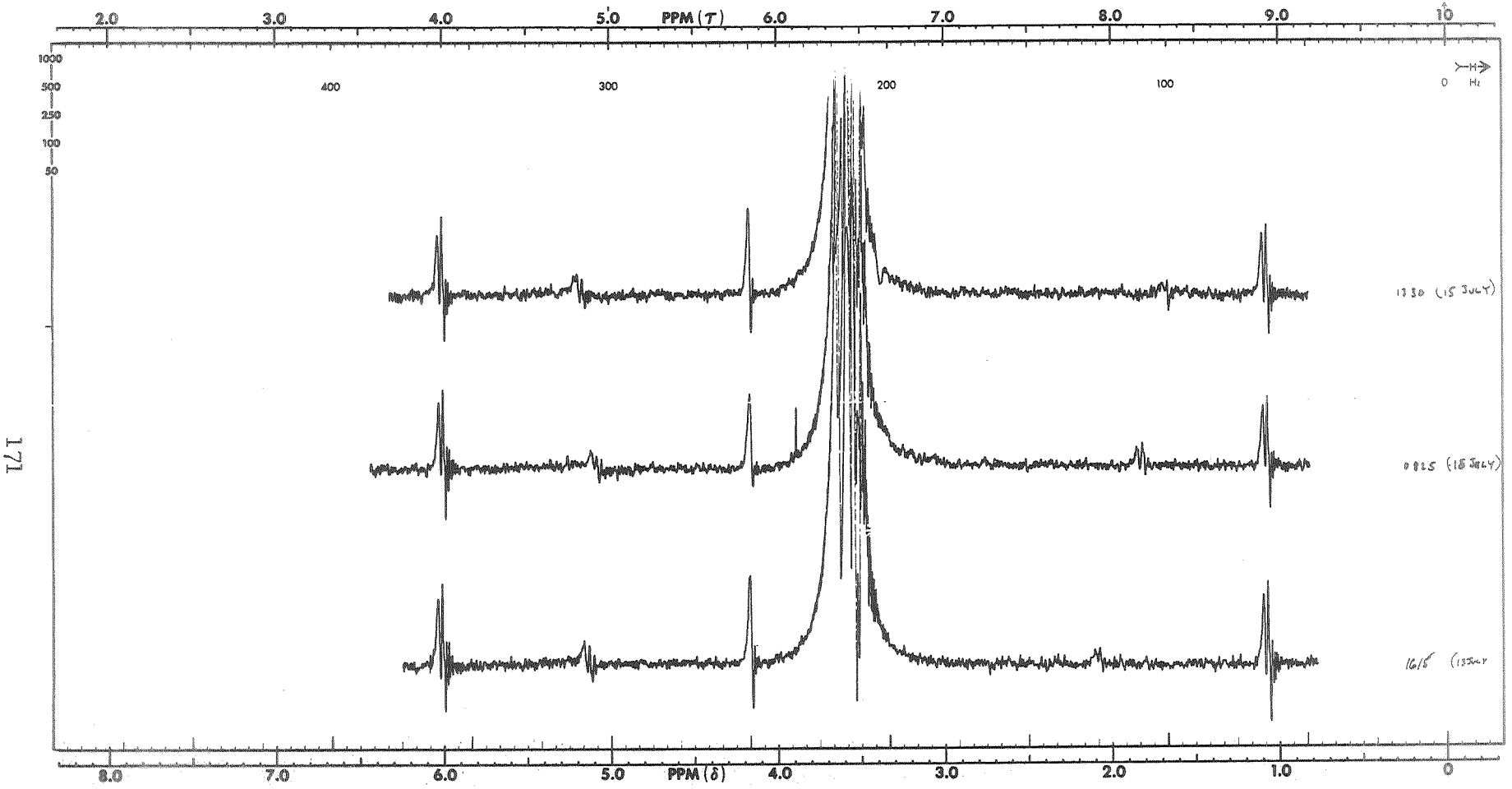

Fig.121. ^{1}H NMR in 1M $LiClO_4$ #3/MF #1 & 2000 ppm H_2O. Time Increases From Bottom to Top

Because the concentration of Li^+ is presumably the same in this specimen as in 1 M $LiAsF_6$/MF and the water proton line in the 1 M $LiAsF_6$/MF has about the same downfield shift, when observable, as that in 1 M $LiClO_4$ the following sequence of reactions may be postulated. When H_2O is first introduced into $LiAsF_6$/MF it solvates Li^+ forming weakly bound $Li[H_2O]_n^+$ complexes. In a short time, minutes to about an hour, interaction with some other species, most likely AsF_6^- breaks up these complexes possibly forming H^+ which in turn catalyzes the conversion of MF to MeOH and HCOOH by an acid catalysis mechanism.

DIMETHYLFORMAMIDE ELECTROLYTES

LiCl $AlCl_3$/DMF

LiClO$_4$ As Additive. High resolution ^1H were run on a specimen of 0.05 M $AlCl_3$ + 0.5 M LiCl/DMF and 0.5 M $LiClO_4$. DMF coordinated by Al^{+3}, i.e., the species $Al[DMF]_6^{+3}$, is observed by virtue of small peaks shifted downfield from the bulk DMF peaks. The downfield shift is less in this specimen than in the 0.05 M $AlCl_3$/DMF due to the presence of $LiClO_4$ and LiCl. It has been reported (Ref.13) that negative ions in the second Al^{+3} coordination sphere (this could be designated the first coordination sphere of $Al[DMF]_6^{+3}$) cause the downfield shift to increase. The difference in the effect of negative ions observed here may be due to ionic strength effects alluded to in Ref. 13 . The spectra show that there is no displacement of complexed DMF by chloride or perchlorate. Thus, the species in solution are $Al[DMF]_6^{+3}$ with possibly some chloride and/or perchlorate in the second Al^{+3} coordination sphere, Li^+, Cl^- and ClO_4^-. If $AlCl_4^-$ is present at all it is not a major species. This is consistent with the observation noted earlier that DMF displaces Cl^- in the first Al^{+3} coordinated sphere.

$LiClO_4$/DMF

MF As Additive. High resolution ^1H spectra were taken on 1 M $LiClO_4$/DMF containing 0.25 M, 1 M, 2 M and 4 M MF. Table 16 shows the chemical shift of the DMF aldehyde proton related to the MF formyl proton (σ_{MF-DMF}), the shift of the MF formyl proton relative to the MF methyl protons (σ_{MF}), and the shift of the DMF aldehyde proton relative to the DMF methyl protons (σ_{DMF}). σ_{DMF} is not changed by the addition of MF although it is reduced somewhat, from 305 Hz in neat DMF, by the addition of 1 M $LiClO_4$. σ_{MF} does decrease as the concentration of MF is increased. The increase is the same as that of σ_{MF-DMF} which checks with the internal MF shift, σ_{MF}. Thus, in these electrolytes the major ionic species are Li^+ and ClO_4^-. There is some interaction of DMF with these ions but the actual interaction cannot be determined. MF added to this electrolyte acts only as a diluent because DMF has a much stronger solvating action.

TABLE 16

CHEMICAL SHIFTS 1 M $LiClO_4$/DMF WITH MF ADDED

MF Concentration (M)	DMF (Hz)	MF (Hz)	MF-DMF (Hz)
0.25	300	271	12.9
1.0	300	271	12.7
2.0	300	270	11.2
4.0	300	268	10.0

$LiAsF_6$/DMF

MF As Additive. This electrolyte was discussed in the previous section.

PHYSICAL PROPERTY DETERMINATIONS

ELECTROLYTE STABILITY STUDIES

Experimental Technique

Electrolyte samples of a few milliliters were placed in test tubes which had been treated according to the standard treatment for glassware. Strips of lithium metal were partially immersed in the liquid. The test tubes were then closed with screw caps which were lined with rubber-backed Teflon, and kept for a day at room temperature. At that time, the samples were removed to a 60 C bath for another 24 hours, except if an exposure of the system to elevated temperature did not seem advisable. Further observations were thereafter made at room temperature.

Visual observations on solution and lithium metal were noted, and the build-up of gas pressure was checked by releasing the screw caps.

Stability of $LiCl+AlCl_3$/PC Solutions Containing Various Additives

Solutions containing $AlCl_3$ in PC generally have a tendency to discolor on standing. From a previous study (Ref. 1) it was concluded that the $Al[PC]_6^{+3}$ species probably is responsible for the observed instability. Several additives were tested to investigate if the species detrimental to the stability of $LiCl+AlCl_3$/PC solutions could be eliminated by interaction with an additive. The results obtained with $LiCl+AlCl_3$/PC solutions and various additives are given in Table 17.

Addition of DMF or DMSO produced solutions of a light yellow color which did not change to a great extent during the stability tests. A pressure build-up was, however, observed, indicating some instability. It is not clear, if the gas evolved was from the reaction of the base electrolyte or from a reaction of the additive with lithium. In the latter case, a more stable additive with similar stabilizing characteristics may be found. It could also be that a reaction only occurs in the beginning and that the solution is stable after an initial period.

Solutions with AN added darkened, but no pressure build-up was noted. Darkening of the solutions was also observed with THF or NM as additive. A light color resulted and remained with MF as additive, but pressure build-up was observed.

TABLE 17

STABILITY OBSERVATIONS ON

$LiCl+AlCl_3$/PC ELECTROLYTES, WITH VARIOUS ADDITIVES,

IN THE PRESENCE OF LITHIUM METAL

Electrolyte	Additive	Initial observation before lithium addition (1-2 week old samples)	Observation after 1 day at room temperature	Observation after 1 day at 60 C
1 M $AlCl_3$ #4/PC #6-5		Dark blackish-purple color; no solid	No change	No change after 30 min; solution turned darker, brownish-black; pressure build-up
1 M $AlCl_3$ #4 + 0.8 M LiCl #3/PC #6-5		Light orange-brown color; no solid	No change	No change after 30 min; solution turned a dark brown; no pressure build-up
1 M $AlCl_3$ #4 + 0.2 M LiCl #3/PC #6-5	1.5 M DMF #7-3	Light yellow color (decanted) from white solid)	No change	No change after 30 min; solution turned slightly darker yellow; slight pressure build-up
1 M $AlCl_3$ #4/PC #6-4	2 M DMF #7-3	Light yellow color; no solid	No change	No change after 30 min; no change in color, slight pressure build-up

TABLE 17 (CONT'D.)

Electrolyte	Additive	Initial observation before lithium addition (1-2 week old samples)	Observation after 1 day at room temperature	Observation after 1 day at 60 C
1 M $AlCl_3$ #4/PC #6-6	0.05 DMSO #1-1	Dark purple-brown; no solid	No change	No change after 1 hour; solution darkened slightly; pressure build-up
1 M $AlCl_3$ #4/PC #6-6	0.15 DMSO #1-1	Dark purple-brown; no solid	No change	No change after 1 hour; solution darkened slightly; pressure build-up
1 M $AlCl_3$ #4/PC #6-6	2.0 M DMSO #1-1	Light yellow, with white precipitate	No change	No change noted; pressure build-up
1 M $AlCl_3$ #4 + 0.8 M LiCl #3/PC #6-6	0.5 M DMSO #1-1	Light yellow; no solid	No change	No change noted; pressure build-up
1 M $AlCl_3$ #4/PC #6-7	0.5 M AN #6-1	Light orange-brown	No change	No change after 1 hour; solution darkened to blackish-brown; no pressure build-up
1 M $AlCl_3$ #4 + 0.4 M LiCl #3/PC #6-7	0.5 M AN #6-1	Light orange-brown	Solution darkened slightly	No change after 1 hour; solution darkened to blackish-brown; no pressure

TABLE 17 (CONT'D.)

Electrolyte	Additive	Initial observation before lithium addition (1-2 week old samples)	Observation after 1 day at room temperature	Observation after 1 day at 60 C
1 M $AlCl_3$ #4/PC #6-6	2 M THF #1	Dark orange-brown	No change	Solution darkened considerably in 1 hour; it turned black with some dark solid dispersed; pressure build-up
1 M AlCl #4/PC #6-6	1 M THF #1	Dark blackish-purple	Solution darkened considerably; pressure build-up	No further change obvious after 1 hour; solution turned very dark (gel-like appearance); some black solid, dispersed; pressure build-up
1 M $AlCl_3$ #4 + 0.8 M LiCl #3/ PC #6-6	1 M THF #1	Dark blackish-purple	Solution darkened slightly	No change obvious after 1 hour; solution darkened slightly; no pressure build-up
1 M $AlCl_3$ #4/PC #7-1	1.5 M NM #1-2	Clear greenish-brown	No change	Solution turned blackish-brown (lithium strip was lighter where submerged in solution); pressure build-up

TABLE 17 (CONT'D.)

Electrolyte	Additive	Initial observation before lithium addition (1-2 week old samples)	Observation after 1 day at room temperature	Observation after 1 day at 60 C
PC #7-4	20 v/o NM	Clear-colorless	No change	No change after 1 week at room temperature
1 M $AlCl_3$ #4/PC #3-1	2 M MF #2-11	Light orange-brown	No change (lithium strip was lighter where submerged in solution)	No change; pressure build-up
1 M $AlCl_3$ #4 + 0.6 M LiCl #3/PC #3-1	2 M MF #2-11	Light orange-brown	No change (lithium strip was lighter where submerged in solution)	No change; pressure build-up
1 M $AlCl_3$ #4/PC #7-1	1 M LiBr #2	Faint pale yellow, with white precipitate	No change	No change; pressure build-up
1 M $AlCl_3$ #4/PC #7-1	0.5 M LiBr #2	Blackish and purple, with some suspended black solid	No change	No change after 1 hour; solution darkened to blackish brown; pressure build-up

The bromide ion, similar to the chloride ion, was expected to displace PC in the $Al[PC]_6^{+3}$ complex. Because of the higher solubility of LiBr than of LiCl in PC, addition of LiBr appeared promising. Problems were encountered, however, in preparing the solutions because of precipitation reactions. Pressure build-ups were observed with the solutions tested.

Because of a heavy emphasis on methyl formate solutions in later parts of the program, the stabilization efforts were not extended beyond these somewhat preliminary studies, and no firm recommendation can be made.

Stability of $LiCl+AlCl_3$/PC With H_2O Added

The stability of 1 M $AlCl_3$ + 0.5 M LiCl/PC to which small amounts of H_2O had been added was investigated, and the results are given in Table 18. No significant differences in stability were observed. It should be remembered that some solid, probably aluminum hydroxide, precipitated during preparation of these solutions and was not present during the stability tests.

TABLE 18

STABILITY OBSERVATIONS ON THE ELECTROLYTE SYSTEM

$LiCl+AlCl_3$/PC & H_2O,

IN THE PRESENCE OF LITHIUM METAL

Solution	Initial observation (1 day old samples; before lithium addition)	Observation after 1 day at room temperature	Observation after 1 day at 60 C	Observation after 1 week at room temperature
1 M $AlCl_3$ #5 + 0.5 M LiCl #3/PC #7-8 & 0 ppm H_2O	Clear orange-brown	Solution turned clear goldish-tan	Solution turned blackish-brown	Pressure build-up
1 M $AlCl_3$ #5 + 0.5 M LiCl #3/PC #7-8 & 100 ppm H_2O	Clear orange-brown	Solution turned clear goldish-tan	Solution turned blackish-brown	Pressure build-up
1 M $AlCl_3$ #5 + 0.5 M LiCl #3/PC #7-8 & 500 ppm H_2O	Clear orange-brown	Solution turned clear goldish-tan	Solution turned blackish-brown	Pressure build-up

Stability of $LiAsF_6$/PC Containing Various Additives

As the results of Table 19 indicate, $LiAsF_6$/PC electrolytes without and with various additives added were found to be stable within the limits of the test applied.

Stability of Several Other Electrolytes Containing LiCl and $AlCl_3$

An electrolyte based on the solvent DMF was found unstable, as shown in Table 20 . The lithium metal appeared to react with DMF.

Methyl formate solutions containing LiCl+$AlCl_3$ appeared to be stable, although some interaction with the lithium was indicated. Such solutions to which some DMSO had been added were less stable.

Stability of $LiAsF_6$/MF Electrolytes

As indicated in Table 21, the stability of $LiAsF_6$/MF solutions was not markedly affected by the addition of DMF or DMSO. Stability problems had been observed with both solvents (Ref.14), and the reaction between lithium and DMF or DMSO therefore, may be inhibited in the presence of $LiAsF_6$. When DMF was added to a $LiClO_4$/MF solution, a reaction with the lithium occurred, and a specific stabilizing effect of $LiAsF_6$ in the above cases was again indicated.

The difference in stability between $LiAsF_6$/MF and $LiClO_4$/MF solutions which was observed in the presence of DMF, was also reflected for solutions containing no additive, as shown in Table 22 . Again, a stabilizing effect of $LiAsF_6$ was demonstrated.

To investigate how much of $LiAsF_6$ was needed to produce this stabilizing effect, experiments were performed with $LiClO_4$/MF solutions containing $LiAsF_6$ an additive. A 0.01 M $LiAsF_6$ content did not produce a stable solution, but a 0.1 M $LiAsF_6$ addition stabilized a 1 M $LiClO_4$/MF electrolyte. This was the case at least for the addition of $LiAsF_6$ #1, originating from the old $LiAsF_6$/MF stock solution provided by the Livingston Electronic Laboratory. Pressure build-up and other indications of decomposition were obtained, however, when $LiAsF_6$ #2 was used, i.e., a pure $LiAsF_6$ synthesized by Midwest Research Institute. These observations were confirmed when 0.1 M $LiAsF_6$ #2 was added to a 1 M $LiClO_4$/MF & 4 M DMF solution.

Because different $LiAsF_6$ materials displayed different effects, it seems that the $LiAsF_6$ per se was not responsible for the characteristic stabilization effect but rather an impurity. Such an impurity could have been present in greater amounts in the $LiAsF_6$ #1/MF solution resulting from the methathesis process, and could have originated either from the solute or the solvent part of the solution.

TABLE 19

STABILITY OBSERVATIONS ON

$LiAsF_6$/PC ELECTROLYTES WITH

VARIOUS ADDITIVES, IN THE PRESENCE OF LITHIUM METAL

Electrolyte	Additive	Initial observation (1 day old samples; before lithium addition)	Observation after 1 day at room temperature	Observation after 1 day at 60 C
1 M $LiAsF_6$ #4/PC #7-8		Clear and colorless	No change	No change
1 M $LiAsF_6$ #4/PC #7-8	4 M DMF #7-3	Clear and colorless	No change	No change
1 M $LiAsF_6$ #4/PC #7-8	4 M DMSO #1-1	Clear and colorless	No change	No change
1 M $LiAsF_6$ #4/PC #7-8	4 M THF #1	Clear and colorless	No change	No change

TABLE 20

STABILITY OBSERVATIONS ON SEVERAL OTHER ELECTROLYTES

CONTAINING LiCl AND $AlCl_3$, IN THE PRESENCE OF LITHIUM METAL

Electrolyte	Additive	Initial observation (2 week old samples; before lithium addition)	Observation after 1 day at room temperature	Observation after 1 week at room temperature
0.05 M $AlCl_3$ #4 + 0.5 M LiCl #3/DMF #1-3	0.5 M $LiClO_4$ #3	Clear - colorless	Solution turned light yellow and a white granular precipitate formed which coated Li strip	No change after 1 hour at 60 C; solution turned darker yellow and contained a white precipitate; most of the original Li strip dissolved; pressure build-up (after 1 day at 60 C)
1 M LiCl #3 + 1 M $AlCl_3$ #4/MF #2-13		Clear and colorless	No change	Lithium strip was lighter with some white solid deposit where submerged
1 M LiCl #3 + 1 M $AlCl_3$ #4/MF #2-12	1 M DMSO #1-1	Clear with tint of yellow and settled white precipitate (supernate used for test)	Solution darkened slightly and a white precipitate formed; pressure build-up; lithium strip was lighter where submerged and had a white crystalline deposit	Same as after 1 day

TABLE 20 (CONT'D.)

Electrolyte	Addition	Initial observation (2 week old samples; before lithium addition)	Observation after 1 day at room temperature	Observation after 1 week at room temperature
1 M $AlCl_3$ #4/MF #2-13	1 M DMSO #1-1	Clear and colorless	Solution turned yellow and lithium strip was very shiny (much lighter) where submerged	Solution darkened slightly
2 M $AlCl_3$ #4 + 2 M LiCl #3/MF #3-3		Clear with pinkish tint	Lithium strip lightened slightly where submerged	Small amount of white precipitate settled at bottom of tube; slight amount of grayish-white deposit formed on lithium strip

TABLE 21

STABILITY OBSERVATIONS ON $LiAsF_6$/MF ELECTROLYTES

CONTAINING DMF OR DMSO AS ADDITIVES, IN THE PRESENCE OF LITHIUM METAL

Electrolyte	Additive	Initial observation (1-2 week old samples; before lithium addition)	Observation after 1 day at room temperature	Observation after 1 week at room temperature
1 M $LiAsF_6$ #1/MF #2-12		Clear with light yellow tint	No change	No change; lithium strip was lighter where submerged in solution
1 M $LiAsF_6$ #1/MF #2-12	2 M DMSO #1-1	Clear with light yellow tint	No change	No change
1 M $LiAsF_6$ #1/MF #2-12	2 M DMSO #1-1	Clear light tan	Brown precipitate settled out and clear supernate remained; lithium strip was lighter where submerged	Same as after 1 day
1 M $LiAsF_6$ #1/MF #2-11	4 M DMF #7-3	Light yellow	No change	No change (observation after 3 days at 25 C)
1 M $LiClO_4$ #3/MF #2-12	4 M DMF #7-3	Colorless	Solution turned light yellow and was bubbling slowly and left goldish deposit on Li strip; pressure build-up	Darkened slightly (observation after 3 days at 25 C)

TABLE 22

STABILITY OBSERVATIONS ON $LiAsF_6$/MF AND $LiClO_4$/MF SOLUTIONS, IN THE PRESENCE OF LITHIUM METAL

Solution	Initial observation (1 day old samples; before lithium addition)	Observation after 1 day at room temperature	Observation after 1 week at room temperature
1 M $LiAsF_6$ #1/MF #3-2	Clear and goldish tint	No change	No change
1 M $LiAsF_6$ #2/MF #3-2	Clear and colorless	No change	Small amount of grayish deposit on lithium strip
1 M $LiClO_4$ #3/MF #3-1	Clear and colorless	Solution turned yellow; lithium strip had a granular silverish deposit; pressure build-up	Solution turned cloudy brown-orange; a brown precipitate formed in solution and deposited on lithium strip; outgassing was observed; pressure build-up
1 M $LiClO_4$ #3/MF #3-2 & 0.01 M $LiAsF_6$ #1	Clear and colorless	Small amount of white precipitate formed in solution, and solution turned light yellow; lithium strip had shiny appearance and had a silverish granular deposit; pressure build-up	Solution turned orange-gold and contained a yellowish precipitate; pressure build-up
1 M $LiClO_4$ #3/MF #3-2 & 0.01 M $LiAsF_6$ #2	Clear and colorless	Solution turned yellow and was outgassing; lithium strip had shiny appearance and had a silverish granular deposit; pressure build-up	Solution turned orange-gold; lithium strip covered with yellowish granular deposit; pressure build-up

TABLE 22 (CONT'D.)

Solution	Initial observation (1 day old samples: before lithium addition)	Observation after 1 day at room temperature	Observation after 1 week at room temperature
1 M $LiClO_4$ #3/MF #2-14 & 0.1 M $LiAsF_6$ #1	Clear and colorless	White precipitate formed; solution was clear and colorless; lithium strip was lighter where submerged	Same as after 1 day
1 M $LiClO_4$ #3/MF #2-14 & 0.1 M $LiAsF_6$ #2	Clear and colorless	Solution was clear and turned light yellow; goldish granular deposit formed on lithium strip	Solution was clear and turned deep yellow; heavy orange-brown deposit formed on lithium strip; pressure build-up
1 M $LiClO_4$ #3/MF #3-2 & 0.1 M $LiAsF_6$ #1 + 4 M DMF #7-3	Clear and colorless	Small amount of white precipitate formed in solution	No change
1 M $LiClO_4$ #3/MF #3-2 & 0.1 M $LiAsF_6$ #2 + 4 M DMF #7-3	Clear and colorless	Solution turned light yellow; lithium strip lightened and had a silverish granular deposit; pressure build-up	Solution turned cloudy brown-orange; thick brown deposit formed on lithium strip; outgassing was observed; pressure build-up

Further experiments, reported on in Table 23 , were performed to elucidate this point. A new solution obtained from Livingston Electronic Laboratory, $LiAsF_6$ #6, was used. This solution did not seem to possess equal stabilizing properties as the original one, $LiAsF_6$ #1. In a concentration of 1 molar, both $LiAsF_6$ #5 and $LiAsF_6$ #6 appeared to render stable solutions.

TABLE 23

STABILITY OBSERVATIONS ON $LiAsF_6$/MF SOLUTIONS IN THE PRESENCE OF LITHIUM METAL

Solution	Initial observation (1 week old samples before lithium addition	Observation after 1 day at room temperature	Observation after 1 week at room temperature
1 M $LiAsF_6$ #5/MF #3-4	Clear, colorless	No change	No change*
1 M $LiAsF_6$ #6/MF #3-7	Clear, colorless	No change	No change**
1 M $LiClO_4$ #3/MF #3-7 & 0.1 M $LiAsF_6$ #6 + 4 M DMF #7-3	Clear, colorless	Light yellow	Light yellow pressure build-up; lithium*** dull, corroded
1 M $LiClO_4$ #3/MF #3-7 & 0.1 M $LiAsF_6$ #5 + 4 M DMF #7-3	Clear, colorless	Light yellow	Light yellow; some pressure build-up; lithium*** dull, somewhat corroded
1 M LiClO, #3/MF #3-7 & 0.1 M $LiAsF_6$ #5 + 4 M DMF #7-3 + 500 ppm H_2O	Clear, colorless	Very light yellow	Light yellow; pressure build-up; lithium*** dull, corroded

Stability Studies on $LiAsF_6$/MF Solutions With Water Added

The stability of 1 M $LiAsF_6$/MF solutions to which small amounts of water had been added was studied. As indicated in Table 24 , the stability in contact with lithium metal was not found to be affected by small amounts of water, except that somewhat more of a white precipitate was observed in the case where the largest amount of water had been added.

*Lithium with yellowish-green coating after 3 months

**Lithium unchanged after 3 months, trace of precipitate

***Lithium replaced by white coherent precipitate after 3 months

TABLE 24

STABILITY STUDIES ON $LiAsF_6$/MF ELECTROLYTES, WITH WATER ADDED, IN THE PRESENCE OF LITHIUM METAL

Solution	Initial observation (no lithium added)	Observation after 1 day at room temperature	Observation after 1 week at room temperature
1 M $LiAsF_6$ #5/MF #3-4	Clear, colorless	No change	No change; trace of white precipitate
1 M $LiAsF_5$ #5/MF #3-4 & 100 ppm H_2O	Clear, colorless	No change	No change; trace of white precipitate
1 M $LiAsF_6$ #5/MF #3-4 & 500 ppm H_2O	Clear, colorless	No change	No change; traces of white precipitate

SOLUBILITY STUDIES

Measurement Procedure

A weighed excess of solute was added in the dry box to the solvent or solution (usually 15 ml) of interest. The volumetric flask was then sealed with a glass stopper and Teflon tape, and the neck of the flask was enclosed in a polyethylene bag containing dry nitrogen. The flask was removed from the dry box and normally stirred by means of a magnetic stirrer for about 3 days at a temperature somewhat above room temperature. Then the sample was placed in a constant-temperature bath held at 25.00±0.02 C to equilibrate for about 3 days. For sampling purposes, the flask remained in the constant-temperature bath and was opened. A sample of the supernatant liquid was taken very quickly with a pipette, and an analysis performed by atomic absorption for one or several elements.

The comments made in Ref. 1 in regard to uncertainties apply again. In cases where interaction between solutes could be suspected, analyses were made for several elements. Errors appeared to occur in the sampling of methyl formate solutions because of the low vapor pressure of this solvent, and concentrations often seemed to be too high by as much as 10 percent.

Solubility of LiCl and $AlCl_3$ as Solutes

The solubilities of LiCl and $AlCl_3$ in propylene carbonate and dimethylformamide were studied in the previous contract (Ref. 1). Some questions had been left unanswered because analyses had not been performed for both the lithium and the aluminum; it was not established, e.g., whether LiCl was soluble up to 0.78 M in a 1 M $AlCl_3$/PC solution (Ref. 1), or whether it was the solubility of a precipitating $LiAlCl_4$ that was actually determined.

In the experiments represented in Table 25, an excess of LiCl (the corresponding concentration is given in parenthesis) was added to 1 M and 0.5 M $AlCl_3$/PC solutions. The solutions were stirred for an hour, later for an additional 16 hours, and then equilibrated at 25 C for about 3 days. Samples of the supernatant liquid were taken and analyzed by atomic absorption to give the results indicated in Table 25 . A sample of 1 M LiCl/DMF with $AlCl_3$ added was treated in the same manner.

Approximately stoichiometric amounts of lithium and aluminum were found in propylene carbonate and, unexpectedly, this was observed at the concentration of 1 molar. Previously, a solubility of only 0.78 M LiCl had been reported for 1 M $AlCl_3$/PC, and 0.66 M LiCl for 1.2 M $AlCl_3$/PC. It appears that LiCl is soluble in stoichiometric amounts to form $LiAlCl_4$ (Li^+ and $AlCl_4^-$ ions) even at a concentration of 1 molar, but that this compound may precipitate very slowly. This would explain various somewhat erratic results on the solubility of LiCl, and the observation that occasionally LiCl+$AlCl_3$/PC solutions could be made up with seemingly excessive LiCl content. It could account also for different solubility values reported for $LiAlCl_4$/PC solutions in the literature.

By dissolving 0.5 M $AlCl_3$ in a 1 M LiCl/DMF solution, an aluminum content of 0.058 M was obtained, the lithium content had increased to 1.30 M, however. A white fluffy precipitate formed, which was very likely an aluminum compound containing solvating solvent. If it is considered that 12.9 moles per liter is the concentration of DMF in a 1 M LiCl/DMF solution, and that 0.4 moles per liter of $AlCl_3$ would coprecipitate 2.4 moles per liter of DMF (assuming a solvation number of 6), then the increase of 30 percent in the lithium concentration appears somewhat high. No further conclusion can be drawn, however, based on this limited experimentation, except that the solubility value of $AlCl_3$ in 1 M LiCl/DMF of Ref. 1 which had been obtained by a chloride titration is most likely erroneous.

For a 0.5 M LiCl + 1.0 M $AlCl_3$/PC & 0.75 M DMF solution, it can be expected, as a first approximation, that the aluminum in the electrolyte selected is completely complexed by either dimethyl formamide molecules or chloride ions, and that the electrolyte composition is

$$0.5\ M\ Li^+ + 0.875\ M\ AlCl_4^- + 0.125\ M\ Al[DMF]_6^{+3}$$

It appears that LiCl is somewhat soluble beyond this stoichiometric composition, to a concentration of 0.55 M. The amount exceeding 0.5 M corresponds approximately to the solubility of LiCl in pure PC (0.04 M at 25 C, according to Ref. 1). It should be noted that the solubility of LiCl is smaller in the presence of the added DMF than in a 1 M $AlCl_3$/PC solution without additive (0.99 M according to results of Table 25, 0.8 M according to Ref. 1).

TABLE 25

SOLUBILITIES OF LiCl AND $AlCl_3$ AT 25 C

Solution	Added Solute	Li Content	Al Content
1 M $AlCl_3$ #4/PC #6-4	LiCl #3 (1.25 M)	0.99 M	1.01 M
0.5 M $AlCl_3$ #4/PC #6-4	LiCl #3 (1 M)	0.51 M	0.52 M
1 M LiCl #3/DMF #7-3	$AlCl_3$ #4 (0.5 M)	1.30 M	0.058 M
0.5 M LiCl #3 + 1 M $AlCl_3$ #4/PC #4-7 & 0.75 M DMF #7-3	LiCl #3 (0.5 M)	0.55 M	1.00 M
0.5 M LiCl #3 + 1 M $AlCl_3$ #4/PC #4-7 & 0.75 M DMF #7-3	LiCl #3 (1.0 M)	0.55 M	0.98 M
0.5 M LiCl #3 + 1 M $AlCl_3$ #4/PC #4-7 & 0.75 M DMF #7-3	-	0.50 M	1.00 M

Solubility of CuF_2 and $CuCl_2$ in LiCl+$AlCl_3$/PC Containing DMF or DMSO as Additives

The solubilities of CuF_2 and $CuCl_2$ in a 0.5 M LiCl + 1 M $AlCl_3$/PC & 0.75 M DMF solution was investigated. The samples were analyzed not only for copper, but also for lithium and aluminum; the results are presented in Table 26.

When CuF_2 is dissolved in the above electrolyte, a dissolution reaction involving the precipitation of LiF could be expected, according to

$$2\ LiCl + CuF_2 = \underline{2\ LiF} + CuCl_2 \qquad (1)$$

In the actual experiment, the lithium concentration did not decrease, however, and a precipitation of LiF evidentally did not occur. The presence of fluorine in dissolved form was verified by NMR investigation of samples of 1 M $AlCl_3$ #4 + 0.5 M LiCl #3/PC #7-4 & 0.75 M DMF #7-3 +

0.25 M CuF_2 #4. Although no fluorine line could be observed in the high resolution spectrum because of excessive line broadening, a strong line was observed in the broadline spectrum. The intensity suggested a fluorine concentration in the order of magnitude corresponding to the copper concentration determined by atomic absorption. Two aluminum lines were found which seem to correspond to the lines observed in respective samples containing no copper halide.

A lower aluminum content was found by analysis, in agreement with results obtained with a similar electrolyte containing no additive. A precipitation of some aluminum fluoride can be suspected:

$$3\ CuF_2 + 2\ AlCl_3 = \underline{2\ AlF_3} + 3\ CuCl_2 \qquad (2)$$

Since the presence of fluorine in solution was verified and the observed ratio of copper content to decrease in aluminum concentration was not stoichiometrically 3:2, a reaction according to equation (2) could not have occured quantitatively. It seemed that not all copper available dissolved, despite the large excess of $AlCl_3$. It can be speculated that a precipitate containing copper and aluminum fluoride may form and that the solubility of such a entity was actually determined. Such compounds, e.g., of the form $Cu(AlF_4)_2$ or $Cu_3(AlF_6)_2$, may contain complexed DMF and thus the DMF content could become an important factor determining the CuF_2 solubility. It would take further investigations, i.e., analysis of the solution for fluoride and DMF, and analysis of the solids, to reach more definitive conclusions.

TABLE 26

SOLUBILITY OF CuF_2, $CuCl_2$, and LiCl IN 0.5 M LiCl #3 + 1 M $AlCl_3$ #4/PC #4-7 & 0.75 M DMF #7-3, AT 25 C

Added Solute	Lithium Content	Aluminum Content	Copper Content
None	0.50 M	1.00 M	-
LiCl #3 (0.5 M)	0.55 M	0.98 M	-
LiCl #3 (1.0 M)	0.55 M	1.01 M	-
CuF_2 #4 (0.75 M)	0.50 M	0.94 M	0.41 M
$CuCl_2$ #2 (0.75 M)	0.49 M	0.98 M	0.185 M
CuF_2 #4 (0.75 M) + LiCl #3 (0.5 M)	0.84 M	0.88 M	0.315 M
$CuCl_2$ #2 (0.75 M) + LiCl #3 (0.5 M)	1.00 M	1.01 M	0.47 M

The presence of a greater amount of LiCl appeared to decrease the solubility of CuF_2 slightly. In the case of $CuCl_2$ a LiCl addition had the adverse effect; with a LiCl content of 0.5 molar the molar ratio of soluble copper to dimethylformamide was 1:4, with a LiCl content of 1 molar it was 2:3, and any suggestions as to what species may form appear to be too speculative at the present time.

In analogy to the previous system, a 0.5 M LiCl + 1 M $AlCl_3$/PC & 0.75 M DMSO electrolyte was also selected to study the solubility of the copper halides; the results are given in Table 27. In general, they are similar to the results presented in Table 26 for the LiCl+$AlCl_3$/PC & DMF system. A voluminous precipitate was observed to form with $CuCl_2$, and the copper content was accordingly somewhat lower in these cases.

Solubility of CuF_2 in LiCl+$AlCl_3$/PC & H_2O

The results of a study of the effect of adding small amount of water to a 1 M $AlCl_3$ + 0.5 M LiCl/PC solution are given in Table 28 . The copper content was found to be lower in solutions to which some water had been added, but the causes of this effect are uncertain. As had been found previously on a 1 M $AlCl_3$ + 0.7 M LiCl/PC solution (Ref. 1) and in the LiCl+$AlCl_3$/PC & DMF system, the aluminum content was slightly decreased, indicating the formation of an aluminum containing precipitate. The aluminum content was somewhat lower when 500 ppm H_2O had been added, but this may be due to the formation of an insoluble aluminum compound as was observed in preparing the solution.

TABLE 27

SOLUBILITY OF CuF_2, $CuCl_2$, AND LiCl IN 0.5 M LiCl #3 + 1 M $AlCl_3$ #4/PC #7-5 & 0.75 M DMSO #1-1, AT 25 C

	Lithium Content	Aluminum Content	Copper Content
None	0.46 M	1.00 M	-
LiCl #3 (0.5 M)	0.58 M	1.05 M	-
LiCl #3 (1.0 M)	0.57 M	1.03 M	-
CuF_2 #4 (0.75 M)	0.50 M	1.01 M	0.48 M
$CuCl_2$ #2 (0.75 M)	0.43 M	1.07 M	0.054 M*
CuF_2 #4 (0.75 M) + LiCl #3 (0.5 M)	0.79 M	0.87 M	0.354 M
$CuCl_2$ #2 (0.75 M) + LiCl #3 (0.5 M)	0.93 M	1.05 M	0.142 M*

*Voluminous precipitate observed

TABLE 28

SOLUBILITY OF CuF_2 IN LiCl + $AlCl_3$/PC SOLUTIONS

CONTAINING SMALL AMOUNTS OF ADDED WATER, AT 25 C

Solute	Electrolyte-Additive Combination	Lithium Content Molar	Aluminum Content Molar	Copper Content Molar
CuF_2 #4 (0.75 M)	1 M $AlCl_3$ #5 + 0.5 M LiCl #3/ PC #7-8	0.45	0.95	0.124
CuF_2 #4 (0.75 M)	1 M $AlCl_3$ #5 + 0.5 M LiCl #3/ PC #7-8 & 100 ppm H_2O	0.45	0.95	0.100
CuF_2 #4 (0.75 M)	1 M $AlCl_3$ #5 + 0.5 M LiCl #3/ PC #7-8 & 500 ppm H_2O	0.45	0.90	0.072
	1 M $AlCl_3$ #5 + 0.5 M LiCl #3/ PC #7-8	0.47	1.02	-
CuF_2 #3	1 M $AlCl_3$ #4 + 0.7 M LiCl #3/ PC #5-5	0.66 (Ref. 1)	0.92 (Ref. 1)	0.063 (Ref. 1)

Solubility of CuF_2 and $CuCl_2$ In Presence of Salicylaldoxime or Phenanthroline

The effect of the addition of salicylaldoxime and phenanthroline on the solubilities of copper halides in selected electrolytes was briefly studied. Both, the copper halide and the organic additive, were added as solids to the basic electrolyte and stirred. The results of the sampling of the supernatant liquid are given in Table 29.

For the case of a 1 M $LiClO_4$/MF solution, the lithium apparently precipitated quantitatively as LiF, and CuF_2 was dissolved by this process. The copper was subsequently precipitated to a large extent by the phenanthroline. With $CuCl_2$, a voluminous precipitate formed so that sampling of a supernatant liquid was not possible.

Similar results were obtained with salicylaldoxime in 1 M $LiAsF_6$. With phenanthroline, a high solubility for CuF_2 was found in this electrolyte.

In all these cases, a higher solubility of the copper halide was observed than in pure 1 M $LiAsF_6$/MF solution. The possibility of depressing the solubility of the cathode material by addition of these additives is not indicated by these cursory studies.

Solubilities of CuF_2 and $CuCl_2$ in Methyl Formate Solutions Containing DMF

The solubilities of CuF_2 and $CuCl_2$ in $LiClO_4$/MF and $LiAsF_6$/MF solutions was studied, as shown in Table 30.

The solubility of CuF_2 in $LiClO_4$/MF was greatly enhanced by the addition of DMF. The reaction

$$2\ Li^+ + CuF_2 = \underline{2\ LiF} + Cu^{+2} \qquad (3)$$

appeared to occur quantitatively, the copper species in solution likely forming a DMF containing complex. The solubility of CuF_2 in 1 M $LiAsF_6$/MF was studied with various amounts of DMF added. If the DMF content was high, lithium precipitated quantitatively, apparently according to equation (3). At lower DMF concentrations, the solubility of CuF_2 was lower, but still increased in comparison to the DMF-free $LiAsF_6$/MF solution. The value for the solubility of CuF_2 obtained with 1 M DMF added is somewhat lower than the respective value obtained with 0.1 M DMF added; but neither the $LiAsF_6$ product used was the same, nor were the DMF batches identical; and this, in addition to some variation in the dissolution procedure, may account for the inconsistency of the results. An irreproducibility was also found with solutions containing no DMF; a solubility of 0.0012 M and 0.0025 M was found with $LiAsF_6$ #4 and $LiAsF_6$ #5, respectively, whereas values of 0.00075 M had been found for CuF_2 with $LiAsF_6$ #1.

TABLE 29

SOLUBILITIES OF COPPER HALIDES, AT 25 C, IN METHYL FORMATE ELECTROLYTES, WITH PHENANTHROLINE OR SALICYLALDOXIME ADDED

Solute	Solution	Solution Appearance	Lithium Content	Copper Content
CuF_2 #4 (1.0 M)	1 M $LiClO_4$ #3/MF #3-1 & "1 M" Phenanthroline #2	Very pale blue; greenish solids	0.0 M	0.023 M
$CuCl_2$ #2 (2.25 M)	1 M $LiClO_4$ #3/MF #3-1 & "1 M" Phenanthroline #2	Ochre colored solid; no free solution	--	--
CuF_2 #4 (0.5 M)	1 M $LiAsF_6$ #4/MF #3-3 & "0.2 M" Phenanthroline #2	Blue color	0.65 M	0.173 M
$CuCl_2$ #2 (0.5 M)	1 M $LiAsF_6$ #4/MF #3-3 & "0.2 M" Phenanthroline #2	Yellowish supernatant; voluminous yellow solid	1.08 M	0.00047 M
CuF_2 #4 (0.5 M)	1 M $LiAsF_6$ #4/MF #3-3 & "0.2 M" Salicylaldoxime #1	Yellowish supernatant; dark green solid	0.99 M	0.018 M
$CuCl_2$ #2 (0.5 M)	1 M $LiAsF_6$ #4/MF #3-3 & "0.2 M" Salicylaldoxime #1	Yellowish supernatant; voluminous ochre colored solid	1.05 M	0.0029 M
CuF_2 #4 (0.5 M)	1 M $LiAsF_6$ #4/MF #3-3	Colorless	1.08 M	0.0012 M
$CuCl_2$ #2 (0.5 M)	1 M $LiAsF_6$ #4/MF #3-3	Yellowish	1.08 M	0.00035 M
--	1 M $LiAsF_6$ #4/MF #3-3	--	1.08 M	--

TABLE 30

SOLUBILITY STUDIES OF CuF_2 AND $CuCl_2$ IN METHYL FORMATE SOLUTIONS CONTAINING DIMETHYLFORMAMIDE, AT 25 C

Solute	Solution	Solution Appearance	Lithium	Copper Content
CuF_2 #4 (1.0 M)	1.00 M $LiClO_4$ #3/MF #3-1	Pale blue; white solid	1.02 M	0.033 M
$CuCl_2$ #2 (1.0 M)	1.00 M $LiClO_4$ #3/MF #3-1	Light yellow-brown; brown-solid	0.97 M	0.0004 M
CuF_2 #4 (1.0 M)	0.98 M $LiClO_4$ #3/MF #3-1 & 3.92 M DMF #7-3	Deep blue; white solid	0.0 M	0.51 M
$CuCl_2$ #2 (1.0 M)	0.98 M $LiClO_4$ #3/MF #3-1 & 3.92 M DMF #7-3	Yellowish; brown solid	1.02 M	0.090 M
CuF_2 #3	1.1 M $LiAsF_6$ #1/MF #2.4			0.00075 M (Ref. 1)
CuF_2 #4 (0.5 M)	1 M $LiAsF_6$ #1/MF #2-12			0.00075 M
$CuCl_2$ #2 (0.5 M)	1 M $LiAsF_6$ #1/MF #2-12			0.0018 M
CuF_2 #4 (0.5 M)	1 M $LiAsF_6$ #1/MF #2-12 & 1 M DMF #7-3			0.0036 M
$CuCl_2$ #2 (0.5 M)	1 M $LiAsF_6$ #1/MF #2-12 & 1 M DMF #7-3			0.0036 M
CuF_2 #4 (0.5 M)	1 M $LiAsF_6$ #4/MF #3-3	Colorless; white solid	1.08 M	0.0012 M
$CuCl_2$ #2 (0.5 M)	1 M $LiAsF_6$ #4/MF #3-3	Yellowish; yellow-brown solid	1.08 M	0.00035 M
	1 M $LiAsF_6$ #4/MF #3-3		1.08 M	
CuF_2 #4 (0.75 M)	1 M $LiAsF_6$ #5/MF #3-4	Colorless	1.11 M	0.0025 M
CuF_2 #4 (0.75 M)	1 M $LiAsF_6$ #5/MF #3-4 & 0.1 M DMF #7-3	Light blue	0.97 M	0.063 M
CuF_2 #4 (0.75 M)	1 M $LiAsF_6$ #5/MF #3-4 & 6 M DMF #7-3	Blue	$<$0.0005 M	0.48 M

The precipitation of LiF according to equation (3) is the driving force for the dissolution of CuF_2. This process seems to occur very slowly, however, as has been shown by other workers for some systems (Ref. 15). It may be presumed that none of the values reported in Table 30 for additive-free solutions represents a true equilibrium. The amount of dissolved CuF_2 depends on the DMF addition, but it is not certain whether DMF only affects the dissolution rate. In addition to the additive there appear to be other factors, possibly impurities in solutes or solvents, which affect the solubility values determined for CuF_2.

In the case of $CuCl_2$, the solubility in $LiClO_4$/MF and $LiAsF_6$/MF solutions was also increased by DMF additions. In view of the high solubility of $CuCl_2$ in DMF this was not surprising. A stoichiometric relationship does not appear to exist however.

A more systematic study of time effects, impurity effects and additive effects would be needed to establish the factors affecting the copper halide solubilities. In addition, it should not be overlooked that the conditions in a partially discharged electrode may be significantly different from shelf life conditions.

Solubility of CuF_2 in Various $LiAsF_6$ Solutions

A difference in the solubility of CuF_2 was observed for two different $LiAsF_6$ products, as indicated by the results given in Table 31. The values obtained using $LiAsF_6$ #6, a stock solution supplied by the Livingston Electronic Laboratory, were significantly higher than the value determined simultaneously with $LiAsF_6$ #5, a high purity product from Midwest Research Institute. Impurities may affect solubilities--or rather the dissolution rates--of CuF_2 significantly. If this is the case, cathode discharge rates may be influenced by the $LiAsF_6$ used in the electrolyte.

Results were sometimes not very reproducible from measurement to measurement, as is evident from comparing the results of Table 31 obtained with 1 M $LiAsF_6$ #5/MF #3-7 with the results previously obtained with 1 M $LiAsF_6$ #5/MF #3-4. It is suspected that the values determined are not equilibrium values and that uncontrolled experimental parameters influenced the results.

Effect of Water Additions to $LiAsF_6$/MF Solutions Upon the Solubility of CuF_2

Results on the solubility of CuF_2 in $LiAsF_6$/MF solution to which small amounts of water had been added are given in Table 32 .

The water additions evidently had a significant effect on the observed copper fluoride solubilities. It can be postulated that a soluble complex involving copper, water(or rather a hydrolysis product since water is known to react with the solution), and possibly hexafluorophosphate ions is formed. A 500 ppm H_2O content corresponds to a water concentration of about 0.03 molar, which corresponds approximately to a 1:2 molar ratio of dissolved copper and water. Again, the time dependence of the results is unknown, and conclusions in regard to stoichiometry are speculative.

TABLE 31

SOLUBILITIES OF COPPER FLUORIDE IN

$LiAsF_6$/MF ELECTROLYTES AT 25 C

Solute	Electrolyte	Lithium Content (Molar)	Copper Content (Molar)
CuF_2 #4 (0.75 M)	1 M $LiAsF_6$ #5/MF #3-7	1.14	0.00063
CuF_2 #4 (0.75 M)	1 M $LiAsF_6$ #6/MF #3-7	1.16	0.0047
CuF_2 #4 (0.75 M)	1 M $LiAsF_6$ #6/MF #4	1.14	0.0046
CuF_2 #4 (0.75 M)	1 M $LiAsF_6$ #5/MF #3-4	1.11	0.0025
CuF_2 #4 (0.75 M)	1 M $LiAsF_6$ #5/MF #3-4	1.17	0.0028

TABLE 32

SOLUBILITIES OF COPPER FLUORIDE IN

$LiAsF_6$/MF ELECTROLYTES AFTER ADDITION OF SMALL AMOUNTS OF WATER, AT 25 C

Solute	Electrolyte-Additive Combination	Lithium Content (Molar)	Copper Content (Molar)
CuF_2 #4 (0.75 M)	1 M $LiAsF_6$ #5/MF #3-4	1.17	0.0028
CuF_2 #4 (0.75 M)	1 M $LiAsF_6$ #5/MF #3-4 & 100 ppm H_2O	1.12	0.0039
CuF_2 #4 (0.75 M)	1 M $LiAsF_6$ #5/MF #3-4 & 500 ppm H_2O	1.14	0.013
	1 M $LiAsF_6$ #5/MF #3-4	1.10	

VISCOSITIES AND DENSITIES

Viscosities were determined by a conventional technique involving measurements of the efflux time of the solutions through a capillary. Commercial Ubbelohde viscometers were employed and calibrated with water and appropriate standard solutions from Cannon Instrument Company. Densities were measured with a chainomatic density balance. The results for viscosities and densities are given in Table 33.

Because no viscosity data are available for a 0.5 M LiCl + 1 M $AlCl_3$/PC solution without any additive, the effect of DMF and DMSO addition, respectively, cannot be identified. The observed viscosity values are, however, very close to the value obtained previously for 1 M $AlCl_3$/PC (57.2 millipoise or 5.72×10^{-3} Newton sec m^{-2} at 25 C, according to Ref. 1).

The addition of DMF caused the viscosity of $LiClO_4$/MF as well as of $LiAsF_6$/MF solutions to increase, evidently due to the higher viscosity of the additive DMF.

The viscosity and density values obtained for 1 M $LiAsF_6$/MF solutions were somewhat irreproducible, but a correlation between the resulting values and the $LiAsF_6$ product used to prepare the solution could not be established.

CONDUCTANCE MEASUREMENTS

Measurement Technique

Specific conductances (λ) of solutions were determined at 1000 Hz using an E.S.I. impedance bridge and capacitance compensation. Freas cells with platinized platinum electrodes were filled with exactly 10 milliliters of solution. Cell constants had been determined accurately with standard aqueous KCl solutions and were approximately 0.4 cm^{-1}. Measurements were made with the conductivity cell dipped into a constant-temperature oil bath at 25.00 ± 0.02 C.

Conductance of LiCl+$AlCl_3$/PC Solutions with Various Additives

Dimethylformamide as Additive. The specific conductances of 1 M $AlCl_3$/PC and 0.2 M $AlCl_3$/PC solutions containing various amounts of LiCl and DMF were measured. The results are given in Table 34 and represented in Figures 122 and 123.

TABLE 33

SOLUTION VISCOSITIES AND DENSITIES AT 25 C

	Density		Viscosity	
	gm/cm^3	Kgm/m^3	millipoise	Newton sec m^{-2}
1 M $AlCl_3$ #4 + 0.5 M LiCl #3/PC #7-1 & 0.75 M DMF #7-3	1.239	1239	58.50	5.850×10^{-3}
1 M $AlCl_3$ #4 + 0.5 M LiCl #3/PC #7-5 & 0.75 M DMSO #1-1	1.248	1248	57.31	5.731×10^{-3}
1 M $LiClO_4$ #3/MF #3-2	1.057	1057	6.18	6.18×10^{-4}
1 M $LiClO_4$ #3/MF #3-2 & 4 M DMF #7-3	1.047	1047	9.70	9.70×10^{-4}
1 M $LiClO_4$ #3/MF #3-2 & 6 M DMF #7-3	1.042	1042	11.35	1.135×10^{-3}
2 M $LiClO_4$ #3/MF #3-1	1.133	1133	11.31	1.131×10^{-3}
2 M $LiClO_4$ #3/MF #3-1 & 2 M DMF #7-3	1.129	1129	15.04	1.504×10^{-3}
2 M $LiClO_4$ #3/MF #3-1 & 4 M DMF #7-3	1.122	1122	21.21	2.121×10^{-3}
1 M $LiAsF_6$ #5/MF #3-4 & 6 M DMF #7-3	1.107	1107	11.97	1.197×10^{-3}
1 M $LiAsF_6$ #5/MF #3-7	1.139	1139	7.31	7.31×10^{-4}
1 M $LiAsF_6$ #6/MF #3-7	1.121	1121	6.81	6.81×10^{-4}
1 M $LiAsF_6$ #7/MF #4	1.125	1125	6.92	6.92×10^{-4}

TABLE 34

SPECIFIC CONDUCTANCE OF PROPYLENE CARBONATE SOLUTIONS CONTAINING $AlCl_3$, LiCl AND DIMETHYLFORMAMIDE, AT 25 C

Electrolyte	Additive	Specific Conductance, $ohm^{-1}\ cm^{-1}$
1 M $AlCl_3$ #4/PC #6-5	-	6.88×10^{-3}
1 M $AlCl_3$ #4 + 0.2 M LiCl #3/PC #6-5	-	6.80×10^{-3}
1 M $AlCl_3$ #4 + 0.4 M LiCl #3/PC #6-5	-	6.75×10^{-3}
1 M $AlCl_3$ #4 + 0.4 M LiCl #3/PC #7-8	-	6.75×10^{-3}
1 M $AlCl_3$ #4 + 0.6 M LiCl #3/PC #6-5	-	6.67×10^{-3}
1 M $AlCl_3$ #4 + 0.8 M LiCl #3/PC #6-5	-	6.58×10^{-3}
1 M $AlCl_3$ #4/PC #6-4	0.5 M DMF #7-3	6.93×10^{-3}
1 M $AlCl_3$ #4 + 0.2 M LiCl #3/PC #6-4	0.5 M DMF #7-3	6.99×10^{-3}
1 M $AlCl_3$ #4 + 0.4 M LiCl #3/PC #6-4	0.5 M DMF #7-3	6.89×10^{-3}
1 M $AlCl_3$ #4 + 0.6 M LiCl #3/PC #6-4	0.5 M DMF #7-3	6.76×10^{-3}
1 M $AlCl_3$ #4 + 0.8 M LiCl #3/PC #6-4	0.5 M DMF #7-3	6.58×10^{-3}*
1 M $AlCl_3$ #4/PC #6-4	1 M DMF #7-3	7.22×10^{-3}
1 M $AlCl_3$ #4 + 0.2 M LiCl #3/PC #6-4	1 M DMF #7-3	7.03×10^{-3}
1 M $AlCl_3$ #4 + 0.4 M LiCl #3/PC #6-4	1 M DMF #7-3	6.64×10^{-3}*
1 M $AlCl_3$ #4/PC #6-5	1.5 M DMF #7-3	6.98×10^{-3}
1 M $AlCl_3$ #4 + 0.2 M LiCl #3/PC #6-5	1.5 M DMF #7-3	6.34×10^{-3}*
1 M $AlCl_3$ #4/PC #6-4	2 M DMF #7-3	4.95×10^{-3}
1 M $AlCl_3$ #4 + 0.5 M LiCl #3/PC #3-1	0.75 M DMF #7-3	6.82×10^{-3}

*Some precipitate observed

TABLE 34(CONT'D.)

Electrolyte	Additive	Specific Conductance, $ohm^{-1}\ cm^{-1}$
0.2 M $AlCl_3$ #4/PC #6-5		2.55×10^{-3}
0.2 M $AlCl_3$ #4 + 0.04 M LiCl #3/PC #6-5		2.58×10^{-3}
0.2 M $AlCl_3$ #4/PC #6-4 and 6-5	0.1 M DMF #7-3	2.57×10^{-3}
0.2 M $AlCl_3$ #4 + 0.04 M LiCl #3/PC #6-4 and 6-5	0.1 M DMF #7-3	2.60×10^{-3}
0.2 M $AlCl_3$ #4/PC #6-4 and 6-5	0.2 M DMF #7-3	2.53×10^{-3}
0.2 M $AlCl_3$ #4 + 0.04 M LiCl #3/PC #6-4 and 6-5	0.2 M DMF #7-3	2.57×10^{-3}
0.2 M $AlCl_3$ #4/PC #6-5	0.3 M DMF #7-3	2.24×10^{-3}
0.2 M $AlCl_3$ #4 + 0.04 M LiCl #3/PC #6-5	0.3 M DMF #7-3	1.99×10^{-3}
0.2 M $AlCl_3$ #4/PC #6-4 and 6-5	0.4 M DMF #7-3	1.46×10^{-3}

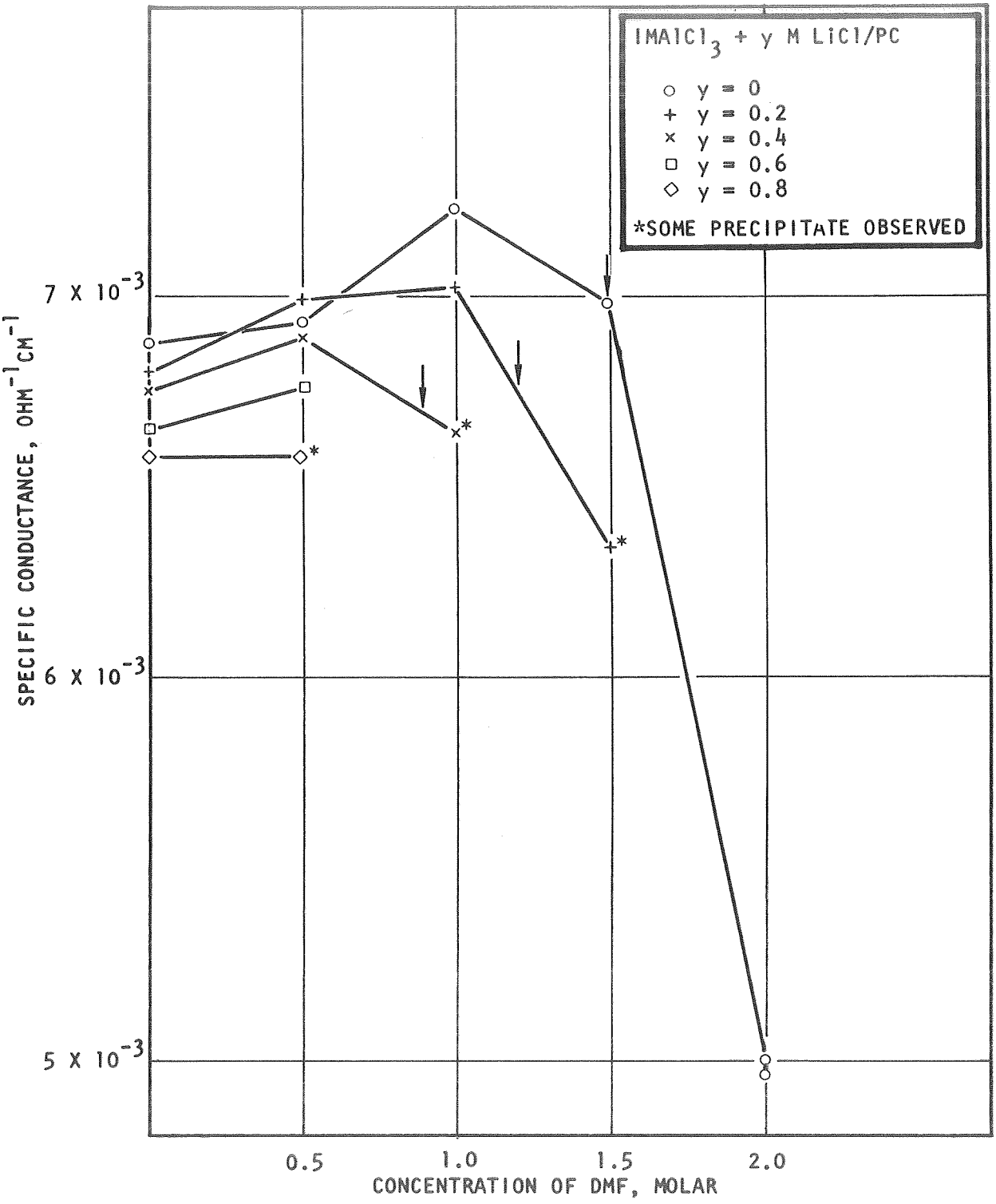

Fig.122.Specific Conductance of 1 M $AlCl_3$/PC Solutions Containing LiCl and/or DMF, at 25 C

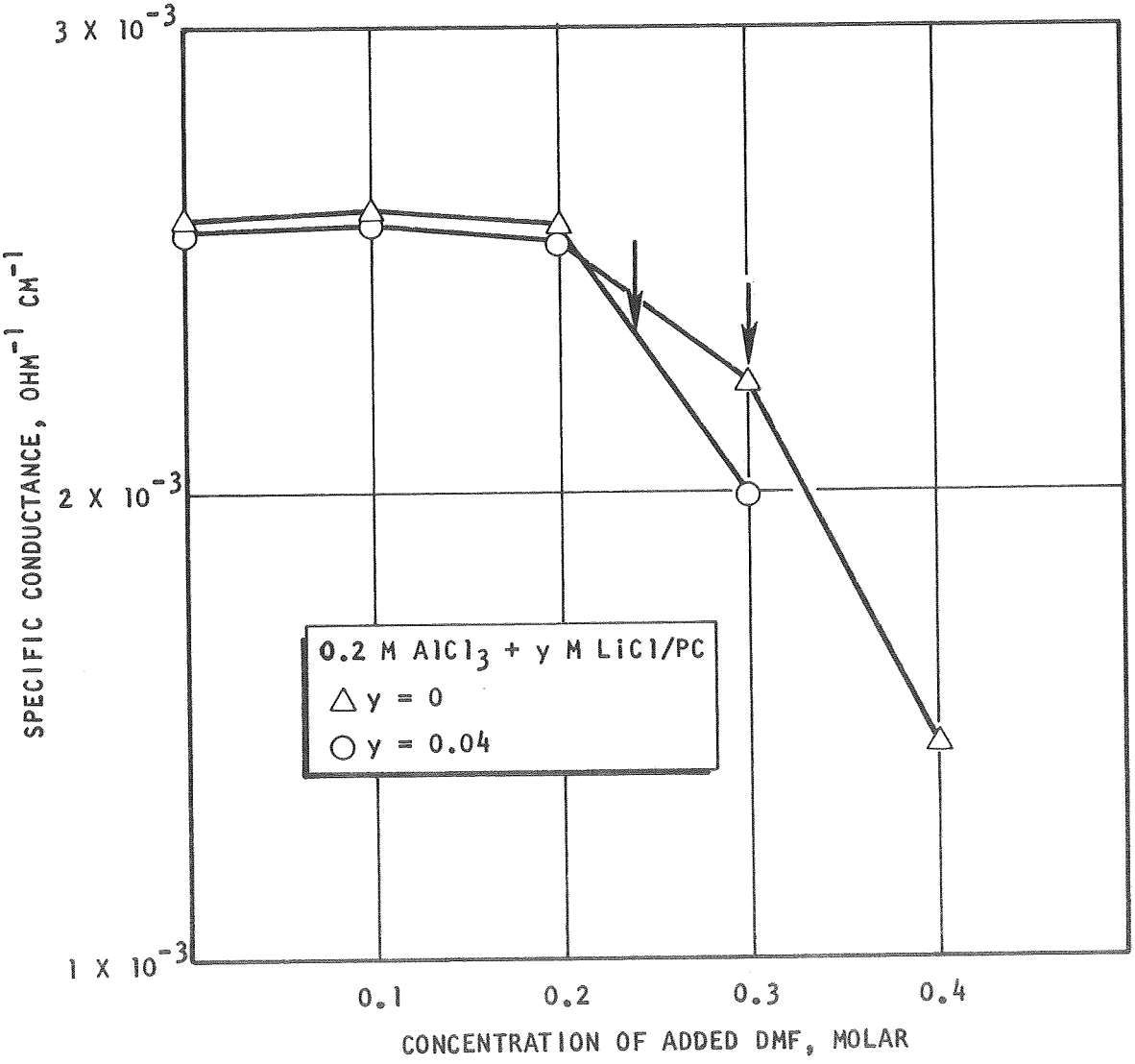

Fig.123. Specific Conductance of 0.2 M $AlCl_3$/PC Solutions Containing LiCl and/or DMF, at 25 C

Upon additions of some DMF, the specific conductance generally increased somewhat; at higher concentrations, a distinct decrease was observed, and the amount of DMF needed to induce this decrease appeared to be smaller the higher the LiCl content of the solution.

From previous studies (Ref.1), it can be expected that DMF replaces PC complexing the aluminum ion:

$$Al[PC]_6^{+3} + 6\ DMF = Al[DMF]_6^{+3} + 6\ PC \qquad (4)$$

The new complex may be more mobile, and a somewhat higher conductance may result.

The amount of DMF needed to complete reaction (4) depends on the concentration of the species $Al[PC]_6^{+3}$. Assuming a quantitative conversion of $AlCl_3$ to $Al[PC]_6^{+3}$ and $AlCl_4^-$, the composition of a 1 M $AlCl_3$/PC solution is 0.25 M $Al[PC]_6^{+3}$ + 0.75 M $AlCl_4^-$. With the coordination number of 6, a DMF content of 1.5 molar is needed to replace all the coordinated PC by DMF. The concentration of $Al[PC]_6^{+3}$ is smaller in solutions which contain LiCl in addition to $AlCl_3$, e.g., 0.4 M LiCl + 1 M $AlCl_3$/PC $\longrightarrow$ 0.15 M $Al[PC]_6^{+3}$ + 0.85 M $AlCl_4^-$. Therefore, the amount of DMF needed to convert all $Al[PC]_6^{+3}$ to $Al[DMF]_6^{+3}$ depends on the LiCl concentration. The DMF concentration corresponding to a complete reaction (4) are marked by vertical arrows in Figures 122 and 123.

It is remarkable that a conductance decrease was found when the DMF addition exceeded the stoichiometric amount according to reaction (4) and there were several explanations for this decrease considered. After all of the $Al[PC]_6^{+3}$ is converted to the DMF complex, a replacement of chloride in $AlCl_4^-$ is expected to follow:

$$AlCl_4^- + 6\ DMF = Al[DMF]_6^{+3} + 4\ Cl^- \qquad (5)$$

This reaction causes an increase in conductive species, but the specific conductance may drop because of an activity effect. If this were the correct explanation, a conductance increase would be expected in dilute solutions (0.2 M $AlCl_3$); this was not the case, however, as Figure 123 shows. The precipitation of conductive species after reaching the equivalence point is an alternate explanation; and some precipitation was actually observed. A third possibility is the elimination of conductive species by the formation of ion pairs occurring as soon as free chloride ions are present.

In conclusion, the results of the conductance experiments support the hypothesis that DMF readily replaces PC in the coordination sphere of the aluminum ion (with a coordination number of 6) and that it also replaces Cl^-.

Dimethyl Sulfoxide As Additive. The specific conductance data obtained with both 1 molar and dilute $AlCl_3$/PC solutions containing LiCl and/or DMSO are given in Table 35. As can be seen in Figures 124 and 125, the results are similar to the data reported above for DMF as the additive. The initial conductance increase upon DMSO addition to solutions 1 molar in $AlCl_3$ was more pronounced than with DMF; the complex ion $Al[DMSO]_6^{+3}$ may be somewhat more mobile than the ion $Al[DMF]_6^{+3}$. A significant difference was not observed in the dilute electrolytes, however. A tendency for a conductance decrease after reaching the stoichiometric concentration for the reaction

$$Al[PC]_6^{+3} + 6\ DMSO = Al[DMSO]_6^{+3} + 6\ PC \qquad (6)$$

was again indicated. In cases where this decrease was observed for the concentrated electrolytes, solutions with higher DMSO contents could not be made up because of the formation of a white precipitate which seemed to form more or less quantitatively past the equivalence point.

Acetonitrile as Additive. Specific conductance data on LiCl+$AlCl_3$/PC solutions with several other solvents as additives are given in Table 36. The addition of acetonitrile produced higher conductance, probably in connection with a decrease in solution viscosity. Some of the data are plotted and compared with similar data obtained with DMF in Figure 126. Whereas the conductance changes were only small in this latter case because of the interaction of DMF with the aluminum species, as discussed above, conductance changes were larger with AN. This solvent does not seem to replace PC in the $Al[PC]_6^{+3}$ complex, or only to a much weaker extent than DMF or DMSO. This is in agreement with conclusions drawn from NMR measurements.

Tetrahydrofuran as Additive. The results of Table 36 indicate that THF has a different influence on the conductance of $AlCl_3$/PC solutions than AN. The conductance of 1 M $AlCl_3$/PC decreased upon addition of 1 M THF, indicating an interaction because a straight viscosity effect would have caused an increase. No NMR evidence was, however, obtained for a reaction involving a significant displacement of PC in the coordinated aluminum species, as in the cases of DMF and DMSO.

A difference in interaction between DMF and THF is also indicated by the conductances of solutions containing LiCl in addition to $AlCl_3$. With higher LiCl content, conductances are lower in the LiCl+$AlCl_3$/PC & DMF system, but higher in the LiCl+$AlCl_3$/PC & THF system. It is suspected that THF forms a strong complex of the form $AlCl_3 \cdot THF$, rather than a complex with Al^{+3} ions having a coordination number of six. Such a complex formation could be the explanation also for the increase of the conductance at the higher THF addition of 2 M; beyond a stoichiometric addition corresponding to $AlCl_3 \cdot THF$, THF will act as a viscosity depressant additive.

TABLE 35

SPECIFIC CONDUCTANCE OF PROPYLENE CARBONATE SOLUTIONS CONTAINING $AlCl_3$, LiCl AND DIMETHYL SULFOXIDE, AT 25 C

Electrolyte	Additive	Specific Conductance, $ohm^{-1}\ cm^{-1}$
	20% DMSO #1-1	1.63×10^{-6}
1 M $AlCl_3$ #4/PC #6-6	0.05 M DMSO #1-1	6.97×10^{-3}
1 M $AlCl_3$ #4/PC #6-6	0.15 M DMSO #1-1	7.07×10^{-3}
1 M $AlCl_3$ #4/PC #6-6	0.30 M DMSO #1-1	7.20×10^{-3}
1 M $AlCl_3$ #4/PC #6-6	0.5 M DMSO #1-1	7.38×10^{-3}
1 M $AlCl_3$ #4 + 0.2 M LiCl #3/PC #6-6	0.5 M DMSO #1-1	7.25×10^{-3}
1 M $AlCl_3$ #4 + 0.4 M LiCl #3/PC #6-6	0.5 M DMSO #1-1	7.13×10^{-3}
1 M $AlCl_3$ #4 + 0.6 M LiCl #3/PC #6-6	0.5 M DMSO #1-1	6.99×10^{-3}
1 M $AlCl_3$ #4 + 0.8 M LiCl #3/PC #6-6	0.5 M DMSO #1-1	6.72×10^{-3}
1M $AlCl_3$ #4/PC #7-4	0.7 M DMSO #1-1	7.58×10^{-3}
1 M $AlCl_3$ #4 + 0.4 M LiCl #3/PC #7-4	0.7 M DMSO #1-1	7.29×10^{-3}
1 M $AlCl_3$ #4 + 0.5 M LiCl #3/PC #7-5	0.75 M DMSO #1-1	7.09×10^{-3}
1 M $AlCl_3$ #4/PC #7-4	0.9 M DMSO #1-1	7.75×10^{-3}
1 M $AlCl_3$ #4 + 0.4 M LiCl #3/PC #7-4	0.9 M DMSO #1-1	7.28×10^{-3}
1 M $AlCl_3$ #4/PC #6-6	1 M DMSO #1-1	7.79×10^{-3}
1 M $AlCl_3$ #4 + 0.4 M LiCl #3/PC #6-6	1 M DMSO #1-1	7.04×10^{-3}
1 M $AlCl_3$ #4/PC #7-4	1.1 M DMSO #1-1	7.90×10^{-3}
1 M $AlCl_3$ #4/PC #7-4	1.3 M DMSO #1-1	7.80×10^{-3}
1 M $AlCl_3$ #4/PC #6-6	1.5 M DMSO #1-1	7.80×10^{-3}

TABLE 35 (CONT'D.)

Electrolyte	Additive	Specific Conductance, $ohm^{-1}\ cm^{-1}$
0.2 M $AlCl_3$ #4/PC #6-6 and 6-5	0.01 M DMSO #1-1	2.56×10^{-3}
0.2 M $AlCl_3$ #4/PC #6-6 and 6-5	0.06 M DMSO #1-1	2.56×10^{-3}
0.2 M $AlCl_3$ #4/PC #6-6 and 6-5	0.1 M DMSO #1-1	2.58×10^{-3}
0.2 M $AlCl_3$ #4 + 0.04 M LiCl #3/PC #6-6 and 6-5	0.1 M DMSO #1-1	2.68×10^{-3}
0.2 M $AlCl_3$ #4 + 0.12 M LiCl #3/PC #6-6 and 6-5	0.1 M DMSO #1-1	2.88×10^{-3}
0.2 M $AlCl_3$ #4 + 0.16 M LiCl #3/PC #6-6 and 6-5	0.1 M DMSO #1-1	2.86×10^{-3}
0.2 M $AlCl_3$ #4/PC #4-7	0.14 M DMSO #1-1	2.61×10^{-3}
0.2 M $AlCl_3$ #4 + 0.08 M LiCl #3/PC #7-4	0.14 M DMSO #1-1	2.80×10^{-3}
0.2 M $AlCl_3$ #4 + 0.08 M LiCl #3/PC #7-4	0.18 M DMSO #1-1	2.79×10^{-3}
0.2 M $AlCl_3$ #4/PC #6-6 and 6-5	0.2 M DMSO #1-1	2.63×10^{-3}
0.2 M $AlCl_3$ #4 + 0.08 M LiCl #3/PC #6-6 and 6-5	0.2 M DMSO #1-1	2.67×10^{-3}
0.2 M $AlCl_3$ #4/PC #7-4	0.26 M DMSO #1-1	2.67×10^{-3}
0.2 M $AlCl_3$ #4/PC #6-6 and 6-5	0.3 M DMSO #1-1	2.52×10^{-3}

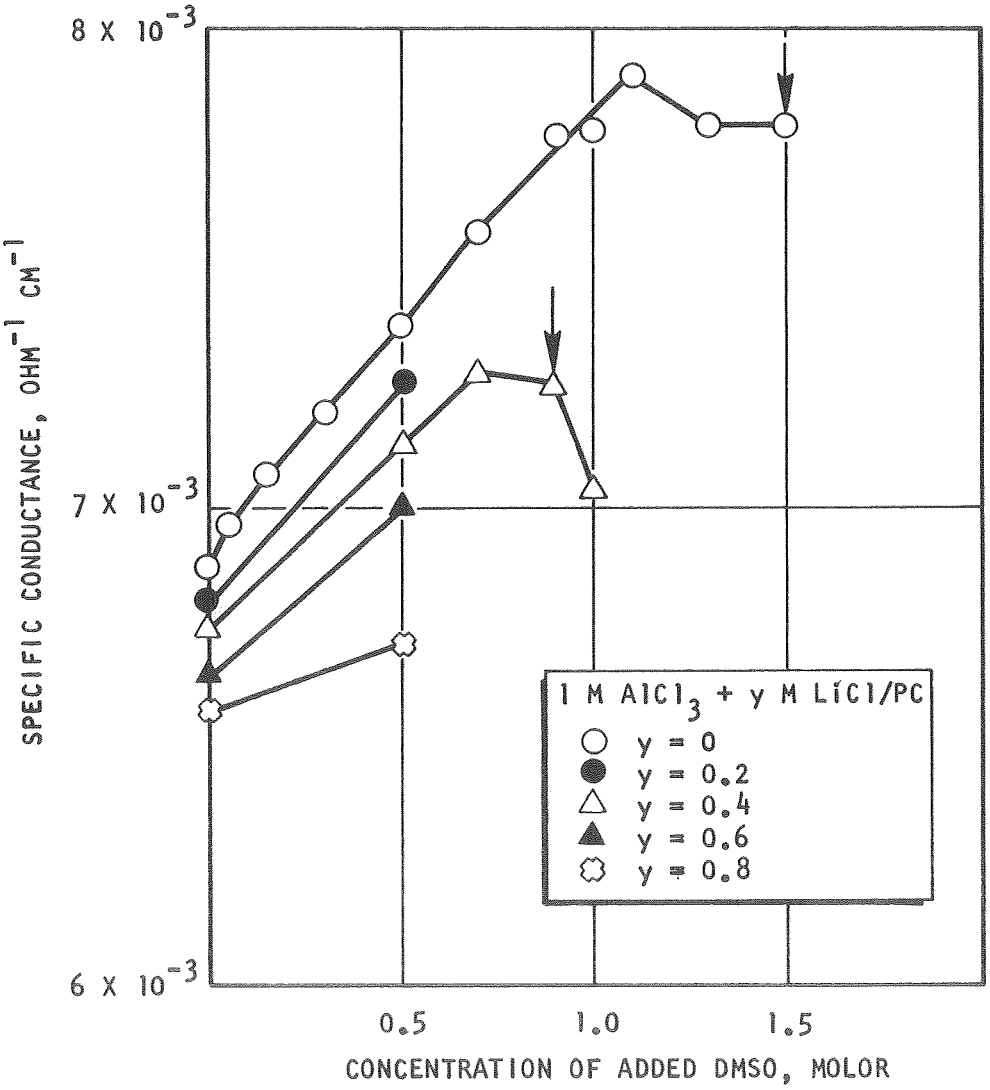

Fig. 124. Specific Conductance of 1 M $AlCl_3$/PC Solutions Containing LiCl and/or DMSO, at 25 C

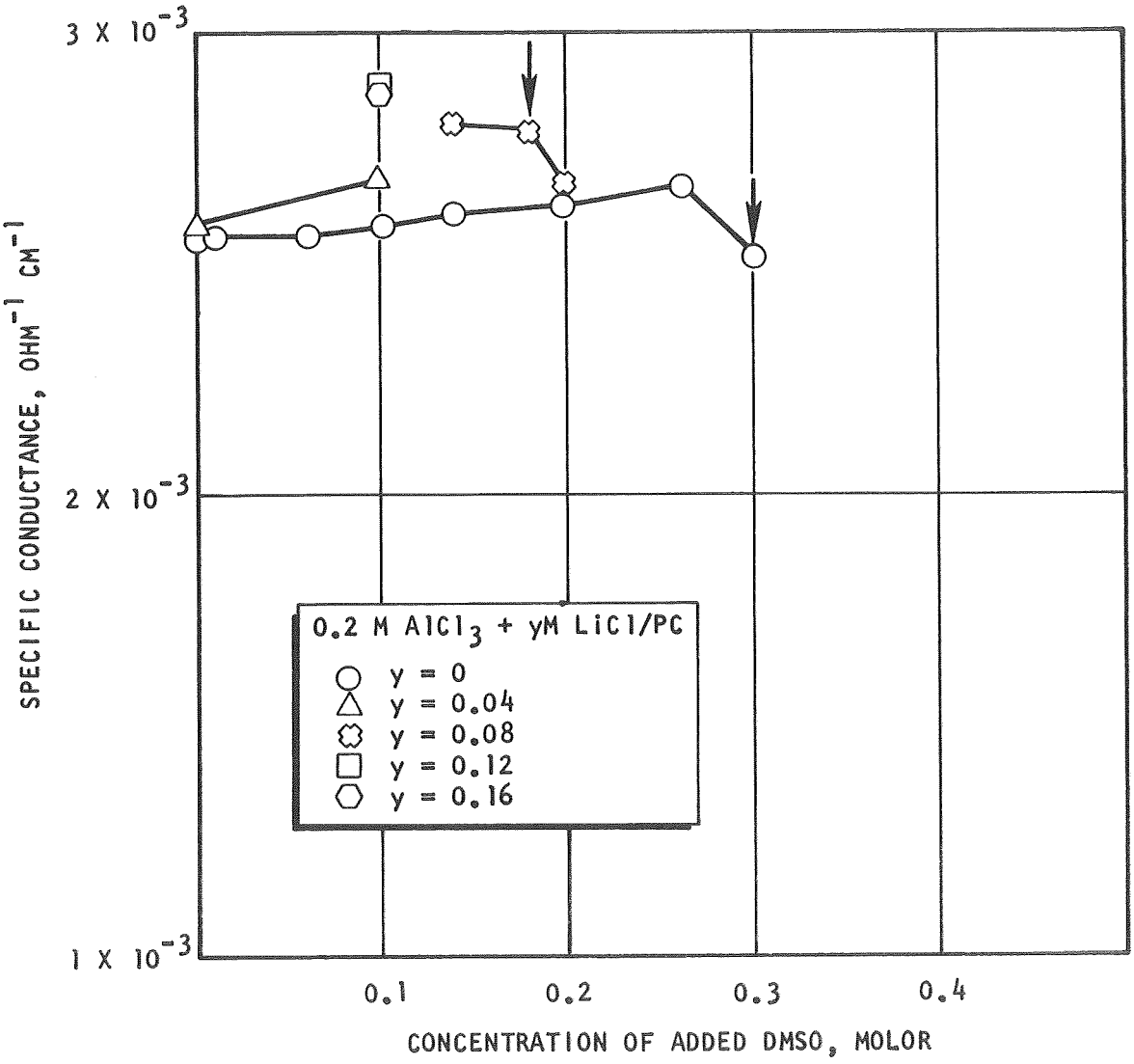

Fig.125. Specific Conductance of 0.2 M $AlCl_3$/PC Solutions Containing LiCl and/or DMSO, at 25 C

TABLE 36

SPECIFIC CONDUCTANCE, AT 25 C, OF PROPYLENE CARBONATE SOLUTIONS CONTAINING $AlCl_3$, LiCl, AND ACETONITRILE, TETRAHYDROFURAN, NITROMETHANE, METHYLFORMATE, OR WATER

Electrolyte	Additive	Specific Conductance, $ohm^{-1}\ cm^{-1}$
PC #6-7	20 v/o AN #6-1	3.63×10^{-6}
1 M $AlCl_3$ #4/PC #6-5		6.88×10^{-3}
1 M $AlCl_3$ #4/PC #6-7	0.5 M AN #6-1	7.50×10^{-3}
1 M $AlCl_3$ #4 + 0.4 M LiCl #3/PC #6-7	0.5 M AN #6-1	7.42×10^{-3}
1 M $AlCl_3$ #4/PC #6-7	1.5 M AN #6-1	8.68×10^{-3}
1 M $AlCl_3$ #4/PC #6-7	3 M AN #6-1	1.064×10^{-2}
1 M $AlCl_3$ #4/PC #6-6	1 M THF #1	6.73×10^{-3}
1 M $AlCl_3$ #4 + 0.2 M LiCl #3/PC #6-6	1 M THF #1	6.95×10^{-3}
1 M $AlCl_3$ #4 + 0.4 M LiCl #3/PC #6-6	1 M THF #1	7.16×10^{-3}
1 M $AlCl_3$ #4 + 0.6 M LiCl #3/PC #6-6	1 M THF #1	7.38×10^{-3}
1 M $AlCl_3$ #4 + 0.8 M LiCl #3/PC #6-6	1 M THF #1	7.57×10^{-3}
1 M $AlCl_3$ #4/PC #6-7	2 M THF #1	6.97×10^{-3}
0.2 M $AlCl_3$ #4/PC #6-5		2.55×10^{-3}
0.2 M $AlCl_3$ #4/PC #6-6 and 6-5	0.2 M THF #1	2.41×10^{-3}
0.2 M $AlCl_3$ #4 + 0.04 M LiCl #3/PC #6-6 and 6-5	0.2 M THF #1	2.55×10^{-3}
0.2 M $AlCl_3$ #4 + 0.08 M LiCl #3/PC #6-6 and 6-5	0.2 M THF #1	2.68×10^{-3}

TABLE 36 (CONT'D.)

Electrolyte	Additive	Specific Conductance, $ohm^{-1}\ cm^{-1}$
0.2 M $AlCl_3$ #4 + 0.12 M LiCl #3/PC #6-6 and 6-5	0.2 M THF #1	2.85×10^{-3}
0.2 M $AlCl_3$ #4 + 0.16 M LiCl #3/PC #6-6 and 6-5	0.2 M THF #1	3.01×10^{-3}
0.2 M $AlCl_3$ #4/PC #6-7	0.4 M THF #1	2.51×10^{-3}
1 M $AlCl_3$ #4/PC #7-1	0.5 M NM #1-2	7.50×10^{-3}
1 M $AlCl_3$ #4/PC #7-1	1.5 M NM #1-2	8.40×10^{-3}
1 M $AlCl_3$ #4/PC #7-1	3 M NM #1-2	9.96×10^{-3}
1 M $AlCl_3$ #4 + 0.4 M LiCl #3/PC #7-1	0.5 M NM #1-2	7.32×10^{-3}
1 M $AlCl_3$ #4/PC #3-1	0.1 M MF #2-11	7.05×10^{-3}
1 M $AlCl_3$ #4/PC #3-1	0.5 M MF #2-11	7.49×10^{-3}
1 M $AlCl_3$ #4/PC #3-1	1 M MF #2-11	8.01×10^{-3}
1 M $AlCl_3$ #4/PC #3-1	2 M MF #2-11	9.12×10^{-3}
1 M $AlCl_3$ #4 + 0.6 M LiCl #3/PC #3-1	1 M MF #2-11	8.09×10^{-3}
1 M $AlCl_3$ #5 + 0.5 M LiCl #3/PC #7-8		6.75×10^{-3}
1 M $AlCl_3$ #5 + 0.5 M LiCl #3/PC #7-8	100 ppm H_2O	6.76×10^{-3}
1 M $AlCl_3$ #5 + 0.5 M LiCl #3/PC #7-8	500 ppm H_2O	6.77×10^{-3}

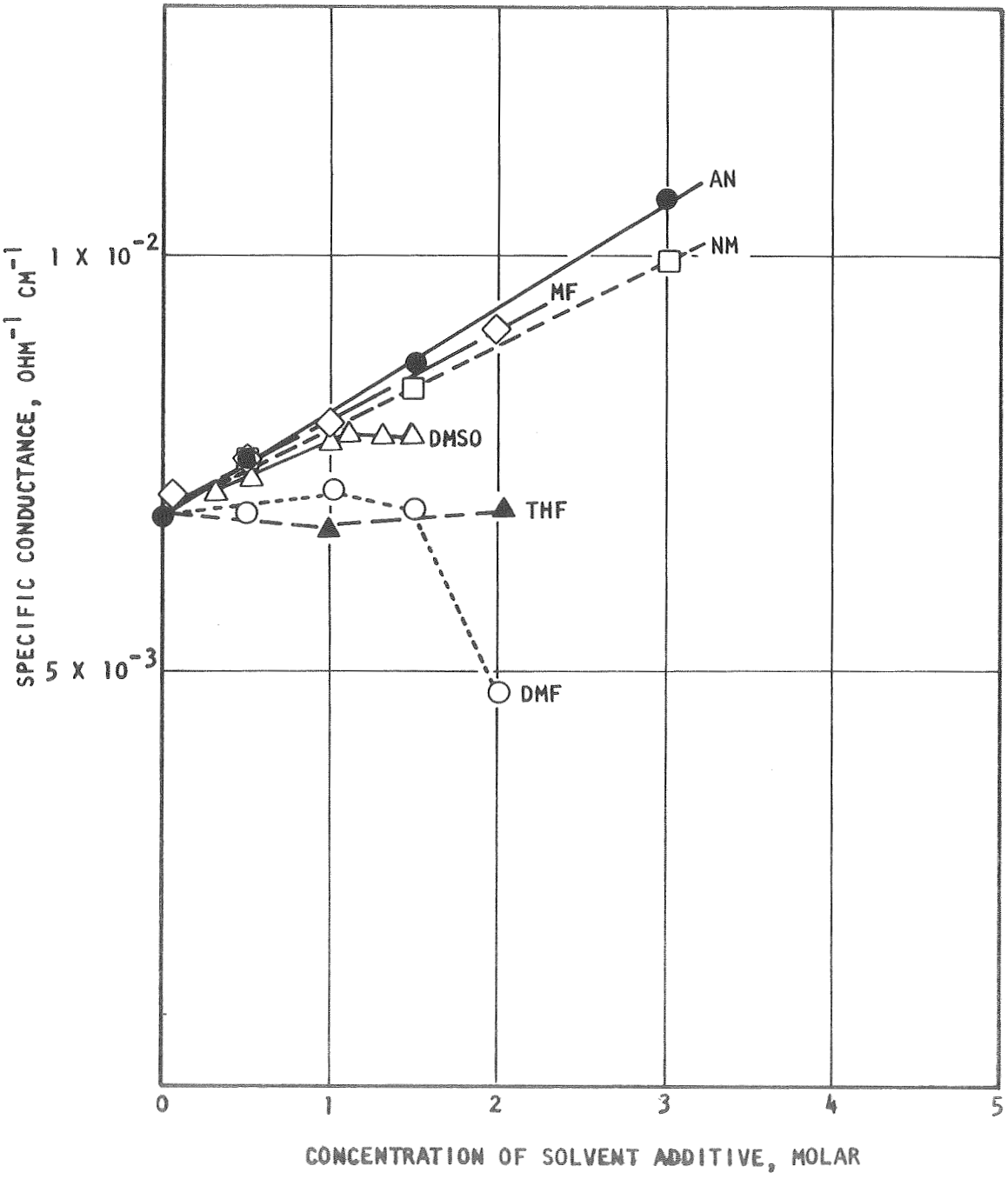

Fig.126. Specific Conductance of 1 M $AlCl_3$/PC Solutions Containing Various Additives, at 25 C

Nitromethane and Methyl Formate as Additives. Results similar to the data obtained with AN as an additive were gathered with NM or MF, indicating a viscosity effect rather than species interactions.

Water as Additive. The addition of small amounts of water did not have any significant effect on the conductance of a 0.5 M LiCl + 1 M $AlCl_3$/PC solution.

LiBr as Additive. Results obtained with LiBr are included in Table 37. The addition of LiBr caused some decrease of the conductance, as had been observed upon addition of LiCl to 1 M $AlCl_3$/PC; substantial precipitation was observed at high LiBr content which also may have contributed to the conductance decrease.

$LiClO_4$ as Additive. Conductance data on the LiCl+$AlCl_3$/PC & $LiClO_4$ system are given in Table 37 and are graphically presented in Figure 127. The conductance of 1 M $AlCl_3$/PC was found to decrease more or less linearly with increasing $LiClO_4$ content. The extent of the decrease indicates an activity effect; according to Ref. 16, the maximum for the specific conductance of $AlCl_3$/PC occurs at a concentration of about 1 molar.

When the same solutions were diluted by taking 4 parts of PC #6-5 and 1 part of $AlCl_3$+$LiClO_4$/PC, the situation was reversed, i.e., the solution conductance increased with greater amounts of $LiClO_4$ added. It may be noted, incidentally, that the conductance could be more than doubled in some cases by a five-fold dilution (compare 1 M $AlCl_3$/PC & 1.5 M $LiClO_4$ and 0.2 M $AlCl_3$/PC & 0.3 M $LiClO_4$). These results caution again--as did the results of the conductometric titration of Ref. 1--against premature conclusions in regard to the concentrations of conductive species based on conductance data. In relatively moderately concentrated nonaqueous solutions, the solution conductance may decrease upon increase of the electrolyte concentration, whereas the opposite may occur at lower concentrations.

Both the behavior of concentrated and of dilute solutions appears to be explainable by the simple effect of addition of $LiClO_4$ (i.e., Li^+ and ClO_4^- ions), without interaction between aluminum and perchlorate according to

$$Al[PC]_6^{+3} + 4\ ClO_4^- = Al(ClO_4)_4^- + 6\ PC \qquad (7)$$

If the nonparticipating species in the case of 1 M $AlCl_3$ are included, reaction (7) becomes:

$$1/4\ M\ Al[PC]_6^{+3} + 3/4\ M\ AlCl_4^- + (1+X)M\ LiClO_4 = 1/4\ M\ Al(ClO_4)_4^- + 1.5\ M\ PC + 3/4\ M\ AlCl_4^- + (1+X)M\ Li^+ + X\ M\ ClO_4^- \qquad (8)$$

TABLE 37

SPECIFIC CONDUCTANCE OF PROPYLENE CARBONATE SOLUTIONS CONTAINING $AlCl_3$, LiCl, AND LiBr OR $LiClO_4$, AT 25 C

Electrolyte	Additive	Specific Conductance $ohm^{-1}\ cm^{-1}$
1 M $AlCl_3$ #4/PC #7-1	0.5 M LiBr #2	5.39×10^{-3}
1 M $AlCl_3$ #4 + 0.5 M LiCl #3/PC #7-1	0.5 M LiBr #2	4.71×10^{-3}
1 M $AlCl_3$ #4/PC #7-1	1 M LiBr #2	2.11×10^{-3}
1 M $AlCl_3$ #4/PC #6-4		6.90×10^{-3}
1 M $AlCl_3$ #4/PC #6-4	0.25 M $LiClO_4$ #3	6.17×10^{-3}
1 M $AlCl_3$ #4/PC #6-4	0.5 M $LiClO_4$ #3	5.26×10^{-3}
1 M $AlCl_3$ #4/PC #6-4	0.75 M $LiClO_4$ #3	4.29×10^{-3}
1 M $AlCl_3$ #4/PC #6-4	1 M $LiClO_4$ #3	3.32×10^{-3}
1 M $AlCl_3$ #4/PC #6-4	1.25 M $LiClO_4$ #3	2.46×10^{-3}
1 M $AlCl_3$ #4/PC #6-4	1.5 M $LiClO_4$ #3	1.74×10^{-3}
1 M $AlCl_3$ #4 + 0.6 M LiCl #3/PC #6-4	1 M $LiClO_4$ #3	2.76×10^{-3}
0.2 M $AlCl_3$ #4/PC #6-4 and 6-5		2.57×10^{-3}
0.2 M $AlCl_3$ #4/PC #6-4 and 6-5	0.05 M $LiClO_4$ #3	3.01×10^{-3}
0.2 M $AlCl_3$ #4/PC #6-4 and 6-5	0.1 M $LiClO_4$ #3	3.52×10^{-3}
0.2 M $AlCl_3$ #4/PC #6-4 and 6-5	0.15 M $LiClO_4$ #3	3.87×10^{-3}
0.2 M $AlCl_3$ #4/PC #6-4 and 6-5	0.2 M $LiClO_4$ #3	4.20×10^{-3}
0.2 M $AlCl_3$ #4/PC #6-4 and 6-5	0.25 M $LiClO_4$ #3	4.43×10^{-3}
0.2 M $AlCl_3$ #4/PC #6-4 and 6-5	0.3 M $LiClO_4$ #3	4.78×10^{-3}
0.2 M $AlCl_3$ #4 + 0.12 M LiCl #3/PC #6-4 and 6-5	0.25 M $LiClO_4$ #3	4.45×10^{-3}

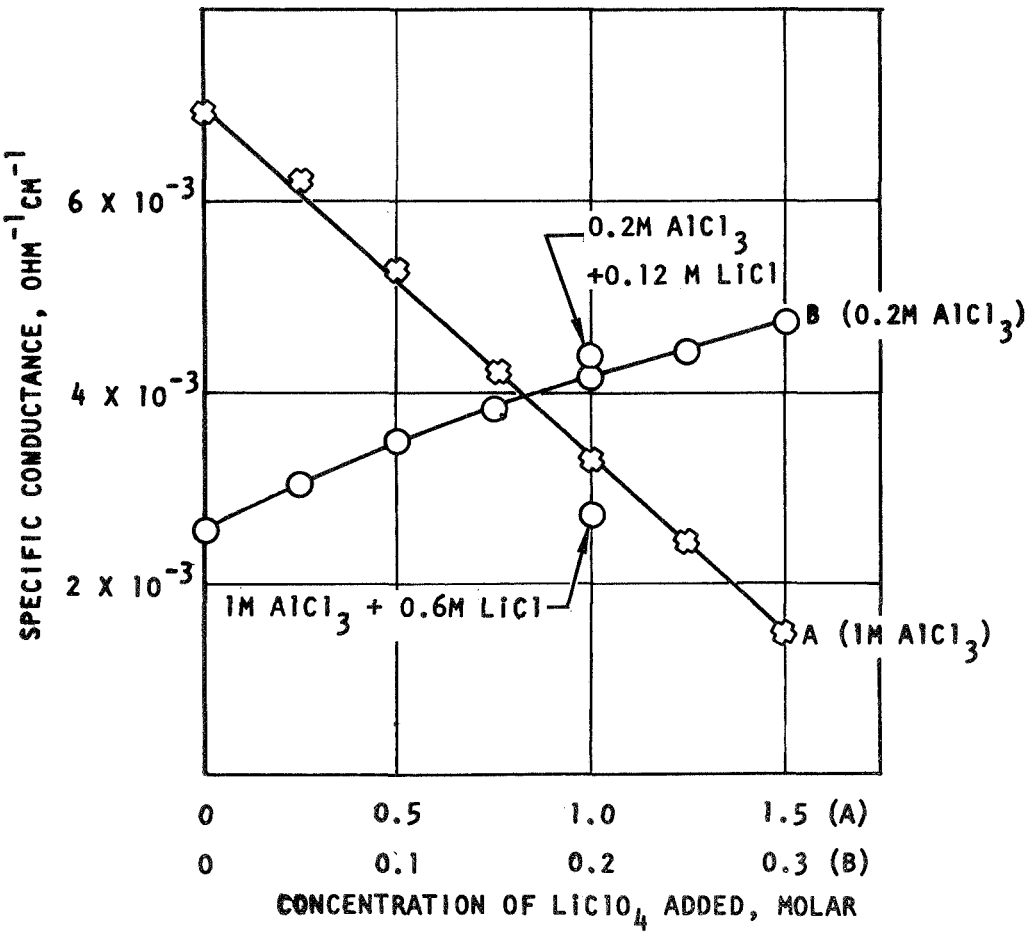

Fig.127. Specific Conductance of $AlCl_3$/PC Solutions Containing LiCl and/or $LiClO_4$, at 25 C

If such a reaction would occur quantitatively, a break point of the conductance curve at 1 M $LiClO_4$ or 0.2 M $LiClO_4$, respectively, would be expected; but such a discontinuity was in actuality not observed, neither in the concentrated nor in the dilute case. Furthermore, a conductance decrease would be expected for reaction (8), at least in dilute solutions (where an increase in conductive species still causes an increase in specific solution conductance), because it can be assumed that $AlCl_4^-$ and $Al(ClO_4)_4^-$ have approximately one-third of the molar conductance of Al^{+3} and four times the one of Li^+.

According to this cursory analysis, it can be concluded that the conductance data provide no evidence for a significant reaction consisting of ClO_4^- ions replacing PC in the $Al[PC]_6^{\ 3}$ complex. It cannot be ruled out, however, that such a reaction could occur to some extent with complexing perchlorate ions being in equilibrium with free perchlorate ions in solutions, as indicated by NMR data.

Conductance of $LiClO_4$/PC and $LiAsF_6$/PC Solutions With Various Solvent Additives

The specific conductance values determined for 1 M $LiClO_4$/PC and 1 M $LiAsF_6$/PC solutions containing various solvent additives are given in Table 38 and are graphically represented in Figure 128. All solvents used as additives have a lower viscosity than propylene carbonate. Conductance increases resulted from their addition, and viscosity effects appear predominant. The addition of a low viscosity solvent to propylene carbonate solutions to increase solution conductance and mass transport appears to be a feasible approach, provided the additive used is sufficiently stable.

Conductance of DMF Solutions With Various Additives

The results obtained upon addition of MF to $LiClO_4$/DMF and $LiAsF_6$/DMF solutions are qualitatively the same as obtained upon addition of the same solvent to propylene carbonate solutions. This can be seen comparing the numbers given in Table 39 with the results of Table 38 and Figure 128.

The conductance of 0.05 M $AlCl_3$ #4 + 0.5 M LiCl #3/DMF #7-3 & 0.5 M $LiClO_4$ #3, i.e., of a solution containing both LiCl and $LiClO_4$, was relatively low and close to the average value of a 1 M LiCl/DMF and a 1 M $LiClO_4$/DMF solution.

TABLE 38

SPECIFIC CONDUCTANCE OF $LiClO_4$ AND $LiAsF_6$ SOLUTIONS IN PROPYLENE CARBONATE, WITH VARIOUS ADDITIVES, AT 25 C

Electrolyte	Additive	Specific Conductance, $ohm^{-1}\ cm^{-1}$
1 M $LiClO_4$ #3/PC #3-1		5.14×10^{-3}
1 M $LiClO_4$ #3/PC #3-1	0.25 M DMF #7-3	5.41×10^{-3}
1 M $LiClO_4$ #3/PC #3-1	1 M DMF #7-3	6.25×10^{-3}
1 M $LiClO_4$ #3/PC #3-1	2 M DMF #7-3	7.57×10^{-3}
1 M $LiClO_4$ #3/PC #3-1	4 M DMF #7-3	1.02×10^{-2}
1 M $LiClO_4$ #3/PC #6-7	0.25 M MF #2-11	5.45×10^{-3}
1 M $LiClO_4$ #3/PC #6-7	1 M MF #2-11	6.28×10^{-3}
1 M $LiClO_4$ #3/PC #6-7	2 M MF #2-11	7.53×10^{-3}
1 M $LiClO_4$ #3/PC #6-7	4 M MF #2-11	1.00×10^{-2}
1 M $LiClO_4$ #3/PC #7-1	2 M NM #1-2	6.38×10^{-3}
1 M $LiClO_4$ #3/PC #7-1	4 M NM #1-2	7.63×10^{-3}
1 M $LiAsF_6$ #2/PC #7-5		6.02×10^{-3}
1 M $LiAsF_6$ #4/PC #7-8		6.04×10^{-3}
1 M $LiAsF_6$ #7/PC #7-8	2 M DMF #7-3	8.22×10^{-3}
1 M $LiAsF_6$ #4/PC #7-8	4 M DMF #7-3	1.050×10^{-2}
1 M $LiAsF_6$ #7/PC #7-8	2 M DMSO #1-1	7.86×10^{-3}
1 M $LiAsF_6$ #4/PC #7-8	4 M DMSO #1-1	8.89×10^{-3}

TABLE 38 (CONT'D.)

Electrolyte	Additive	Specific Conductance, $ohm^{-1}\ cm^{-1}$
1 M $LiAsF_6$ #7/PC #7-8	2 M THF #1	8.71×10^{-3}
1 M $LiAsF_6$ #4/PC #7-8	4 M THF #1	1.13×10^{-3}
1 M $LiAsF_6$ #7/PC #7-8	2 M NM #1-1	8.07×10^{-3}
1 M $LiAsF_6$ #4/PC #7-8	4 M NM #1-2	1.030×10^{-2}
1 M $LiAsF_6$ #2/PC #7-5	2 M MF #2-14	9.15×10^{-3}

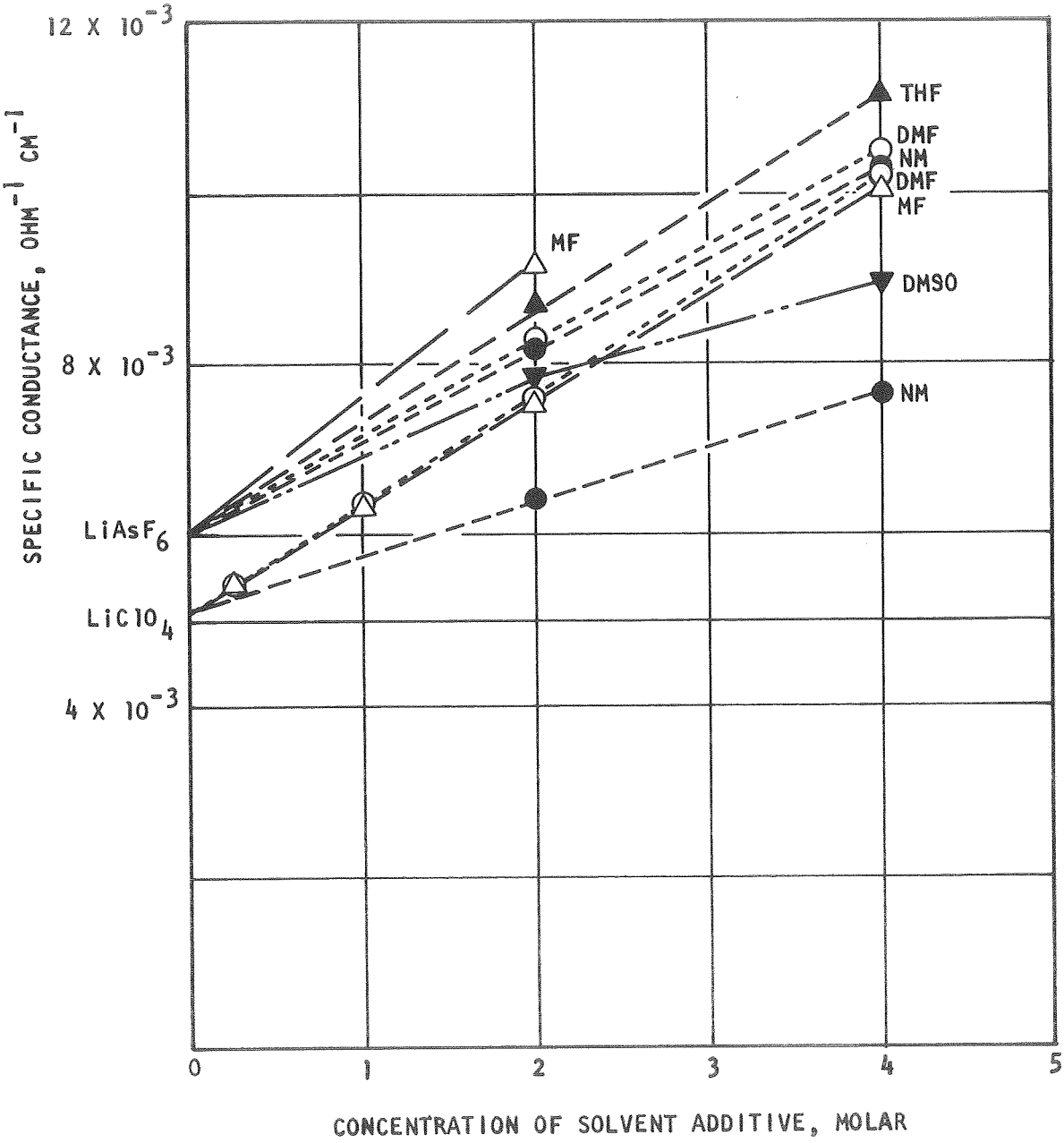

Fig.128. Specific Conductance of 1 M $LiClO_4$/PC and 1 M $LiAsF_6$/PC Solutions Containing Various Additives, at 25 C

Conductance of Methyl Formate Solutions
Without and With Various Additives

Results obtained with $LiAsF_6$/MF, $LiClO_4$/MF and $LiCl+AlCl_3$/MF solution without or with various additives are presented in Table 40, and are discussed below for the various electrolytes.

Values obtained with MF solutions are not always as well reproducible as desired. Deviations may be caused by the low vapor pressure of methyl formate which facilitates concentration changes by solvent evaporation.

TABLE 39

SPECIFIC CONDUCTANCE OF SEVERAL

DIMETHYLFORMAMIDE SOLUTIONS AT 25 C

Electrolyte	Additive	Specific Conductance, ohm^{-1} cm^{-1}
1 M $LiClO_4$ #3/DMF #7-3		2.11×10^{-2}
1 M $LiClO_4$ #3/DMF #7-3	0.25 M MF #2-11	2.10×10^{-2}
1 M $LiClO_4$ #3/DMF #7-3	1 M MF #2-11	2.18×10^{-2}
1 M $LiClO_4$ #3/DMF #7-3	2 M MF #2-11	2.26×10^{-2}
1 M $LiClO_4$ #3/DMF #7-3	4 M MF #2-11	2.41×10^{-2}
1 M $LiAsF_6$ #4/DMF #7-3	6 M MF #3-3	2.60×10^{-2}
0.05 M $AlCl_3$ #4 + 0.5 M LiCl #3/DMF #7-3	0.5 M $LiClO_4$ #3	1.32×10^{-2}

$LiAsF_6$/MF. The conductances of $LiAsF_6$/MF solutions is relatively high, as demonstrated by the values given in Table 40 and by literature data (Ref. 15). The conductance of such solutions was decreased by solvent additives such as DMF, DMSO, and THF. This would be consistent with a simple viscosity effect.

The addition of small amounts of water had no effect on the conductance of a 1 M $LiAsF_6$/MF solution.

TABLE 40

SPECIFIC CONDUCTANCE OF METHYL FORMATE ELECTROLYTES WITH VARIOUS ADDITIVES, AT 25 C

Electrolyte	Additive	Specific Conductance, $ohm^{-1}\ cm^{-1}$
MF #2-11		6.6×10^{-7}
0.5 M $LiAsF_6$ #1/MF #2-11		1.60×10^{-2}
1 M $LiAsF_6$ #1/MF #2-11		3.18×10^{-2}
1 M $LiAsF_6$ #5/MF #3-4		3.38×10^{-2}
2 M $LiAsF_6$ #5/MF #3-4		4.63×10^{-2}
1 M $LiAsF_6$ #5/MF #3-7		3.28×10^{-2}
1 M $LiAsF_6$ #6/MF #3-7		3.21×10^{-2}
1 M $LiAsF_6$ #6/MF #4		3.20×10^{-2}
1 M $LiAsF_6$ #7/MF #4		3.28×10^{-2}
1 M $LiAsF_6$/MF		2.97×10^{-2} *
2 M $LiAsF_6$/MF		4.02×10^{-2} *
3 M $LiAsF_6$/MF		3.35×10^{-2} *
Sat. $LiAsF_6$/MF		2.95×10^{-2} *
1 M $LiAsF_6$ #1/MF #2-11	2 M PC #7-1	3.10×10^{-2}
1 M $LiAsF_6$ #1/MF #2-11	1 M DMF #7-3	3.05×10^{-2}
1 M $LiAsF_6$ #1/MF #2-11	2 M DMF #7-3	2.91×10^{-2}
1 M $LiAsF_6$ #1/MF #2-11	4 M DMF #7-3	2.79×10^{-2}
2 M $LiAsF_6$ #5/MF #3-4	6 M DMF #7-3	2.46×10^{-2}
1 M $LiAsF_6$ #1/MF #2-12	2 M DMSO #1-1	2.57×10^{-2}

*According to Ref. 15; at 26-28 C

TABLE 40 (CONT'D.)

Electrolyte	Additive	Specific Conductance, $ohm^{-1}\ cm^{-1}$
1 M $LiAsF_6$ #1/MF #2-12	2 M THF #1	2.88×10^{-2}
1 M $LiAsF_6$ #5/MF #3-4		3.88×10^{-2}
1 M $LiAsF_6$ #5/MF #3-4	100 ppm H_2O	3.34×10^{-2}
1 M $LiAsF_6$ #5/MF #3-4	500 ppm H_2O	3.35×10^{-2}
1 M $LiClO_4$ #3/MF #2-11		1.33×10^{-2}
1 M $LiClO_4$ #3/MF #2-13		1.203×10^{-2}
2 M $LiClO_4$ #3/MF #2-14		2.43×10^{-2}
2 M $LiClO_4$ #3/MF #3-1		2.50×10^{-2}
3 M $LiClO_4$ #3/MF #3-1		2.75×10^{-2}
1 M $LiClO_4$/MF		1.57×10^{-2} *
2 M $LiClO_4$/MF		2.85×10^{-2} *
3 M $LiClO_4$/MF		2.97×10^{-2} *
4 M $LiClO_4$/MF		2.36×10^{-2} *
1 M $LiClO_4$ #3/MF #2-11	0.25 M DMF #7-3	1.26×10^{-2}
1 M $LiClO_4$ #3/MF #2-11	1 M DMF #7-3	1.42×10^{-2}
1 M $LiClO_4$ #3/MF #2-11	4 M DMF #7-3	2.34×10^{-2}
1 M $LiClO_4$ #3/MF #3-2	4 M DMF #7-3	2.30×10^{-2}
1 M $LiClO_4$ #3/MF #3-2	6 M DMF #7-3	2.55×10^{-2}
1 M $LiClO_4$ #3/MF #3-2	6 M DMF #7-3	2.53×10^{-2}
2 M $LiClO_4$ #3/MF #3-1	2 M DMF #7-3	2.20×10^{-2}
2 M $LiClO_4$ #3/MF #3-1	4 M DMF #7-3	2.14×10^{-2}

*According to Ref. 15; at 26-28 C

TABLE 40 (CONT'D.)

Electrolyte	Additive	Specific Conductance, $ohm^{-1}\ cm^{-1}$
1 M $LiClO_4$ #3/MF #2-12	2 M PC #7-1	1.72×10^{-2}
1 M $LiClO_4$ #3/MF #2-12	2 M THF #1	1.01×10^{-2}
1 M $LiClO_4$ #3/MF #2-14	0.1 M $LiAsF_6$ #2	1.60×10^{-2}
1 M $LiClO_4$ #3/MF #3-2	0.1 M $LiAsF_6$ #2 + 4 DMF #7-3	2.36×10^{-2}
1 M $LiClO_4$ #3/MF #3-4	1 M $LiAsF_6$ #5	3.68×10^{-2}
1 M $LiClO_4$ #3/MF #3-4	1 M $LiAsF_6$ #5 + 6 M DMF #7-3	2.24×10^{-2}
1 M $LiClO_4$ #3/MF #3-4	2 M $LiAsF_6$ #5	3.46×10^{-2}
1 M $LiClO_4$ #3/MF #3-4	2 M $LiAsF_6$ #5 + 6 M DMF #7-3	1.41×10^{-2}
2 M $LiClO_4$ #3/MF #3-4	1 M $LiAsF_6$ #5	3.10×10^{-2}
2 M $LiClO_4$ #3/MF #3-4	1 M $LiAsF_6$ #5 + 6 M DMF #7-3	1.40×10^{-2}
1 M $AlCl_3$ #4/MF #2-13		1.15×10^{-2}
1 M $AlCl_3$ #4 + 1 M LiCl #3/MF #2-12		3.86×10^{-2}
2 M $AlCl_3$ #4 + 2 M LiCl #3/MF #3-3		4.25×10^{-2}
1 M $AlCl_3$ #4 + 1 M LiCl #3/MF #3-3	1 M $LiAsF_6$ #3	4.04×10^{-2}
1 M $AlCl_3$ #4/MF #2-13	2 M PC #7-1	1.59×10^{-2}
1 M $AlCl_3$ #4 + 1 M LiCl #3/MF #2-12	2 M PC #7-1	3.37×10^{-2}
1 M $AlCl_3$ #4/MF #2-13	2 M THF #1	8.05×10^{-3}
1 M $AlCl_3$ #4 + 1 M LiCl #3/MF #2-12	2 M THF #1	3.34×10^{-2}
1 M $AlCl_3$ #4/MF #2-13	1 M DMSO #1-1	1.16×10^{-2}
1 M $AlCl_3$ #4 + 1 M LiCl #3/MF #2-12	1 M DMSO #1-1	2.30×10^{-2}

$LiClO_4$/MF. These solutions, compared to $LiAsF_6$/MF solutions of the same concentrations, display lower specific conductances. This can be explained by a stronger ion-pair formation by $LiClO_4$. In increasing the $LiClO_4$ concentration from 1 to 2 molar, the equivalent conductance was found to increase slightly; this unexpected result could be explained by the formation of triple ions.

Higher solution conductances were found in 1 M $LiClO_4$/MF solution with a DMF content. In Figure 129, these results are contrasted with the respective results obtained with 1 M $LiAsF_6$/MF. Since DMF has a higher viscosity than MF, a viscosity effect would have caused a conductance decrease as in the case of $LiAsF_6$/MF & DMF. It is assumed that the break-up of ion pairs by the introduction of DMF is the overriding effect. This was not the case for 2 M $LiClO_4$/MF and 3 M $LiClO_4$/MF solutions, where conductance decreases were observed when DMF was added. In these cases, the action of DMF could be basically the same, but instead of break-up of ion pairs, a transformation of triple ions to ion pairs could be prominent, thus causing a conductance decrease.

Since the specific conductance of a 1 M $LiClO_4$/DMF solution is 2.03 x 10^{-2} ohm^{-1} cm^{-1} at 25 C, the results shown in Table 40 indicate that a ratio of MF:DMF exists where the conductance of a 1 M $LiClO_4$ solution reaches a maximum. From a conductometric titration not reported here in detail, it appears that such a composition is close to the investigated 1 M $LiClO_4$/MF & 6 M DMF.

Although the conductance of 1 M $LiClO_4$/MF solutions can be significantly improved by solvent additives, this cannot readily be achieved at higher concentrations. The maximum conductance for $LiClO_4$/MF with or without additives, was observed for an approximately 3 M $LiClO_4$/MF solution. These results are similar to the results obtained at the Livingston Electronic Laboratory for methyl formate-butyrolactone mixtures containing $LiClO_4$ (Ref. 17); these results are reproduced in Figure 130. The highest conductance was observed for an approximately 3 molar solution containing no butyrolactone; but at lower solute concentrations, addition of some butyrolactone generally improved the solution conductance.

$LiClO_4$+$LiAsF_6$/MF. $LiAsF_6$ as the solute is advantageous because of its stabilizing properties and because of the resulting high conductance. This solute has a relatively high formula weight, however, and a partial substitution by a lighter solute would be beneficial. Solutions containing $LiClO_4$ and $LiAsF_6$ in methyl formate were therefore studied. A 1 M $LiClO_4$/MF & 1 M $LiAsF_6$ electrolyte was found to have some promise, but the other combinations all showed lower specific conductances. An effort to improve conductances of mixed electrolytes through DMF addition was not successful. Decreases of conductances were observed, but more than viscosity effects seemed to be involved.

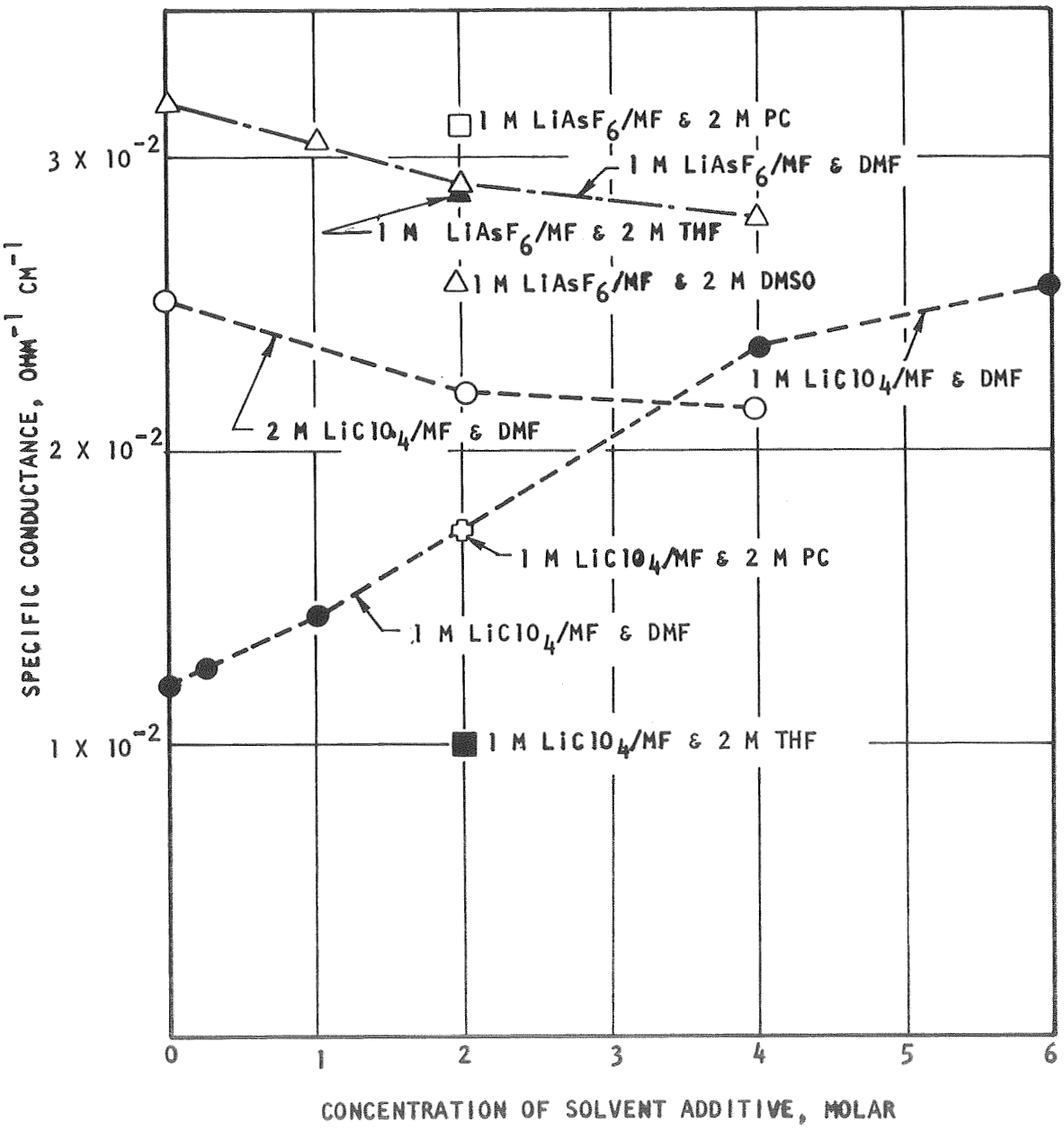

Fig.129. Specific Conductance of $LiClO_4$/MF and $LiAsF_6$/MF Solutions Containing Various Additives, at 25 C

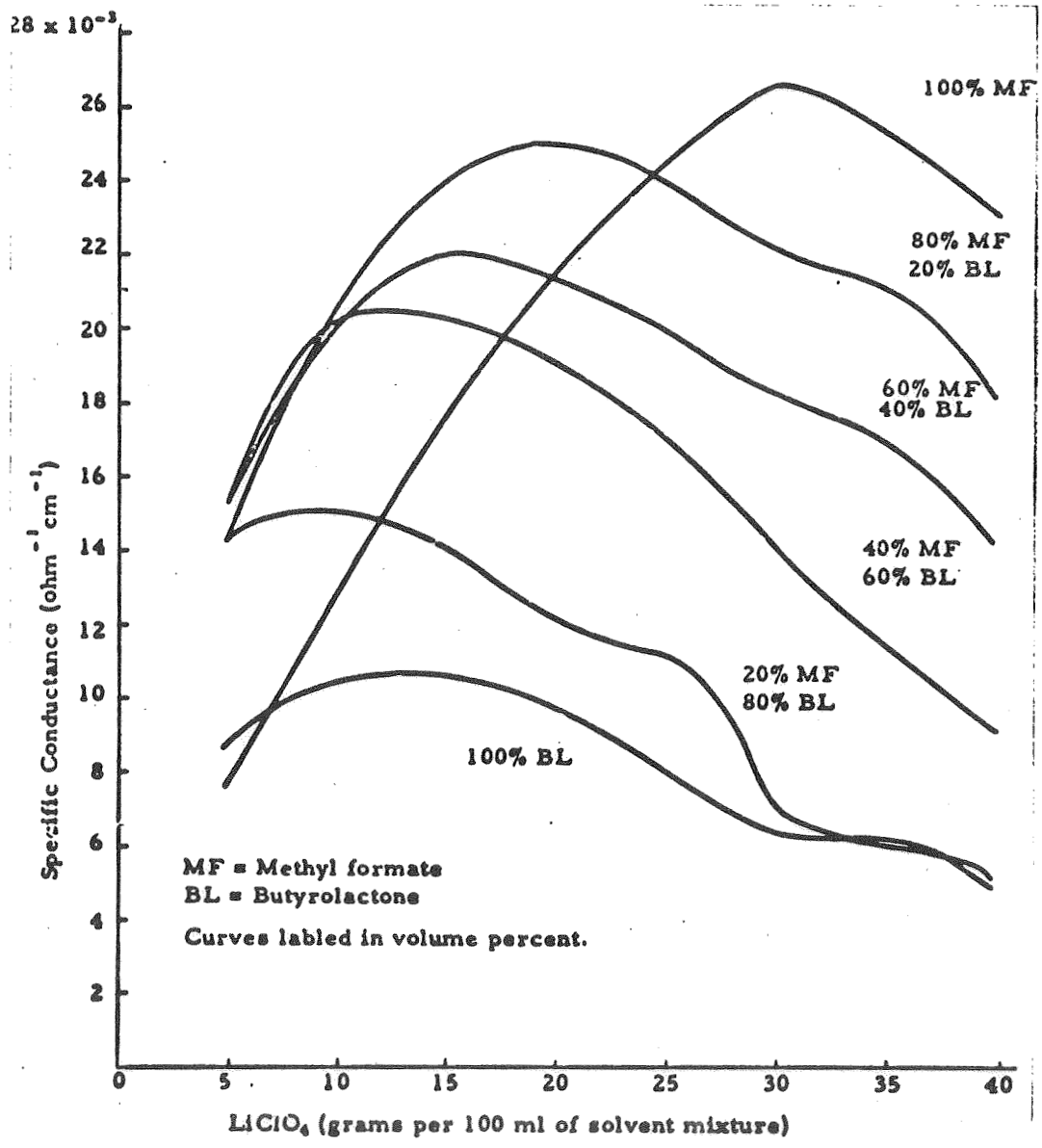

Fig. 130. Specific Conductance of $LiClO_4$ Solutions in Methyl Formate - Butyrolactone Mixtures, From Ref. 17

$LiCl+AlCl_3/MF$. The comparatively low conductance of 1 M $AlCl_3/MF$ (1.15×10^{-2} ohm^{-1} cm^{-1} at 25 C) is enhanced by the addition of lithium chloride (3.86×10^{-2} ohm^{-1} cm^{-1} at 25 C for 1 M $AlCl_3$ + 1 M LiCl/MF). It appears that, if there is no excess of chloride ions, a significant amount of the aluminum is present in such a form that it does not contribute to the solution conductance. Upon addition of LiCl, it appears that Li^+ and $AlCl_4^-$ form and that these ions have no great tendency to form ion pairs. A 2 M LiCl + 2 M $AlCl_3/MF$ solution displayed one of the highest conductances observed with organic electrolytes.

The presence of PC improved the conductance of 1 M $AlCl_3/MF$, whereas it was not significantly affected by DMSO addition; THF addition resulted in a lower conductance. These solvent additives decreased the conductances in the $LiCl+AlCl_3/MF$ electrolyte in all cases. A great deal of further data would be necessary to arrive at suggestions as to what species equilibria exist in these electrolytes and how they are affected by the various additives.

TRANSFERENCE EXPERIMENTS

A Hittorf cell was used, as described in Ref. 1. Silver electrodes were employed, and a current of 16 ma or 12 ma was applied for 500 minutes. Changes of lithium and aluminum concentrations in the cell were determined by atomic absorption analysis.

Data on the experiment performed with a 1 M $AlCl_3$ + 0.5 M LiCl/PC & 0.75 M DMF electrolyte are given in Table 41 , and data obtained with 1 M $AlCl_3$ + 0.5 M LiCl/PC & 0.75 M DMSO in Table 42 . Because of the complicated electrolyte compositions, a quantitative evaluation is not possible. The contribution of the aluminum ions to the conductance was predominantly anionic, in accordance with the presumed ionic compositions of the electrolyte included in Table 41 and 42 , respectively. The accumulation of aluminum in the anolyte appeared to be relatively low compared to the loss of aluminum observed for the catholyte. A possible source of error may be the trapping of some aluminum in the bulky anode deposit. The relatively small contribution to the conductance by the lithium ion reflects the low mobility of this ion due to solvation (Ref. 1).

A transference experiment was also performed with a 1 M $LiClO_4/MF$ & 6 M DMF electrolyte (Table 43). The results were inconclusive, apparently because of inaccuracies of the analyses. Due to the high vapor pressure of methyl formate, sampling of solutions by pipetting frequently leads to excessively high lithium contents. Another source of error may be the loss of some solvent during the course of the experiment, although care was taken to perform it in a relatively cool (22 C) room. Because high accuracy of the analysis results is imperative for a quantitative evaluation of the transference experiment, the procedure would have to be revised for accurate measurements with methyl formate.

TABLE 41

TRANSFERENCE EXPERIMENT WITH AN

$AlCl_3$+LiCl/PC & DMF ELECTROLYTE

Electrolyte:	1 M $AlCl_3$ #4 + 0.5 M LiCl #3/PC #3-1 & 0.75 M DMF #7-3
Presumed Composition:	0.125 M $Al(DMF)_6^{+3}$ + 0.5 M Li^+ + 0.875 M $AlCl_4^-$
Total Charge:	480 Coulombs (16 ma for 500 minutes)
Electrodes:	Silver
Change of Lithium Content in Anolyte:	$-\ 8.6 \times 10^{-4}$ mole (corresponds to 83 Coulombs)
Change of Aluminum Content in Anolyte:	$+\ 8.7 \times 10^{-4}$ mole (corresponds to n x 84 Coulombs)
Change of Lithium Content in Catholyte (Including Lithium Deposit)	$+\ 1.06 \times 10^{-3}$ mole (corresponds to 102 Coulombs)
Change of Aluminum Content in Catholyte:	$-\ 3.8 \times 10^{-3}$ mole (corresponds to n x 366 Coulombs)

TABLE 42

TRANSFERENCE EXPERIMENT WITH AN

$AlCl_3$+LiCl/PC & DMSO ELECTROLYTE

Electrolyte:	1 M $AlCl_3$ #4 + 0.5 M LiCl #3/PC #7-8 & 0.75 M DMSO #1-1
Presumed Composition:	0.125 M $Al(DMSO)_6^{+3}$ + 0.5 M Li^+ + 0.875 M $AlCl_4^-$
Total Charge:	480 Coulombs (16 ma for 500 minutes)
Electrodes:	Silver
Change of Lithium Content in Anolyte:	-9.4×10^{-4} mole (corresponds to 90 Coulombs)
Change of Aluminum Content in Anolyte:	$+1.37 \times 10^{-3}$ mole (corresponds to n x 132 Coulombs)
Change of Lithium Content in Catholyte (Including Lithium Deposit)	$+6.2 \times 10^{-4}$ mole (corresponds to 60 Coulombs)
Change of Aluminum in Catholyte:	-4.3×10^{-3} mole (corresponds to n x 460 Coulombs)

TABLE 43

TRANSFERENCE EXPERIMENT WITH A

$LiClO_4$/MF & DMF ELECTROLYTE

Electrolyte:	1 M $LiClO_4$ #3/MF #3-3 & 6 M DMF #7-3
Total Charge:	360 Coulombs (12 ma for 500 minutes)
Electrodes:	Silver
Change of Lithium Content in Anolyte:	-1.96×10^{-3} mole (corresponds to 190 Coulombs)
Change of Lithium Content in Catholyte (Including Lithium Deposit)	-2.7×10^{-4} mole (corresponds to 26 Coulombs)

MEASUREMENT OF DIFFUSION COEFFICIENTS

Diffusion rates given in Table 44 were determined by the porous disk method which had been used in previous measurements (Ref. 1 and 18). The method does not lead to unambiguous results for multi-component systems such as the ones studied. However, the relationship between the logarithm of the change of the apparent weight and the time was linear; therefore, a diffusion of different entities with different diffusion rates is not indicated.

For the electrolytes containing $LiCl+AlCl_3$, the values calculated for the diffusion coefficients were close to the value of 3.04×10^{-6} cm^2 sec^{-1} (3.04×10^{-10} m^2 sec^{-1}) found previously for a 0.7 M LiCl + 1 M $AlCl_3$/PC solution (Ref. 1). The insensitivity of the diffusion results to the addition of DMF or DMSO may be due to minimal changes in solution viscosity because the additives form strong complexes with aluminum and are in effect not a solvent component in the systems tested.

The diffusion coefficient of a 1 M $LiClO_4$/MF solution was decreased from 1.68×10^{-5} cm^2 sec^{-1} (1.68×10^{-9} m^2 sec^{-1}) at 25 C (Ref. 1) to 1.16×10^{-5} cm^2 sec^{-1} (1.16×10^{-9} m^2 sec^{-1}) at 25 C upon addition of 6 M DMF. This is consistent with a viscosity increase observed. The additives DMF and DMSO do not seem to solvate the solute preferentially, at least not very strongly; in this respect DMF and DMSO appear to be similar to water, which is not very strongly bound to Li^+ ions according to Ref. 19.

TABLE 44

DIFFUSION COEFFICIENTS AT 25 C, AS

DETERMINED BY THE POROUS DISK METHOD

Electrolyte-Additive Combination	Solvent	Diffusion Coefficient $cm^2\ sec^{-1}$	$m^2\ sec^{-1}$
0.5 M LiCl#3 + 1 M $AlCl_3$ #4/ PC #7-1 & 0.75 M DMF #7-3	PC #7-2, 7-3	2.94×10^{-6}	2.94×10^{-10}
0.5 M LiCl #3 + 1 M $AlCl_3$ #4/ PC #7-5 & 0.75 M DMSO #1-1	PC #7-6, 7-7	3.03×10^{-6}	3.03×10^{-10}
1 M $LiClO_4$ #3/MF #3-2 & 6 M DMF #7-3	MF #3-5	1.16×10^{-5}	1.16×10^{-9}

SUMMARY OF RESULTS

PREPARATION AND ANALYSIS OF SOLVENTS

Purification and/or analysis procedures were established for the solvents methyl formate, dimethyl sulfoxide, nitromethane, and tetrahydrofuran. Propylene carbonate, dimethylformamide and acetonitrile were purified and analyzed according to the methods developed on the previous contract (Ref. [1]).

In general, it appears that aprotic solvents can be purified without excessive efforts to achieve water contents of 10-50 ppm and similar organic impurities contents. In some cases, e.g., for propylene carbonate, impurity contents can be reduced by another order of magnitude with relatively modest efforts.

Vapor phase chromatography is the most convenient, sufficiently sensitive analysis method for aprotic solvents. It is well suited for routine analysis. One should bear in mind, however, that an analysis on one column material does not constitute a complete analysis.

ALUMINUM COMPLEXES FORMED WITH VARIOUS SOLVENTS AND IONS

The aluminum ion, Al^{+3}, is a strongly coordinating ion and the first coordination sphere is occupied by solvents and/or ions depending upon their relative solvating or complexing strengths. The present results established the following order of decreasing solvating or complexing strength as:

$$DMSO,\ H_2O,\ DMF,\ Cl^-,\ Br^-,\ PC,\ ClO_4^-,\ AN,\ MF,\ THF,\ NM$$

Positions in this sequence may not be exact. For example, H_2O and DMSO, Cl^- and Br^-, and PC and ClO_4^- may be reversed. This sequence is based mainly on NMR results and supported by evidence from conductance measurements. In the presence of dimethylformamide in a $AlCl_3$/PC solution, for instance, the $Al[DMF]_6^{+3}$ complex forms more easily than the $Al[PC]_6^{+3}$ complex, as indicated from the replacement of NMR peaks corresponding to the latter species by peaks attributed to the DMF complex upon addition of DMF to $AlCl_3$/PC. Not only solvents but also ions enter the competition as complexing agents, and it can be shown by NMR evidence that, for instance, Cl^- ions occupy an intermediate position in complexing ability between DMF and PC.

Interactions between additives and existing species in solutions can be indicated by conductance measurements also. An interaction is indicated, for instance, in cases where conductance changes are not occurring as expected based on consideration of solution viscosities.

Table 45 presents a summary of the species present in solutions containing $AlCl_3$ as a solute.

The solvents DMSO and DMF both displace PC in the $Al[PC]_6^{+3}$ complex and also are able to displace Cl^- ions from the $AlCl_4^-$ complex. Acetonitrile, methyl formate, and nitromethane, however, cannot displace PC from $Al[PC]_6^{+3}$ in appreciable amounts. When additives easily displace PC from the $Al[PC]_6^{+3}$ there is in general a distribution of mixed complexes $Al[(PC)_{6-x}(DMSO)_x]^{+3}$ for example, where x can take on several values. The relative population of these species varies with the concentration of additive. Small concentrations of mixed complexes also occur with additives such as AN which are lower than PC in the complexing sequence given above at higher additive concentrations.

In addition to the direct displacement of PC to form the $Al[DMF]_6^{+3}$ complex, DMF seems to have another effect. An equilibrium which is reached only after long periods of time seems to exist, similar to the one observed for the $CuCl_2$/DMF system (Ref. 1). It is suspected that, bridged complexes occur ultimately at the expense of both $AlCl_4^-$ and $Al[DMF]_6^{+3}$.

Tetrahydrofuran is a special case because it appears to form etherates with $AlCl_3$. Its position in the above sequence is therefore somewhat artificial.

The Br^- ions have similar properties to the Cl^- ions, whereas ClO_4^- complexes much more weakly, although it can compete with PC.

Water is an exceptional case among the additives because of its protic character. Hydrolysis of the aluminum ion was suspected to occur.

SPECIES FORMED IN $LiClO_4$ AND $LiAsF_6$ SOLUTIONS

A summary of the results on species studies in $LiClO_4$ and $LiAsF_6$ solutions is given in Table 46 .

The predominant species found in $LiClO_4$ and $LiAsF_6$ solutions were, as expected, Li^+-ions and ClO_4^--or AsF_6^--ions, respectively. In the case of $LiAsF_6$, the existence of an additional asymmetric species was indicated. Such a species could be AsF_5 resulting from the dissociation of the AsF_6^- ion, it could be an ion with hydroxyl or other groups substituted for a fluorine ion or it could be a charged particle multiplet with AsF_6^- as a participant. The concentration of asymmetric species appeared to be reduced in the presence of DMF or DMSO, whereas other solvents primarily acted as diluents.

TABLE 45

SUMMARY OF SPECIES IN VARIOUS ELECTROLYTES CONTAINING $AlCl_3$

Electrolyte	Additive	Species	Remarks
$LiCl+AlCl_3/PC$	--	Li^+, $AlCl_4^-$, $Al[PC]_6^{+3}$	Cl^- displaces PC from first coordination sphere of Al^{+3}
	DMSO	Li^+, $AlCl_4^-$, $Al[PC]_{6-x}[DMSO]_x^{+3}$, $Al[DMSO]_6^{+3}$	DMSO displaces PC then Cl^-; may be further changes with time.
	DMF	Li^+, $AlCl_4^-$, $Al[PC]_{6-x}[DMF]_x^{+3}$, $Al[DMF]_6^{+3}$, $Al_2Cl_xDMF_{6-x}^{+(6-x)}$	DMF displaces PC then Cl^-; stable bridged (?) complexes formed in time.
	AN	Li^+, $AlCl_4^-$, $Al[PC]_6^{+3}$	Small concentrations of complexes containing AN at high AN concentration
	MF	Li^+, $AlCl_4^-$, $Al[PC]_6^{+3}$	Small concentration of complexes containing MF at high MF concentrations
	THF	Li^+, $AlCl_4^-$, $Al[PC]_6^{+3}$, $AlCl_3 \cdot THF(?)$	Etherate almost surely present
	NM	Li^+, $AlCl_4^-$, $Al[PC]_6^{+3}$	NM acts as diluent only

TABLE 45
(Continued)

Electrolyte	Additive	Species	Remarks
	$LiClO_4$	Li^+, $AlCl_4^-$, $Al[PC]_6^{+3}$ $Al[PC]_x[ClO_4]_y^{+3-y}$(?)	ClO_4^- competes with PC in first coordination sphere of Al^{+3}
	LiBr	Li^+, $AlCl_xBr_{4-x}^-$(?) $Al[PC]_6^{+3}$	Data quite skimpy on this system
	H_2O	Li^+, $AlCl_4^-$, $Al[PC]_6^{+3}$ $Al[OH]_4^-$(?)	Addition of H_2O produces a gel which precipitates; may redissolve in time at low water concentration
$LiCl+AlCl_3$/DMF	--	Li^+, Cl^-, $Al[DMF]_6^{+3}$	No $AlCl_4^-$
	$LiClO_4$	Li^+, Cl^-, $Al[DMF]_6^{+3}$ ClO_4^-	No mixed complexes
$LiCl+AlCl_3$/MF	--	Li^+, $AlCl_4^-$, $Al[MF]_6^{+3}$	Cl^- displaces MF
	DMSO	Li^+, $AlCl_4^-$, $Al[MF]_6^{+3}$ $Al[DMSO]_6^{+3}$	DMSO displaces MF then Cl^-

TABLE 45

(Continued)

Electrolyte	Additive	Species	Remarks
	PC	Li^+, $AlCl_4^-$, $Al[MF]_6^{+3}$ $Al[MF]_{6-x}[PC]_x$, $Al[PC]_6^{+3}$	PC competes with and tends to displace MF
	THF	Li^+, $AlCl_4^-$, $Al[MF_6]^{+3}$ $AlCl_3 \cdot THF$ (?)	Etherate almost surely present

TABLE 46

SUMMARY OF SPECIES IN $LiClO_4$ AND $LiAsF_6$ ELECTROLYTES

Electrolyte	Additive	Species	Remarks
$LiClO_4$/PC	--	Li^+, ClO_4^-	--
	DMF	Li^+, ClO_4^-	May be some interaction of DMF with Li^+
	MF	Li^+, ClO_4^-	MF is diluent
	NM	Li^+, ClO_4^-	NM is diluent
$LiAsF_6$/PC	--	Li^+, AsF_6^-, AsF_5(?)	Some species such as AsF_5 which is asymmetric relative to the As is almost surely present
	DMSO, DMF	Li^+, AsF_6^-, AsF_5(?)	Concentration of asymmetric species reduced
	MF, THF, NM	Li^+, AsF_6, AsF_5 (?)	Apparently act as diluents only

TABLE 46

(Continued)

Electrolyte	Additive	Species	Remarks
$LiClO_4$/DMF	--	Li^+, ClO_4^-	
	MF	Li^+, ClO_4^-	MF is primarily a diluent
$LiAsF_6$/DMF	--	Li^+, AsF_6^-	Asymmetric species not present
	MF	Li^+, AsF_6^-	MF is primarily a diluent
$LiClO_4$/MF	--	Li^+, ClO_4^-	Strong ion pairing
	DMF	Li^+, ClO_4^-	May be some interaction of DMF with Li^+, ion pairing reduced
	PC, THF	Li^+, ClO_4^-	Apparently act as diluent only, ion pairing reduced with PC
$LiAsF_6$/MF	--	Li^+, AsF_6^-, AsF_5 (?)	Some species asymmetric relative to As is almost surely present

TABLE 46

(Continued)

Electrolyte	Additive	Species	Remarks
	DMSO, DMF	Li^+, AsF_6^-, AsF_5 (?)	Concentration of asymmetric species reduced
	PC, THF	Li^+, AsF_6^-, AsF_5 (?)	Primarily diluents
	$AlCl_3$		Gel formed on addition of $AlCl_3$
	H_2O (small amounts)	Li^+, AsF_6^-, AsF_5 (?) MeOH, HCOOH	De-esterification of MF to MeOH and HCOOH stoichiometrically

Strong ion association presumably due to the low dielectric constant of the solvent was indicated for $LiClO_4$/MF solutions by conductance measurements. An irregular behavior of the equivalent conductances as a function of electrolyte concentration had been found for both $LiClO_4$/MF and $LiAsF_6$/MF solutions (Ref. 1), and is indicative of ion association in these solutions. The effect is much weaker for $LiAsF_6$ than for $LiClO_4$, however, which is also confirmed by a comparison of the conductance of 1 M $LiClO_4$/MF (1.2×10^{-2} ohm^{-1} at 25 C) with the conductance of 1 M $LiAsF_6$/MF (3.2×10^{-2} ohm^{-1} cm^{-1} at 25 C).

Upon addition of DMF or PC to 1 M $LiClO_4$/MF, the solution conductance increased significantly, presumably because of a break-up of ion pairs.

As discussed later, water addition of MF solutions resulted in a hydrolysis of the methyl formate, i.e., in a chemical decomposition of the solvent.

STABILITY OF METHYL FORMATE SOLUTIONS

Methyl formate is inherently unstable in the presence of lithium metal. This applies also to $LiClO_4$ solutions in this solvent, but $LiAsF_6$ produces stable solutions.

Within the tests applied, methyl formate solutions with one molar or higher $LiAsF_6$ contents were found to be stable. The stabilizing effect of $LiAsF_6$ was such that no decomposition was observed even after addition of dimethylformamide.

It was found that the stabilization effect depended on the amount of $LiAsF_6$ present. Addition of 0.1 M $LiAsF_6$ to 1 M $LiClO_4$/MF produced a stabilizing effect, but not a 0.01 M $LiAsF_6$ addition. Inconsistent results were obtained with $LiAsF_6$ from different sources, purer materials generally having less stabilization effects.

The mechanism by which this stabilization is achieved is not known. It appears to be, at least to some extent, an impurity effect. Lithium metal may be made unreactive by a protective coating such as perhaps LiF or of lithium methylate.

WATER ADDITION TO $AlCl_3$/PC AND $LiAsF_6$/MF

Upon addition of up to 2000 ppm water to 1 M $AlCl_3$ + 0.5 M LiCl/PC, no water proton line was observed in NMR studies, although such a line was found upon addition of water to pure propylene carbonate. It is thought that precipitation of aluminum hydroxide occurred when the solutions were prepared, particularly since the formation of a precipitate was actually observed. The solution studied was decanted

and the precipitate discarded, although there were some indications that a redissolution might have occurred over long time periods. A decrease in the observed intensity of the NMR peak due to Al^{+3} coordinated PC is consistent with this assumption. Whereas no significant change in conductance was observed upon water addition, the solubility (or dissolution rate) of CuF_2 appeared to be slightly reduced.

In the case of $LiAsF_6$/MF solutions, added water had a significant effect on the measured values for the solubility of CuF_2. With water, higher copper contents were obtained, contrary to the results obtained in $LiCl+AlCl_3$/PC. The conductance was not affected.

Water added to $LiAsF_6$/MF hydrolyzes MF to methanol and formic acid. This reaction does not occur, or only at a much slower rate, in pure methyl formate or in $LiClO_4$/MF. $LiAsF_6$, therefore, catalyzes the hydrolysis but the mechanism is subject to conjecture at the present time. Since the hydrolysis appears to depend on the $LiAsF_6$ product and results were erratic, impurities, possibly of acidic or basic character, seem to be a determining factor. Such impurities could originate in the solute used, but also in the solvent. Slight impurities in the sample tubes could have affected the NMR results. This means for a practical case that "inert" battery compounds such as battery case, electrode grids or inert conductors might affect battery electrolyte characteristics in addition to impurities originally contained in the electrolyte.

THE SOLUBILITY OF COPPER HALIDES

The solubility of copper halides, the prospective electroactive cathode materials, is of particular significance. A high solubility leads to excessive self-discharge; on the other hand, a sufficiently high solubility may be necessary to maintain adequate battery discharge rates.

The precipitation of LiF should be a force for the dissolution of CuF_2; cupric fluoride dissolves and lithium fluoride precipitates leaving behind a "new" copper compound which may stay in solution or may also, at least partially, precipitate. Such a mechanism is actually expected to occur for $LiClO_4$ and $LiAsF_6$ solutions.

$$2\ LiClO_4 + CuF_2 = \underline{2\ LiF} + Cu(ClO_4)_2$$

$$2\ LiAsF_6 + CuF_2 = \underline{2\ LiF} + Cu(AsF_6)_2$$

This mechanism was indicated for many cases where a decrease of the lithium content was detected which was in direct stoichiometric relationship to the amount of CuF_2 available. It was not ascertained, however, if CuF_2 can dissolve to result in appreciable quantities of a precipitate of the new copper compound.

Often the above reactions were suspected to occur, but only at very slow rates so that solubility values determined would not reflect true equilibrium values. Addition of a proper additive can accelerate the reaction, however, as has been demonstrated for the addition of DMF to propylene carbonate solutions, or of H_2O to methyl formate solutions. In practice, it has to be expected that the self-discharge rates will depend on the impurity contents in the electrolyte.

In certain cases, e.g., in a 0.5 M LiCl + 1 M $AlCl_3$/PC and 0.75 M DMF electrolyte, CuF_2 was found to dissolve in large amounts without the precipitation of lithium fluoride. The presence of fluorine in solution was verified in such a case by NMR studies, and it appears that aluminum complexes containing fluoride form. It would be interesting to investigate the reversibility of the cupric fluoride cathode in such an electrolyte.

REFERENCES

1. Properties of Nonaqueous Electrolytes, Contract NAS3-8521, Report NASA CR-1425, by R. Keller, J. N. Foster, D. C. Hanson, J. F. Hon, and J. S. Muirhead, Rocketdyne, A Division of North American Rockwell Corporation, Canoga Park, California, August 1969.

2. Preparation of Pure Hexafluoroarsenate, Contract NAS3-12979, Report NASA CR-72640, by E. W. Lawless, Midwest Research Institute, Kansas City, Missouri, 1970.

3. Develop Methods for Preparation of Pure Copper (II) Fluoride and Develop Analytical Techniques for Determination of Impurities, Contract NAS3-10942, Report NASA CR-72571, by J. R. Lundquist, Pacific Northwest Laboratories, A Division of Battelle Memorial Institute, Richland, Washington, June 1969.

4. J. A. Pople, W. G. Schneider, and H. J. Bernstein, "High-Resolution Nuclear Magnetic Resonance," McGraw-Hill Book Co., Inc., New York, 1959.

5. J. W. Emsley, J. Feeney, and L. H. Sutcliffe, "High Resolution Nuclear Magnetic Resonance Spectroscopy," Vols. 1 and 2, Pergamon Press, Oxford, 1965.

6. A. Abragram, "The Principles of Nuclear Magnetism," Oxford University Press, London, 1961.

7. R. Pottel, "Chemical Physics of Ionic Solutions," edited by B. E. Conway and R. G. Barradas, Chapter 25, John Wiley and Sons, Inc., New York, 1966.

8. M. St. J. Arnold and K. J. Packer, Mol. Phys. 10, 141 (1966).

9. J. Bacon, R. J. Gillespie, and J. W. Quail, Canad. J. Chem. 41, 3063 (1963).

10. Masuo Suzuki and Ryogo Kubo, Mol. Phys. 7, 201 (1964).

11. M. St. J. Arnold and K. J. Packer, Mol. Phys. 14, 241 (1967).

12. M. St. J. Arnold and K. J. Packer, Mol. Phys. 14, 249 (1967).

13. W. G. Movius and N. A. Matwiyoff, J. Phys. Chem. 72, 3063 (1968).

14. Aprotic Organic Electrolytes, NASA Technology Handbook, Contract NAS8-5604, by R. Keller, Rocketdyne, A Division of North American Rockwell, Canoga Park, California, draft submitted August 1970.

15. Development of High Energy Density Primary Batteries, Contract NAS3-10613, Report NASA CR-72535, by S. G. Abens, W. C. Merz, and C. R. Walk, Livingston Electronic Laboratory, Honeywell, Inc., Montgomeryville, Pennsylvania, April 1968.

16. New Cathode-Anode Couples Using Nonaqueous Electrolytes, Contract AF33(616)-7957, Report No. ASD-TDR-62-837, by J. E. Chilton and G. M. Cook, Lockheed Missiles & Space Co., Sunnyvale, California, December 1962.

17. Development of High Energy Density Primary Batteries 200 Watthours Per Pound Total Battery Weight Minimum, Contract NAS3-6004, Report NASA CR-54803, by S. G. Abens, T. X. Mahy, W. Merz, and W. F. Meyers, Livingston Electronic Corporation, Montgomery, Pennsylvania, June 1965.

18. J. M. Sullivan, D. C. Hanson, and R. Keller, J. Electrochem. Soc. 117, 779 (1970).

19. Study of the Composition of Nonaqueous Solutions of Potential Use in High Energy Density Batteries, Contract AF19(628)6131, Report AFCRL-69-0470, by J. N. Butler, D. R. Cogley, J. C. Synnott, and G. Holleck, Tyco Laboratories, Inc., Watham, Massachusetts, September 1969.

DISTRIBUTION LIST

FOR CONTRACT NAS3-12969

National Aeronautics & Space Administration
Lewis Research Center
21000 Brookpark Road
Cleveland, Ohio 44135
Attn: Dr. L. Rosenblum (MS 302-1)
H. J. Schwartz (MS 309-1)
Dr. J. S. Fordyce (MS 309-1)
J. E. Dilley (MS 500-309)
Technology Utilization Office (MS 3-19)
R. B. King (MS 309-1)
D. G. Soltis (MS 309-1)
V. Hlavin (MS 3-14)
Library (MS 60-3)
Report Control (MS 5-5)
G. M. Ault (MS 3-13)
J. Toma (MS 302-1)

National Aeronautics & Space Administration

Washington, D. C. 20546
Attn: RNW/E. M. Cohn
U/Technology Utilization Office
SCC/A M. Greg Andrus
MTG/R. Livingston
UT/Dr. E. N. Case

National Aeronautics & Space Administration
Goddard Space Flight Center
Greenbelt, Maryland 20771
Attn: Thomas Hennigan, Code 716.2
Gerald Halpert, Code 735
Joseph Sherfey, Code 735
Louis Wilson, Code 450

National Aeronautics & Space Administration
Langley Research Center
Instrument Research Division
Hampton, Virginia 23365
Attn: J. E. Zanks (MS 488)

National Aeronautics & Space Admin.
Geo C. Marshall Space Flight Center
Huntsville, Alabama 35812
Attn: C. B. Graff (S&E-ASTR-EP)

National Aeronautics & Space Admin.
Manned Spacecraft Center
Houstin, Texas 77058
Attn: William R. Dusenbury (EP-5)

Attn: W. E. Rice (EP-5)
Attn: Forrest E. Eastman (EE-4)

National Aeronautics & Space Admin.
Langley Research Center
Langley Station
Hampton, Virginia 23365
Attn: Harry Ricker

National Aeronautics & Space Admin.
Scientific & Technical Information
Center: Input
P. O. Box 33
College Park, Maryland 20740
(2 copies plus 1 reproducible)

National Aeronautics & Space Admin.
Ames Research Center
Pioneer Project
Moffett Field, California 94035
Attn: Arthur Wilber/A. S. Hertzog

National Aeronautics & Space Admin.
Ames Research Center
Moffett Field, California 94035
Attn: Jon Rubenzer
Code PBS, MS 244-2

Jet Propulsion Laboratory
4800 Grove Drive
Pasadena, California 91103
Attn: A. A. Uchiyama (MS 198-220)
Dr. R. Lutwack (MS 190-220)
D. Runkle (MS 198-220)

Department of the Army

U. S. Army Mobility Equipment R&D Center
MERDC
Fort Belvoir, Virginia 22060
Electro Technology Lab
Energy Conversion Research Division

Commanding General
U. S. Army Weapons Command
Attn: AMSWE-RDR, Mr. G. Reinsmith
Rock Island Arsenal
Rock Island, Illinois 61201

U. S. Army Research Office
Box CM, Duke Station
Durham, North Carolina 27706
Attn: Dr. Wilhelm Jorgensen

U. S. Army Research Office
Chief, R&D
Department of the Army
3D442, The Pentagon
Washington, D. C. 20546

U. S. Army Natick Laboratories
Clothing and Organic Materials Div.
Natick, Massachusetts 01762
Attn: L. A. Spano

Commanding Officer
U. S. Army Electronics R&D Labs
Fort Monmouth, New Jersey 07703
Attn: Power Sources Division (AMSEL-KL-P)

Army Materiel Command
Research Division
AMCRD-RSCM-T-7
Washington, D. C. 20315
Attn: John W. Crellin

Army Materiel Command
Development Division
AMCRD-DE-MO-P
Washington, D. C. 20315
Attn: Marshall D. Aiken

U. S. Army TRECOM
Fort Eustis, Virginia 23604
Attn: Leonard M. Bartone (SMOFE-ASE)
Dr. R. L. Eshols (SMOFE-PSG)

U. S. Army Mobility Command
Research Division
Warren, Michigan 48090
Attn: O. Renius (AMSMO-RR)

Harry Diamond Laboratories
Room 300, Building 92
Conn. Ave & Van Ness St., N. W.
Washington, D. C. 20438
Attn: Nathan Kaplan

Department of the Navy

Office of Naval Research
Arlington, Virginia 22217
Attn: Director, Power Program
Code 473

Office of Naval Research
Department of the Navy
Arlington, Virginia 22217
Attn: H. W. Fox (Code 472)

Naval Research Laboratory
Washington, D. C. 20360
Attn: Dr. J. C. White, Code 6160

Naval Ship R&D Center
Annapolis, Maryland 21402
Attn: J. H. Harrison, Code A731

Naval Air Systems Command
Department of the Navy
Washington, D. C. 20360
Attn: (Code AIR-340C)

Commanding Officer

U. S. Naval Ammunition Depot
Crane, Indiana 47522
Attn: D. Miley, Code QEWE

U. S. Naval Observatory
4301 Suitland Road
Suitland, Maryland 20390
Attn: R. E. Trumbule (STIC)
Bldg. 52

Naval Ordnance Laboratory
Silver Spring, Maryland 20910
Attn: Philip D. Cole (Code 232)

Naval Ship Engineering Center
Center Bldg.
Prince George's Center
Hyattsville, Maryland 20782
Attn: C. F. Viglotti (Code 6157D)

Bureau of Naval Weapons
Department of the Navy
Washington, D. C. 20360
Attn: Whitewall T. Beatson
(Code RAAE-52)

Naval Ship Systems Command
Washington, D. C. 20360
Attn: Bernard B. Rosenbaum
Code 03422

Department of the Air Force

Aero Propulsion Laboratory
Wright-Patterson AFB, Ohio 45433
Attn: James E. Cooper, APIP-1

AF Cambridge Research Lab
Attn: CRFE
L. G. Hanscom Field
Bedford, Massachusetts 01731
Attn: Dr. R. Payne

AF Cambridge Research Lab
L. G. Hanscom Field
Bedford, Massachusetts 01731
Attn: Edward Raskind (Wing F) (CREC)

Headquarters, U. S. Air Force (AFRDR-AS)
Washington, D. C. 20325
Attn: Major G. Starkey

Headquarters, U. S. Air Force (AFRDR-AS)
Washington, D. C. 20325
Attn: Lt. Col. William G. Alexander

Rome Air Development Center, ESD
Attn: Frank J. Mollura (EMRED)
Griffis AFB, New York 13440

Space Systems Division
Los Angeles Air Force Station
Los Angeles, California 90045
Attn: HQSAMSO
(SMTAE/Lt R. Ballard)

Other Government Agencies

National Bureau of Standards
Washington, D. C. 20234
Attn: Dr. W. J. Hamer

National Bureau of Standards
Washington, D. C. 20234
Attn: Dr. A. Brenner

Office, Sea Warfare System
The Pentagon
Washington, D. C. 20310
Attn: G. B. Wareham

U. S. Atomic Energy Commission
Auxiliary Power Branch (SNAP)
Division of Reactor Development
Washington, D. C. 20325
Attn: Lt. Col. George H. Ogburn, Jr.

Lt. Col. John H. Anderson
Advanced Space Reactor Branch
Division of Reactor Development
U. S. Atomic Energy Commission
Washington, D. C. 20325

Mr. Donald A. Hoatson
Army Reactors, DRD
U. S. Atomic Energy Commission
Washington, D. C. 20545

Bureau of Mines
4800 Forbes Avenue
Pittsburgh, Pa. 15213
Attn: Dr. Irving Wender

Clearing House for Scientific &
Technical Information
5285 Port Royal Road
Springfield, Virginia 22151

Private Organizations

Aerojet-General Corporation
Chemical Products Division
Azusa, California 91702
Attn: William H. Johnson

Aerojet-General Corporation
Von Karman Center
Bldg. 312, Dept. 3111
Azusa, California 91703
Attn: Mr. Russ Fogle

Aeronutronic Division of Philco Corp.
Technical Information Services
Ford Road
Newport Beach, California 92663

Aerospace Corporation
P. O. Box 95085
Los Angeles, California 90045
Attn: Library Acquisition Group

Aerospace Corporation
Systems Design Division
2350 East El Segundo Boulevard
El Segundo, California 90246
Attn: John G. Krisilas

A.M.F.
Attn: R. J. Mosny/M. S. Mintz
689 Hope Street
Stamford, Connecticut 06907

American University
Mass. & Nebraska Avenue, N.W.
Washington, D. C. 20016
Attn: Dr. R. T. Foley
Chemistry Department

Arthur D. Little, Inc.
Acorn Park
Cambridge, Massachusetts 02140
Attn: Dr. James D. Birkett

Atomics International Division
North American Aviation, Inc.
8900 DeSota Avenue
Canoga Park, California 91304
Attn: Dr. H. L. Recht

Battelle Memorial Institute
505 King Avenue
Columbus, Ohio 43201
Attn: Dr. C. L. Faust

Bell Laboratories
Murray Hill, New Jersey 07974
Attn: U. B. Thomas/D. O. Feder

The Boeing Company
P. O. Box 3999
Seattle, Washington 98124
Attn: Sid Gross, MS 88-06

Borden Chemical Company
Central Research Lab.
P. O. Box 9524
Philadelphia, Pennsylvania 19124

Burgess Battery Company
Foot of Exchange Street
Freeport, Illinois 61032
Attn: M. E. Wilke, Chief Eng.

C & D Batteries
Division of Eltra Corporation
3043 Walton Road
Plymouth Meeting, Pennsylvania 19462
Attn: Dr. Eugene Willihnganz

Calvin College, Science Bldg.
3175 Burton St., S.E.
Grand Rapids, Michigan 49506
Attn: Prof T. P. Dirkse

Communications Satellite Corporation
Comsat Labs
P. O. Box 115
Clarksburg, Maryland 20734
Attn: Mr. Robt. Strauss

Catalyst Research Corporation
6308 Blair Hill Lane
Baltimore, Maryland 21209
Attn: Mr. F. Tepper

ChemCell Inc.
150 Dey Road
Wayne, New Jersey 07470
Attn: Peter D. Richman

Cubic Corporation
9233 Balboa Avenue
San Diego, California 92123
Attn: Librarian

Delco Remy Division
General Motors Corporation
2401 Columbus Avenue
Anderson, Indiana 46011
Attn: J. A. Keralla

Bellcomm, Inc.
955 Lenfant Plaza North, S.W.
Washington, D. C. 20024
Attn: B. W. Moss

Energy Research Corporation
15 Durant Avenue
Bethel, Connecticut 06801
Attn: M. Klein

Dynatech Corporation
17 Tudor Street
Cambridge, Massachusetts 02139
Attn: R. L. Wentworth

Eagle-Picher Industries, Inc.
Post Office Box 47
Joplin, Missouri 64801
Attn: E. P. Broglio

ESB Inc.
Post Office Box 11097
Raleigh, North Carolina 27604
Attn: Director of Engineering

Electromite Corporation
2117 South Anne Street
Santa Ana, California 92704
Attn: R. H. Sparks

ESB Inc.
Research Center
19 West College Avenue , P.O.Box 336
Yardley, Pennsylvania 19067
Attn: Librarian

Electrochemical & Water Desalination Technology
13401 Kootenay Drive
Santa Ana, California 92705
Attn: Dr. Carl Berger

Electrochimica Corporation
1140 O'Brien Drive
Menlo Park, California 94025
Attn: Dr. Morris Eisenberg

E. I. DuPont Nemours & Co.
Engineering Materials Laboratory
Wilmington, Delaware 19898
Attn: J. M. Williams
Bldg. 304

Energetics Science, Inc.
4461 Bronx Blvd.
New York, New York 10470
Attn: Dr. H. G. Oswin

Elgin National Watch Company
107 National Street
Elgin, Illinois 60120
Attn: T. Boswell

Emhart Corporation
Box 1620
Hartford, Connecticut 06102
Attn: Dr. W. P. Cadogan

Engelhard Industries, Inc.
497 Delancy Street
Newark, New Jersey 07105
Attn: Dr. J. G. Cohn

Dr. Arthur Fleischer
466 South Center Street
Orange, New Jersey 07050

General Electric Company
P. O. Box 43, R&D Center
Schenectady, New York 12301
Attn: Dr. R. P. Hamlen

General Electric Company
Space Systems
P. O. Box 8555
Philadelphia, Pennsylvania 19101
Attn: K. L. Hanson, Room 2700

General Electric Company
Battery Business Section
P. O. Box 114
Gainesville, Florida 32601
Attn: P. R. Voyentzie

General Electric Company
Research & Development Center
Post Office Box 8
Schenectady, New York 12301
Attn: Whitney Library

Dr. P. L. Howard
Centreville, Maryland 21617

General Telephone & Electronics Labs
Bayside, New York 11352
Attn: Dr. Paul Goldberg

Gould Ionics, Inc.
P. O. Box 1377
Canoga Park, California 91304
Attn: Dr. J. E. Oxley

Globe-Union, Inc.
P. O. Box 591
Milwaukee, Wisconsin 53201
Attn: Dr. E. Y. Weissman

General Electric Company
777 - 14th Street, N.W.
Washington, D.C. 20005
Attn: D. F. Schmidt

Gould-National Batteries, Inc.
Engineering & Research Center
2630 University Avenue, S. E.
Minneapolis, Minnesota 55418
Attn: D. L. Douglas

Gulton Industries
Battery & Power Services Division
212 Durham Avenue
Metuchen, New Jersey 08840
Attn: D. J. Mager

Grumman Aerospace Corporation
OAO Project
Bethpage, Long Island, N.Y. 11714
Attn: S. J. Gaston (Plant 41)

Hughes Aircraft Corporation
Centinda Ave. & Teale Street
Culver City, California 90230
Attn: T. V. Carvey

G. & W. H. Corson, Inc.
Plymouth Meeting
Pennsylvania 19462
Attn: Dr. L. J. Minnick

Hughes Aircraft Corporation
Bldg. 366, M.S. 524
El Segundo, California 90245
Attn: M. E. Ellison

Hughes Research Labs. Corp.
3011 Malibu, California 90265
Attn: T. M. Hahn

ITT Federal Laboratories
500 Washington Avenue
Nutley, New Jersey 07110
Attn: Dr. P. E. Lighty

ITT Research Institute
10 West 35th Street
Chicago, Illinois 60616
Attn: Dr. H. T. Francis

Institute for Defense Analyses
R&E Support Division
400 Army-Navy Drive
Arlington, Virginia 22202
Attn: Mr. R. Hamilton

Institute for Defense Analyses
R&E Support Division
400 Army-Navy Drive
Arlington, Virginia 22202
Attn: Dr. R. Briceland

Idaho State University
Department of Chemistry
Pocatello, Idaho 83201
Attn: Dr. G. Myron Arcand

Heliotek
12500 Gladstone Avenue
Sylmar, California 91342
Attn: Dr. H. N. Seiger

International Nickel Co.
1000-16th St., N.W.
Washington, D. C. 20036
Attn: N. A. Matthews

John Hopkins University
Applied Physics Laboratory
8621 Georgia Avenue
Silver Spring, Maryland 20910
Attn: Richard E. Evans

Johns-Manville R&E Center
Post Office Box 159
Manville, New Jersey 08835
Attn: J. S. Parkinson

Leesona Moos Laboratories
Lake Success Park, Community Drive
Great Neck, New York 11021
Attn: Dr. A. Moos

Honeywell Inc.
Livingston Electronic Laboratory
Route 309
Montgomeryville, Pennsylvania 18936
Attn: Library

Lockheed Missiles & Space Company
Post Office Box 504
Sunnyvale, California 94088
Attn: R. E. Corbett
Dept. 62-25, Bldg 157

Life Systems, Inc.
23715 Mercantile Road
Cleveland, Ohio 44122
Attn: Dr. R. A. Wynveen

Lockheed Missiles & Space Company
Dept. 62-30
3251 Hanover Street
Palo Alto, California 94304
Attn: J. E. Chilton

Lockheed Missiles & Space Company
Technical Information Center
3251 Hanover Street
Palo Alto, California 93404

Mallory Battery Company
South Broadway & Sunnyside Lane
Tarrytown, New York 10591
Attn: R. R. Clune

P. R. Mallory & Co., Inc.
Northwest Industrial Park
Burlington, Massachusetts 01803
Attn: Dr. Per Bro

P. R. Mallory & Company, Inc.
Technical Services Laboratory
Indianapolis, Indiana 46206
Attn: A. S. Doty

P. R. Mallory & Co., Inc.
3029 E. Washington Street
Indianapolis, Indiana 46206
Attn: Technical Librarian

Marquardt Corporation
16555 Saticoy Street
Van Nuys, California 91406
Attn: Dr. H. G. Krull

Martin Company
Electronics Research Department
P. O. Box #179
Denver, Colorado 80201
Attn: William B. Collins, MS 1620
Attn: M. S. Imanura, MS F8845
J. Leuthard

Material Research Corporation
Orangeburg, New York 10962
Attn: V. E. Adler

McDonnell Douglas Astronautics Company
5301 Bolsa Avenue
Huntington Beach, California 92647
Attn: Dr. G. Moe, Bldg 11-3-12, MS 12
A. D. Tonelli, MS 17, Bldg 22

Melpar
Technical Information Center
7700 Arlington Boulevard
Falls Church, Virginia 22046

North American Rockwell
Autonetics Division
P. O. Box 4181
Anaheim, California 92803
Attn: R. F. Fogle GF18

Metals and Controls Division
Texas Instruments, Inc.
34 Forrest Street
Attleboro, Massachusetts 02703
Attn: Dr. J. W. Ross

Midwest Research Institute
425 Volker Boulevard
Kansas City, Missouri 64110
Attn: Physical Science Laboratory

North American Rockwell Corp.
12214 Lakewood Boulevard
Downey, California 90241
Attn: Burton M. Otzinger

North American Rockwell Corp.
Rocketdyne Division
6633 Canoga Avenue
Canoga Park, California 91304
Attn: Library

North American Rockwell Corp.
Space Division
Downey, California 90241
Attn: Dr. James Nash

Oklahoma State University
Stillwater, Oklahoma 74075
Attn: Prof. William L. Hughes
School of Electrical Engineering

Dr. John Owen
P. O. Box 87
Bloomfield, New Jersey 07003

Power Information Center
University City Science Institute
3401 Market St., Rm. 2107
Philadelphia, Pennsylvania 19104

Prime Battery Corporation
15600 Cornet Street
Santa Fe Springs, Calif., 90670
Attn: David Roller

Portable Power Sources Corp.
166 Pensylvania Avenue
Mount Vernon, New York 10552
Attn: L. Schulman

RAI Research Corporation
225 Marcus Boulevard
Hauppauge, L.I., New York 11787

Philco Corporation
Division of the Ford Motor Company
Blue Bell, Pennsylvania 19422
Attn: Dr. Phillip Colet

Radio Corporation of America
Astro Corporation
P. O. Box 800
Hightstown, New Jersey 08540
Attn: Seymour Winkler

Philco-Ford Corporation
Power & Control Engr Dept, MS R26
3939 Fabian Way
Palo Alto, California 94303
Attn: Mr. D. C. Briggs

Radio Corporation of America
415 South Fifth Street
Harrison, New Jersey 07029
Attn: Dr. G. S. Lozier
Bldg. 18-2

Southwest Research Institute
P. O. Drawer 28510
San Antoinio, Texas 78206
Attn: Library

Sonotone Corporation
Saw Mill River Road
Elmsford, New York 10523
Attn: A. Mundel

Thomas A. Edison Research Laboratory
McGraw Edison Company
Watchung Avenue
West Orange, New Jersey 07052
Attn: Dr. P. F. Greiger

Texas Instruments, Inc.
P. O. Box 5936
Dallas, Taxas 75222
Attn: Dr. Isaac Trachtenberg

Stanford Research Institute
19722 Jamboree Boulevard
Irvine, California 92664
Attn: Dr. F. R. Kalhammer

TRW Systems, Inc.
One Space Park
Redondo Beach, California 90278
Attn: Dr. Herbert P. Silverman (R-1/2094)
Dr. W. R. Scott (M-2/2154)

TRW, Inc.
23555 Euclid Avenue
Cleveland, Ohio 44117
Attn: Librarian (TIM 3417)

Tyco Laboratories, Inc.
Bear Hill
Hickory Drive
Waltham, Massachusetts 02154
Attn: Dr. Jose Giner

Unified Sciences Associates, Inc.
2925 E. Foothill Blvd.
Pasadena, California 91107
Attn: Dr. S. Naiditch

Union Carbide Corporation
Development Laboratory Library
P. O. Box 6056
Cleveland, Ohio 44101

Union Carbide Corporation
Parma Laboratory
Post Office Box 6116
Parma, Ohio 44130
Attn: Dr. Robert Powers

University of California
Space Science Laboratory
Berkeley, California 94720
Attn: Dr. C. W. Tobias

University of Pennsylvania
Electrochemistry Laboratory
Philadelphia, Pennsylvania 19104
Attn: Prof. John O'M. Bockris

University of Teledo
Toledo, Ohio 43606
Attn: Dr. Albertine Krohn

Westinghouse Electric Corporation
Research and Development Center
Churchill Borough
Pittsburgh, Pennsylvania 15235
Attn: Dr. C. C. Hein/Dr. A. Langer

Yaroney Electric Corporation
82 Mechanic Street
Pawcatuck, Connecticut 02891
Attn: Director of Engineering

Whittaker Corporation
3850 Olive Street
Denver, Colorado 80237
Attn: L. K. White

Western Electric Company
Suite 802, RCA Building
Washington, D. C. 20006
Attn: R. T. Fiske